

The Role of Active Site Residues in Cytochrome  
P450 BM3 from *Bacillus megaterium*

Thesis submitted for the degree of  
Doctor of Philosophy  
at the University of Leicester

by

Catherine Frances Oliver BSc (Bradford)  
Centre for Mechanisms of Human Toxicity  
University of Leicester

May 1998

UMI Number: U530415

All rights reserved

INFORMATION TO ALL USERS

The quality of this reproduction is dependent upon the quality of the copy submitted.

In the unlikely event that the author did not send a complete manuscript and there are missing pages, these will be noted. Also, if material had to be removed, a note will indicate the deletion.



UMI U530415

Published by ProQuest LLC 2013. Copyright in the Dissertation held by the Author.  
Microform Edition © ProQuest LLC.

All rights reserved. This work is protected against  
unauthorized copying under Title 17, United States Code.



ProQuest LLC  
789 East Eisenhower Parkway  
P.O. Box 1346  
Ann Arbor, MI 48106-1346

## *Acknowledgements*

There are three groups of people who have been influential during my time here at Leicester, both as a technician and as a post-graduate student. It is at this time that I hope to acknowledge and thank the relevant people. Firstly I would like to thank all the people with whom I have come into contact, either as work colleagues or friends throughout the University, many of whom have gone on to pastures new. Those I would like to mention include all members of the Biological NMR Centre, past and present and people associated with the P450 group, but especially S. Barnes, M. Barnes, J. M. B. Boyle, A. Howells, V. A. Galbraith, A. N. J. Shaw, and Drs. J. and A. Basran, R. M. A. Bellingham, R. O. Frederick, B. L. Hawkins, K. S. Lilley, S. Modi and V. Ramesh. Next, I would like to say two enormous thank yous, to Prof. G.C.K. Roberts for his supervision and overview of my Ph.D. project, as well as, most importantly Glaxo Wellcome for provided the funding. Finally I would like to thank my family and in particular my husband Martin, as without his constant love and support this would not have been possible.

## ***Abstract***

Cytochrome P450 BM3 from *Bacillus megaterium* represents a novel form of P450 consisting of a single polypeptide chain incorporating both reductase and cytochrome P450, reminiscent of mammalian P450 systems. The crystal structure highlighted two important active site residues; arginine 47, postulated to interact with the carboxylate group on the fatty acid substrate and phenylalanine 87 which was possibly involved in creating a lipophilic pocket where the terminal methyl of the fatty acid substrate is sequestered and protected from hydroxylation.

Arginine 47 to glutamate (R47E) mutation resulted in a change from a positive to a negative charge and a decrease in the overall length of the side chain at this position. The  $k_{cat}$ ,  $K_m$  and  $K_d$  were determined using fatty acids and trimethylammonium compounds, the latter being better substrates for the R47E proteins. Complete reaction mixtures for wild type and R47E mutant were analysed by NMR to confirm the presence of hydroxylated products. Paramagnetic relaxation measurements established that laurate bound closer to the iron of the mutant protein for both the ferric and ferrous state.

The arginine 47 to cysteine (R47C) mutation investigated the effect of complete removal of any charge and allowed chemical modification with either iodoacetic acid to recreate "glutamic acid" or iodopropionic acid creating an "unnatural" amino acid side chain at this position. The chemically modified proteins were kinetically characterised using lauric acid and all the trimethylammonium compounds as substrates.

The last mutation was phenylalanine 87 to alanine (F87A). Products of hydroxylation were separated using reverse phase HPLC and then examined by NMR. The F87A mutation's predominant product was terminally hydroxylated lauric acid, as opposed to  $\omega$ -1 hydroxylated product with the wild type enzyme. Paramagnetic relaxation measurements showed in the reduced protein, the substrate's terminal methyl group was bound 3.1Å from the iron making it available for hydroxylation.

## *Abbreviations and Symbols*

A	Adenine
ADP	2', 5'-adenosine diphosphate
AMP	2'-adenosine monophosphate
APS	Ammonium persulphate
bp	Base pair
BSA	Bovine serum albumin
C	Cytosine
CPR	NADPH-cytochrome P450 reductase
DEAE	Diethylaminoethyl
DMF	Dimethylformamide
DNA	Deoxyribonucleic acid
DNase	Deoxyribonuclease
dsDNA	Double stranded DNA
DTNB	Dithionitrobenzoate
DTT	Dithiothreitol
EDTA	Ethylenediamine tetraacetic acid
EM water	Double distilled water
ES-MS	Electrospray mass spectrometry
F87A	Phenylalanine 87 to alanine
FAD	Flavin adenine dinucleotide
FMN	Flavin mononucleotide
FPLC®	Fast protein liquid chromatography
G	Guanine
GdmCl	Guanidinium hydrochloride
HCl	Hydrochloric acid
id	Internal diameter
IOAc	Iodoacetic acid
IOPr	Iodopropionic acid
IPTG	$\beta$ -D-isopropyl-thiogalactopyranoside
K <sub>d</sub>	Equilibrium dissociation constant

$k_{cat}$	Turnover number
$K_M$	Michaelis-Menten constant
MALDI-TOF	Matrix assisted laser desorption ionisation time of flight
MW	Molecular weight
NADH	$\beta$ -nicotinamide adenine dinucleotide (reduced form)
NADP <sup>+</sup>	$\beta$ -nicotinamide adenine dinucleotide phosphate (oxidised form)
NADPH	$\beta$ -nicotinamide adenine dinucleotide phosphate (reduced form)
NOS	Nitric oxide synthase
NMR	Nuclear magnetic resonance
NTB	Nitrothiobenzoate
P450 BM3	Cytochrome P450 BM3 from <i>Bacillus megaterium</i>
PAGE	Polyacrylamide gel electrophoresis
PCR	Polymerase chain reaction
PEG	Polyethylene glycol
PMSF	Phenylmethylsulphonyl fluoride
R47C	Arginine 47 to cysteine
R47E	Arginine 47 to glutamic acid
RNA	Ribonucleic acid
RNase	Ribonuclease
rpm	Revolutions per minute
SDM	Site-directed mutagenesis
SDS	Sodium dodecylsulphate
ssDNA	Single stranded DNA
T	Thymine
TMA	Trimethylammonium
TAE	Tris-acetate-EDTA buffer
TE	Tris-EDTA buffer
TEMED	N, N, 'N, 'N-tetramethylethylenediamine
$T_m$	Melting temperature
v/v	Volume to volume ratio
w/v	Weight to volume ratio
X-gal	5-bromo-4-chloro-3-indolyl- $\beta$ -galactopyranoside

## Contents

<i>Title</i>	Page
<i>Acknowledgements</i>	ii
<i>Abstract</i>	iii
<i>Abbreviations</i>	iv
<i>Contents</i>	vi
<b>Chapter 1: Introduction.....</b>	<b>1</b>
<b>1.1 Why Study the Cytochrome P450 Family of Enzymes.....</b>	<b>1</b>
<b>1.2 The Cytochrome P450s.....</b>	<b>2</b>
1.2.1 A Brief History of Studies involving Cytochrome P450s.....	2
1.2.2 Evolution of the Cytochrome P450s.....	3
1.2.3 Classification of the Cytochrome P450s .....	4
1.2.4 General Properties of the Cytochrome P450s .....	5
1.2.5 General Features of Cytochrome P450 Isoenzymes .....	6
1.2.6 Structural Organisation of Cytochromes P450.....	7
1.2.7 Self Sufficient Cytochrome P450 Catalytic Systems.....	9
<b>1.3 Catalytic Mechanism of Action for the Cytochrome P450s .....</b>	<b>10</b>
1.3.1 Cytochrome P450 Catalytic Cycle Based on Data from P450 cam .....	10
1.3.2 The “Peroxide Shunt” Mechanism.....	13
<b>1.4 Cytochrome P450 and Nitric Oxide Synthase .....</b>	<b>14</b>
<b>1.5 P450 cam from <u>Pseudomonas putida</u> .....</b>	<b>15</b>
1.5.1 General Background on P450 cam .....	15
1.5.2 The Crystal Structure of P450 cam.....	16
<b>1.6 P450 BM3 from <u>Bacillus megaterium</u> .....</b>	<b>20</b>
1.6.1 General Properties of P450 BM3 .....	20
1.6.1.1 Induction of P450 BM3 .....	23
1.6.1.2 The Reductase Domain of P450 BM3 .....	24
1.6.1.3 The Haem Domain of P450 BM3.....	25
1.6.2 X-ray Crystal Structure for the Haem Domain of P450 BM3.....	27
1.6.2.1 Overall Structure of the Haem Domain of P450 BM3 .....	27
1.6.2.2 The Substrate Binding Pocket.....	28
1.6.2.3 Important Residues Within the Substrate Binding Pocket .....	29
1.6.2.4 Comparison of the Open and Closed Conformations of the Substrate Access Channel of the Haem Domain of P450 BM3.....	29
1.6.3 Significance of the P450 BM3 Crystal Structure with Regard to Cytochrome P450s in General .....	33
<b>1.7 Comparison of All Known Cytochrome P450 Structures .....</b>	<b>33</b>

<b>1.8 Overall Aims and Objectives of the Work Described in this Thesis .....</b>	<b>37</b>
<b>Chapter 2: Materials and Methods .....</b>	<b>38</b>
<b>2.1 Chemicals and Reagents .....</b>	<b>38</b>
<b>2.2 Bacterial Strains .....</b>	<b>39</b>
<b>2.3 Expression Plasmids.....</b>	<b>39</b>
<b>2.4 Protein Purification .....</b>	<b>41</b>
2.4.1 Production and Initial Purification of Intact Cytochrome P450 BM3 and its Haem Domain.....	41
2.4.2 Further Purification of Intact P450 BM3 .....	43
2.4.3 Further Purification of the Haem Domain of Cytochrome P450 BM3 .....	44
2.4.4 Protein Analysis by SDS-PAGE .....	44
<b>2.5 Mass Spectroscopy and N-Terminal Sequencing .....</b>	<b>44</b>
<b>2.6 Chemical Modification of Free Protein Thiols.....</b>	<b>45</b>
<b>2.7 Ellman Assay for Free Thiols .....</b>	<b>45</b>
<b>2.8 HPLC Analysis of Products of Hydroxylation.....</b>	<b>46</b>
2.8.1 Production of Hydroxylated Products .....	46
2.8.2 Extraction of Hydroxylated Products .....	46
2.8.3 HPLC Purification of Hydroxylated Products.....	47
<b>2.9 Spectroscopic Assays .....</b>	<b>47</b>
2.9.1 Bradford Assay to determine Protein Concentration .....	47
2.9.2 Enzyme Kinetic Assays .....	47
2.9.3 Method for Determination of the Binding Constant, $K_d$ .....	48
2.9.4 Alternative Method for Determination of the Binding Constant, $K_d$ .....	49
2.9.5 Hydrogen Peroxide Assay .....	49
<b>2.10 NMR Spectroscopy .....</b>	<b>50</b>
2.10.1 Preparation of Samples for NMR Spectroscopy.....	50
2.10.2 NMR Spectroscopy to Identify Products of Hydroxylation and Measure Distances Between the Haem Iron and Substrate Protons.....	51
<b>2.11 Oxygen Consumption Assay .....</b>	<b>53</b>
<b>2.12 Oligonucleotides.....</b>	<b>54</b>
2.12.1 Purification of Synthesised Custom Oligonucleotides.....	54
2.12.2 Alternative Purification of Synthesised Custom Oligonucleotides.....	56
2.12.3 Phosphorylation of Oligonucleotides for Mutagenesis.....	56
<b>2.13 General DNA Methods .....</b>	<b>57</b>
2.13.1 Preparation of Bacterial Cell Stocks .....	57
2.13.2 Preparation of <i>E. coli</i> Competent Cells.....	57
2.13.2.1 Preparation of <i>E. coli</i> Competent Cells using Calcium Chloride.....	57
2.13.2.2 Hanahan's Method for Preparation of <i>E. coli</i> Competent Cells .....	58
2.13.2.3 Chung and Miller's Method for Preparation of <i>E. coli</i> Competent Cells.....	58
2.13.3 Bacterial Transformation with Phagemid Vectors .....	59
2.13.4 Bacterial Transformation with Double Stranded Replicative Form Phage DNA ..	59
2.13.5 Double Stranded DNA Purification .....	60

2.13.5.1 DNA Purification using Promega Magic Minipreps .....	60
2.13.5.2 Double Stranded DNA Purification using Promega Wizard Minipreps .....	61
2.13.5.3 Double Stranded DNA Purification using Hybaid Recovery .....	62
2.13.5.4 Double Stranded DNA Purification using Qiagen-tip 20 .....	62
2.13.6 Restriction Enzyme Digestion .....	63
2.13.7 Preparation of Single Stranded Phagemid DNA.....	64
2.13.8 Isolation of Single Stranded DNA by PEG Precipitation.....	65
<b>2.14 Site-directed Mutagenesis.....</b>	<b>65</b>
2.14.1 Site-directed Mutagenesis of Single Stranded Phagemid DNA.....	66
2.14.2 Control System for the Mutagenesis Reaction .....	68
2.14.3 Analysis of Mutagenesis Samples by Agarose Gel Electrophoresis.....	69
<b>2.15 DNA Automated Sequencing.....</b>	<b>69</b>
2.15.1 PCR of Single and Double Stranded DNA for Automated Sequencing .....	69
2.15.2 Phenol/Chloroform Extraction of PCR Products.....	70
2.15.3 Revised Method for the PCR of DNA for Automated Sequencing .....	70
2.15.4 Extraction of PCR Products from the Revised Method .....	71
2.15.5 Improved Automated Sequencing using Dimethylsulphoxide (DMSO) .....	72
<b>2.16 Computer Packages for DNA and Protein Analysis .....</b>	<b>72</b>
<b><i>Chapter 3: Protein Purification and Site-directed Mutagenesis .....</i></b>	<b><i>74</i></b>
<b>3.1 Introduction .....</b>	<b>74</b>
<b>3.2 Molecular Biology, involving Gene Manipulation and Protein Expression .....</b>	<b>75</b>
3.2.1 Site-Directed Mutagenesis .....	75
3.2.2 Gene Sequencing .....	81
3.2.3 Gene Sequencing for Mutant Expression Systems .....	82
3.2.4 Protein Expression .....	83
<b>3.3 Protein Purification .....</b>	<b>83</b>
3.3.1 Purification of Wild Type Proteins .....	83
3.3.2 Mutant Protein Purification .....	88
3.3.3 Incorporation of the P450 Haem .....	91
<b>3.4 Protein Characterisation .....</b>	<b>95</b>
3.4.1 Spectral Characterisation of the Wild Type and Mutant Intact P450 BM3 and its Haem Domain.....	95
3.4.2 Mass Spectrometry of Wild Type Intact P450 BM3 and its Haem Domain .....	95
3.4.2.1 MALDI-TOF Mass Spectrometry of the Wild Type Intact P450 BM3 .....	97
3.4.2.2 Electrospray Mass Spectrometry of the Wild Type Intact P450 BM3 .....	98
3.4.2.3 Electrospray Mass Spectrometry of the Wild Type Haem Domain.....	98
3.4.3 N-Terminal Sequencing of Both Wild Type and Mutant Proteins.....	99
<b>3.5 Discussion.....</b>	<b>100</b>
<b><i>Chapter 4: R47E Mutants of P450 BM3 .....</i></b>	<b><i>110</i></b>
<b>4.1 Introduction .....</b>	<b>110</b>
<b>4.2 Protein Expression and Characterisation .....</b>	<b>110</b>

<b>4.3 Electrospray Mass Spectroscopy .....</b>	<b>111</b>
<b>4.4 Optical Spectroscopy and Enzyme Assays.....</b>	<b>113</b>
4.4.1 Determination of the Catalytic Constant, $k_{cat}$ and the Michaelis Menten Constant $K_M$ .....	113
4.4.2 Substrate Binding.....	124
4.4.2.1 Substrate Binding by Optical Spectroscopy .....	124
4.4.2.2 Binding of C12 Substrate Measured by Competition .....	130
4.4.3 Hydrogen Peroxide Formation .....	134
4.4.4 Oxygen Consumption.....	137
<b>4.5 NMR Spectroscopy .....</b>	<b>139</b>
<b>4.6 Discussion.....</b>	<b>144</b>
<b><i>Chapter 5: R47C Mutants of P450 BM3 .....</i></b>	<b>152</b>
<b>5.1 Introduction .....</b>	<b>152</b>
<b>5.2 Protein Expression and Characterisation .....</b>	<b>154</b>
<b>5.3 Electrospray Mass Spectroscopy .....</b>	<b>154</b>
<b>5.4 Determination of the Number of Free Thiols.....</b>	<b>156</b>
<b>5.5 Chemical Modification .....</b>	<b>159</b>
5.5.1 Determination of the Optimum Conditions for Chemical Modification with Iodoacetate.....	160
5.5.2 Determination of the Optimum Conditions for Chemical Modification with Iodopropionate .....	163
5.5.3 Control of Chemical Modification .....	163
5.5.4 Structural Integrity of Chemically Modified Enzymes .....	165
<b>5.6 Optical Spectroscopy and Enzyme Assays.....</b>	<b>165</b>
5.6.1 Determination of the Catalytic Constant, $k_{cat}$ and the Michaelis Menten Constant $K_M$ .....	165
5.6.2 Substrate Binding.....	171
<b>5.7 Discussion.....</b>	<b>177</b>
<b><i>Chapter 6: F87A Mutants of P450 BM3 .....</i></b>	<b>188</b>
<b>6.1 Introduction .....</b>	<b>188</b>
<b>6.2 Protein Expression and Purification .....</b>	<b>189</b>
<b>6.3 Electrospray Mass Spectroscopy .....</b>	<b>189</b>
<b>6.4 Optical Spectroscopy and Enzyme Assays.....</b>	<b>191</b>
6.4.1 Substrate Binding.....	191
6.4.2 Determination of the Catalytic Constant, $k_{cat}$ and the Michaelis Menten Constant $K_M$ .....	196
6.4.3 Hydrogen Peroxide Formation .....	197
<b>6.5 Identification of Products of Hydroxylation from the F87A mutant P450 BM3. 199</b>	

6.5.1 HPLC Purification of Products of Hydroxylation.....	199
6.5.2 1D Proton NMR of Complete Reaction Mixtures for both the Wild Type and F87A Mutant P450 BM3 .....	202
<b>6.6 NMR Spectroscopy .....</b>	<b>202</b>
<b>6.7 Discussion.....</b>	<b>208</b>
<b><i>Chapter 7: General Discussion .....</i></b>	<b>218</b>
<b><i>Appendix.....</i></b>	<b>229</b>
<b>A1 Reagent Solutions.....</b>	<b>229</b>
<b>A2 Growth Media.....</b>	<b>238</b>
<b>A3 Spectrophotometric Conversions for DNA .....</b>	<b>239</b>
<b>A4 Calculation of the Melting Temperature of Oligonucleotides .....</b>	<b>239</b>
<b><i>References .....</i></b>	<b>240</b>

## ***Chapter 1: Introduction***

### ***1.1 Why Study the Cytochrome P450 Family of Enzymes?***

To manipulate enzymes for applications, such as novel detoxification or modulating physiological processes by gene therapy, it is important to establish the relationships of a protein structure to its function. Haem proteins, specifically cytochromes P450s, present good model systems for understanding the interaction of structure and function, since these enzymes contain exactly the same prosthetic group yet exhibit diverse functions, catalysing a broad range of mainly oxidative reactions on an equally broad range of substrates (Darwish *et al.*, 1991). Many of the hydroxylation reactions occur with a high degree of regio- and stereoselectivity. So clearly the active sites of the P450s must differ substantially from one another to accommodate substrates of different size, shape and electrostatic properties (Li and Poulos, 1997). The ability to predict whether a molecule would be a substrate from knowledge of the active site structure and an understanding of the factors that determine substrate specificity are critical if new activities and specificities are to be engineered into P450 enzymes by mutagenesis. A great deal of interest also surrounds the possibility of harnessing the catalytic power of these enzymes for industrial processes, such as the catalysis of stereospecific oxidations *in vitro*. In addition, elucidation of the factors that determine substrate specificity is required to understand, predict, and attempt to modulate the metabolism of pharmaceuticals and other xenobiotics (De Voss and Ortiz de Montellano, 1995). In the case of human enzymes this might lead to the rational design of inhibitors and/or pro-drugs that would take advantage of the activity of these enzymes *in vivo*.

The cytochrome P450 BM3 from *Bacillus megaterium* was chosen for the present work due to its relationship with two different classes of enzymes: mammalian microsomal fatty acid hydroxylases of P450 Family 4, which display approximately 30% sequence identity with P450 BM3 (Ruettinger *et al.*, 1989) and nitric oxide synthase (NOS) which is purported to be the first example of a catalytically self-sufficient cytosolic mammalian P450-like enzyme, a fusion protein containing a flavin

domain analogous to NADPH-P450 reductase and a haem domain, exhibiting a similar protein domain organisation to P450 BM3 (White and Marletta, 1992). Cytochrome P450 BM3 also provides a useful model as it possesses the distinct advantages of being soluble and expression systems are available for production in large quantities for use in biophysical studies.

## **1.2 The Cytochrome P450s**

### **1.2.1 A Brief History of Studies Involving Cytochrome P450s**

The cytochrome P450s (EC 1.14.14.1, non-specific monooxygenase) were discovered about 40 years ago, when pharmacologists were intrigued by the observation that “hexobarbital sleeping time” of animals could be used as an indicator of the effectiveness of various compounds to alter the rate of drug metabolism (Bernhardt, 1995). By 1958, Klingenberg and Garfinkel independently observed the presence of a pigment in rat liver microsomes which absorbed light at 450nm after treatment with the reducing agent sodium dithionite and gassing with carbon monoxide. It was not until 1964 that the haemprotein nature of this CO-binding pigment was proven by Omura and Sato. The identification of this pigment as a *b*-type cytochrome with an atypical absorption maximum, referred to as the Soret band, of the CO complex at 450nm led the authors to designate it cytochrome P450 and describe it as “a new cytochrome of unusual properties”. The name P450 therefore represents a pigment absorbing light at 450nm. The appearance of the ferrous haem-carbonyl absorption maximum near 450nm is quite different from that exhibited by other haem proteins such as myoglobin which has a maximum at 435nm and horseradish peroxidase whose maximum is at 438nm (Black and Coon, 1987).

The studies of Estabrook *et al.* (1963) established the catalytic function of P450s. They showed that this pigment was the final component of an electron-transfer chain that catalysed the oxidation of substrates. Specifically, their experiments indicated that P450s present in the microsomal fraction of the adrenal cortex were responsible for the 21-hydroxylation of 17 $\alpha$ -hydroxyprogesterone. The P450s correspond to a superfamily of haem-containing enzymes widely distributed in mammalian, plant and

microbial systems which possess a unique cysteine thiolate (S-) ligand to the haem iron. In the last 10 years a new definition of P450 has been introduced based on their common structural properties - "haem-thiolate" protein instead of the term cytochrome for P450s. This is because, in almost all of its activities, P450 does not function simply as an electron carrier transferring electrons to other proteins (Black and Coon, 1987). Other examples of haem-thiolate protein are the nitric oxide synthases which are discussed in more detail below in Section 1.4.

### ***1.2.2 Evolution of the Cytochrome P450s***

It is now widely accepted that the P450 gene superfamily is very old, the ancestral gene having existed before the time of prokaryote/eukaryote divergence. On examination of the amino acid sequence alignments, most P450 proteins are markedly different. However there is a 10 residue region involved in haem binding located near the carboxy-terminus of all P450s that exhibits a high degree of similarity (Adesnik and Atchison, 1986; Nebert and Gonzalez, 1987; Waterman, 1992). These findings suggest that all P450 genes have diverged from the same ancestral gene, which probably existed more than 2 billion years ago (Nebert *et al.*, 1989). The earliest P450s to emerge were those that metabolised steroids and fatty acids. The fatty acid metabolising P450 Family 4 and the steroid-inducible P450 Family 3 diverged more than 1 billion years ago (Nelson and Stroebel, 1987). It appears therefore that the earliest P450s may have evolved to maintain mammalian membrane integrity through metabolism of lipids and steroids (Gonzalez, 1990).

It seems likely that the P450 enzymes originated during early evolution to provide the organism with oxidative and peroxidative metabolism of important endogenous molecules, as well as the breakdown of environmental chemicals to be utilised for energy (Nelson *et al.*, 1993). As some organisms developed a wide array of toxins to escape the fate of being eaten, others developed strategies to deal with these toxic substances (Gonzalez and Nebert, 1990). The structural diversity of these compounds requiring detoxification led to the evolution of a complex system to deal with these xenobiotics. As most of these xenobiotics are lipophilic and not readily excretable, a

complex pathway has evolved to convert them to more hydrophilic metabolites. The first step in this process entails the introduction of an oxygen atom into the compound and this reaction is mainly catalysed by the cytochrome P450s.

### ***1.2.3 Classification of the Cytochrome P450s***

The first classification of the cytochrome P450s was made in 1991 by Nebert *et al.*. In this paper 154 different P450 genes and 7 putative pseudogenes were described in a total of 23 eukaryotic and 6 prokaryotic species. By 1993, Nelson *et al.* were describing 221 genes and 12 putative pseudogenes. The most recent review by Nelson *et al.* (1996) details 481 P450 genes and 22 pseudogenes. These genes were described in 85 eukaryotic (including vertebrates, invertebrates, fungi and plants) and 20 prokaryotic species. 74 gene families have been identified with 14 families further divided into 26 subfamilies in mammals.

A P450 gene is named including the italicised root symbol “*CYP*” (“*Cyp*” for mouse and drosophila) denoting cytochrome P450, an Arabic number denoting the P450 family, a letter indicating the subfamily when two or more subfamilies exist within that family and a second Arabic numeral to represent the individual gene (Nebert *et al.*, 1991). The cDNAs, mRNAs and proteins in all species (including mouse) should include all capital letters and without italics.

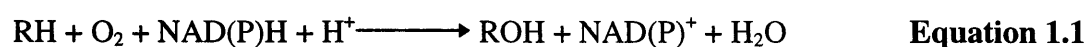
Members of the same gene family are defined as usually having  $\leq 40\%$  sequence identity with a protein from another P450 family. This definition was made arbitrarily but subsequently has been shown to be very useful. If the protein sequence is less than 40% identical to any other sequence, then the new sequence constitutes the first member of a new family. The P450 protein sequences within a given gene family are  $>40\%$  identical. There are always exceptions to any rule and here sequences from Families 2, 4, 6, 11, 52 and 105 provide examples. They range from CYP4C1, CYP4D1 and CYP4E1 insect sequences that display between 26 and 42% identity with other Family 4 members to the bacterial CYP105C1 protein which exhibits 39.5% identity with CYP105A1 protein (Nelson *et al.*, 1996). Sequences within the same

family that are at least 60% identical are grouped into subfamilies. Genes within a defined subfamily have been found to be nonsegregating, that is, they reside on the same gene cluster (Nelson *et al.*, 1996). These clusters most likely have arisen via gene duplication events, most likely during the last 400 million years (Nelson and Strobel, 1987). The individual P450 enzymes are then given specific numbers (although not if only one gene is present). The main characteristics of the most important cytochrome P450 families will be discussed briefly.

CYP2 represents the largest family of cytochrome P450s consisting of 10 subfamilies concerned mainly with the bioconversion of drugs, testosterone hydroxylation and metabolism of ethanol, acetone and acetoacetone (Gonzalez, 1990; Nelson *et al.*, 1993). The CYP3 family has one subfamily subdivided into 12 individual enzymes, the most important being P450 3A4 as it is the most abundant P450 in human liver and is involved in the metabolism of a variety of very different drugs and xenobiotics such as nifedipine, cyclosporine, erythromycin, gestodene and aflatoxins (Li *et al.*, 1995). This variety of substrates makes P450 3A4 one of the most important enzymes for drug metabolism. The best studied cytochrome P450 is P450 cam, a soluble, bacterial P450 involved in the catabolism of camphor by *Pseudomonas putida*. P450 cam (CYP101) was the first P450 for which a three-dimensional structure became available (Poulos *et al.*, 1985) and as a result numerous structural and functional studies have been performed with it.

#### ***1.2.4 General Properties of the Cytochrome P450s***

The cytochrome P450 enzymes are ubiquitous in nature and present in a broad range of species including plants, fungi, bacteria, insects and mammals. The P450 system catalyses the following reaction:



In the presence of oxygen and the reduced form of either nicotinamide adenine dinucleotide (NADH) or nicotinamide adenine dinucleotide phosphate (NADPH) and

one or more electron transfer proteins, they catalyse the monooxygenation of a wide variety of hydrophobic substances of both exogenous and xenobiotic origin through the insertion of one atom of molecular oxygen into the substrate with the concomitant reduction of the other atom to water. They catalyse many diverse reactions including hydroxylation, N- O- and S-dealkylation, N-oxidation, sulphoxidation, deamination, epoxidation, dehydrogenation, dehydration, deformylation, dehalogenation, peroxidation and N-oxide reduction.

The biochemical processes in which this monooxygenation step is important include bile acid formation, steroid hormone synthesis, the metabolism of fat-soluble vitamins (A and D), certain polyunsaturated fatty acid oxygenations, (Wen and Fulco, 1987; Guengerich, 1991). Many of these enzymes also metabolise a wide range of man-made chemicals including drugs, environmental chemicals and pollutants. The number of man-made “environmental chemicals” has been estimated as greater than 200000, most of which are thought to be potential substrates for P450s though some may act as inducers or inhibitors (Porter and Coon, 1991). Some of the transformations, particularly with xenobiotics leads to more polar compounds that are more readily excreted directly or after conjugation with water soluble agents. The metabolism of foreign compounds can frequently produce toxic metabolites with much greater cytotoxicity, mutagenicity or carcinogenicity, some of which have been implicated as agents responsible for birth defects and other forms of toxicity, as well as tumour initiation and progression (Nebert *et al.*, 1996).

### ***1.2.5 General Features of Cytochrome P450 Isoenzymes***

The primary structures contain up to 547 amino acid residues with an average molecular weight of 50000 Daltons (Da)  $\pm$  10000Da. The first 20 amino-terminal residues of the microsomal P450s are highly hydrophobic with polar or charged side chains found only rarely. This region constitutes a noncleaved membrane insertion signal and stop-transfer anchor sequence. The microsomal P450s are synthesised on the endoplasmic reticulum and the hydrophobic N-terminus directly interacts with a signal recognition particle which mediates the insertion into the membrane during

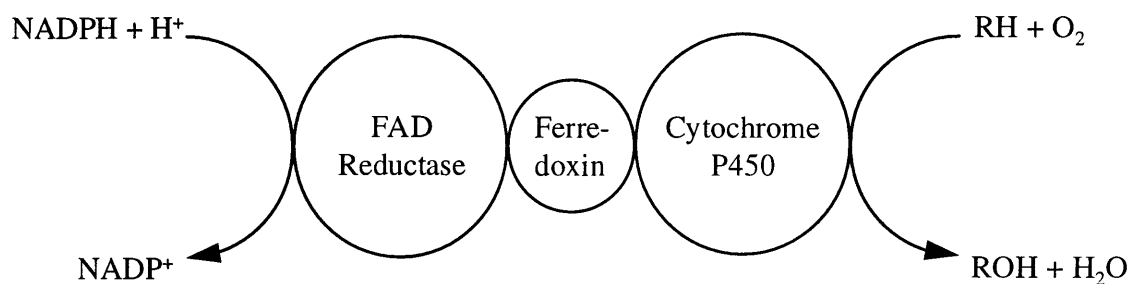
translation (von Wachenfeldt and Johnson, 1995). The stop-transfer sequence interrupts translocation and anchors the protein in the membrane (Sakaguchi *et al.*, 1992). The hydrophobic, anionic and cationic amino acid residues in the known covalent structures represent approximately 37, 11 and 14% respectively of the total residues. These values vary little from sequence to sequence suggesting that the structures are related. Sequence alignments of various cytochrome P450s indicate the C-terminal half of the sequences show greater homology overall than the N-terminal portion (Gotoh and Fujii-Kuriyama, 1989; Lewis, 1995). This difference may be due to functional core residues residing in the C-terminus region, whereas the reduced homology at the N-terminal reflects a response to environmental and evolutionary pressures or results from spontaneous random mutations that would not be tolerated if they occurred within the C-terminal region. This is discussed further in Section 1.7.

### ***1.2.6 Structural Organisation of Cytochromes P450***

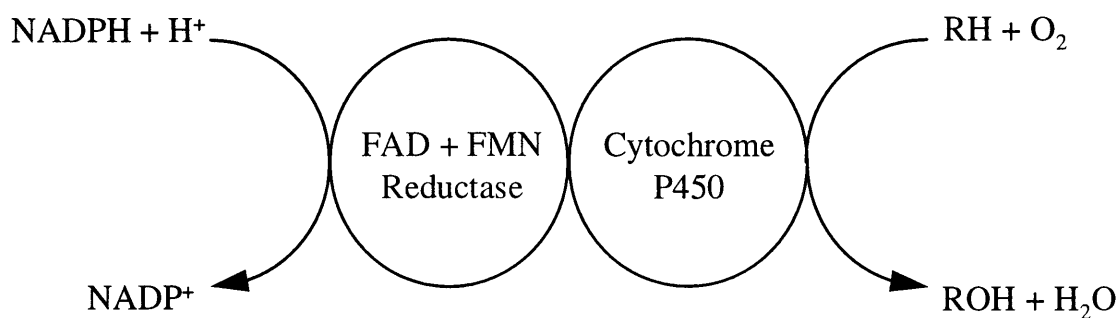
The cytochromes P450 require an external electron donor to provide the electrons necessary for oxygen activation and the subsequent substrate hydroxylation. The P450 monooxygenase systems are therefore classified into two groups based on the minimum number of protein components necessary to reconstitute the monooxygenase activity (Figure 1.1).

Class I P450s (Figure 1.1a) have been identified in mitochondria and most bacteria. These P450 systems are made up of two major parts; the first part being the P450 enzyme, where the mitochondrial P450s are located in the intrinsic membrane and the bacterial P450s are all soluble, while the other forms the electron transfer components that have been isolated in the soluble form. The electron transfer components consist of an iron sulphur protein which shuttles electrons to the P450 from a flavin adenine dinucleotide (FAD)- or flavin mononucleotide (FMN)- containing reductase which associates with the nicotinamide dinucleotide.

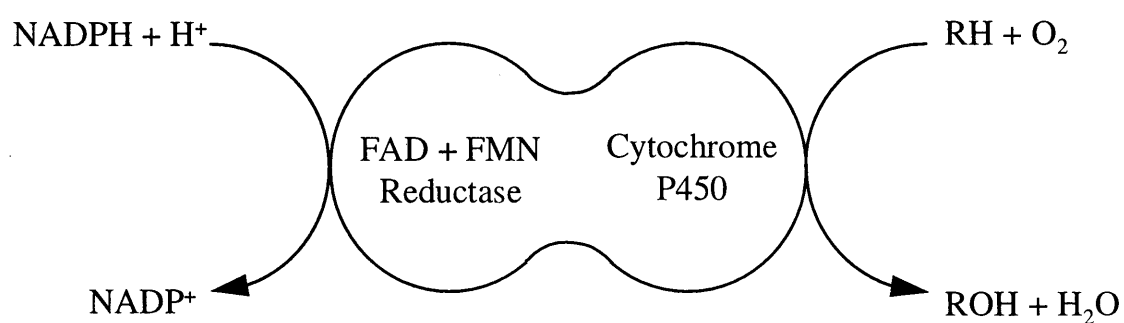
Figure 1.1b depicts the microsomal Class II P450 monooxygenase which is located in the endoplasmic reticulum of eukaryotic cells and consists of an NADPH-cytochrome



a) Class I: Mitochondrial and Most Bacterial P450 Monooxygenases, e.g. P450 cam



b) Class II: Microsomal P450 Monooxygenases, e.g. P450 4A1



c) Class II: P450 BM3 Monooxygenase from *Bacillus megaterium*

**Figure 1.1:** Comparison of mitochondrial, microsomal and bacterial P450 monooxygenase systems.

the endoplasmic reticulum of eukaryotic cells and consists of an NADPH-cytochrome P450 reductase (CPR: EC 1.6.2.4), a flavoprotein containing one FMN and one FAD molecule, which transfers electrons from NADPH to the P450.

Class I and Class II P450 systems differ substantially in their degree of amino acid sequence identity (Nelson *et al.*, 1993) as well as the way in which they receive reducing equivalents from nicotinamide cofactors.

Figure 1.1c illustrates the only known example to date of a bacterial, self-sufficient, one protein P450-dependent monooxygenase, the 119kDa fatty acid monooxygenating P450 BM3 from *Bacillus megaterium*. P450 BM3 is essentially composed of the two protein component system and is therefore uniquely classified as the only prokaryotic member of the Class II monooxygenases. A fungal self-sufficient, one protein P450-dependent monooxygenase has also been identified in *Fusarium oxysporum* MT-811, designated P450 foxy (CYP55; Shoun *et al.*, 1985; Nakayama *et al.*, 1996). On purification this fatty acid hydroxylase was shown to closely resemble P450 BM3 with respect to structure and function (Nakayama *et al.*, 1996). P450 BM3 was the system under study during the research and is discussed in greater detail later.

### ***1.2.7 Self Sufficient Cytochrome P450 Catalytic Systems***

The production of engineered self-sufficient cytochrome P450s is a growing field. They have been found to be useful when studying drug metabolism, as when these proteins are expressed alone they exhibit low levels of expression. The catalytic power of these fusion enzymes can be harnessed for practical purposes, including the stereospecific synthesis of fine organic chemicals, the degradation or detoxification of hazardous compounds in the environment and the development of plants with resistance to specific pesticides (Sibbesen *et al.*, 1996). This final use has already been demonstrated by Shiota *et al.* (1994) where they developed a cytochrome P450-P450 reductase fusion protein that conveyed resistance to the herbicide chlortoluron in tobacco plants. So far to date the majority of self-sufficient P450 catalytic systems have utilised the Class II membrane-bound mammalian P450 enzymes. The first fusion

protein to appear was constructed from rat P450 1A1 with the N-terminal truncated rat P450 reductase (Murakami *et al.*, 1987). These fusion proteins have been expressed in yeast (*Saccharomyces cerevisiae*) and bacterial (*Escherichia coli*) host systems (For a review of the current literature see Yabusaki, 1995 and references therein) providing a number of advantages with regard to high yield, low cost and ease of handling.

To date there has only been one example of an engineered bacterial fusion protein and that is the triple fusion protein of putidaredoxin reductase-putidaredoxin-cytochrome P450 cam (Sibbesen *et al.*, 1996), though a triple fusion protein has been developed for the mitochondrial Class I P450 system consisting of cytochrome P450 scc fused to adrenodoxin and adrenodoxin reductase (Harikrishna *et al.*, 1993). At protein concentrations less than 0.3  $\mu\text{M}$ , the catalytic rate for the P450 cam fusion protein was slightly higher than that for the 1:1:1 (putidaredoxin reductase:putidaredoxin:P450 cam) reconstituted system. However the catalytic rate of the reconstituted system exhibited a higher order concentration dependence, suggesting that overall the fusion protein was less efficient than the reconstituted wild type system (Sibbesen *et al.*, 1996). Therefore it appears that more work is required to maximise the potential for this area of cytochrome P450 research.

### ***1.3 Catalytic Mechanism of Action for the Cytochrome P450s***

#### ***1.3.1 Cytochrome P450 Catalytic Cycle Based on Data from P450 cam***

Various authors have discussed the catalytic cycle of the cytochrome P450s in detail (White and Coon, 1980; Sligar and Murray, 1986; Black and Coon, 1987; Dawson, 1988; Sariaslani, 1991; Bernhardt, 1995; Mueller *et al.*, 1995). Below is a concise account of the cycle as it is known at present. The generally accepted mechanism of the cytochrome P450-dependent substrate conversion is depicted in Figure 1.2. P450 catalysis typically begins with the substrate-free, oxidised (ferric iron) state. This protein has a redox potential of about -300mV with the haem iron in the low-spin six-coordinated form. Solution of the X-ray structure of the substrate-free cytochrome P450 cam unambiguously reported water or OH<sup>-</sup> as the sixth ligand, trans to the thiolate proximal ligand provided by the cysteine coordination (Poulos *et al.*, 1986).

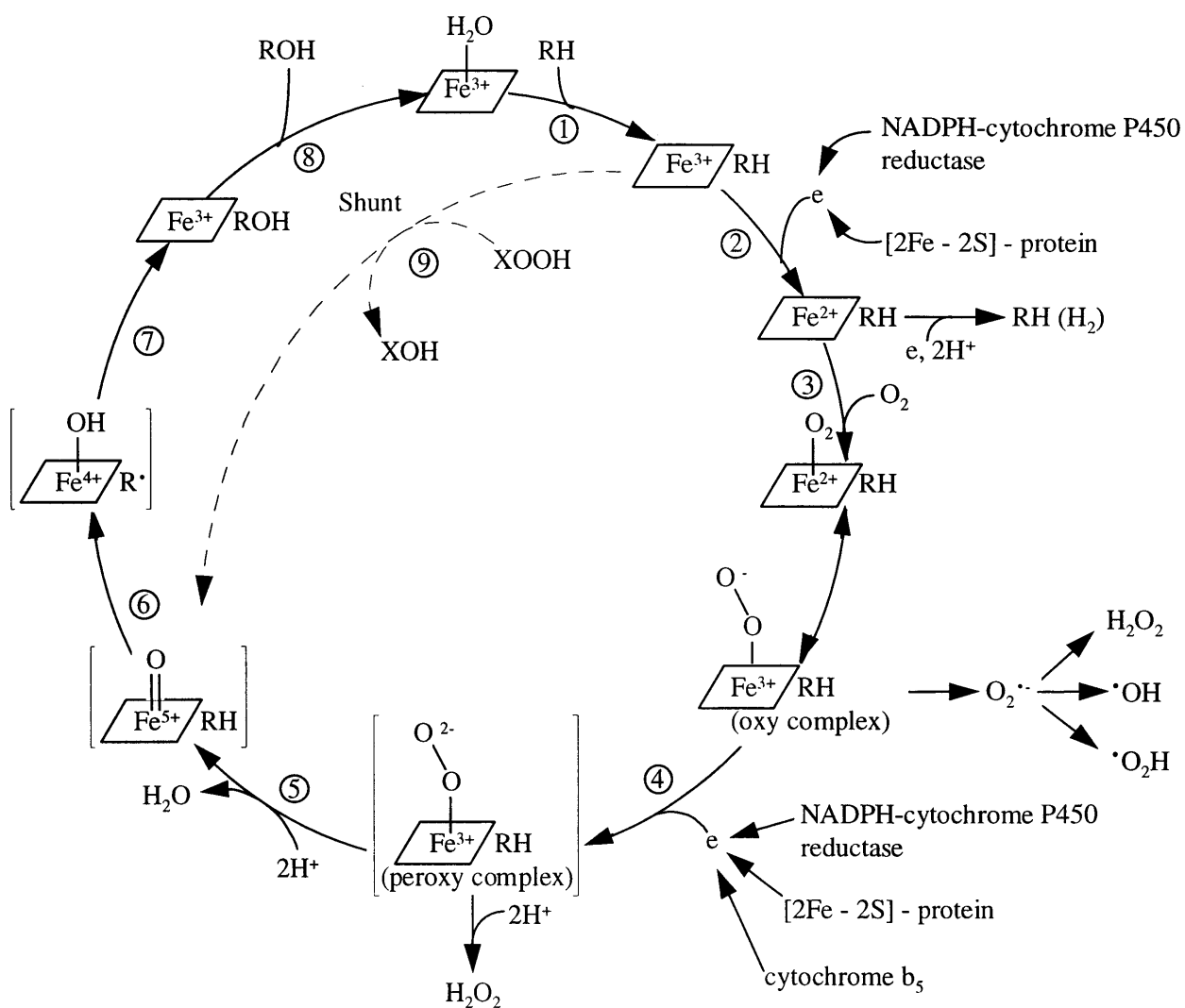


**Figure 1.2:** The reaction cycle of the cytochrome P450s, based on experiments performed on P450 cam. Uncoupling side reactions and sources of electrons have been shown (Adapted from Bernhardt, 1995).

The first step of the reaction cycle is the formation of the enzyme-substrate complex. This fundamental aspect of molecular recognition defines the regio- and stereoselectivity of the oxygenation process as well as the “fit” within the substrate binding site that excludes water. This ensures the efficient coupling of reducing equivalents from the electron transfer proteins, be they the iron sulphur protein of the Class I P450s or the NADPH-cytochrome P450 reductase of the Class II P450s.

The binding of the substrate to the P450 active site results in dehydration of the haem iron environment and a concomitant shift of the enzyme redox potential from -300mV to -170mV. The shift in redox potential is necessary as the potential, for example, for the iron sulphur protein electron donor in the subsequent first electron transfer operates at -200mV. This means that the substrate binding induced change in redox potential acts as a physiological control for the initial electron transfer.

The binding of the substrate can be followed by observing spectral changes of the P450 in the near UV spectral region (Soret Band) and in the visible spectral region caused by spin-state changes of the protein. The majority of substrates being metabolised by cytochrome P450s produce a "Type I" difference spectrum which is characterised by a minimum at 417nm and a maximum at 387nm. Many inhibitors, which bind directly to the haem iron, produce "Type II" difference spectrum with absorption maxima between 425nm and 445nm and minima between 390nm and 420nm. Some compounds such as alcohols and ketones give rise to "Inverse type I" difference spectrum, characterised by an absorption maximum at about 420nm and a minimum at 385-390nm.

The second step of the reaction cycle is the introduction of the first electron where the oxidised iron ( $3^+$ ) is reduced to iron ( $2^+$ ). This is accomplished by electron transfer from either NADPH-dependent reductase or via a ferredoxin (Figure 1.1). Implicit in this event is the formation of a specific complex between the two macromolecules. It has been suggested that the dynamics and structure of the donor-acceptor complex plays a key role in the overall efficiency and regulation of the electron transfer process.

The third step of the reaction cycle involves the binding of molecular oxygen to the one-electron reduced haemprotein. In P450 cam the oxyferrous state is fairly stable, autoxidising only very slowly to ferric P450 cam and  $O_2^{\bullet-}$  to produce a ferric-superoxide species (Sligar *et al.*, 1974). Referring to Figure 1.2, from this complex a superoxide anion radical can be released, where the negatively charged dioxygen favours the binding of a proton or hydrogen.

Step 4 of the reaction cycle is the introduction of the second electron, which in some situations can be facilitated by another microsomal haemprotein, cytochrome  $b_5$  (Bonfils *et al.*, 1981). From the (RH)  $\text{Fe}^{3+} (\text{O}_2^{2-})$  complex hydrogen peroxide can be formed. Due to the fact that the cytochrome P450 is a one-electron donor, oxygen activation is a two step process (Peterson *et al.*, 1977).

The events occurring after the delivery of the second electron have been the subject of debate in the P450 community for many years. The mechanism depicted in Figure 1.2 details only one of the two mooted reaction mechanisms. None of the bracketed species have been observed directly. The mechanism involves the reduction of the ferric-peroxy species, which may exist alternatively as a ferrous-superoxide species. Two protons are delivered to the active site to facilitate the loss of one atom of oxygen as water and generate a high-valent iron-oxo species. Although depicted as an  $\text{Fe}^{5+}=\text{O}$  moiety, this species can be stabilised as  $\text{Fe}^{4+}=\text{O-porphyrin}^{+}$  (White and Coon, 1980). Another depiction of this species is  $[\text{FeO}]^{3+}$ , which avoids the implications of a specific iron-oxo bonding.

In the presence of excess protons, cytochrome P450s are capable of exhibiting NADPH oxidase activity in that the activated oxygen generated can be directly reduced to water. However, generally the next step is hydrogen abstraction from the substrate to generate a substrate radical species (step 6) followed by recombination of the resulting carbon radical and hydroxyl radical to produce a stable hydroxylated product (step 7). Finally, the hydroxylated product dissociates and the cycle can start again (step 8).

### **1.3.2 The “Peroxide Shunt” Mechanism**

Aside from the conventional cycle, an alternative reaction path has been discovered and is referred to as the peroxide shunt reaction. In this pathway the substrate can be hydroxylated immediately by various oxygen atom donors such as iodosobenzene, sodium periodate, sodium chlorite and peroxides, including hydrogen peroxide and cumene hydroperoxide without the necessity of interaction with an electron-donating system and molecular oxygen, as illustrated in step 9 (Hycay *et al.*, 1976). The peroxy

compound may undergo homolytic cleavage, with the  $XO^{\bullet}$  radical abstracting a hydrogen atom from the substrate to give XOH. Recombination of the substrate radical and hydrogen radical would then proceed to yield ROH.

#### ***1.4 Cytochrome P450 and Nitric Oxide Synthase***

The nitric oxide synthases (NOSs: EC 1.14.13.39) catalyse the oxygenation of L-arginine by nicotinamide adenine dinucleotide phosphate (NADPH) and molecular oxygen ( $O_2$ ) with formation of citrulline and NO. The formation of citrulline and NO from  $N^{\omega}$ -hydroxy-L-arginine can also be efficiently catalysed by microsomal cytochrome P450s (Boucher *et al.*, 1992). They are the only mammalian proteins that catalyse a P450-like hydroxylation reaction and P450 reductase-like NADPH reduction within the same protein; an attribute shared with P450 BM3 and P450 foxy. These possess a carboxy-terminal FAD- and FMN-containing reductase domain (Bredt *et al.*, 1991; McMillan *et al.*, 1992; White and Marletta, 1992) and an N-terminal domain that possesses haem and displays cytochrome P450-like properties (Stuehr *et al.*, 1992; McMillan *et al.*, 1992; White and Marletta, 1992) such as a Fe(II)-CO complex exhibiting a Soret peak at 450nm and on binding the substrate L-arginine there is a shift in the Soret peak from 418nm (low spin  $Fe^{3+}$ ) to 390nm (high spin  $Fe^{3+}$ ). The original signature sequence FXXGXXXCXG for P450 proteins was found in 202 of 205 sequences (Nelson *et al.*, 1993), a signature that is not present in the NOSs. McMillan *et al.* (1992) suggested putative cysteine thiolate donors in rat neuronal (Cys-415), bovine endothelial (Cys-186) and murine macrophage (Cys-194) NOSs, by sequence inspection observing the presence of a conserved dodecapeptide within the three forms. These are compared with the sequences of other haemproteins in Table 1.1.

To search for any other resemblance to P450 sequences, the first 501 residues of mouse NOS, corresponding to a putative haem domain, were aligned with 57 P450 sequences each from different families. This failed to demonstrate the presence of the I and L helices that are considered the structural determinants for the P450s. Thus although the NOSs are haem containing monooxygenases, structurally these enzymes

are at most distantly related to the cytochrome P450s and likely represent an example of convergent evolution (Nelson *et al.*, 1993).

**Table 1.1:** Comparison of haem binding peptides in various haem proteins (Adapted from McMillan *et al.*, 1996).

Enzyme	Peptide Sequence	Reference
Rat nNOS	W R N A S R - C V G R	Bredt <i>et al.</i> (1991)
Murine iNOS	W R N A P R - C I G R	Xie <i>et al.</i> (1992)
Bovine cNOS	W R N A P R - C V G R	Lamas <i>et al.</i> (1992)
P450 BM3	F G N G P R N C I G	Ruettinger <i>et al.</i> (1989)
P450 cam	F G H G S H L C L G	Ungar <i>et al.</i> (1986)

## 1.5 P450 cam from *Pseudomonas putida*

### 1.5.1 General Background on P450 cam

Cytochrome P450 cam (CYP101) from *Pseudomonas putida* ATCC 17453 was first isolated by Gunsalus and co-workers in 1967. It consists of 414 amino acid residues, with an approximate molecular weight of 45 kDa and was subsequently shown to catalyse the oxidation of the monoterpene camphor to 5-exo-camphor (Figure 1.3). This hydroxylation reaction is the first step in the degradation of camphor, to the final products of acetate and isobutyrate, which allows *P. putida* to utilise camphor as its sole carbon and energy source (Martinis *et al.*, 1991). As P450 cam is a soluble enzyme obtainable in relatively large amounts and high purity, it has been extensively used as a model to investigate the chemical and biophysical mechanisms of P450 catalysis (White and Coon, 1980; Poulos *et al.*, 1987; Raag *et al.*, 1991; Poulos and Raag, 1992; Loida and Sligar, 1993).

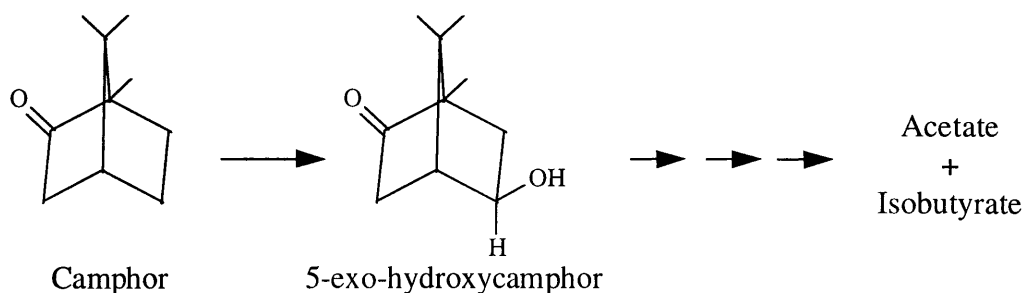


**Figure 1.3:** Diagrammatic representation of the cytochrome P450 catalysed hydroxylation of camphor to 5-exo-hydroxycamphor by P450 cam, to its final degradation products.

P450 cam is an example of Class I cytochrome P450s and as such requires two auxiliary proteins, the flavoprotein putidaredoxin reductase (PDR) and the iron-sulphur protein putidaredoxin (PR), containing a ferredoxin-type 2Fe-2S centre, for catalytic activity. These two proteins mediate the transfer of electrons from NADH via the PDR then PR to the haemprotein. All three proteins necessary for P450 cam catalytic reaction have been cloned and heterologously expressed in *E. coli* (Koga *et al.*, 1985; Ungar *et al.*, 1986; Peterson *et al.*, 1990). Although P450 cam has traditionally been associated with camphor, it has also been associated with the metabolism of other compounds including styrenes, ethylbenzene, nicotine and chlorinated hydrocarbons, catalysing a range of reactions including carbon hydroxylation, epoxidation, sulphoxidation and dehalogenation, though rather poorly in some cases (Sibbesen *et al.*, 1996).

### 1.5.2 The Crystal Structure of P450 cam

The first three-dimensional structure of a P450 cytochrome was reported by Poulos *et al.* in 1985 (Figure 1.4). This 2.6Å resolution structure of P450 cam was obtained from the ferric substrate-bound form of the cytochrome P450. Shortly after the x-ray crystal structure at 2.2Å resolution was produced for the substrate-free P450 cam (Poulos *et al.*, 1986) and in the presence of several inhibitor complexes (Poulos and Howard, 1987). The availability of crystal structures of P450 cam with a variety of bound ligands and of several mutant forms of the protein make it the best structurally

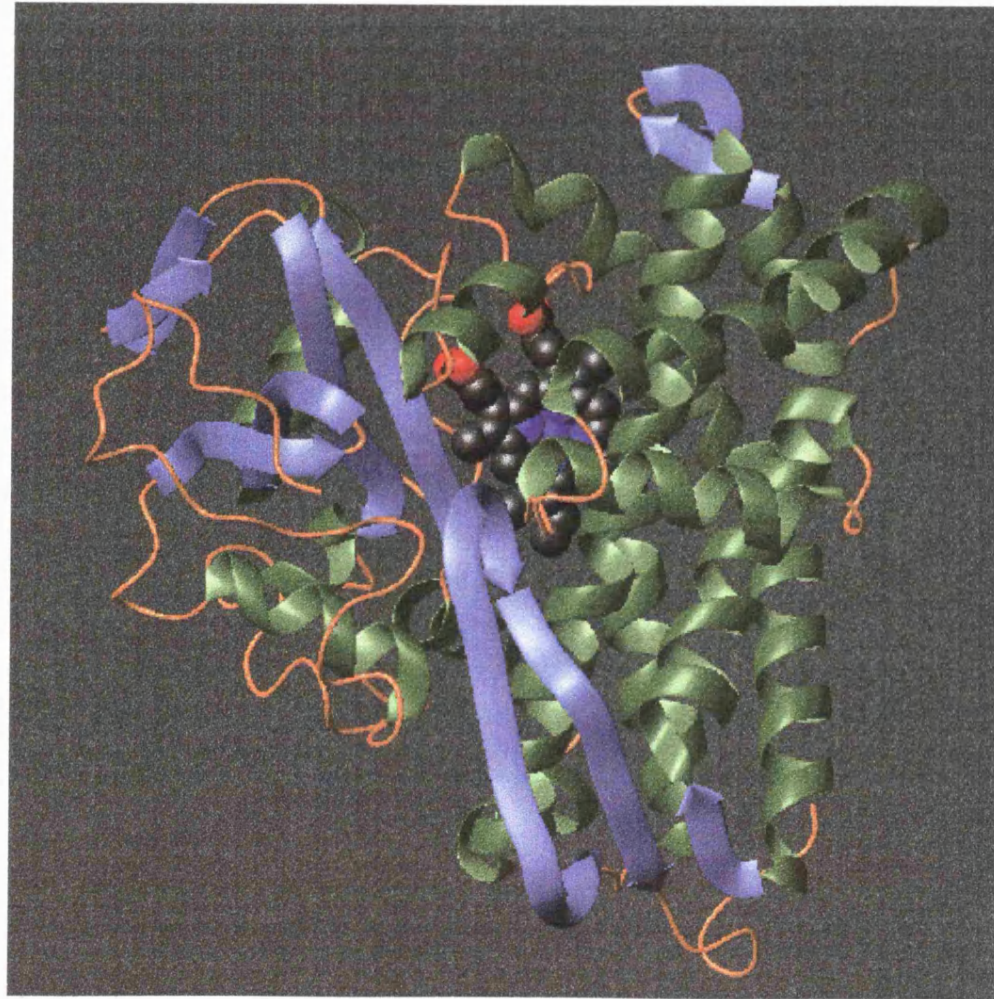


**Figure 1.4:** Ribbon diagram to display the overall folding and secondary structure of the substrate-free P450 cam (Poulos *et al.*, 1986). The  $\alpha$  helices are shown in green, the  $\beta$  strands in blue and the random coil in orange.

characterised P450 enzyme (Poulos and Howard, 1987; Raag *et al.*, 1990; Raag and Poulos, 1991; Raag *et al.*, 1993).

The general shape of the protein approximates to a flattened triangular prism with a maximum dimension of about 60Å and a minimum dimension of about 30Å;  $\alpha$ -helices constitute approximately 40% of the total structure, with 10% antiparallel  $\beta$ -sheet. If viewed from an edge, the molecule is domed on top (distal surface) and flat on the bottom (proximal surface). The L or proximal helix donates the cysteinate ligand (C357) to the iron atom. On comparison of the camphor-free and camphor-bound P450 cam, there is no evidence of any suitable path from the protein surface to the active site that would permit substrate binding. It would thus appear that conformational dynamics must play a significant role in the process of substrate binding. The most significant alteration on substrate binding occurs at the active site, which in the absence of substrate is filled with six water molecules. On substrate binding all water is displaced thus facilitating the production of the high-spin pentacoordinated ferric centre.

The active site is a buried cleft isolated from bulk solvent, that is mainly hydrophobic in nature offering neither acid or base groups to aid in catalysis (Poulos *et al.*, 1987). The bound substrate, camphor, is therefore held in place by hydrophobic interactions and by hydrogen bonding of the carbonyl oxygen to tyrosine 96, such that the substrate is located above pyrrole ring A with the iron atom facing the 5-exo position. Such an orientation accounts for the stereoselective hydroxylation characteristic of the cytochrome. Phenylalanine 87 (F87) and leucine 244 (L244) lie in contact with the substrate carbonyl and valine 247 (V247) and valine 295 (V295) further define the camphor envelope by completely enclosing the substrate and orientating it towards the haem (Poulos *et al.*, 1985).

In the X-ray crystal structure of P450 cam, the side chain hydroxyl of threonine 252 (T252; Figure 1.5), rather than the peptidyl nitrogen, forms a hydrogen bond with the carbonyl oxygen of glycine 248. This unique hydrogen bond produces a local deformation, or kink, in the distal I helix, which is directly adjacent to the active site and haem iron. This distortion widens helix I at this point providing a binding pocket

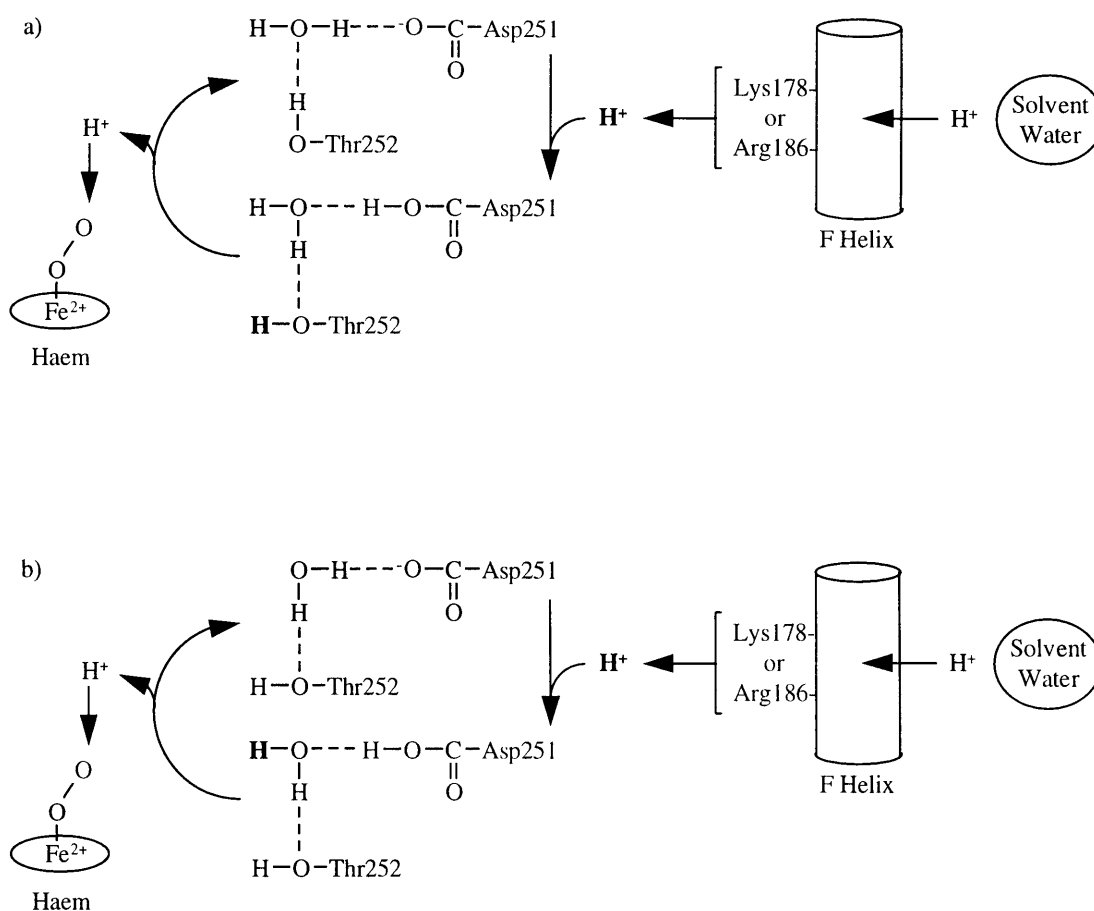


**Figure 1.5:** Proposed oxygen activation mechanism from a) Gerber and Sligar (1994) and b) Kimata *et al.* (1995). Adapted from Kimata *et al.* (1995).

for molecular oxygen (Poulos *et al.*, 1987). Several groups (Poulos *et al.*, 1985; Poulos *et al.*, 1987; Gerber and Sligar, 1994) have suggested that this conserved threonine may have a unique role in oxygen binding, activation and proton transfer during the catalytic cycle (Figure 1.5a). T252 is in a position to hydrogen bond with the iron-bound oxygen and to assist in polarisation. Input of the second electron is presumed to result in O-O bond cleavage with the formation of hydroxide ion and the iron-oxene intermediate (see Figure 1.2). As shown in Figure 1.5a), the proton transfer pathway is proposed to consist of aspartate 251 of the I helix and either lysine178 or arginine 186 of the F helix. Experiments using the unnatural amino acid O-methyl-threonine, in which the free hydroxyl group is replaced with a methoxy group, indicated that the hydroxyl group is not a pre-requisite for the O-O bond cleavage

(Kimata *et al.*, 1995). To explain the results obtained Kimata *et al.* (1995) proposed the alternative proton relay system shown in Figure 1.5b). The side chains oxygens of Thr252 and Asp251 function to keep a water molecule through hydrogen bonds and the water, instead of the hydroxyl group of Thr252, acts as the terminal proton donor for bond cleavage (Kimata *et al.*, 1995).

## **1.6 P450 BM3 from Bacillus megaterium**

### **1.6.1 General Properties of P450 BM3**

This protein was discovered during experiments designed to look for temperature-sensitive particulate preparations from *Bacillus* that would carry out the  $\Delta^5$  desaturation of palmitate. P450 BM3 (Figure 1.6) is a soluble P450-dependent monooxygenase from *Bacillus megaterium* ATCC 14581. In addition to the *b* haem moiety, P450 BM3 contains 1 molecule each of FAD and FMN per molecule of haem (Narhi and Fulco, 1986). Due to the presence of noncovalently bound FAD and FMN in its structure, P450 BM3 possesses a distinctive absorption spectrum in the 450nm to 475nm region.

Using partially purified preparations of P450 BM3 it was demonstrated that this enzyme catalyses hydroxylation (in the  $\omega$  minus 1, 2 and 3 positions) of long chain saturated and mono-unsaturated fatty acids, fatty amides and alcohols, and epoxidation and/or hydroxylation of medium chain mono-unsaturated fatty acids (Miura and Fulco, 1975; Ho and Fulco, 1976; Fulco, 1991). It is by far the most catalytically active P450 reported to date, the turnover rate is 100-1000 times higher than the rates of most P450 enzymes depending on O<sub>2</sub> and NADPH (Nahri and Fulco, 1986). With long chain fatty acids (C14-16), it exhibits a specific activity of greater than 4500 moles substrate oxygenated per mole of haem per minute.

P450 BM3 is a single polypeptide containing 1048 amino acid residues with a peptide molecular weight of 117641 Da. Narhi and Fulco (1987) showed that when the substrate-bound P450 BM3 was subjected to limited trypsin digestion, two domains were formed and these on analysis were analogous to the mammalian Class II P450

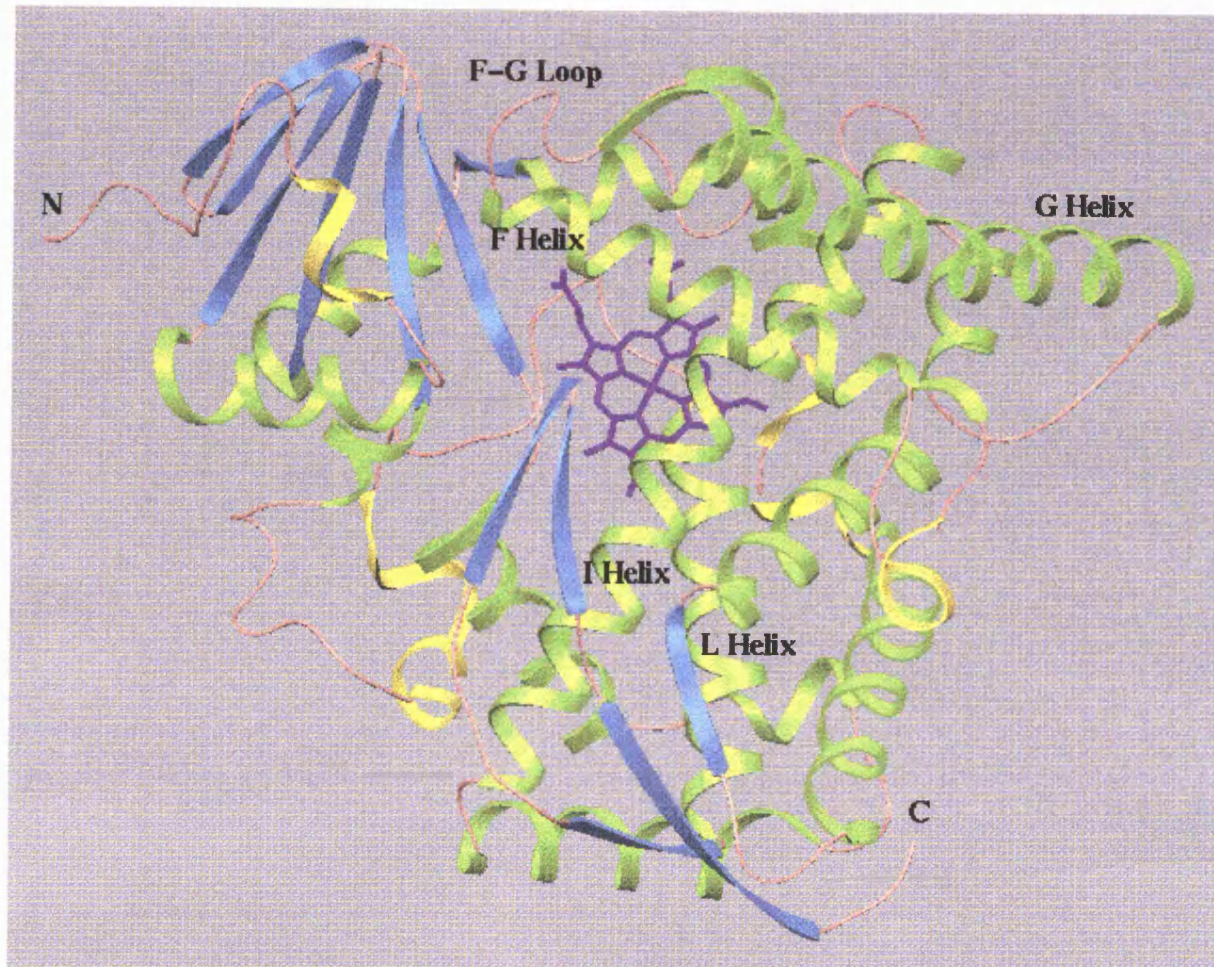


**Figure 1.6:** Schematic diagram of the haem domain of P450 BM3 from *Bacillus megaterium*. The structure reported by Ravichandran *et al.* (1993) represents residues 1-457, as no electron density is observed for the last 14 residues, suggesting that the carboxy-terminal is highly disordered. The F, G, I and L helices have been marked, as well as the F-G loop that is involved in substrate binding.

system (Figure 1.7).

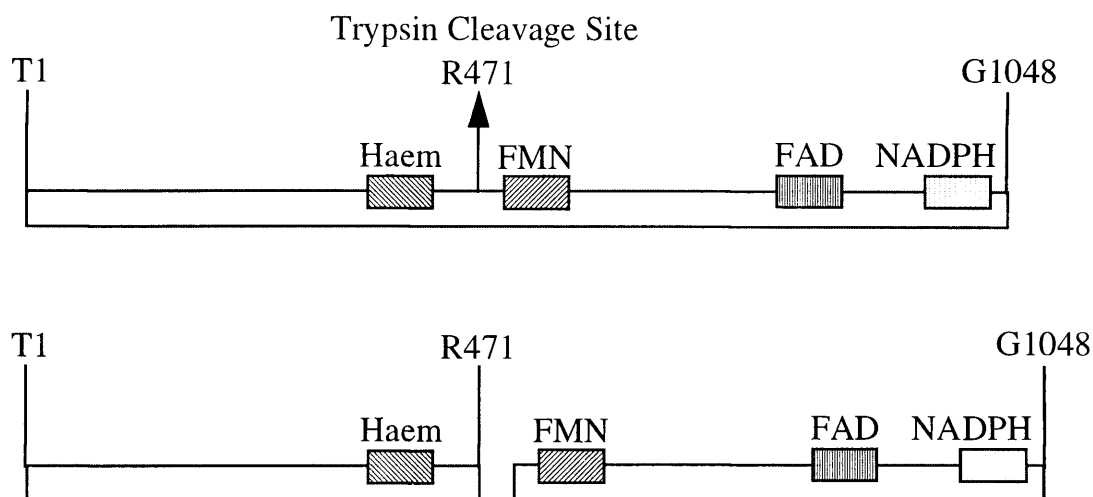


**Figure 1.7:** Schematic representation of the structure of cytochrome P450 BM3 showing the regions involved in substrate, haem, flavin and NADPH binding. The formation of separate but functional P450 and reductase domains by trypsin treatment of P450 BM3 in the presence of fatty acid is also illustrated. Adapted from Fulco, 1991.

With the N-terminal threonine of the mature polypeptide counting as residue 1, the trypsin cleavage site of P450 BM3 is between residues arginine 471 and lysine 472, generating a N-terminal “haem” domain of 471 residues of molecular mass 53220 Da retaining the haem moiety, linked to a 577 residue C-terminal “reductase” domain peptide of 63939 Da molecular mass containing both flavins and the NADPH binding site. The reductase is analogous in structure and function to mammalian NADPH dependent cytochrome P450 reductase and can function as a cytochrome c reductase as well as transferring electrons to P450 (Narhi and Fulco, 1987). On closer examination, the 53 kDa peptide, produced by trypsin digestion, constituted three haem containing peptides (TI, TII and TIII). All these peptides exhibit the characteristic spectral properties of a P450 in the presence of CO and sodium dithionite. The TI peptide binds substrate, whereas both TII and TIII cannot and were found to lack the first 9 and 15 N-terminal amino acids. It was therefore suggested that one or more of the first 9 residues of P450 BM3 were important for substrate binding.

The extent of the similarity between P450 BM3 and the mammalian Class II P450 systems was made more apparent after the gene encoding P450 BM3 was cloned and sequenced (CYP102; Ruettinger *et al.*, 1989). Subsequently expression systems for the individual domains were also developed (Li *et al.*, 1991; Oster *et al.*, 1991; Miles *et al.*, 1992). The monooxygenase activity of the intact P450 BM3 can be reconstituted using the individual domains, though the activity reported for the reconstituted system varies considerably (Boddupalli *et al.*, 1992; Miles *et al.*, 1992; Modi *et al.*, 1995a). Comparison to previously characterised P450s and reductases (Porter and Kasper, 1986; Nebert *et al.*, 1989; Porter, 1991) highlighted several regions containing highly conserved segments corresponding to regions proposed to be binding sites for the haem moiety, the flavins FMN, FAD and the coenzyme NADPH.

#### ***1.6.1.1 Induction of P450 BM3***

Cytochrome P450 BM3 has been shown to be induced as much as 100 fold by the well known mammalian P450 inducer phenobarbital, as well as by other barbiturate analogues (Narhi and Fulco, 1982, Kim and Fulco, 1983; Ruettinger *et al.*, 1984). In a study of barbiturate-mediated induction of P450 BM3, DNA was obtained that contained not only the gene for the cytochrome P450 but the regulatory region as well (Wen and Fulco, 1987). The regulatory gene, designated *bm3R1*, is located in an open reading frame immediately upstream of the P450 BM3 structural gene, encoding the protein Bm3R1, which acts as a repressor that negatively regulates the expression of the P450 BM3 gene (Shaw and Fulco, 1992). It has been postulated that the barbiturate effect in mediating the induction of P450 BM3 is such that the barbiturate interacts directly with the Bm3R1 repressor and dissociates it from its operator, allowing cotranscription of the *bm3R1* gene and P450 BM3 genes (Shaw and Fulco, 1992; Shaw and Fulco 1993). It has been suggested that the barbiturate inducers mimic an as yet unknown endogenous inducer(s) in *Bacillus megaterium* that functions by releasing the binding of the Bm3R1 repressor from its operator (Shaw and Fulco, 1993). More recently it has been demonstrated that various peroxisome proliferators

can also serve as potent inducers of P450 BM3 (English *et al.*, 1994) as well as sodium palmitate and sodium dodecyl sulphate (Shaw *et al.*, 1996).

### **1.6.1.2 The Reductase Domain of P450 BM3**

The reductase domain of P450 BM3 exhibits 33% sequence identity to the mammalian microsomal NADPH-cytochrome P450 reductase (CPR; NADPH-ferrihaemoprotein reductase, EC 1.6.2.4) even though it lacks the large, extremely hydrophobic string of residues normally found at the N-terminal region of the mammalian reductase (Ruettinger *et al.*, 1987). These proteins belong to a distinct family of flavoproteins with sites for both FAD and FMN to bind as well as a binding site for the nicotinamide cofactor, NADPH, which also includes the various isoforms of NOS. The function of the reductase is to transfer electrons from the reduced pyridine nucleotide to the haem of the P450. The sequence of electron transfer has been established to be from NADPH to FAD then to FMN via a series of internal one-electron reactions involving semiquinone intermediates (Vermillion *et al.*, 1981).

The simplest model shows the CPR enzyme to consist of three functional domains. The first domain (6kDa) is hydrophobic and located at the N-terminal of the protein, serving to anchor the molecule to the endoplasmic reticulum. This is followed by two soluble, hydrophilic catalytic domains. The first domain, of approximately 170 amino acid residues, is homologous to bacterial flavodoxins, most noticeably *Desulfovibrio vulgaris* flavodoxin, implying that this portion functions as a FMN-binding domain. The final C-terminal domain is homologous to ferredoxin-NADP<sup>+</sup> reductase and NADH cytochrome *b5* reductase (Porter and Kasper, 1986; Porter, 1991) indicating that this region binds both FAD- and NADPH. Sequence comparisons suggest that the cytochrome-P450 reductase gene arose through the fusion of the ancestral genes for flavodoxin and ferredoxin-NADP<sup>+</sup> reductase (Porter and Kasper, 1986).

The structure of rat liver CPR has been determined at 2.6Å resolution (Wang *et al.*, 1997). The overall shape of the molecule is an oval-shaped bowl that is approximately 50Å deep x 70Å wide x 60Å high and the cofactors lie in the middle of the bowl. The

structure is composed of four domains: (1) a FMN binding domain consisting of a five-stranded parallel  $\beta$ -sheet flanked by 5  $\alpha$ -helices, with the FMN positioned at the tip of the C-terminal side of the  $\beta$ -sheet, (2) a FAD binding domain, the core of which is an anti-parallel flattened  $\beta$ -barrel, (3) an NADP(H) binding domain which is another five-stranded parallel  $\beta$ -sheet sandwiched by 5  $\alpha$ -helices and (4) a connecting domain, situated between the two flavin binding domains comprising mainly of  $\alpha$ -helices (Wang *et al.*, 1997).

### **1.6.1.3 The Haem Domain of P450 BM3**

When considering the amino acid sequence of the haem domain of P450 BM3, it appears to possess 41% similarity to rat P450 3A1, 34% similarity to either P450 4A1 or P450 4A4 (both from rabbits) but only 21% similarity with P450 cam, that equates to 25% sequence identity to the microsomal P450s of Family 4 with only 15% sequence identity to P450 cam (Ruettinger *et al.*, 1989). This difference is further emphasised by the fact that P450 BM3 segregates with the eukaryotic Families 4 and 52 in the P450 phylogenetic tree (Nelson *et al.*, 1993). The sequence alignment for the haem domain consisting of the first 457 amino acids of P450 BM3 with the bacterial P450 cam (CYP101; *Pseudomonas putida*), P450 terp (CYP108; *Pseudomonas sp.*) and P450 eryF (CYP107A1; *Saccharopolyspora erythraea*), for which there are three dimensional x-ray crystal structures available and the microsomal P450 4A1 as representative of the Family 4 cytochrome P450s has been depicted in Figure 1.8. This structure-based alignment was initially performed by M. J. Sutcliffe and is based on that published by Hasemann *et al.* (1995) for various P450s. The sequences were aligned so as not to violate the conserved motifs observed in the crystal structures. Those residues within the other P450s which are identical to P450 BM3 are shown with a black background and the secondary structural elements are depicted above the first sequence. This figure shows quite clearly that P450 BM3 has a higher sequence identity with the Family 4 enzyme than with the bacterial P450s with known structure, emphasising that the structure of P450 BM3 has more in common with the mammalian P450s as opposed to those bacterial P450s.

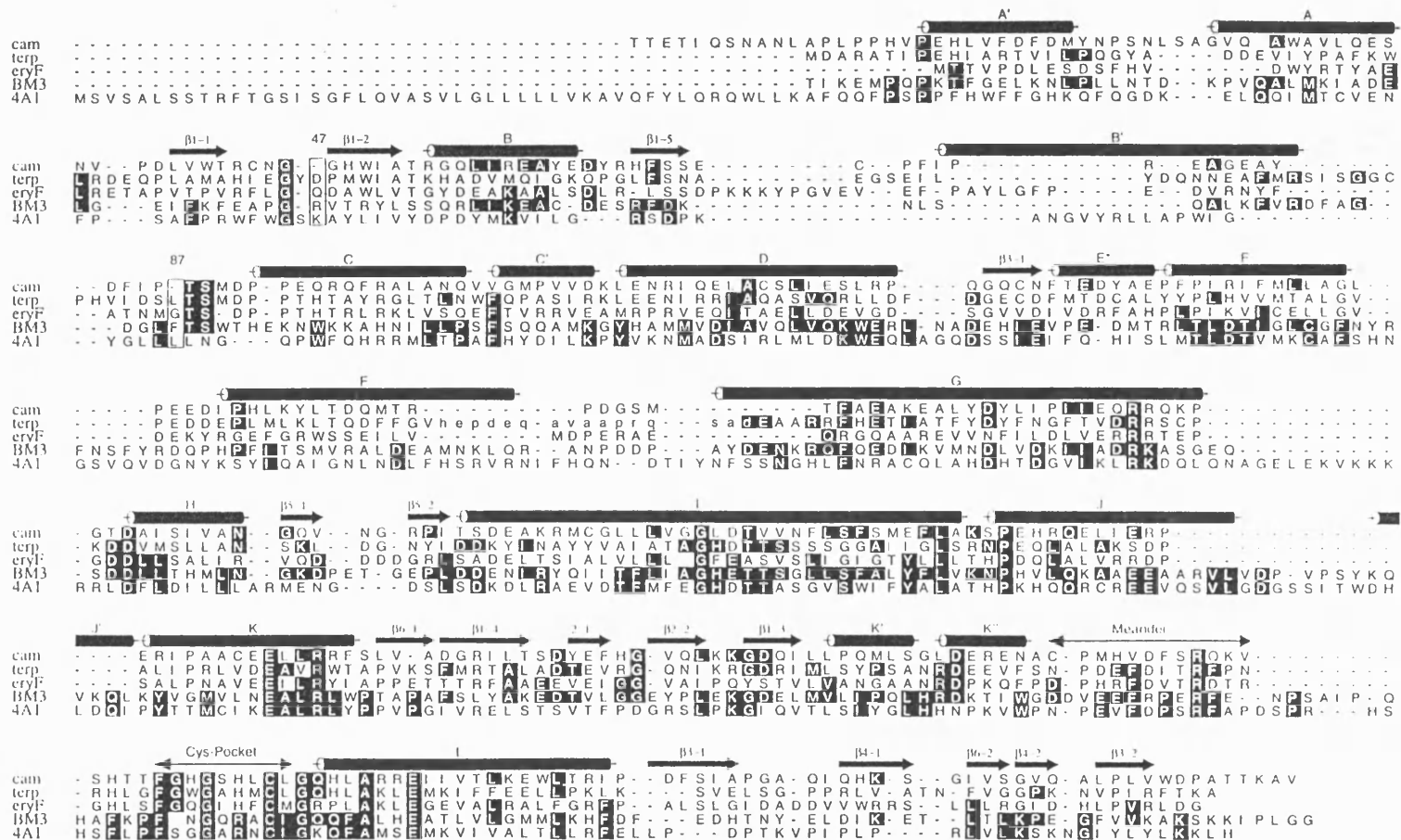


**Figure 1.8:** Sequence alignment for P450 cam, P450 terp, P450 cam, P450 eryF, P450 BM3 and P450 4A1. The figure indicates the positions of the structural elements of  $\beta$  sheet and  $\alpha$  helices relative to the sequence alignment as well as indicating were the sequences are identical to P450 BM3 by shading the relevant residues.

## ***1.6.2 X-ray Crystal Structure for the Haem Domain of P450 BM3***

In 1993, Ravichandran *et al.* published the first x-ray crystal structure for a Class II cytochrome P450, with that of the substrate-free form of the haem domain of P450 BM3 refined to 2.0Å (Figure 1.6). It was not until 1997 that the structure of the haem domain of P450 BM3 complexed with the fatty acid substrate palmitoleic acid was published (C16:Δ<sup>9</sup>; Li and Poulos, 1997). A comparison of the substrate-bound and substrate-free forms reveals major conformational differences indicating that substrate binding in P450 BM3 induces structural change.

### ***1.6.2.1 Overall Structure of the Haem Domain of P450 BM3***

The three dimensional structure of the haem domain of P450 BM3 included only residues 1 to 457, as the last 14 residues at the carboxy-terminal could not be detected, presumably due to these residues being either highly dynamic or absent through proteolytic cleavage (See Chapter 3, Section 3.4.3.3). The molecule is a triangular prism with an edge length of approximately 65Å and thickness of approximately 35Å. The structure can be conveniently split into two domains, one consisting mainly of α-helices and the other of β-sheet, referred to as the α and β domains respectively. The α-domain represents 70% and the β domain represents 22% of the structure overall. The haem is embedded between the I helix and the L helix of the α domain, with no part of it coming into direct contact with bulk solvent. As with the structures for the substrate-free P450 cam (Poulos *et al.*, 1985; Poulos *et al.*, 1986), in the substrate-free form of P450 BM3 the low spin, oxidised iron is hexacoordinated with cysteine residue 400 and either a water molecule or a hydroxide ion as the axial ligand. A comparison between the tertiary structure of P450 cam and P450 BM3 shows that the overall fold and percentages of α-helices and β-sheet of these proteins is essentially conserved, even though the amino acid sequence identity is only 16%. There are however a number of key differences that can only be appreciated on close inspection of the two structures (Poulos *et al.*, 1987; Ravichandran *et al.*, 1993). There are substantial differences between the A, B', C, G and H helices and there are two helices missing,

corresponding to  $\beta 2$  in P450 cam (Poulos *et al.*, 1987). The C-terminus of the I helix and the L helix appear to be structurally conserved. P450 BM3 has four major insertions relative to P450 cam: (1) ten residues including a  $3_{10}$  helix with flanking loops between the E and F helices, (2) 11 residues between the F and G helices which extends both helices, (3) the longest insertion of 17 residues between the J and K helices which results in elongation of the J helix by two turns and the formation of a new helix, J' and (4) seven residues centred around isoleucine 385 which consists of two  $3_{10}$  helices. There are no deletions in P450 BM3 relative to P450 cam, suggesting that P450 cam represents a minimal structure (Ravichandran *et al.*, 1993). There are some structural modifications within the other elements of the P450 BM3 structure. The C helix is followed by the D helix which is shortened in P450 BM3 by nine residues and is replaced by two  $3_{10}$  helices at the C-terminal end, which have been implicated in a putative docking site for the reductase domain in the intact P450 BM3 (Ravichandran *et al.*, 1993). The last difference between the P450 crystal structures of P450 BM3 and P450 cam resides in the 50Å long I helix. A conserved threonine residue in the I helix, threonine 252 (T252) in P450 cam and threonine 268 (T268) in P450 BM3, has been implicated in O<sub>2</sub> binding and is thought to be important in O<sub>2</sub> activation during the P450 catalytic cycle (Poulos *et al.*, 1987; Imai *et al.*, 1989; Martinis *et al.*, 1989). With the substrate-bound P450 cam it was proposed that the role of the I helix disruption around the T252 is to form a pocket adjacent to the axial ligand such that O<sub>2</sub> can bind to the haem iron, as discussed in more detail in Section 1.5.2. In the substrate-free enzyme, this pocket is thought to contain a water molecule (Poulos *et al.*, 1986). In P450 BM3, the I helix distortion is located within the next turn of the helix, where the O $\gamma$  of threonine 268, instead of its amide nitrogens, forms a hydrogen bond with the carbonyl oxygen of alanine 264. This pocket is however occluded by the carbonyl oxygen from alanine 264 (A264), which is hydrogen bonded to both the water axial ligand and the conserved threonine (Ravichandran *et al.*, 1993; Hasemann *et al.*, 1995).

### **1.6.2.2 The Substrate Binding Pocket**

The substrate binding pocket, depicted in Figure 1.9, provides access to the active site

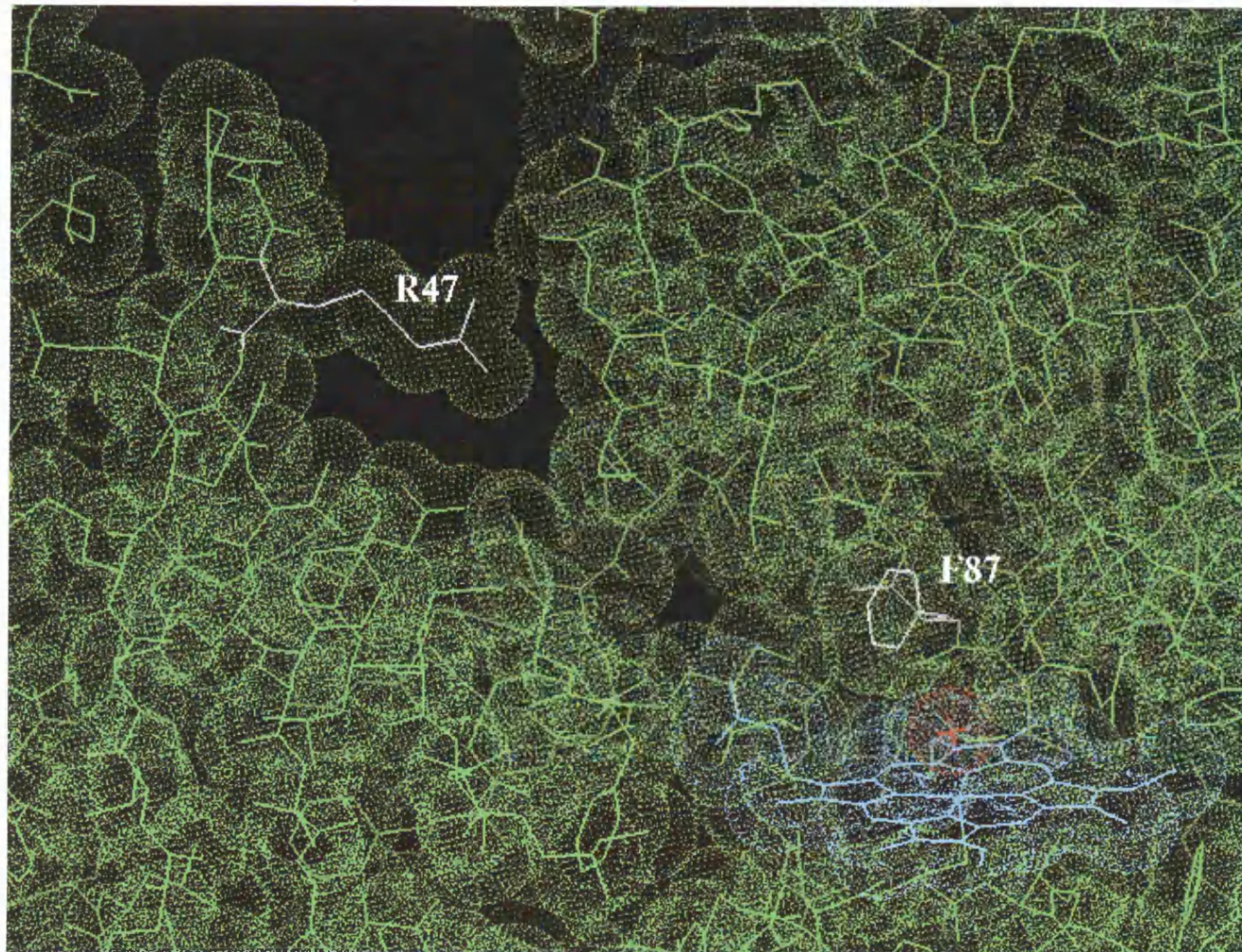


**Figure 1.9:** Van der Waals surface of the substrate binding pocket of the haem domain of cytochrome P450 BM3 from *Bacillus megaterium*. The cone shaped substrate binding pocket runs diagonally across the figure toward the active site haem at the bottom of the picture. The residue side chains for arginine 47 and phenylalanine 87 have also been highlighted (Ravichandran *et al.*, 1993).

located by the haem moiety. This access takes the form of a long hydrophobic channel approximately 8Å to 10Å in diameter and 20Å in length and is defined by  $\beta$ -sheet 1, residues 14 to 25 of the  $\beta$  domain and the B' helix, F helix and  $\beta$ -sheet 4 of the  $\alpha$  domain. This funnel shaped channel is mainly lined with mostly hydrophobic residues such as phenylalanine 42, tyrosine 51, leucine 181, methionine 185, leucine 188, alanine 328, alanine 330 and methionine 354. The solvent exposed hydrophobic residues of leucine 14, leucine 17, proline 45 and alanine 191 may be important as a substrate docking region (Ravichandran *et al.*, 1993).

### ***1.6.2.3 Important Residues Within the Substrate Binding Pocket***

The substrate-free structure highlighted the residues arginine 47 (R47) and phenylalanine 87 (F87) which appear to be important in substrate recognition. The open end of the substrate binding pocket, close to the molecule surface is flanked by the side chain of R47. The side chain of this residue is not well defined and it has been suggested that the guanidinium group may be involved in the binding of different length fatty acids (Ravichandran *et al.*, 1993; Graham-Lorence *et al.*, 1994). The aromatic ring of F87 forms close van der Waals force interactions with the haem on the distal side and is perpendicular to the plane. This residue could be important in forming the lipophilic pocket mentioned earlier involved in sequestering the  $\omega$ -end of a fatty acid, which is not hydroxylated by the enzyme (Ravichandran *et al.*, 1993).

### ***1.6.2.4 Comparison of the Open and Closed Conformations of the Substrate Access Channel of the Haem Domain of P450 BM3***

Of the known P450 structures, three, that is P450 cam, P450 eryF and P450 BM3 have been solved in the substrate-bound form (Poulos *et al.*, 1987; Li and Poulos, 1997; Cupp-Vickery and Poulos, 1995). Of these, only P450 cam and P450 BM3 have been solved in both the substrate-free and substrate-bound forms (Poulos *et al.*, 1986; Poulos *et al.*, 1987; Ravichandran *et al.*, 1993; Li and Poulos, 1997). The substrate-bound structures show that the substrate access channel is closed making it too small to allow substrate entry. This therefore suggests that there must be an opening motion of

the channel to allow access, though with P450 cam and P450 eryF this has yet to be demonstrated. In contrast the structure of the haem domain of P450 BM3 in the substrate-free form shows that the substrate access channel is open (Ravichandran *et al.*, 1993; Li and Poulos, 1995). Furthermore, two independent molecules within the crystal lattice exist which exhibit large differences around the substrate binding channel such that the binding pocket in molecule 2 is in a more open conformation than molecule 1. Attempts to solve the substrate-bound complex by soaking substrate-free crystals in a solution containing substrate either had no effect on the structure or lead to crystal cracking. This and energy minimisation and molecular dynamic simulations suggest that the access channel can undergo a large opening and closing motion (Li and Poulos, 1995; Paulsen and Ornstein, 1995). The successful crystallisation of P450 BM3 bound with the substrate palmitoleic acid allowed comparison of the open and closed conformations (Li and Poulos, 1997).

A comparison between the substrate-free and the substrate-bound structures (Figure 1.10) showed that the largest changes occurred around the F and G helices and the loop that connects them. This F-G loop forms one side of the access opening channel, while  $3_{10}$  helix (residues 16-20) and the  $\beta$ -sheet containing arginine 47 forms the other. These regions move closer together on substrate binding resulting in closure of the access channel and new intramolecular contacts. This is also accompanied by ordering of the F-G loop, which is not so well resolved in the substrate-free enzyme. The majority of conformational changes involving ordered elements of the secondary structure are as a result of the repositioning of the F and G helices. The other areas of movement on substrate binding extend to the G/H helices loop, the H helix and all the way to the I helix. The I helix in both the substrate-free and substrate-bound crystal structure is well ordered such that  $1\text{\AA}$  changes between the substrate-free and substrate-bound forms is significant (Li and Poulos, 1997). In the substrate-bound structure of P450 BM3, the axial water ligand is displaced so that A264 is no longer restricted by the water ligand hydrogen bond. This results in a movement of A264 of about  $1\text{\AA}$  away from the iron which creates sufficient room near the iron for  $\text{O}_2$  to bind and the T268 region in the complex now resembles the P450 cam-substrate complex (Li and Poulos, 1997).

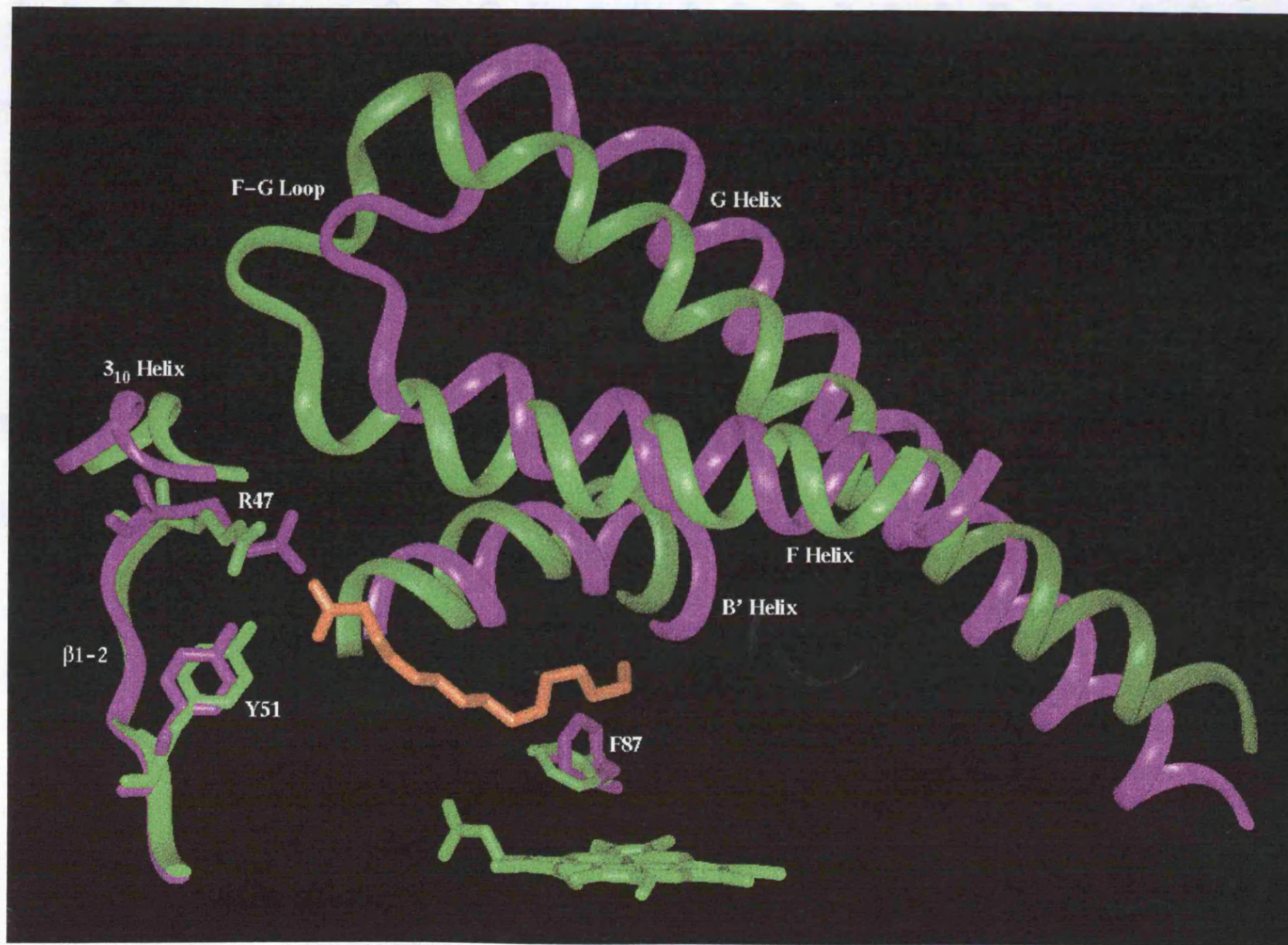


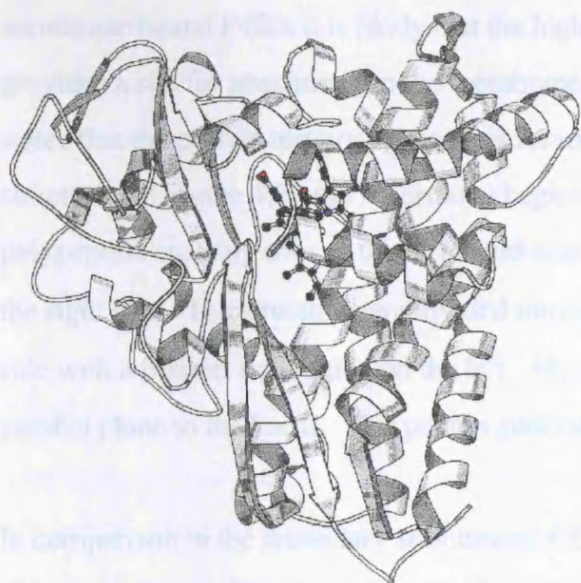
**Figure 1.10:** A comparison of selected regions between the substrate-free (purple) and substrate-bound (green) structures, in the presence of the substrate, palmitoleic acid (orange).

### ***1.6.3 Significance of the P450 BM3 Crystal Structure with Regard to Cytochrome P450s in General***

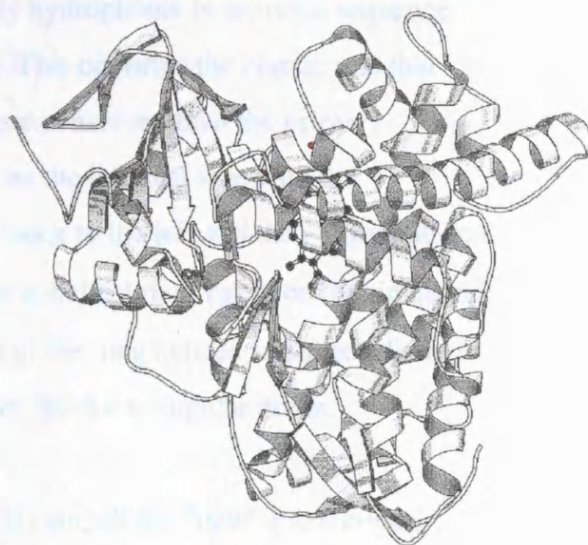
Homology modelling has been used by various groups to generate three dimensional models for P450s other than those for which an x-ray crystal structure already exists (Lewis, 1995; Lewis and Lake, 1995; Modi *et al.*, 1996a). The publication of the crystal structure of P450 BM3 has permitted the derivation of more accurate models of mammalian P450s which previously had to rely on the structure of P450 cam as a model template. This is due to the increased sequence identity and presumed structural homology of P450 BM3 with the mammalian P450s. Consequently the key functional and structural residues are more highly conserved, by about 90% between P450 BM3 and microsomal P450s, than by using the P450 cam model which exhibits approximately 80% conservation. The P450 cam model also has about 50 amino acid residues missing from the aligned P450 cam sequence and only the membrane-anchoring N-terminal stretch of approximately 20 residues is unmatched between the cytosolic prokaryotic P450 BM3 and the membrane bound microsomal P450s (Lewis and Lake, 1995). P450s modelled to date include: P450 1A1 and P450 1A2 (Lewis, 1995), P450 2A1, P450 2A4, P450 2A5, and P450 2A6, isoenzymes of the 2A Family (Lewis and Lake, 1995), P450 2B1 (Szklarz *et al.*, 1995), P450 2B6 and P450 2C9 (Lewis, 1995), P450 2D6 (de Groot *et al.*, 1996; Modi *et al.*, 1996), P450 3A4, P450 4A4 and P450 4A11 (Lewis, 1995), P450 arom (CYP19; Amarneh *et al.*, 1993; Graham-Lorence *et al.*, 1995) and P450 choP (CYP105C1; Chang and Loew, 1996).

### ***1.7 Comparison of All Known Cytochrome P450 Structures***

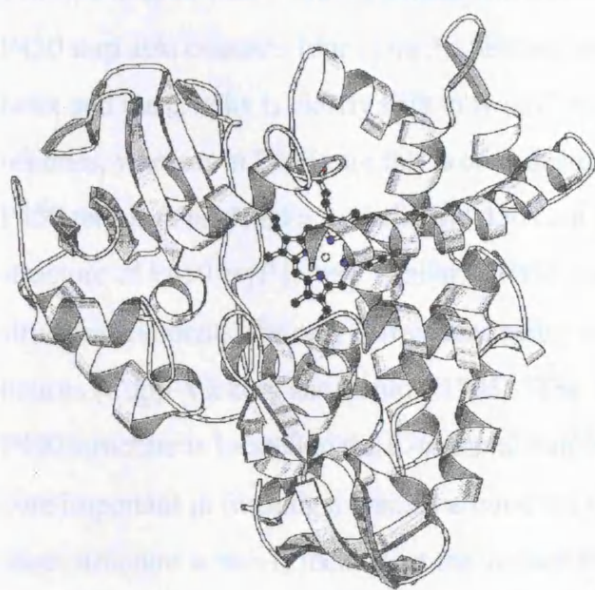
Three dimensional crystal structures have been solved for P450 cam and the haem domain of P450 BM3, as already discussed, as well as for P450 terp from *Pseudomonas sp.* (Hasemann *et al.*, 1994) and P450 eryF from *Saccharopolyspora erythraea* (Cupp-Vickery and Poulos, 1995) and these are depicted in Figure 1.11. The most important observation to arise from these structures is that they all possess the same overall fold and topology despite having low sequence identities of less than 20% (See Figure 1.8). Therefore it seems likely that all cytochrome P450s, including



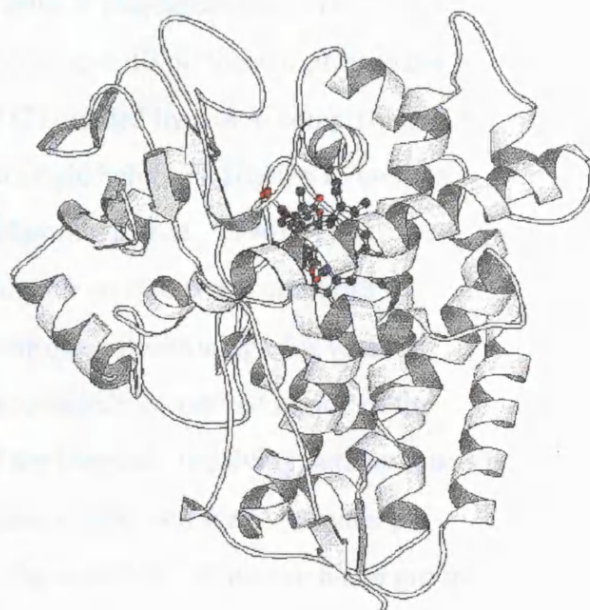
P450 cam



P450 BM3



P450 terp



P450 eryF

**Figure 1.11:** Schematic diagrams for P450 cam, the haem domain of P450 BM3, P450 terp and P450 eryF. The diagrams for P450 cam and P450 eryF are depicted with substrate bound. These diagrams obtained from the P450 World Wide Web site at <http://www.icgeb.trieste.it/p450>.

those which are membrane bound, share this overall structure. With the case of the membrane bound P450s it is likely that the highly hydrophobic N-terminal sequence provides a site for attachment to the membrane. This confirms the classic rule that states that the protein tertiary structure is far more conserved than the primary structure. In Figure 1.11 the N-terminal begins on the lefthand side with the polypeptide crossing over to the righthand side, back to the left and then terminates on the right side. The structures are divided into an  $\alpha$ -helical rich region on the righthand side with a  $\beta$ -sheet rich region on the left. Most of the long helices and sheets lie in a parallel plane to the haem. This pattern generates the flat triangular prism.

In comparison to the secondary structure of P450 cam, all the “new” P450 crystal structures show differences in the number and form of structural elements. The differences between P450 BM3 and P450 cam have already been described. Briefly they involve two  $\beta$  strands missing, corresponding to  $\beta$ 2 in P450 cam (Poulos *et al.*, 1987), a total of four extra  $3_{10}$  helices and a new helix, J' (Ravichandran *et al.*, 1993). P450 terp also contains four extra  $3_{10}$  helices, an extra  $\alpha$ -helix A' located prior to the A helix and the C helix is clearly split in two (C and C') divided by a loop comprising of 5 residues, whereas in P450 cam this is considered a single helix. Finally the K' helix in P450 terp is considered a  $3_{10}$  helix in P450 cam (Hasemann *et al.*, 1994). The overall structure of P450 eryF is very similar to P450 cam with no significant additions of structural elements, the only differences being in the exact positioning of several  $\alpha$ -helices (Cupp-Vickery and Poulos, 1995). The most highly conserved region of the P450 structure is located in the C-terminal half of the molecule involving both an inner core important in forming a bracket around the haem moiety and the C-terminal  $\beta$ -sheet structure which is located on the surface of the molecule. When the haem groups for the crystal structures are overlaid, the conserved “core structure” which spans both the domains can be readily identified. The most highly conserved structures are a four helix bundle consisting of helices D, I, L and the anti-parallel helix E, helix J and K,  $\beta$ -sheets 1 and 2, the haem-binding region and the 14 amino acid “meander” just N-terminal of the haem-binding region (Graham-Lorence and Peterson, 1996a). The backbone hydrogen bonding of the I helices in the immediate vicinity of the haem moiety deviates from the normal  $\alpha$ -helical pattern in all the P450 crystal structures.

With the exception of P450 eryF this distortion is centred around a threonine residue; T252 in P450 cam, T268 in P450 BM3 and T271 in P450 terp. P450 eryF has an alanine (A245) in the position homologous to T252 in P450 cam. The local distortion in the I helix is stabilised by a network of hydrogen bonds involving the side chains of two nearby residues and three ordered water molecules. Glutamic acid 360 stabilises the distortion by hydrogen bonding with the carbonyl of glycine 242 through a water molecule and the side chain of serine 246 (Cupp-Vickery and Poulos, 1995).

The N-terminal half of the P450s is less well conserved than the protein core. It has been suggested that the regions that show the greatest structural difference are involved in substrate recognition and binding and those involved in redox partner binding (Graham-Lorence and Peterson, 1996b). These elements require more flexibility and would therefore be subject to greater topological variability as they would incorporate a greater number of amino acid substitutions for the specific purpose of altering substrate specificity without affecting haem binding (Poulos *et al.*, 1987). It is worth noting that a substrate access channel is apparent in P450 BM3, P450 eryF and P450 terp but there is no evidence of one in P450 cam. In each of the P450 structures the active site is composed of residues from the B-B' loop ( $\beta$ 1-5 in P450 BM3), the B'-C loop,  $\beta$ 1-4,  $\beta$ 4, the top of the F helix in P450 eryF and a portion of the I helix (Graham-Lorence and Peterson, 1996b). There are many differences between the four crystal structures, though the most dramatic is the rotation of the B' helix. In P450 BM3 and P450 terp the B' helix is rotated approximately 90° about the helical axis relative to P450 cam with the helical axis parallel to the haem plane, whereas in P450 eryF the B' helix axis is nearly perpendicular to haem plane. This movement of the B' helix may be required to enlarge the active site and may be critical in the binding of bulky substrates (Cupp-Vickery and Poulos, 1995). The antiparallel F and G helices vary greatly in length and position within all the P450 structures and the F-G loop, which has major insertions in both the structures for P450 BM3 and P450 terp, is highly flexible and therefore does not occupy a single conformation. It has been suggested that the F-G loop may act as a flexible flap or lid over the substrate access channel (Graham-Lorence and Peterson, 1996b).

The last residues to be considered are those on the proximal face of the P450 proteins, those postulated to be involved in the binding of the redox partner. These include the B, C, J, J', K, and L helices as well as the carboxy-terminal of the meander and the haem-binding region involved in redox partner binding (Graham-Lorence and Peterson, 1996b). The shape of the putative docking region is similar in P450 cam and P450 terp, but different in P450 BM3. This is not unexpected as both P450 cam and P450 terp are Class I P450s binding small iron sulphur proteins and P450 BM3 is a Class II protein binding a NADPH-dependent P450 reductase. The redox partner binding surface is relatively flat for the Class I P450s with four positively charged residues near the centre, whereas for P450 BM3 the region is like a bowl containing almost exclusively hydrophobic and aromatic residues surrounded by numerous negatively and positively charged residues (Hasemann *et al.*, 1995; Graham-Lorence and Peterson, 1996b).

### ***1.8 Overall Aims and Objectives of the Work Described in this Thesis***

Mutational and kinetic studies were performed to explore the structure and functional relationship of the *Bacillus megaterium* P450 BM3. These studies centred on arginine 47 and phenylalanine 87, the two residues highlighted in the crystal structure of the haem domain of P450 BM3, in an attempt to further define their role within the active site with regard to substrate specificity and the catalytic mechanism of the enzyme.

## ***Chapter 2: Materials and Methods***

### ***2.1 Chemicals and Reagents***

Deuterated methanol, dodecyltrimethylammonium bromide, ferrous ammonium sulphate, hexadecyltrimethylammonium bromide, hydrogen peroxide iodopropionic acid, tetradecyltrimethylammonium bromide and potassium thiocyanate were obtained from Aldrich Chemical Co. *EcoR* I and *BamH* I, with their respective buffers E4 and E6, were purchased from Amersham. Dye Deoxy Terminator solution was obtained from Applied Biosystems Ltd (via K. S. Lilley). Ammonium persulphate, Chelex 100 and hydroxyapatite resin were purchased from Bio Rad Ltd. T4 polynucleotide kinase was purchased from Cambio. Deuterium oxide (99.9% and 99.96%) and 99% deuterated methanol were purchased from Goss Scientific Instruments Ltd. Protogel was supplied by Flowgen Instruments Ltd.

Low melting point agarose, restriction enzymes *EcoR* I, *Kpn* I and *Xba* I and sodium dodecylsulphate were purchased from Gibco BRL Ltd. Isopropyl- $\beta$ -D-thiogalactopyranoside and 5-bromo-4-chloro-3-indolyl-galactopyranoside were purchased from NovoChem. 2', 5'-ADP sepharose, DEAE sephadex, Microspin S200 HR, NAP5 and PD10 columns and sephacel S300 were purchased from Pharmacia LKB Ltd.

DNA Magic Minipreps column, DNA Magic Minipreps DNA purification resin and lambda/*Hind* III DNA molecular weight markers were purchased from Promega.

Adenosine 2'-monophosphate, ampicillin, benzamidine HCl, brilliant blue G250, brilliant blue R, DEAE sephadex, dimethylformamide, dimethylsulphoxide, dithionitrobenzoate, dithiothreitol, deoxyribonuclease I, glycerol, guanidine hydrochloride, iodoacetic acid, lambda/*Hind* III DNA molecular weight marker, lauric acid sodium salt, lysozyme, mineral oil, myristic acid sodium salt,  $\beta$ -nicotinamide adenine dinucleotide phosphate (both oxidised and reduced form) tetrasodium salt, N, N, 'N, 'N-tetramethylethylenediamine, palmitic acid sodium salt, phenylmethylsulphonyl fluoride, polyethylene glycol, protein high molecular weight markers, ribonuclease A,

dodecyl-, tetradecyl- and hexadecyl-trimethylammonium bromide were purchased from Sigma Chemical Co.

The helper phage VSCM13, used in the production of single stranded plasmid DNA was obtained from Stratagene. Agar bacterial (Agar No. 1), bactotryptone and yeast extract were supplied by Unipath Ltd.

All other chemicals used were purchased from either Sigma Chemical Co. or Fisher Ltd and were at least of analytical grade.

## 2.2 Bacterial Strains

For all DNA manipulations the *E. coli* host strains used were either TG1 with genotype of *supE*, *hsd* $\Delta$ 5, *thi*,  $\Delta$ (*lac*<sup>-</sup> *proAB*), F' [*traD36 proAB*<sup>+</sup> *lacI*<sup>q</sup> *lacZ* $\Delta$ M15] or DH5 $\alpha$  with genotype of F-,  $\phi$ 80*dlacZ* $\Delta$ M15, *recA1*, *endA1*, *gyrA96*, *thi-1*, *hsdR17* (*r<sub>k</sub>*<sup>-</sup>, *m<sub>k</sub>*<sup>+</sup>), *supE44*, *relA1*, *deoR*,  $\Delta$ (*lacZYA-argF*)U169. XL1 Blue, with the genotype *supE44*, *hsdR17*, *recA1*, *endA1*, *gyrA46*, *thi*, *relA1*, *lac*<sup>-</sup> F' [*proAB*<sup>+</sup> *lacI*<sup>q</sup> *lacZ* $\Delta$ M15 *Tn10* (*tet*<sup>r</sup>)] and TG1 were the bacterial strains used for protein expression. All *E. coli* host strains were maintained using glucose minimal media plates to select for the F' episome.

## 2.3 Expression Plasmids

All the expression vectors in *E. coli* host strain XL Blue 1 were obtained as a gift from Dr J. S. Miles, Department of Biochemistry, University of Glasgow, Glasgow, UK.

The three P450 BM3 expression systems are (Figure 2.1):

- 1) The entire *CYP102* gene obtained from genomic DNA, encoding cytochrome P450 BM3 from *Bacillus megaterium*. The gene, known to reside on a 4,957bp *Bgl* II fragment, was cloned into the *Bam*H I site of pUC119 (Vieira and Messing, 1987) to give pJM23.
- 2) A 1.5 kbp fragment from the *CYP102* gene was amplified, introducing a stop codon

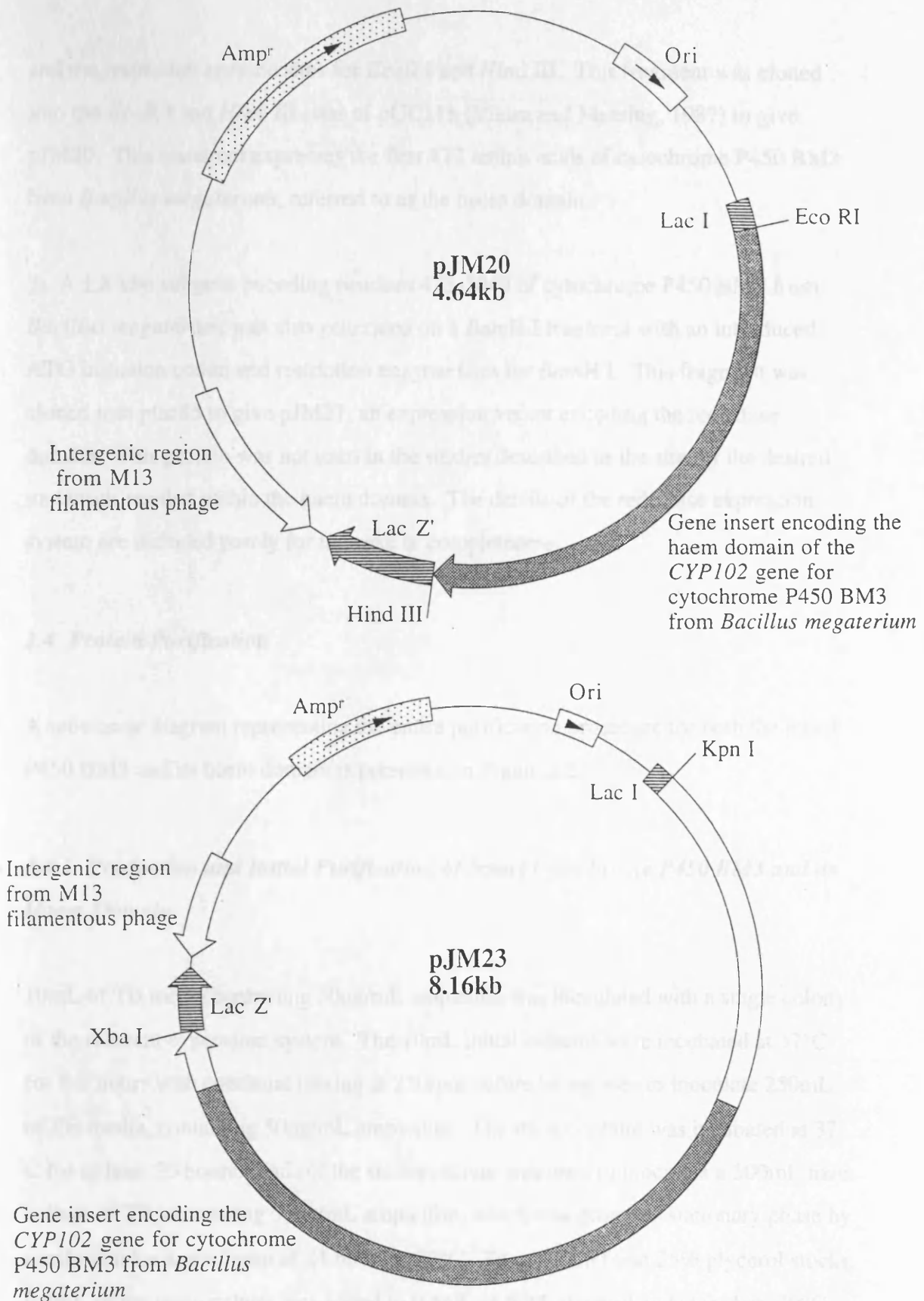


**Figure 2.1:** Schematic structural representation of the expression vectors pJM20 and pJM23 used in site-directed mutagenesis experiments. The regions encoding the open reading frames for the haem domain of P450 BM3 and the intact enzyme respectively are under the control of the lac promoter which is heavily shaded.

and the restriction enzyme sites for *EcoR* I and *Hind* III. This fragment was cloned into the *EcoR* I and *Hind* III sites of pUC118 (Vieira and Messing, 1987) to give pJM20. This construct expresses the first 472 amino acids of cytochrome P450 BM3 from *Bacillus megaterium*, referred to as the haem domain.

3) A 1.8 kbp subgene encoding residues 473-1049 of cytochrome P450 BM3 from *Bacillus megaterium* was also generated on a *Bam*H I fragment with an introduced ATG initiation codon and restriction enzyme sites for *Bam*H I. This fragment was cloned into ptac85 to give pJM27, an expression vector encoding the reductase domain. This protein was not used in the studies described as the site for the desired mutations resided within the haem domain. The details of the reductase expression system are included purely for the sake of completeness.

## **2.4 Protein Purification**

A schematic diagram representing the entire purification procedure for both the intact P450 BM3 and its haem domain is presented in Figure 2.2.

### **2.4.1 Production and Initial Purification of Intact Cytochrome P450 BM3 and its Haem Domain**

10mL of TB media containing 50µg/mL ampicillin was inoculated with a single colony of the relevant expression system. The 10mL initial cultures were incubated at 37°C for 8-9 hours with continual mixing at 250rpm before being used to inoculate 250mL of TB media, containing 50µg/mL ampicillin. The starter culture was incubated at 37°C for at least 20 hours. 5mL of the starter culture was used to inoculate a 500mL main culture of TB, containing 50µg/mL ampicillin, which was grown to stationary phase by incubation for a minimum of 24 hours at 37°C. To maintain fresh 25% glycerol stocks, 0.5mL of the main culture was added to 0.5mL of 50% glycerol and stored at -70°C. The main cultures for the pJM20 expression system, that is, the expression system for the haem domain of cytochrome P450 BM3 also included 0.5mL of 0.2M IPTG prior to inoculation with the starter culture.

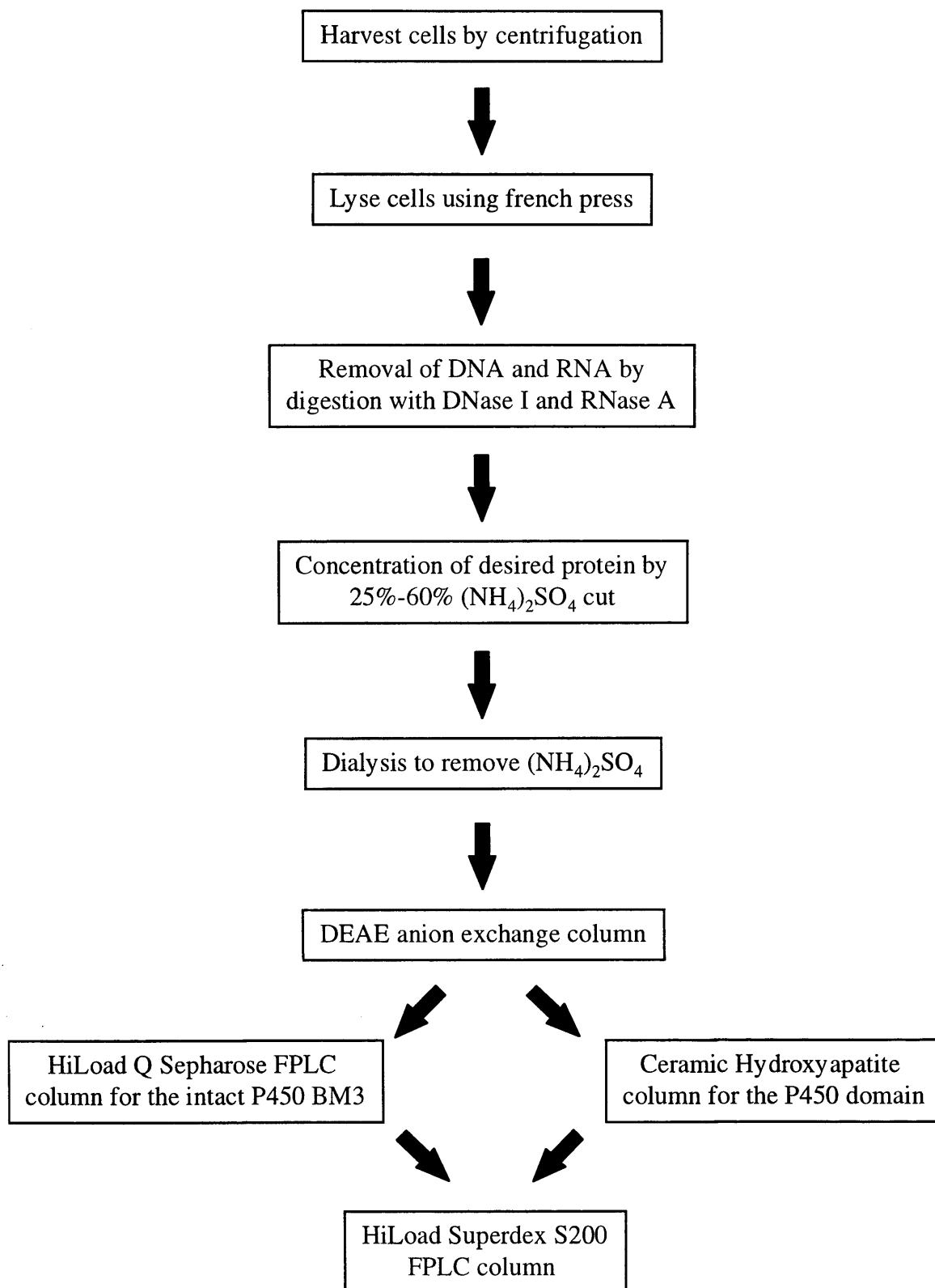


**Figure 2.2:** Schematic diagram depicting the purification of intact P450 BM3 and its haem domain.

All the following procedures were carried out at 4°C when possible. The cells were harvested by centrifugation of the main culture media at 10000rpm for 15 minutes. The supernatant was removed and the pellets washed with buffer A (See the Appendix, Section A1 for the contents of all buffers and solutions used) before freezing at -20°C. The pellets were thawed at 4°C and resuspended in 3 volumes of buffer A. The resuspended cells were broken by passage twice through a French Press (2.5cm id x 17cm, Power Laboratory Press, American Instrument Co. Inc.) before centrifugation at 35000rpm for 1 hour. The supernatant, saved as the “cell free extract”, was incubated at 37°C for 45 minutes with 0.5mL of 10mg/mL solutions of DNase I and RNase A, to degrade any nucleic acids present. The resulting solution was subjected to ammonium sulphate precipitation, collecting the 25-60% ammonium sulphate pellet. This pellet was dialysed extensively into buffer A before loading onto a DEAE-sephadex ion-exchange column which had been pre-equilibrated with buffer A. The protein was eluted using a linear gradient of 0.1-0.5M KCl in buffer A. Fractions which had an absorbance ratio  $A_{418}/A_{280nm}$  greater than 0.5 for intact P450 BM3 and a ratio greater than 1.0 for its haem domain were pooled and retained for further purification.

#### **2.4.2 Further Purification of Intact P450 BM3**

The retained fractions from DEAE-sephadex purification were dialysed into FPLC buffer before concentration using a 30 kDa molecular weight cut off (MWCO) dialysis membrane in an Amicon Stirred Cell. The concentrated sample was loaded onto a HiLoad 26/10 Q sepharose high performance column attached to a Pharmacia LKB FPLC system and eluted using a linear gradient of 250-450mM KCl in FPLC buffer. Fractions with an absorbance ratio  $A_{418}/A_{280nm}$  greater than 0.6 for intact P450 BM3 were pooled, dialysed against either buffer A, if using the standard chromatography gel filtration column, or FPLC buffer, if finishing purification using the FPLC system. The protein was concentrated before the final purification step of gel filtration using either a sephacel S300 (2.6cm id x 100cm) or a HiLoad 26/60 Superdex 200 prep grade FPLC column. The absorbance ratio  $A_{418}/A_{280nm}$  of intact P450 BM3 should be 0.7 for pure protein. After the protein was verified as pure by SDS-PAGE analysis as detailed in Section 2.4.4, it was stored in buffer A containing 50% glycerol at -20°C.

### ***2.4.3 Further Purification of the Haem Domain of Cytochrome P450 BM3***

The retained fractions from DEAE-sephadex purification were dialysed into buffer HA before concentration using a 30 kDa MWCO dialysis membrane in an Amicon Stirred Cell. The concentrated sample was loaded onto a pre-equilibrated ceramic hydroxyapatite column (3cm id x 28.5cm) and eluted with a linear gradient of 25-450mM potassium phosphate. Fractions with an absorbance ratio  $A_{418}/A_{280\text{nm}}$  greater than 1.2 were pooled, dialysed into either buffer A or FPLC buffer and concentrated as before. The haem domain was finally purified to homogeneity by gel filtration using either a sephacel S300 (2.6cm id x 100cm) or a HiLoad 26/60 Superdex 200 prep grade FPLC column. The absorbance ratio  $A_{418}/A_{280\text{nm}}$  should be at least 1.55, though preferably 1.7 for pure protein. The verified pure haem domain was stored in buffer A containing 50% glycerol at -20°C.

### ***2.4.4 Protein Analysis by SDS-PAGE***

Protein samples were analysed for purity by SDS-PAGE using a Bio Rad Protean II Mini PAGE gel apparatus. Samples were loaded onto a 3% stacking gel above a 8% separating gel, as described in appendix A1. The gel was run at 100V for approximately 1.5 hours or until the bromophenol blue dye front was at the bottom of the separating gel. After carefully disassembling the gel apparatus, the gel was immersed in SDS-PAGE coomassie blue stain solution for 1 hour followed by SDS-PAGE destain for 2 hours or sufficient time for complete destaining of the gel. The destain was removed and the gel stored in 6% acetic acid until it was dried on a Bio Rad Model 583 Gel Dryer for 45 minutes at 80°C.

## ***2.5 Mass Spectroscopy and N-Terminal Sequencing***

Mass spectroscopy was performed on intact P450 BM3 and its haem domain using both electrospray ionisation and Matrix Assisted Laser Desorption Ionisation (MALDI) sampling devices. Protein samples for electrospray ionisation were dialysed into water and diluted 2 fold using HPLC grade acetonitrile containing 0.2% trifluoroacetic acid

(TFA), resulting in 50% (v/v) water and 50% (v/v) acetonitrile with 0.1% TFA. 10 $\mu$ L of sample was loaded into a mobile phase of 1:1 v/v acetonitrile:water. For MALDI analysis, samples were dialysed into water and diluted 2 fold using saturated sinapinic acid (70:30 v/v water:methanol). 2 $\mu$ L of sample was loaded. Mass spectroscopic analysis was performed by J. H. Lamb and G. M. A. Sweetman using either a Fisons Quatro B. Q., Tandem Quadrupole Instrument with Electrospray Ionisation or a Fisons T. O. F., MALDI Time of Flight Mass Spectrometer.

The N-terminal sequences of protein samples of intact P450 BM3 and its haem domain in 0.1M sodium bicarbonate were determined by gas-phase microsequencing.

Sequencing was performed by E. A. Cavanagh and K. S. Lilley using an Applied Biosystems 476A Protein Sequencer.

## ***2.6 Chemical Modification of Free Protein Thiols***

Chemical modification of the accessible free thiols of the wild type and R47C mutant intact P450 BM3 and its haem domain was performed at room temperature using the chemical modifying agents iodoacetic and iodopropionic acid. Adventitious oxidation of the thiols was avoided by purifying and storing the protein sample using buffer A, containing 0.2mM DTT. Prior to chemical modification the proteins were transferred into enzyme assay buffer using a PD10 column. The modifying agent was added in a 20 fold molar excess over the protein and mixed thoroughly. After 10 minutes incubation the modification reaction was stopped by addition of a 40 fold molar excess of  $\beta$ -mercaptoethanol. Excess  $\beta$ -mercaptoethanol and the conjugated excess modifying agent and  $\beta$ -mercaptoethanol mixture was removed using either a NAP5, NAP10 or PD10 column depending on the volume of protein modified.

## ***2.7 Ellman Assay for Free Thiols***

The Ellman assay (Ellman, 1959) measures the amount of nitrothiobenzoate (NTB) released upon reaction of a thiol with dithionitrobenzoate (DTNB) by monitoring the absorbance at 412nm, from which the number of free thiols present in a protein can be

calculated. The assay was performed at 25°C, both in the absence and the presence of 6M guanidinium chloride, which denatures the protein to allow all thiols present within the protein to react with the DTNB

A known concentration of protein was added to 0.1M phosphate buffer, pH 8 such that the final volume was 1mL and its absorbance at 412nm measured against a reference that contained only buffer. 50µL of 3mM DTNB was added to each cuvette and thoroughly mixed. The absorbance difference between the sample and reference cuvette was monitored for up to 30 minutes, until there was no further increase in the absorbance at 412nm. From the increased absorbance the molar concentration of thiol was calculated from the molar absorbance of the NTB anion that has an  $\epsilon_{412}=13700 \text{ M}^{-1} \cdot \text{cm}^{-1}$  in 6M guanidinium chloride and  $\epsilon_{412}=14150 \text{ M}^{-1} \cdot \text{cm}^{-1}$  in its absence.

## ***2.8 HPLC Analysis of Products of Hydroxylation***

### ***2.8.1 Production of Hydroxylated Products***

20mg of lauric acid substrate was added to 10mL of 0.1M phosphate buffer at pH 8. This represented a gross excess of substrate with respect to the final enzyme concentration and was used to prevent further reaction of hydroxylated products. The solution was heated to 70°C and allowed to cool to room temperature. An NADPH regenerating system was added containing 3.3mM glucose-6-phosphate, 1.3mM NADP<sup>+</sup>, 3.3mM magnesium chloride and 0.4U/mL glucose-6-phosphate dehydrogenase (Penman *et al.*, 1993). The catalytic reaction was initiated on addition of either wild type or mutant intact P450 BM3 to a final concentration of 3µM. The reaction was allowed to proceed for 3 hours before termination by acidification using HCl to pH 3-3.2.

### ***2.8.2 Extraction of Hydroxylated Products***

The acidified reaction mixtures were extracted twice with 20mL ethyl acetate. The separated pooled ethyl acetate layers were washed with 4mL double distilled water, to ensure that all protein material was removed, and then evaporated at room temperature

under a stream of nitrogen gas.

### **2.8.3 HPLC Purification of Hydroxylated Products**

HPLC purification of hydroxylated products was performed using a method based on that of Okita *et al.* (1991). The extracts of the hydroxylation mixtures were dissolved in 2mL 75% methanol of which 100 $\mu$ L was injected onto a 0.46cm x 25cm C18 reverse phase S5 ODS2 column (Phase Separations). An isocratic elution with 38% methanol/62% aqueous 0.2% acetic acid was employed for 30 minutes followed by 100% methanol for a further 30 minutes. It was impossible to follow the separation by UV spectroscopy so 1mL fractions were collected throughout the separation. These were evaporated to dryness and only those fractions that contained any residue were investigated further by 1D proton NMR spectroscopy.

## **2.9 Spectroscopic Assays**

### **2.9.1 Bradford Assay to determine Protein Concentration**

Under appropriate conditions, the acidic and basic groups of proteins interact with organic dyes to form coloured precipitates. This dye-binding phenomenon can be readily exploited for quantitative analysis. This approach was popularised by Bradford (1976) using Coomassie Brilliant Blue G250. 1.0mL of Bradford Assay reagent is added to 0.1mL of protein solution and mixed. The resulting solution is incubated at room temperature for 5 to 60 minutes and the absorbance monitored at 595nm against a 1.1mL buffer blank containing 1.0mL Bradford Assay reagent. Plastic cuvettes are used as the protein-dye complex binds to glass surfaces. The concentration was calculated from a calibration curve constructed using 0.1mg/mL solution of bovine serum albumin (BSA).

### **2.9.2 Enzyme Kinetic Assays**

All ultraviolet-visible spectroscopy and enzyme assays were performed using either a

Beckman DU 650 Spectrophotometer or a Hewlett Packard 8452A Diode Array Spectrophotometer. Protein concentrations were measured by the method of Omura and Sato (1964) using  $\epsilon=96000 \text{ M}^{-1}.\text{cm}^{-1}$  at 418nm for intact P450 BM3 and  $\epsilon=77500 \text{ M}^{-1}.\text{cm}^{-1}$  at 418nm for its haem domain and  $\epsilon=91000 \text{ M}^{-1}.\text{cm}^{-1}$  at 450nm to measure the specific content of P450 haem for either protein.

Fatty acid hydroxylation was measured spectrophotometrically as described by Matson *et al.* (1977). This involved determining the substrate-specific rate of NADPH oxidation in the presence of 0.1M phosphate buffer, pH 8.0 (enzyme assay buffer), substrate,  $\text{O}_2$  and 0.2mM NADPH. The stock solutions of fatty acid substrate used were 2mM sodium laurate, 100 $\mu\text{M}$  sodium myristate and 10 $\mu\text{M}$  sodium palmitate; all were freshly prepared in enzyme assay buffer. For the trimethylammonium bromide compounds the stock solutions were 1mM dodecyl-, 200 $\mu\text{M}$  tetradecyl- and 50 $\mu\text{M}$  hexadecyl trimethylammonium bromide. The decrease in absorbance at 340nm was followed at 25°C using an extinction coefficient of  $\epsilon=6220 \text{ M}^{-1}.\text{cm}^{-1}$  to estimate the number of moles of NADPH oxidised. For association and dissociation equilibrium constant determination, the solution of fatty acid was incubated with the protein for up to 30 minutes at 25°C before measuring the absorbance at 418nm.

### 2.9.3 Method for Determination of the Binding Constant, $K_d$

Equilibrium constants for substrate binding were estimated by fitting the following equation (He *et al.*, 1991) to the changes in absorbance at 418nm measured on addition of substrate to protein:

$$\Delta A = \frac{\Delta A_{\infty}}{2E} \left[ E + S + K_d - \left( \{E + S + K_d\}^2 - 4ES \right)^{1/2} \right] \quad \text{Equation 2.1}$$

where E and S represent the concentrations of enzyme (intact P450 BM3 or P450 domain) and substrate, respectively,  $\Delta A$  and  $\Delta A_{\infty}$  are the changes in absorption at, respectively, the substrate concentration S and at saturating substrate concentrations and  $K_d$  is the equilibrium dissociation constant of the enzyme-substrate complex.

#### 2.9.4 Alternative Method for Determination of the Binding Constant, $K_d$

The equilibrium dissociation constant ( $K_d$ ) for some of the substrates used with either the wild type or mutant proteins could not always be determined, because the change in absorbance from 418nm to 390nm due to the low to high spin shift of the haem iron was small. In such circumstances the  $K_d$ s were determined using a competitive binding assay, where the binding of a substrate with known  $K_d$  is affected by the binding of the substrate under investigation. The observed dissociation constant ( $K_d(\text{obs})$ ) of the known substrate in the presence of a known concentration of the test substrate (S2) is related to that concentration by the following expression (Modi *et al.*, 1989):

$$K_d(\text{obs}) = K_{d1} + \left( K_{d1} \times \frac{S2}{K_{d2}} \right) \quad \text{Equation 2.2}$$

where  $K_{d2}$  is the dissociation constant of the substrate under investigation and  $K_{d1}$  is the dissociation constant for the binding of the substrate with known  $K_d$  in the absence of the test substrate.

#### 2.9.5 Hydrogen Peroxide Assay

Determination of hydrogen peroxide ( $\text{H}_2\text{O}_2$ ) is dependent on a method that is sensitive enough to be able to determine  $1\mu\text{M}$   $\text{H}_2\text{O}_2$  without interfering with monooxygenase dependent hydroxylation reactions, eliminates the influence of various substrates or products on the oxidation reaction, permits inhibition of catalase so that measurement of rate and extent of  $\text{H}_2\text{O}_2$  formation is possible and allows determination of possible degradation of  $\text{H}_2\text{O}_2$  by residual catalase, peroxidase or NADPH-dependent monooxygenase activity.

The method used to assay hydrogen peroxide was based on that described by Hildebrandt *et al.*, (1978). This chemical assay depends on the formation of  $\text{Fe}(\text{SCN})_3$  from ferrous ammonium sulphate and potassium thiocyanate upon oxidation of  $\text{Fe}^{2+}$  to

$\text{Fe}^{3+}$ . Initially a calibration curve for hydrogen peroxide generation was produced. A series of 300 $\mu\text{L}$  solutions containing varying concentrations of peroxide between 0 and 150 $\mu\text{M}$  was set up, each containing 30 $\mu\text{L}$  of enzyme buffer. 100 $\mu\text{L}$  4M guanidine hydrochloride/400mM acetic acid, 500 $\mu\text{L}$  10mM ferrous ammonium sulphate and 200 $\mu\text{L}$  2.5M potassium thiocyanate were added to each solution. The solutions were mixed and incubated at room temperature for 5-60 minutes until a red colour developed. The solutions were decanted into plastic cuvettes and the absorbance monitored at 480nm against a distilled water blank. The concentration of hydrogen peroxide was calculated using a molar extinction coefficient  $\epsilon_{480}=9600 \text{ M}^{-1}.\text{cm}^{-1}$ .

To compare hydrogen peroxide formation and NADPH consumption a subtly different NADPH consumption assay is required. A 1mL reaction volume contained 0.1mL enzyme assay buffer, 0.1mL 2mM substrate, 0.2mL substrate (either 2mM lauric acid or 1mM C12 dodecyltrimethylammonium bromide) and 0.6mL double distilled water. The enzymatic reaction performed at 25°C was monitored for 1 minute, to determine the non-enzymatic rate, before addition of 5 $\mu\text{L}$  of enzyme and monitored for a further 4 minutes at 340nm.

Peroxide production for the sample solutions was measured with time so the rate could be calculated. A 2mL reaction volume of the amended NADPH consumption assay was performed at 25°C. 300 $\mu\text{L}$  of the incubation mixture was transferred to a 7mL bijoux containing 100 $\mu\text{L}$  of 4M guanidine hydrochloride/400mM acetic acid at appropriate time intervals. When all the incubation mixture was finished, the assay for hydrogen peroxide was performed as for the calibration curve. From these results the rate of hydrogen peroxide production was calculated with respect to protein concentration.

## **2.10 NMR Spectroscopy**

### **2.10.1 Preparation of Samples for NMR Spectroscopy**

The sample fractions obtained from HPLC purification of the products of hydroxylation were analysed by NMR spectroscopy. This was to determine whether hydroxylation had occurred and if so at which position on the hydrocarbon chain of the

substrate. Each HPLC fraction that displayed some residue was resuspended in 0.5mL of 99% deuterated methanol.

NMR spectroscopy was also used to identify the products formed within complete reaction mixtures. All enzyme assays were performed *in situ* within the NMR tube. All solutions were made up in 0.1M phosphate buffer, pH\*8 in  $^2\text{H}_2\text{O}$  (the notation pH\* refers to a pH meter reading that has not been corrected for isotope effects on the glass electrode). 100 $\mu\text{L}$  of 10mM substrate, 100 $\mu\text{L}$  of 10mM NADPH were added to 300 $\mu\text{L}$  of 0.1M phosphate buffer, pH\*8 in an NMR tube and mixed. A 1D proton NMR spectrum was recorded of the sample. To this reaction mixture, either wild type or mutant intact P450 BM3 was added to a final concentration not in excess of 10 $\mu\text{M}$  to initiate the catalytic reaction. The solution was mixed and incubated for 2 hours at room temperature before a second 1D proton NMR spectrum was obtained. Alternatively, 100 $\mu\text{L}$  of 10mM substrate, 100 $\mu\text{L}$  of 10mM NADPH were added to 300 $\mu\text{L}$  of 0.1M phosphate buffer, pH\*8 in a 7mL bijoux. The resulting solution was incubated overnight at room temperature with continual mixing before being transferred to an NMR tube.

### ***2.10.2 NMR Spectroscopy to Identify Products of Hydroxylation and Measure Distances Between the Haem Iron and Substrate Protons***

Proton NMR measurements were performed at either 250MHz or 600MHz using either a Bruker AR250 spectrometer or a Bruker AMX600 spectrometer. Studies to determine the frequency dependence of the relaxation rate were performed by S. Modi and additionally involved measurements at 300 and 500MHz. Samples contained 0.5-6.0mM substrate and 2 $\mu\text{M}$ -4mM either wild type or mutant haem domain in 0.1M phosphate buffer, pH\*8 in  $^2\text{H}_2\text{O}$ . The ferrous state of the haem domain was prepared in a glovebox under argon/nitrogen with a 5- to 10- fold excess of sodium dithionite. All buffers were pretreated with Chelex 100 to remove any traces of free metal ions. The sample temperature was 300K unless otherwise stated. Proton chemical shifts were referred to the resonance of  $\text{H}^2\text{HO}$  as a secondary reference at 4.78 ppm. Distances from the haem iron and substrate were measured by paramagnetic relaxation

as described by Modi *et al.* (1995). The longitudinal relaxation time ( $T_1$ ) was measured by the inversion recovery method, using the (180- $\tau$ -90°-acquire) pulse sequence (Hahn, 1950; Sass and Ziessow, 1977).

The longitudinal relaxation rate,  $R_{1,obs}$ , was determined by fitting the measured peak height as a function of the interpulse delay,  $\tau$ , to an exponential by nonlinear regression. Under fast exchange conditions, the measured relaxation rate is the weighted average of the relaxation rates of the free and bound substrates ( $R_{1,f}$  and  $R_{1,b}$  respectively):

$$R_{1,obs} = p_f R_{1,f} + p_b R_{1,b} \quad \text{Equation 2.3}$$

where the  $p_f$  ( $=[S_f]/S_o$ ) and  $p_b$  ( $=[S_b]/S_o$ ) are the fraction of the substrate in the free and bound state respectively and the  $[S_f]$ ,  $[S_b]$  and  $S_o$  are the free, bound and total substrate concentrations. Since under these conditions the substrate concentration is much greater than the protein concentration,  $p_f \approx 1$ , and a stoichiometry of 1:1 for enzyme and substrate (Modi *et al.*, 1995b) so:

$$R_{1,obs} - R_{1,f} = \frac{E_o}{K_d + S_o} (R_{1,f} + R_{1,b}) \quad \text{Equation 2.4}$$

where  $E_o$  and  $S_o$  are the total enzyme and substrate concentrations respectively and  $K_d$  is the dissociation constant of the enzyme-substrate complex. In these experiments,  $R_{1,p}$ , the paramagnetic contribution to the relaxation rate of the protons in the bound substrate due to the unpaired electrons of the haem iron is to be determined. Each of the  $R_{1,obs}$  values measured using the paramagnetic protein must be corrected by subtracting the values measured under the same conditions in the presence of a diamagnetic control ( $R_{1,d}$ ), in this case the reduced CO complex of the haem domain. Equation 2.4 therefore becomes:

$$(R_{1,obs} - R_{1,d}) - R_{1,f} = \frac{E_o}{K_d + S_o} (R_{1,p} - R_{1,f}) \quad \text{Equation 2.5}$$

Estimates of  $K_d$  and  $R_{1,P}$  can be obtained by measuring ( $R_{1,obs}-R_{1,d}$ ) as a function of protein and/or substrate concentration and fitting the data to equation 2.5.

The paramagnetic contribution,  $R_{1,P}$ , to the relaxation rate on the protons of the bound substrate arising from the unpaired electrons on the haem iron is related to the iron-proton distance by the Solomon-Bloembergen equation (Solomon and Bloembergen, 1956; Dwek, 1973; Jardetzky and Roberts, 1981):

$$R_{1,P} = \frac{1}{T_{1,M}} = \frac{2}{15} \frac{\gamma_I^2 \gamma^2 S(S+1) \beta^2}{r^6} \left( \frac{3\tau_c}{1 + \omega_I^2 \tau_c^2} + \frac{7\tau_c}{1 + \omega_S^2 \tau_c^2} \right) \quad \text{Equation 2.6}$$

where  $r$  is the distance of the proton from the haem iron,  $\omega_I$  and  $\omega_S$  are the nuclear and electron Larmor frequencies respectively and  $\tau_c$  is the effective correlation time of the dipolar interaction. In the present case  $\tau_c$  is determined by the electron spin relaxation time. The correlation time for both the wild type and mutant protein was estimated by measuring  $R_{1,P}$  at 250, 500 and 600MHz and fitting the data to equation 2.4 (Modi *et al.*, 1995b).

## 2.11 Oxygen Consumption Assay

An oxygen consumption assay (Plummer *et al.*, 1995) was used to quantify the amount of oxygen consumed during the catalytic reaction of the wild type and mutant intact P450 BM3 enzymes. The oxygen tension in a 2mL incubation volume was measured using a glass chamber that was connected to a heated stirring water bath. This vessel contained a Clark electrode that was attached to a Lloyds Instruments Graphic 1002 chart recorder. To calibrate the system, oxygenated double distilled water was added to the glass chamber and the oxygen tension monitored to establish a baseline for an oxygen saturated solution. Sodium dithionite was added until there was no change in the trace. The change in oxygen tension represents 100% and 0% oxygen saturation in water, where 100% oxygen saturation is 390 $\mu$ M. 1.6mL of 0.1M phosphate buffer, pH 8, 0.2mL of substrate and 0.2mL of 2mM NADPH was added to the chamber and

was allowed to equilibrate at 37°C for 2 minutes before the reaction was initiated by addition of 10µL of a known concentration of enzyme. The catalytic reaction was allowed to proceed for 3 minutes and the initial rate of oxygen uptake determined from the linear part of the oxygen monitor trace at the onset of the reaction.

## **2.12 Oligonucleotides**

All custom oligonucleotides for mutagenesis and automated DNA sequencing were synthesised by D. A. Langton or K. S. Lilley using either an Applied Biosystems Automated 380B DNA Synthesiser or an Applied Biosystems Automated 394 DNA/RNA Synthesiser. The custom oligonucleotides synthesised were as detailed in Table 2.1 below. Two M13/pUC sequencing primers were purchased from New England BioLabs: a reverse sequencing primer, #1233, of which the 5' end annealed to a site 48 nucleotides upstream from the *EcoR* I site and a sequencing primer, #1244, whose 5' end annealed to a site 47 nucleotides downstream of the *Hind* III site. Both oligonucleotides were reconstituted using 1mL of sterile Elga Maxima deionised (EM) water to produce 0.35pmol/µL and 0.40pmol/µL solutions respectively. These oligonucleotides were used for control PCR reactions to assess the purity of the templates used and to determine the orientation of the CYP102 gene for intact cytochrome P450 BM3 in the expression vector pJM23.

### **2.12.1 Purification of Synthesised Custom Oligonucleotides**

The custom oligonucleotides, described in Table 2.1, were delivered in ammonium hydroxide solution which it was necessary to remove before their use in DNA manipulations. This was mostly achieved by ethanol precipitation. 80µL oligonucleotide solution was added to 100µL EM water and 20µL 3M ammonium acetate at either pH 5.2 or 4.8. 400µL 100% ethanol was added (equivalent to 2 volumes), the solution mixed and incubated at -80°C for 20 minutes. After centrifugation at 13000 rpm for 15 minutes, the supernatant was removed and the pelleted oligonucleotide washed with 70% ethanol that had been stored at -20°C. All traces of ethanol were removed by evaporation before resuspending the

**Table 2.1:** Details of all custom oligonucleotides synthesised, stating their length in base pairs and calculated melting temperature ( $T_m$ ) as specified in the Appendix.

Purpose for Oligonucleotide	Name	Oligonucleotide Sequence 5' to 3' <sup>a</sup>	Length (bases)	Calculated $T_m$ ( $^{\circ}\text{C}$ ) <sup>b</sup>
Mutagenesis	R47E	GCGCGTTACT <b><u>TTC</u></b> ACCAGGCGC	21	70
	R47C	TAGCGCGTTAC <b><u>GCA</u></b> ACCAGGCGCCT	25	82
	F87A	GTCCAGCTTG <b><u>TCGCT</u></b> AACCCGTCTC	25	80
Sequencing	ds Seq. 1	GGTGTAGAAGAGAGTCTGTGGG	22	68
	ds Seq. 2	CGTGATTTTGCAGGAGACGG	20	62
	ds Seq. 3	CGAGCAAATCCAGACGACCC	20	64
	ds Seq. 4	GCACGAGTTCTAGTAGATCCTG	22	66
	ds Seq. 4a	GCTTAAATATGTCGGCATGGTC	22	68
	ds Seq. 5	GGTCAGCGTGCGTGTATCGG	20	66
	ds Seq. 6	GGAACAGCTGAAGGAACGGC	20	64
	ds Seq. 7	CGGTGAAGCAGATGCAAGCG	20	64
	ds Seq. 8	GGAGATCATTAGGTGTTATTCCTC	25	70
	ds Seq. 9	CCTACAAAGAACAAGTGCTGGC	22	66
	ds Seq. 10	CCAAAAGACCTGAAACGCC	20	62
ds Seq. 11	GCACTTCTATATTTGCGGAGACGG	24	72	

<sup>a</sup>: The codon involved in the desired mutation is written in bold and underlined.

<sup>b</sup>: The  $T_m$  was calculated according to the formula shown in the Appendix, Section A4.

oligonucleotide in 100 $\mu$ L EM water to calculate the concentration of pure oligonucleotide. If a low yield of oligonucleotide was obtained, the procedure was repeated using 3 times the volumes of starting solutions.

### ***2.12.2 Alternative Purification of Synthesised Custom Oligonucleotides***

There is another easier method for the removal of ammonium hydroxide from the oligonucleotide solutions, that described by Sawadogo and Van Dyke (1991). 100 $\mu$ L of oligonucleotide solution was vortexed vigorously with 1mL of n-butanol for 15 seconds and then centrifuged for 1 minute at 13000 rpm. The single H<sub>2</sub>O containing n-butanol phase was removed and discarded. It was sometimes necessary to repeat the n-butanol extraction to achieve complete removal of contaminants for some oligonucleotide preparations. In these cases, the pellet was redissolved in 100 $\mu$ L H<sub>2</sub>O and extracted with n-butanol as described. Following n-butanol extraction, the pellet was dried under vacuum and resuspended in EM water.

### ***2.12.3 Phosphorylation of Oligonucleotides for Mutagenesis***

The oligonucleotide used in mutagenesis was phosphorylated at the 5' end to ensure ligation after extension by T7 DNA polymerase. After calculating the oligonucleotide concentration, an aliquot of the pure oligonucleotide solution was adjusted to 1.6pmol/ $\mu$ L. This is equivalent to 0.025AU units per mL per base, so for an 21mer oligonucleotide solution the concentration should be at 0.525 AU units/mL. 30 $\mu$ L oligonucleotide solution, 3 $\mu$ L kinase buffer and 2 units T4 polynucleotide kinase (PNK) were added together in a microcentrifuge tube, mixed and incubated at 37°C for 15 minutes. Incubation at 70°C for 10 minutes caused heat inactivation of the PNK and thus terminated the reaction. The phosphorylated oligonucleotide was stored at -20°C prior to use.

## **2.13 General DNA Methods**

### **2.13.1 Preparation of Bacterial Cell Stocks**

Both glycerol and LB agar plate stocks were prepared for all vectors, both wild type and mutant, used in DNA manipulations. A single colony from a freshly prepared minimal media agar plate containing 50µg/mL ampicillin was used to inoculate 10mL of 2YT media containing 50µg/mL ampicillin. This was incubated overnight at 37°C with continual mixing at 250rpm. The following morning a loopful of culture was used to inoculate a fresh LB agar plate containing 50µg/mL ampicillin, which was then incubated at 37°C overnight before storage at 4°C. To create a glycerol stock, 0.7mL culture was added to 0.3mL of sterile 50% glycerol, giving a final concentration of glycerol of 15%, the solution mixed and frozen on dry ice before storage at -80°C.

### **2.13.2 Preparation of *E. coli* Competent Cells**

#### **2.13.2.1 Preparation of *E. coli* Competent Cells using Calcium Chloride**

*E. coli* host cells can be transformed by double stranded DNA vectors only if they have been made “competent”. There are several ways of achieving this, though treatment by calcium chloride (CaCl<sub>2</sub>) is a quick and easy method, though competent cells produced in this manner have only a limited storage life. The cells can be stored on ice but the efficiency of transformation drops after 24 hours. Therefore this method is useful when competent cells are required at short notice or if a single experiment is planned.

A single colony of cells was picked from a glucose minimal media plate and used to inoculate 10mL of 2YT media which was incubated overnight at 37°C. 400µL of the overnight culture was used to inoculate 40mL of 2YT which was incubated at 37°C with continual mixing for approximately 2 hours until the absorbance at 600nm of the culture was about 0.3. The cells were harvested by centrifugation at 3000 xg for 5 minutes. The pelleted cells were gently resuspended in 20mL of pre-chilled sterile 50mM CaCl<sub>2</sub>. After incubating on ice for 20 minutes, the resuspended cells were

harvested again by centrifugation at 3000 xg for 5 minutes. The competent cells were resuspended in 4mL of 50mM CaCl<sub>2</sub> and stored on ice until required.

#### ***2.13.2.2 Hanahan's Method for Preparation of E. coli Competent Cells***

This method of transformation is based on the protocol of Hanahan (1985) and although a more involved method than that using calcium chloride, generates cells that possess a much higher transformation efficiency, which can be maintained upon storage at -80°C for several months.

30mL of SOB media was inoculated with a colony of cells from a glucose minimal media plate, which was incubated overnight at 37°C with continual mixing. 8mL of the overnight culture was used to inoculate a flask containing 200mL SOB media that was incubated at 37°C until the absorbance at 600nm reached approximately 0.3. The culture was transferred to four polypropylene tubes, rapidly chilled in a ice water bath and incubated on ice for 15 minutes. The cells were pelleted by centrifugation at 3000 xg for 5 minutes at 4°C and the supernatant thoroughly removed. The cells were gently resuspended in 16mL transformation buffer 1 and incubated on ice for 15 minutes. The cells were pelleted as before (3000 xg for 5 minutes at 4°C) and gently resuspended in 16mL transformation buffer 2. These competent cells were stored on ice for no longer than a few hours before use, or were aliquoted into 200µL quantities that were flash frozen in liquid nitrogen before storage at -80°C.

#### ***2.13.2.3 Chung and Miller's Method for Preparation of E. coli Competent Cells***

The quickest and easiest method used for the production of competent cells was the method devised by Chung and Miller (1993). This is a one step method where the bacteria are grown to early exponential growth, harvested and are then treated with a single transformation buffer which is also used for storage of the competent cells.

A single colony of cells was picked from a glucose minimal media plate and used to inoculate 5mL of LB media which was incubated overnight at 37°C. 400µL of the overnight culture was used to inoculate 40mL of LB media which was incubated at 37°C with continual mixing for approximately 2 hours until the absorbance at 600nm of the culture was between 0.3 and 0.5. The cells were pelleted by centrifugation at 1000 xg for 10 minutes. The pelleted cells were gently resuspended in 4mL of pre-chilled sterile TSS solution. After incubating on ice for 5-15 minutes, the resuspended cells were ready to use in a transformation reaction or to be aliquoted into 200µL quantities that were flash frozen in liquid nitrogen before storage at -80°C. For transformation the DNA was added followed by gentle mixing and incubation on ice for 5-60 minutes. According to the authors there was no requirement for a heat shock step during transformation, though the conventional method was used with no difference in transformation efficiencies.

### ***2.13.3 Bacterial Transformation with Phagemid Vectors***

A positive transformation control containing 1-5ng DNA and a negative transformation control containing no DNA were performed with every transformation reaction. 300µL competent cells were dispensed into each pre-chilled 50mL polypropylene tubes. 10µL of double stranded DNA or repolymerisation reaction from the final stage of the mutagenesis protocol was added and the solution gently mixed to avoid damaging the delicate competent cells. The cells were incubated on ice for 40 minutes before heat shocking by incubation at 42°C for 45 seconds followed by incubation on ice for 5 minutes. 100µL of 2YT was added to each tube and the cells were incubated at 37°C for 30 minutes with continual mixing at 250 rpm. The content of each tube was poured onto an LB agar plate containing 50µg/mL ampicillin, spread, allowed to dry before inverting the plate for incubation overnight at 37°C.

### ***2.13.4 Bacterial Transformation with Double Stranded Replicative Form Phage DNA***

In addition to preparing competent cells for the transformation, it was also necessary to

prepare fresh *E. coli* host cells for plating out transformed double stranded replicative form (RF) phage DNA. A single colony of cells was picked from a glucose minimal media plate and used to inoculate 10mL of 2YT media which was incubated overnight at 37°C. 20mL of 2YT was inoculated with 200µL of the overnight culture and incubated at 37°C with continual mixing for approximately 2 hours until the absorbance at 600nm of the culture was about 0.3. The cells were incubated on ice until they were required.

Transformation of double stranded RF phage DNA from the mutagenesis control reactions was performed by the same method as the phagemid DNA to the point of cell incubation after heat shocking. After the cells were incubated for 5 minutes, the tubes were allowed to reach room temperature. 200µL of lawn cells, 40µL of 100mM IPTG, 40µL of 2% X-Gal and 4mL of molten H top agar were added to each tube, mixed by rolling and immediately poured onto an LB agar plate. The mix was spread by rolling on the plate and allowed to dry before inverting the plate for incubation overnight at 37°C

### ***2.13.5 Double Stranded DNA Purification***

Various methods were tried and tested for the purification of double stranded DNA. Originally only Promega Magic Minipreps were used. Promega then reformulated their DNA purification resin and it was felt that afterwards the purity and yields were insufficient. As a result other purification systems were investigated and pure DNA from all methods were used at various stages throughout the project.

#### ***2.13.5.1 DNA Purification using Promega Magic Minipreps***

A 5mL or 10 mL 2YT culture containing 50µg/mL ampicillin was inoculated with a single colony and incubated overnight at 37°C. The cell pellet was harvested by centrifugation at 13000 rpm for 5 minutes and the supernatant completely removed. The cells were resuspended using 200µL of cell resuspension solution and transferred to a microcentrifuge tube before addition of 200µL of cell lysis solution. The solutions

were mixed by inversion and 200µL of neutralisation solution was added before mixing by inversion. The tube was centrifuged at 13000 rpm for 5 minutes and the supernatant containing the DNA transferred to a fresh tube. 1mL of Magic Minipreps DNA Purification Resin was added, mixed and the solution applied to a Magic Minicolumn via a 2mL disposable syringe. The Magic Minicolumn was washed with 2mL column wash solution before centrifugation at 13000 rpm for 20 seconds to dry the resin. The pure plasmid DNA was eluted from the column using 50µL of either sterile EM water or TE buffer and stored at -20°C.

#### ***2.13.5.2 Double Stranded DNA Purification using Promega Wizard Minipreps***

The method for purification of double stranded plasmid DNA using the Promega Wizard Minipreps was essentially identical to that for the Promega Magic Minipreps, the only difference being the DNA purification resin used. The Promega Magic Minipreps were initially employed though at a later date Promega withdrew this product and published an alternative purification strategy for the purification of pUC derived plasmid DNA for use with ABI automated sequencing using the Promega Wizard Minipreps. This was then the method used when purifying DNA.

The cell pellet was obtained as in the previous method and the cells resuspended using 300µL of cell resuspension solution and 2µL 20mg/mL RNase A and transferred to a microcentrifuge tube before addition of 300µL of cell lysis solution. The solutions were mixed by inversion till clear and 300µL of neutralisation solution was added before mixing by inversion. The tube was centrifuged at 13000 rpm for 3 minutes and the supernatant containing the DNA transferred to a fresh tube. The supernatant was respun at 13000 rpm for 3 minutes and the clear supernatant transferred equally to two fresh tubes, approximately 400µL per tube. 500µL of Wizard Miniprep DNA Purification Resin was added to each tube, mixed and incubated at room temperature for 5 minutes with occasional mixing. The resin and DNA mix from both tubes was applied to a Magic Minicolumn via a 5mL disposable syringe. The Magic Minicolumn was washed with 4mL column wash solution before centrifugation at 13000 rpm for 1 minute to dry the resin. 100µL of sterile EM water at 70°C was applied to the top of

the Minicolumn and the Minicolumn incubated at room temperature for 1 minute. To elute the pure plasmid DNA the Minicolumn was centrifuged at 13000 rpm for 1 minute and the eluant reapplied to the top of the column before being respun. The DNA was analysed for purity and concentration against known standards as a spectrophotometer could not be used to assess concentration. The method yielded DNA concentrations of between 200 and 250ng/ $\mu$ L and was stored at -20°C.

#### ***2.13.5.3 Double Stranded DNA Purification using Hybaid Recovery***

A 5mL LB culture containing 50 $\mu$ g/mL ampicillin was inoculated with a single colony and incubated overnight at 37°C. A cell pellet was harvested by centrifugation of 1.5mL culture in a microcentrifuge tube at 13000 rpm for 30 seconds and the supernatant completely removed. The cells were resuspended by adding 50 $\mu$ L of pre-lysis buffer and mixed by vortexing. 100 $\mu$ L of alkaline lysis solution was added directly into the cell suspension and mixed by pipetting until the solution was clear. 75 $\mu$ L of neutralisation solution was added and mixed by vortexing. The tube was centrifuged at 13000 rpm for 2 minutes and the supernatant containing the DNA transferred to a kit-supplied spin filter placed in a microcentrifuge vial. 250 $\mu$ L of binding buffer was added to the spin filter and mixed with the supernatant by pipetting before centrifugation at 13000 rpm for 1 minute. The spin filter was washed with 350 $\mu$ L wash solution before centrifugation at 13000 rpm for 1 minute. The liquid in the collection vial was poured off and the spin filter centrifuged again at 13000 rpm for 1 minute to ensure all liquid was removed. The spin filter was transferred to a fresh vial. The pure plasmid DNA was eluted from the filter by adding 50 $\mu$ L of either sterile EM water or TE buffer, briefly vortexing to resuspend the binding buffer and centrifuging at 13000 rpm for 30 seconds to collect the DNA in the bottom of the vial before storage at -20°C.

#### ***2.13.5.4 Double Stranded DNA Purification using Qiagen-tip 20***

The Qiagen-tip 20 plasmid kit was used as an alternative method for DNA purification for some of the preparations. This system is long established as a reliable method for

the rapid purification and isolation of pure supercoiled DNA with high yields, depending on the copy number of the plasmid used. The only notable disadvantage was difficulty in handling the columns if a large number of samples were to be purified.

A 5mL LB culture containing 50µg/mL ampicillin was inoculated with a single colony and incubated overnight at 37°C. The cell pellet was obtained by centrifugation at 13000 rpm for 5 minutes and the supernatant completely removed. 0.3mL of buffer P1 was added and the cell pellet resuspended by vortexing and transferred to a microcentrifuge tube. 0.3mL of buffer P2 was added directly into the cell suspension, mixed gently until the solution was clear and incubated at room temperature for 5 minutes. 0.3mL of chilled buffer P3 was added immediately but gently and the mixture incubated on ice for 10 minutes. The tube was centrifuged at 10000 rpm for 15 minutes and the supernatant containing the DNA was removed promptly to a fresh microcentrifuge tube. A Qiagen-tip 20 was equilibrated by applying 1mL of buffer QBT and the column allowed to empty by gravity flow. The supernatant containing the DNA was applied to the top of the Qiagen-tip 20 and allowed to enter the resin by gravity. The Qiagen-tip 20 was then washed with 4x 1mL buffer QC. The pure plasmid DNA was eluted from the column using 0.8mL buffer QF. The DNA was precipitated by adding 0.7 volumes of isopropanol previously equilibrated to room temperature and centrifuging immediately at 13000rpm for 30 minutes. As the resulting pellet was glassy in appearance and was therefore difficult to see, the outside of the microcentrifuge tube was marked before centrifugation so the pellet was more easily located. The supernatant was carefully removed and the DNA washed with 1mL of cold 70% ethanol, air dried for 5 minutes and the DNA redissolved in 50µL of either sterile EM water or TE buffer before storage at -20°C.

### **2.13.6 Restriction Enzyme Digestion**

Restriction enzyme digestions were carried out on the expression vectors before and after site-directed mutagenesis to confirm the presence of the correct gene inserts. The gene for the haem domain of cytochrome P450 BM3 was known to reside on a *EcoR* I-*Hind* III fragment in the construct pJM20. The reaction mixture for the double

digestion using both enzymes contained 14µL EM water, 2µL of 10x REact 3 buffer, 2µL plasmid DNA containing in total 1µg DNA, 1µL of 10U/µL *EcoR* I and 1µL of 10U/µL *Hind* III and was incubated for 1 hour at 37°C before terminating the reaction by addition of 2µL of DNA stop dye.

The *CYP102* gene resided on a *Bgl* II fragment that was ligated into the *Bam*H I site of pUC119 creating pJM23. This destroyed both sites, so restriction enzyme digestion was performed using the *Xba* I and *Kpn* I sites located upstream and downstream, respectively, of the insert. The only common buffer that did not display non-specific restriction enzyme digestion of the DNA, that is star activity, supported 60% enzyme efficiency. Therefore the reaction mixture containing 14µL EM water, 2µL of 10x REact 1 buffer, 2µL plasmid DNA containing in total 1µg DNA, 1µL of 10U/µL *Xba* I and 1µL of 10U/µL *Kpn* I was incubated overnight at 37°C before terminating the reaction by addition of 2µL of DNA stop dye. Restriction enzyme digests were analysed by electrophoresis on a 1% agarose gel containing 1µg/mL ethidium bromide.

### **2.13.7 Preparation of Single Stranded Phagemid DNA**

Both expression vectors used contained the intergenic region (IG) from M13 filamentous phage. Phagemids containing this region will be secreted as single stranded f1 packaged phage when infected with a helper phage, for example R408 or VSCM13. This removes the need to ligate our cloned genes into M13 prior to site-directed mutagenesis.

10mL of TYP medium was inoculated using a single colony from a glucose minimal media plate containing 50µg/mL ampicillin and incubated at 37°C for 6 to 7 hours with continual mixing at 250rpm. 5mL of TYP containing 50µg/mL ampicillin was inoculated with sufficient culture such that the absorbance at 600nm was approximately 0.1 and was incubated until the  $A_{600nm}$  reached approximately 0.5 (about 45 minutes). VSCM13 helper phage was added to a multiplicity between 10 and 20 (phage:cell ratio of between 10:1 and 20:1) and the culture incubated overnight at 37°C. The overnight culture was transferred to microcentrifuge tubes and incubated at 70°C for 15 minutes

to denature any proteins in solution. The tubes were centrifuged at 13000 rpm for 5 minutes and the supernatant containing the virions removed. The supernatant was centrifuged again to ensure complete removal of all cell debris.

#### ***2.13.8 Isolation of Single Stranded DNA by PEG Precipitation***

Single stranded DNA was isolated by PEG precipitation to ensure complete removal of contaminating proteins or degraded DNA and RNA that can interfere, as the nucleic acid fragments can act as primers during mutagenesis. 200µL PEG/NaCl solution was added to each microcentrifuge tube, mixed and incubated at room temperature for 15 minutes. The tubes were centrifuged at 13000 rpm for 5 minutes and the supernatant containing the single stranded DNA removed. The supernatant was centrifuged again to ensure complete removal of all remaining traces of PEG. 100µL TE buffer was added to each tube and the pellet resuspended by vortexing for 30 seconds. 50µL phenol:0.1M Tris HCl at pH 8.0 was added to each tube, vortexed for 20 seconds before centrifugation at 13000 rpm for 5 minutes. The upper aqueous layer was transferred to a fresh microcentrifuge tube and 100µL 24:1 chloroform:iso-amyl alcohol was added to each tube, vortexed, before centrifugation at 13000 rpm for 5 minutes. The upper aqueous layer was again transferred to a fresh microcentrifuge tube and 10µL of 3M sodium acetate at pH 6 and 250µL 100% ethanol were added. The solution was mixed and incubated at -80°C for 20 minutes. After centrifugation at 13000 rpm for 15 minutes, the supernatant was removed and the DNA pellet washed with 70% ethanol that had been stored at -20°C. All traces of ethanol were removed before resuspending all 5 pellets in 50µL EM water by transferring the volume from tube to tube. The solution was centrifuged again at 13000 rpm for 5 minutes and the supernatant transferred to a fresh tube, leaving behind any precipitated protein. The single stranded DNA was stored at -20°C.

#### ***2.14 Site-directed Mutagenesis***

Site-directed mutagenesis was performed using the Sculptor *in vitro* mutagenesis system as purchased from Amersham International plc.. The principle of this system is

illustrated in Figure 2.3. An oligonucleotide, designed to introduce the desired mutation, is annealed to the single stranded template that contains the target DNA cloned into either an M13 or phagemid vector. The annealed primer is extended using T7 DNA polymerase and ligated with T4 ligase to form the heteroduplex.

Any remaining single stranded wild type template is removed using T5 exonuclease leaving only the mutant heteroduplex. The extension reaction utilises a base analogue of deoxy-cytosine triphosphate, dCTP $\alpha$ S, which has a sulphur atom substituted for oxygen at the alpha phosphate. After treatment with the restriction enzyme *Nci* I only the wild type strand of the duplex will be nicked, as the phosphorothiolate bonds in the mutant strand are resistant to cleavage. Exonuclease III is used to digest the nicked non-mutant strand and a double stranded mutant homoduplex is generated using DNA polymerase I and T4 DNA ligase.

#### ***2.14.1 Site-directed Mutagenesis of Single Stranded Phagemid DNA***

The complete mutagenesis reaction was carried out in one day and is composed of 6 steps, after any of which the reaction can be frozen to be continued at another time.

1) Annealing the oligonucleotide to the single stranded DNA template. 2 $\mu$ L of 1 $\mu$ g/ $\mu$ L single stranded template, 1 $\mu$ L of 1.6pmol/ $\mu$ L oligonucleotide, 1 $\mu$ L Buffer A and 5 $\mu$ L water were added to a microcentrifuge tube, mixed and incubated at 70°C for 5 minutes followed by incubation at 37°C for 30 minutes.

2) Extension and ligation of the mutant strand. After centrifugation at 13000xg for 1 minute, 10 $\mu$ L dNTP mix A, 1 $\mu$ L (2.5 units) T4 DNA ligase and 1 $\mu$ L (0.8 units) T7 DNA polymerase were added to the tube and mixed. The reaction was incubated at room temperature for 10 minutes, followed by 30 minutes at 37°C. The enzymes were heat inactivated by incubation at 70°C for 15 minutes. 1 $\mu$ L (sample 1) was removed and added to 9 $\mu$ L EM water before storing at -20°C for analysis by gel electrophoresis.

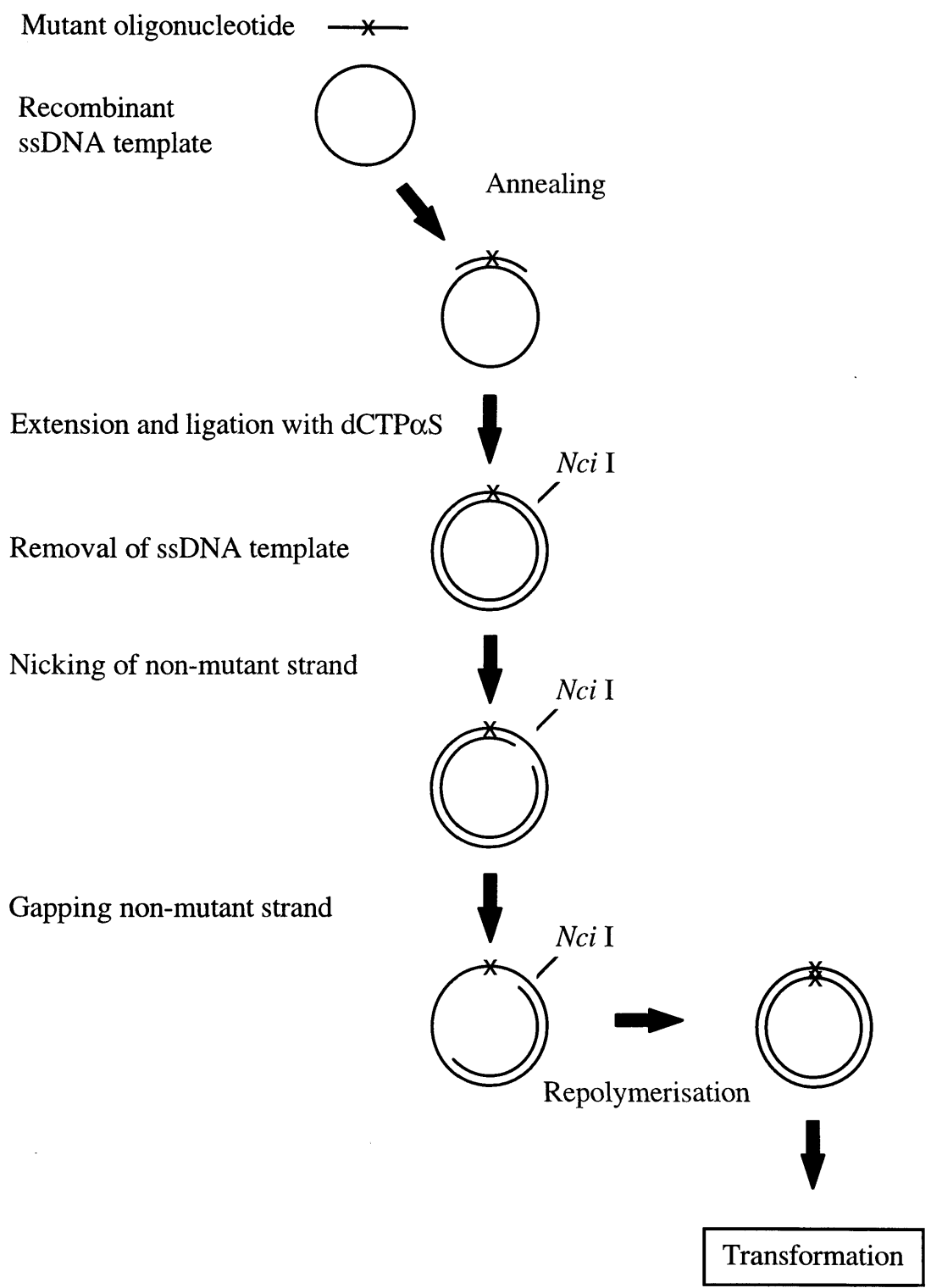


**Figure 2.3:** Schematic representation of the protocol for site-directed mutagenesis using the Sculptor *in vitro* mutagenesis system as purchased from Amersham International plc. (Taken from the Amersham Protocol)

3) Removal of the single stranded, non-mutant DNA. 50 $\mu$ L buffer B and 2 $\mu$ L (2000 units) of T5 exonuclease were added with mixing to the extension reaction. The solution was incubated at 37°C for 30 minutes before the enzyme was heat inactivated by incubation at 70°C for 20 minutes. 5 $\mu$ L (sample 2) was removed and stored at -20°C for analysis by gel electrophoresis.

4) Nicking of the non-mutant strand. To the T5 digestion, 5 $\mu$ L buffer C and 1 $\mu$ L (5 units) restriction enzyme *Nci* I were added, mixed and incubated at 37°C for 90 minutes. 10 $\mu$ L (sample 3) was removed and stored at -20°C for analysis by gel electrophoresis.

5) Digestion of the non-mutant strand. To the reaction containing the nicked DNA, 20 $\mu$ L buffer D and 1 $\mu$ L (160 units) exonuclease III were added, mixed and incubated at 37°C for 30 minutes. 10 $\mu$ L (sample 4) was removed and stored at -20°C for analysis by gel electrophoresis.

6) Repolymerisation of the gapped DNA. 20 $\mu$ L dNTP mix B, 1 $\mu$ L (3.5 units) DNA polymerase I and 1 $\mu$ L (2,5 units) T4 DNA ligase were added to the exonuclease reaction. After a final incubation at 37°C for 60 minutes, 15 $\mu$ L (sample 5) was removed and stored at -20°C for analysis by gel electrophoresis.

#### **2.14.2 Control System for the Mutagenesis Reaction**

A control template and control oligonucleotide are supplied with the kit to monitor the performance of the system. The template DNA is single stranded M13 mp8 that has a single base mutation that introduces a stop codon in the  $\beta$ -galactosidase gene.

Mutagenesis using the control 16mer oligonucleotide will result in removal of the stop codon and complete expression of the  $\beta$ -galactosidase gene. Efficiency of mutagenesis is determined by using blue/white selection of plaques, as in the presence of the inducer IPTG and dye substrate X-Gal only plaques expressing functional  $\beta$ -galactosidase will be blue in colour whereas plaques generated from template DNA will be colourless.

Efficiency of mutagenesis is expressed as the percentage of blue plaques present after mutagenesis control reactions.

### ***2.14.3 Analysis of Mutagenesis Samples by Agarose Gel Electrophoresis***

The samples taken throughout the mutagenesis reactions were defrosted at room temperature. Two markers, one of lambda/*Hind* III and the other containing 500ng of single stranded template DNA, were also prepared. 2 $\mu$ L DNA stop dye was added to the markers and each sample before they were loaded onto a 1% agarose gel containing 1 $\mu$ g/mL ethidium bromide. The samples were separated by electrophoresis at 100V until the dye front had moved about 5cm.

### ***2.15 DNA Automated Sequencing***

The PRISM Ready Reaction DyeDeoxy Terminator cycle Sequencing kit was especially designed for the preparation of samples for sequence analysis on the Applied Biosystems Model 373A DNA Sequencer. The terminator premix contains four dye-labelled dideoxy nucleotides: G, A, T, and C DyeDeoxy terminators so that all four termination reactions are performed in the same tube. Also present in the terminator premix are dITP, which minimises band compression, and AmpliTaq DNA polymerase that is thermally stable so can be used at higher temperatures to minimise secondary structure formation and non-specific primer binding. Automated DNA sequencing was carried out by Dr. K. S. Lilley on an Applied Biosystems 373A DNA Sequencer.

#### ***2.15.1 PCR of Single and Double Stranded DNA for Automated Sequencing***

The quantity of DNA required varied according to the nature of the template DNA, that is, whether it was single or double stranded. 0.5 $\mu$ g template DNA with 0.8 pmol of sequencing primer was used for single stranded DNA sequencing, whereas for double stranded DNA template sequencing, 0.5 $\mu$ g of DNA used with 3.2 pmol of sequencing primer produced the best results. The reaction mixture, in a 0.6mL

microcentrifuge tube, contained 9.5µL terminator premix, 1µL template DNA, 1µL primer and 8.5µL sterile EM water and was overlaid with mineral oil to prevent evaporation during the thermal cycling. The tubes were transferred directly from ice to a Biometra TRIO-Thermblock thermal cycler preheated to 96°C, after which thermal cycling was immediately initiated. The thermal cycle used for sequencing reactions was: rapid thermal ramping to 96°C, 96°C for 30 seconds, rapid thermal ramp to 50°C, 50°C for 15 seconds rapid thermal ramp to 60°C and 60°C for 4 minutes. 25 cycles were completed before ramping to 4°C. “Ramping” of temperatures involved either increasing or decreasing the temperature at a rate of 1°C per second. The total time required for these sequencing reactions was 2 hours and 47 minutes.

### ***2.15.2 Phenol/Chloroform Extraction of PCR Products***

Phenol/chloroform extraction was performed to purify the termination products, as any residual terminators may obscure the first 20 to 50 bases of the sequence. At the end of thermal cycling the reaction mix was removed from under the mineral oil and transferred to a fresh microcentrifuge tube. 80µL of water was added to dilute the sample before addition of 100µL of phenol:water:chloroform. The solution was mixed and centrifuged at 13000 rpm for 5 minutes. The upper aqueous phase was transferred to a fresh tube and reextracted with a second aliquot of phenol:water:chloroform mixture. Extension products were precipitated by adding 15µL of 2M sodium acetate, pH 4.5 and 300µL of 100% ethanol. After incubation at -80°C for 20 minutes, the tube was centrifuged at 13000 rpm for 15 minutes and the supernatant removed. The pelleted products were washed with 70% ethanol that had been stored at -20°C. All traces of ethanol were removed before the extension products were sent for automated DNA sequencing.

### ***2.15.3 Revised Method for the PCR of DNA for Automated Sequencing***

With the revised method for PCR of single and double stranded DNA for automated sequencing, the AmpliTaq DNA polymerase has been replaced with a new enzyme, AmpliTaq DNA polymerase, FS. This enzyme was designed specifically for use in

fluorescent cycle sequencing and so avoids the requirement for high concentrations of the dye-labelled terminators required by AmpliTaq DNA polymerase due to discrimination against incorporation of dideoxynucleotides. The dNTP mix also differs in that dITP has been included with the exclusion of dGTP to minimise band compression.

The quantity of DNA required varied according to the nature of the template DNA, whether it was single or double stranded, though was less than originally used. 0.05-0.1µg single stranded template DNA or 0.3-0.5µg of double stranded template DNA was used with 3.2 pmol of sequencing primer to give the best results. The reaction mixture, in a 0.6mL microcentrifuge tube, contained 8µL terminator premix, 1.0-2.5µL template DNA, 1µL primer and an appropriate volume of sterile EM water to make the final volume 20µL. The reaction mixture was overlaid with mineral oil and the tubes were transferred from ice to a Biometra TRIO-Thermblock thermal cycler preheated to 96°C, after which thermal cycling immediately began. The thermal cycle used was: rapid thermal ramping to 96°C, 96°C for 10 seconds, rapid thermal ramp to 50°C, 50°C for 5 seconds rapid thermal ramp to 60°C and 60°C for 4 minutes. 25 cycles were completed before ramping to 4°C. The total time required was 2 hours and 35 minutes.

#### ***2.15.4 Extraction of PCR Products from the Revised Method***

Phenol/chloroform extraction of the PCR sequencing products is no longer necessary as the amount of the dye terminators used has been significantly reduced. Ethanol precipitation was performed to effectively remove minimal traces of unincorporated terminators that are occasionally seen in front of the sequence data. Even though two methods for ethanol precipitation are recommended the method used was considered to be the most reliable and to give the best results as carryover of unincorporated dye terminators was minimised.

At the end of thermal cycling the reaction mix was removed from under the mineral oil and transferred to a fresh microcentrifuge tube. Extension products were precipitated

by adding 2 $\mu$ L of 3M sodium acetate, pH 4.6 and 50 $\mu$ L of 95% ethanol. 3M sodium acetate, pH 5.2 and 3M potassium acetate, pH 5.6 appear to work equally well. After incubation at -80°C for 20 minutes, the tube was centrifuged at 13000 rpm for 15 minutes and the supernatant removed as completely as possible. The pelleted products were washed twice with 250 $\mu$ L of 70% ethanol that had been stored at -20°C. All traces of ethanol were removed by gyrovap before the extension products were sent for automated DNA sequencing.

#### ***2.15.5 Improved Automated Sequencing using Dimethylsulphoxide (DMSO)***

S. G. Burgett and P. R. Roestek, Jr. (Unpublished Results) found that double stranded templates containing a high concentration of guanine and cytosine generally produced shorter readable sequences than other templates when analysed by fluorescent dye sequencing. The results suggested that either strong secondary structures or rapid reannealing of template DNA strand was responsible. To combat this phenomenon, they developed a method where 5% DMSO was included in the PCR mixture.

This method was only performed in the presence of double stranded DNA. The reaction mixture, in a 0.6mL microcentrifuge tube, contained 8 $\mu$ L terminator premix, 1.0-2.5 $\mu$ L containing 0.5 $\mu$ g template DNA, 1 $\mu$ L of 3.2 pmol primer, 2 $\mu$ L DMSO and an appropriate volume of sterile EM water to make the final volume 20 $\mu$ L. The reaction mixture was overlaid with mineral oil and the tubes were transferred from ice to a Biometra TRIO-Thermblock thermal cycler preheated to 96°C, after which thermal cycling immediately began. The thermal cycle used for sequencing reactions was: rapid thermal ramping to 95°C, 95°C for 1 minute, rapid thermal ramp to 50°C, 50°C for 15 seconds rapid thermal ramp to 60°C and 60°C for 4 minutes. 25 cycles were completed before ramping to 4°C. The total time required was 3 hours.

#### ***2.16 Computer Packages for DNA and Protein Analysis***

DNA sequence data was analysed using DNA Strider version 1.0, Sequence Editor version 1.0.3, Sequence Navigator and MacVector version 4.1.4 for the Apple

Macintosh and Molecular Biology Wisconsin Genetics Group (GCG) suite of packages on the University of Leicester IRIX system. These programs allowed easy manipulation of data from the gene sequences, oligonucleotides for mutagenesis and sequencing and automated DNA sequencing results. Plasmid Artist version 1.13 for the Apple Macintosh was used to generate schematic representations of the expression systems used. Cameleon v3.31 (Oxford Molecular Ltd) and Alscript version 2.0 (Barton, 1993) on a Silicon Graphics work station were used to generate the sequence alignment. XWIN-NMR, version xwin-nmr 1.3 on a Silicon Graphics work station was used analyse the NMR spectra. Insight II (Biosym Technologies) on a Silicon Graphics work station was used for viewing and manipulating the crystal structures of the haem domain of P450 BM3 from *Bacillus megaterium* (Ravichandran *et al.* 1993) and the crystal structure for the haem domain with substrate bound (Li and Poulos, 1997). Enzfitter, version 1.05, from Elsevier-Biosoft was used to calculate  $k_{cat}$  and  $K_M$  values from enzyme assay results. Microsoft Excel version 5.0, and Microsoft PowerPoint version 4.0, for PC and Kaleidagraph version 2.1.3 for Apple Macintosh were used as graphic packages.

## ***Chapter 3: Site-Directed Mutagenesis and Protein Purification***

### ***3.1 Introduction***

Site-directed mutagenesis (SDM) is an invaluable technique for studying protein structure-function relationships which allows the researcher to substitute selected amino acid residues. This procedure when combined with recombinant DNA technology can result in the expression of large amounts of enzyme, thus providing a powerful approach for testing hypotheses for the role of individual amino acids or intramolecular regions which may mediate functions, such as catalysis, derived from knowledge of the three dimensional x-ray crystal structure, enzyme kinetics, chemical modification and bioorganic chemistry (Plapp, 1995). Single site-directed mutagenesis, resulting in a mutant protein with one altered amino acid is a frequently used technique to test a residues structural and functional significance, as well as to engineer stability and enzymatic properties. Also, engineering of enzymes, specifically cytochrome P450s, to achieve high catalytic turnover and low uncoupling is of particular interest in biotechnology and bioremediation research. It was therefore proposed to undertake a variety of mutagenesis experiments to explore the structure-function relationship of P450 BM3 from *Bacillus megaterium* using high level expression systems for the intact enzyme and the isolated haem domain derived by Miles *et al.*, (1992). The thrust of the experiments was aimed at understanding the role of individual amino acid residues within the substrate binding site of the enzyme.

The published crystal structure of the P450 BM3 haem domain (Ravichandran *et al.*, 1993) was used to design single residue substitutions to investigate the substrate specificity and regioselectivity of the enzyme. Inspection of this structure indicated there were two obvious candidates for further analysis by site-directed mutagenesis within the substrate binding site, and these were the residues arginine 47 (R47) and phenylalanine 87 (F87). It was proposed that the side chain guanidinium group of Arg47, the only charged residue located at the opening of the substrate access channel, interacts electrostatically with the fatty acid substrate carboxylate thereby orienting the substrate for carbon chain hydroxylation near the haem moiety (Peterson *et al.*, 1994).

It was also suggested that the aromatic ring of Phe87, which forms close van der Waals interactions with the haem, could be important in forming the lipophilic pocket involved in sequestering the  $\omega$ -end of a fatty acid, which is not hydroxylated by the enzyme (Miura and Fulco, 1975; Ravichandran *et al.*, 1993).

### 3.2 Molecular Biology, involving Gene Manipulation and Protein Expression

#### 3.2.1 Site-Directed Mutagenesis

Site directed mutagenesis was performed using the Sculptor *in vitro* mutagenesis system as purchased from Amersham International plc on the expression systems for intact P450 BM3 and its haem domain. The custom oligonucleotides, as described in Table 2.1 in the materials and methods chapter, were annealed to single stranded DNA (Figure 3.1): oligonucleotide R47E creating the mutation of arginine to glutamic acid at position 47, oligonucleotide R47C creating the mutation of arginine to cysteine at position 47 and oligonucleotide F87A creating the mutation of phenylalanine to alanine at position 87. Both the R47E and F87A mutations required the most extensive change to the gene sequence as when changing the codon used for arginine (CGT) to that of glutamic acid (GAA) and phenylalanine (TTT) to alanine (GCG), all 3 bases were mutated. The R47C mutation entailed a double base mutation where the CGT codon to was changed to TGC, the codon used for cysteine.

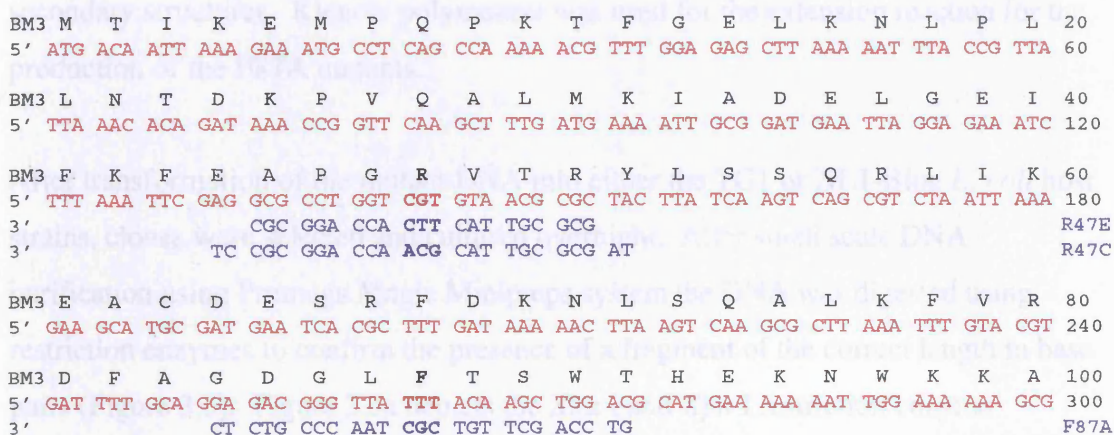
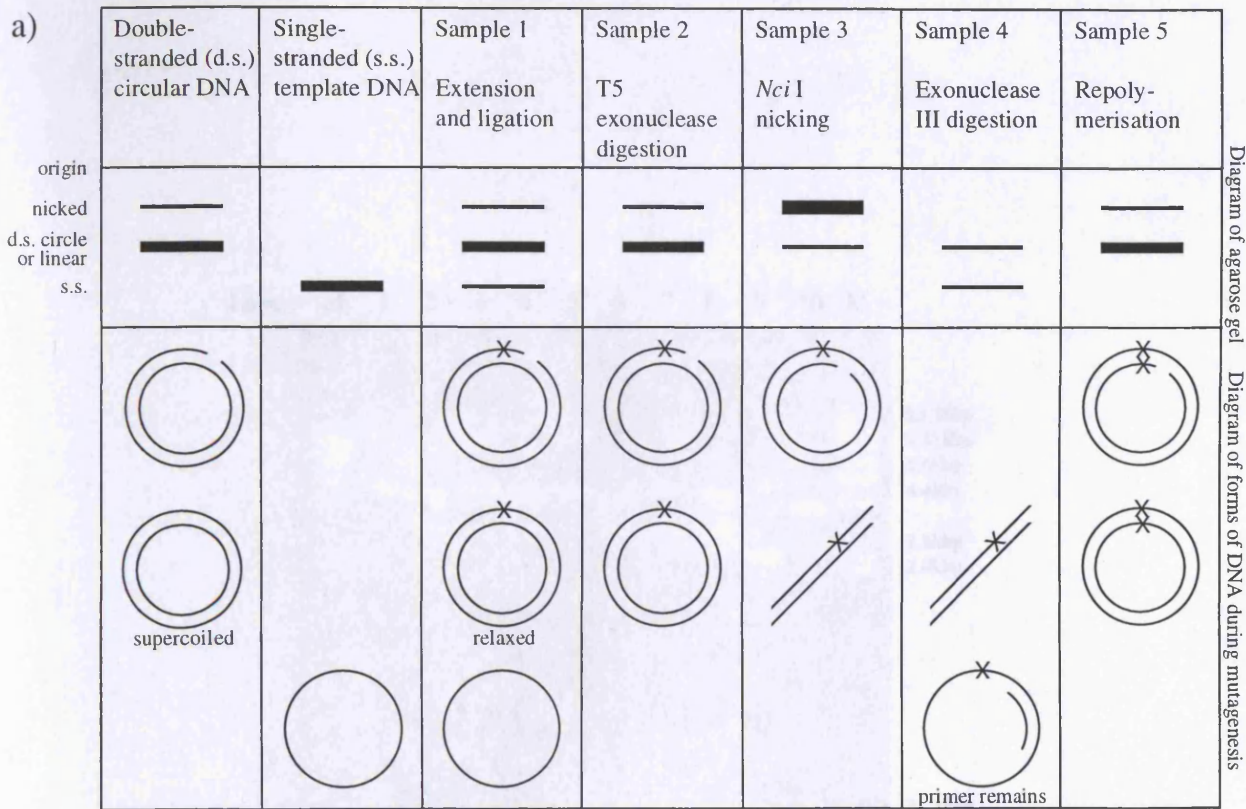


**Figure 3.1:** The nucleotide sequence (red) for the first 100 residues of the P450 BM3 gene, with the translated protein sequence (black). Also illustrated at their position of annealing are the mutant oligonucleotides used in site-directed mutagenesis (blue) with the variant codon in bold type.

Initial mutagenesis experiments proved unsuccessful resulting either in an absence of colonies after transformations using the resulting mutated DNA or in colonies whose DNA was later shown to contain the original wild type gene. Samples were taken after each step of the mutagenesis procedure and analysed by agarose gel electrophoresis (Figure 3.2).

All the desired mutations were eventually successfully generated after minor changes to the recommended protocol for the Sculptor *in vitro* mutagenesis system described by Amersham. The changes involved using twice the concentration of mutant oligonucleotide so that the ratio of mutant oligonucleotide to template DNA was increased from 4:1 to 8:1, doubling the incubation time when extending and ligating after annealing the mutant oligonucleotide and increasing the incubation time in the presence of T5 exonuclease to ensure all non-mutant single stranded DNA is thoroughly removed. Increasing the concentration of oligonucleotide increases the amount of primer in the correct conformation to bind and by competition reduces the effect of self-annealing of the template. Later kits for the Sculptor *in vitro* mutagenesis system included Klenow polymerase. This is particularly useful where the mutant oligonucleotide and/or the template is capable of forming secondary structures. Klenow polymerase allows the extension reaction to be performed at 16°C and this lower temperature appears to stabilise the oligonucleotide-template complex and reduce melting that would allow either the oligonucleotide or the template to reform secondary structures. Klenow polymerase was used for the extension reaction for the production of the F87A mutants.

After transformation of the mutant DNA into either the TG1 or XL1-Blue *E. coli* host strains, clones were selected and cultured overnight. After small scale DNA purification using Promega Magic Minipreps system the DNA was digested using restriction enzymes to confirm the presence of a fragment of the correct length in base pairs (Figure 3.3). Figure 3.3a depicts the *Xba* I and *Kpn* I restriction enzyme digestion of 10 samples of DNA obtained from clones produced after transformation of TG1 *E. coli* host strain with pJM23 R47E, the expression vector for the R47E mutant of intact P450 BM3. Of the 10 mutant intact P450 BM3 clones analysed, the DNA from 7 of the clones contained an insert of the correct length, when compared to the



b)

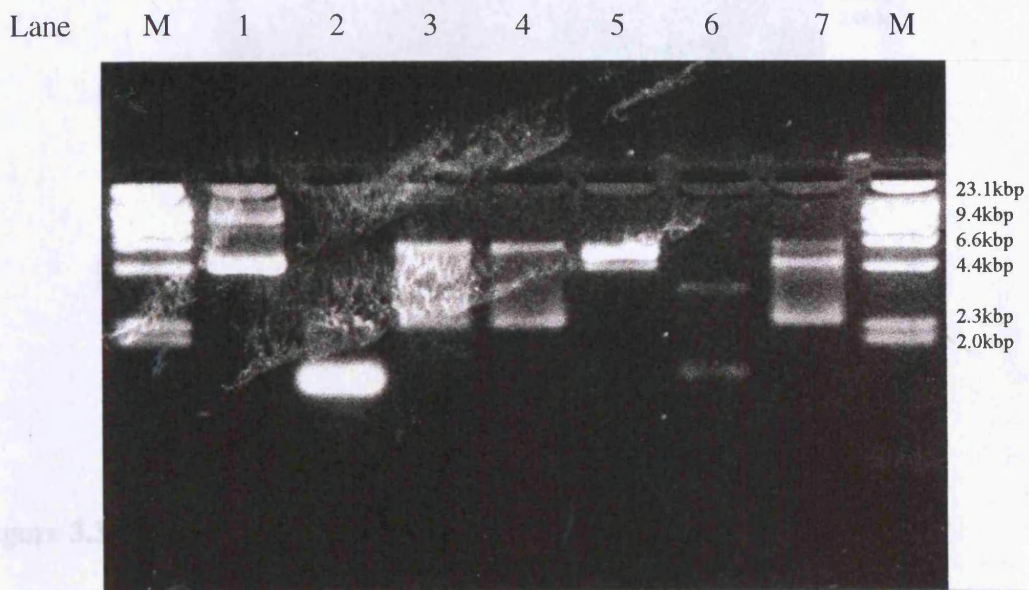


**Figure 3.2:** Analysis of the samples obtained during the mutagenesis reaction, both diagrammatically (a; Taken from the Amersham Protocol) and by agarose gel electrophoresis for the R47C mutation of pJM20, the expression vector for the haem domain of P450 BM3 (b). Lane M, lambda/*Hind* III DNA markers; lane 1, d.s. pJM20; lane 2, s.s. pJM20; lane 3, sample 1; lane 4, sample 2; lane 5, sample 3; lane 6, sample 4; lane 7, sample 5.

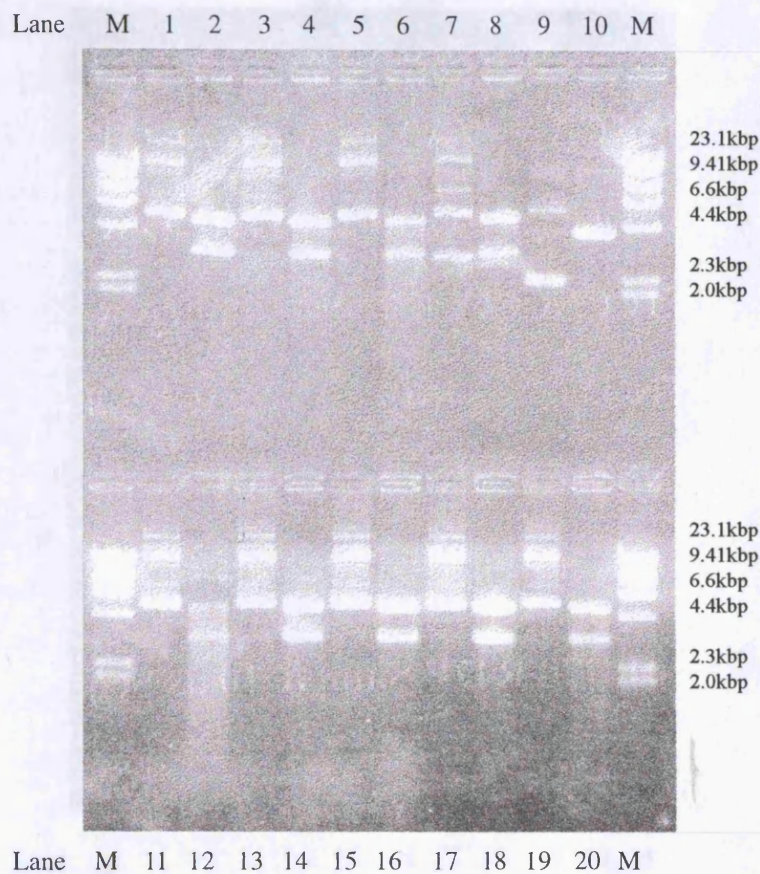
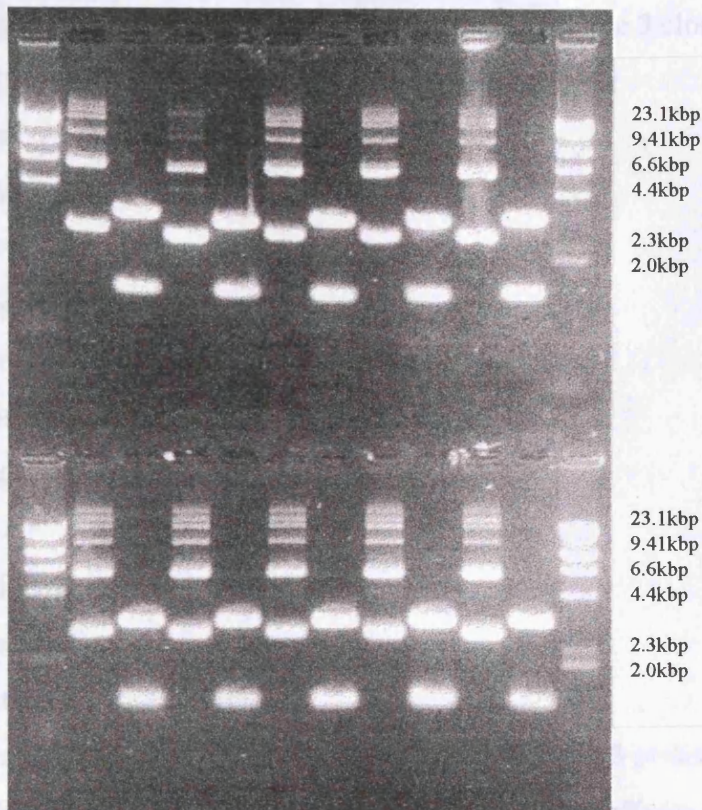


**Figure 3.3a:** Restriction enzyme digestion using *Xba* I and *Kpn* I for the digestion of 10 clones from the R47E mutation of pJM23, the expression vector for intact P450 BM3 to verify the presence of a gene of the correct length. *Lane M*, lambda/*Hind* III DNA markers; *lane 1 and 2*, pJM23 R47E clone 1; *lane 3 and 4*, pJM23 R47E clone 2; *lane 5 and 6*, pJM23 R47E clone 3; *lane 7 and 8*, pJM23 R47E clone 4; *lane 9 and 10*, pJM23 R47E clone 5; *lane 11 and 12*, pJM23 R47E clone 6; *lane 13 and 14*, pJM23 R47E clone 7; *lane 15 and 16*, pJM23 R47E clone 8; *lane 17 and 18*, pJM23 R47E clone 9; *lane 19 and 20*, pJM23 R47E clone 10. All even numbered lanes are those containing the restriction enzyme digest.

Lane M 1 2 3 4 5 6 7 8 9 10 M



Lane M 11 12 13 14 15 16 17 18 19 20 M

**Figure 3.3b:** Restriction enzyme digestion using *EcoR* I and *Hind* III for the digestion of 10 clones from the R47E mutation of pJM20, the expression vector for the haem domain of P450 BM3 to verify the presence of a gene of the correct length. Lane M, lambda/*Hind* III DNA markers; lane 1 and 2, pJM20 R47E clone 1; lane 3 and 4, pJM20 R47E clone 2; lane 5 and 6, pJM20 R47E clone 3; lane 7 and 8, pJM20 R47E clone 4; lane 9 and 10, pJM20 R47E clone 5; lane 11 and 12, pJM20 R47E clone 6; lane 13 and 14, pJM20 R47E clone 7; lane 15 and 16, pJM20 R47E clone 8; lane 17 and 18, pJM20 R47E clone 9; lane 19 and 20, pJM20 R47E clone 10. All even numbered lanes designated are those containing the restriction enzyme digest.

lambda/*Hind* III DNA marker used. Figure 3.3b depicts the *Eco*R I and *Hind* III restriction enzyme digestion of 10 samples of DNA obtained from clones produced after a similar transformation using pJM20 R47E, the expression vector for the R47E mutant of the haem domain from P450 BM3. All of the DNA obtained from the 10 mutant haem domain clones contained an insert of the correct length, when compared to the lambda/*Hind* III DNA marker used. The uncut DNA from the 3 clones displaying an insert of incorrect length appeared to be of a smaller size to that of the other clones. The reduction in DNA size may have been due to deletion of DNA during the mutagenesis reactions.

The clones containing a fragment displaying an insert of DNA of the correct length for either the intact P450 BM3 or its haem domain were amplified by PCR using an appropriate sequencing primer to verify the presence of the desired change. The ds Seq. 1 primer was used for intact P450 BM3 and the commercial reverse sequencing primer, #1233 was used for the haem domain. The mutagenic success varied with the mutation made and which expression vector template was used. M13 mp8 mutagenesis controls performed simultaneously with some of the mutagenesis experiments indicated an average efficiency of mutagenesis of 87%, in accordance with manufacturers expectations. For the R47E mutant intact P450 BM3 protein, of 7 clones sequenced 6 included the CGT to GAA mutation, giving an efficiency of mutation at 86% whereas for the R47E mutant haem domain 7 out of 10 (70%) contained the desired mutation. The CGT to TGC change in the R47C mutation resulted in 1 out of 3 (33%) mutant haem domain and 4 out of 9 (44%) mutant intact P450 BM3. Finally the F87A mutation of TTT to GCG resulted in 5 out of 7 (71%) mutant haem domain and 2 out of 3 (67%) mutant intact P450 BM3. These results represent the clones which were successfully sequenced, not necessarily the total number of clones sent for sequencing. The mutation frequency for both the R47C and F87A clones were lower than that for the R47E mutation, with that for the R47C being the lowest. This may have been due to the presence of A and T nucleotides at the 5' and 3' ends of the oligonucleotide, which ideally should have been GC rich to stabilise annealing to the template.

### **3.2.2 Gene Sequencing**

To detect any spurious mutations introduced by the polymerase, it is important to sequence the entire structural gene after mutagenesis. For each mutation, one clone for the intact enzyme and two for the haem domain were fully sequenced. The DyeDeoxy Terminator cycle sequencing kits used with the Applied Biosystems DNA Sequencer is capable of correctly sequencing up to 450bp according to the manufacturers instructions, though in practise approximately 350bp is usual. The sequencing oligonucleotides were designed to anneal to the DNA template at 300bp intervals resulting in successful sequencing of 350bp overlapping segments of the genes. The same sequencing primers could be used to sequence both the intact P450 BM3 gene and the gene for its haem domain as the sequences were sufficiently identical except at the start of the haem domain gene where the region upstream of the P450 BM3 gene had been removed. All sequencing primers were analysed using the Wisconsin Genetics Group (GCG) suite of packages to assess for either hairpin or dimer formation and the MacVector programme to ensure a single annealing site within the open reading frame for the different genes, calculated with up to 5 bases mismatched. PCR amplification sequencing reactions were performed on double stranded samples of mutant DNA using the oligonucleotides specified in Table 2.1 in the materials and methods chapter. Oligonucleotides ds Seq. 1 to ds Seq. 11 were used to sequentially analyse the mutant genes for intact P450 BM3, whereas the commercial oligonucleotide #1233 with ds Seq. 2 to ds Seq. 5 were used to sequence the genes for the haem domain.

The results obtained from sequencing reactions using the sequencing primer ds Seq. 4 in general generated sequences that were unrecognisable, though they did contain small sequences corresponding to the expected sequence. On viewing the ds Seq. 4 sequencing chromatograms using the Sequence Editor programme, it was apparent that at the positions where there was an incorrectly assigned base a smaller fluorescence peak corresponding to the correct base was also present, though a stronger peak corresponding to an incorrect base was also present. This suggested that the primer was probably not annealing correctly to the template DNA. The nonsense sequences

produced may have been due to the formation of a secondary DNA structure as the region of the gene being sequenced by ds Seq. 4 is predominantly composed of the bases C and G, for example a DNA loop, despite using the annealing temperature of 50°C. Annealing the primer to the template across the base of a loop would generate two sequences: one corresponding to the loop and the other corresponding to template DNA across the base of the loop. An alternative primer was designed, designated ds Seq. 4a, and this was successfully used to sequence this region of both genes. Sequencing was further aided by using 5% DMSO in the PCR mixture, which according to S. G. Burgett and J. P. Roestek, Jr. (Unpublished results) reduced the risk of either strong local secondary structures or rapid reannealing of template DNA which results from double stranded templates containing a high concentration of guanine and cytosine.

### 3.2.3 Gene Sequencing for Mutant Expression Systems

All the clones generated for mutants of both the intact P450 BM3 and its haem domain, with one exception were shown not to contain any unwanted mutations. When sequencing the gene for the F87A mutant of the intact P450 BM3 three anomalies were found. The sequencing reactions were repeated and these confirmed the presence of three spontaneous mutations in the sequence within the haem domain corresponding to the amino acid residues 429-432 (Figure 3.4).

Residue Number	429	430	431	432
Wild Type Amino Acid Sequence	Y	E	L	D
Wild Type Gene Sequence	TAC	GAG	CTG	GAT
F87A Mutant Gene Sequence	<u>G</u> AC	<u>A</u> AG	CTG	<u>G</u> AC
F87A Mutant Amino Acid Sequence	D	K	L	D

**Figure 3.4:** Sequence data from the F87A mutant intact P450 BM3 to illustrate the spontaneous mutation of three nucleotides within the haem domain and the resulting change in amino acid sequence.

Figure 3.4 illustrates that there were three substitutions in the nucleotide sequence for the F87A mutant intact protein though these only resulted in transformation with two of the amino acid residues at positions 429 and 430, changing from tyrosine (Y) and glutamate (E) to aspartate (D) and lysine (K), respectively. The third mutation was silent, that is the change in the genotype had no effect on the phenotype of the amino acid residue.

### **3.2.4 Protein Expression**

The double stranded mutant vectors, which had been fully sequenced, were transformed into the *E. coli* host strain, either TG1 or XL1-Blue. Overnight cultures of these cells were analysed by SDS-PAGE to verify protein expression. Figure 3.5 is an example of this, illustrating the cell lysates from the F87A mutation of the intact P450 BM3 and its haem domain. These cell lysates revealed proteins at 119kDa for the intact P450 BM3 protein and 54kDa for the haem domain, indicating that the mutant proteins were expressed. The purifications of the mutant proteins of the intact P450 BM3 and its haem domain were then undertaken.

## **3.3 Protein Purification**

### **3.3.1 Purification of Wild Type Proteins**

Expression of the wild type intact P450 BM3 and its haem domain was performed using the vectors pJM23 and pJM20 respectively, which were obtained as gifts from Dr John Miles, Glasgow University (Miles *et al.*, 1992). The expression of the intact P450 BM3 was independent of the inducing agent IPTG, as it is constitutively expressed in *E. coli* using its own promoter located upstream of the inserted P450 BM3 gene cloned into the pUC119 expression vector. Wen and Fulco (1987) showed that this constitutive expression in *E. coli* is due to the absence of one or more components present in *B. megaterium* which are required to interact with the regulatory sequences to produce repression. The intact P450 BM3 and its haem domain were purified as described in the Material and Methods chapter. The original protocol used was essentially identical to those published by Li *et al.*, (1991), Miles *et al.* (1992) and

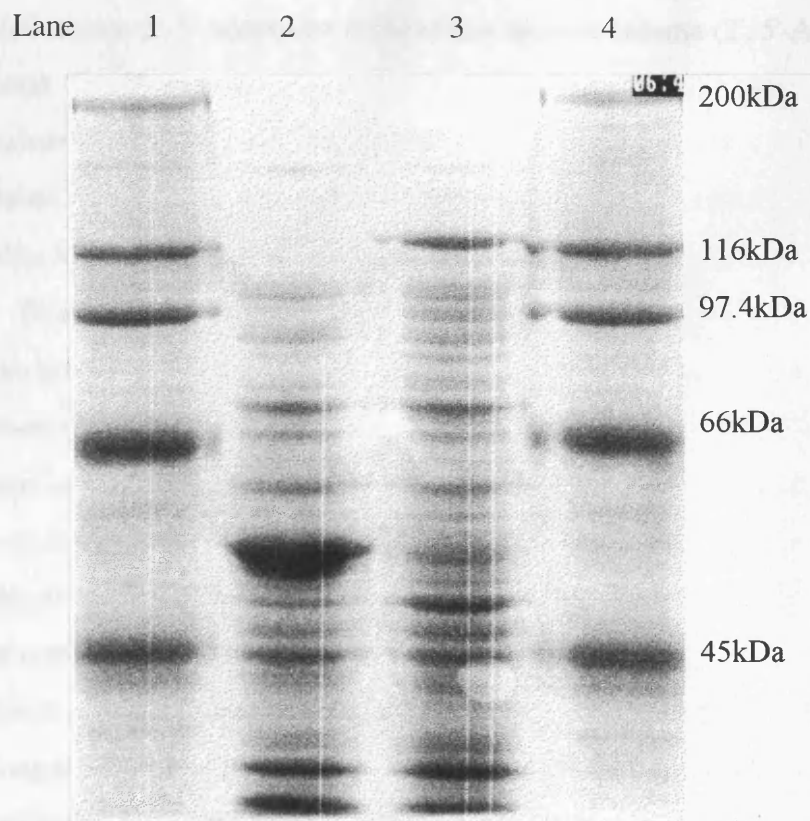


**Figure 3.5:** SDS polyacrylamide gel of *E. coli* cell lysates from the F87A mutant expression systems for intact P450 BM3 from *Bacillus megaterium* and its haem domain, visualised by coomassie blue staining. *Lane 1* and *4*, high molecular weight markers; *lane 2*, pJM23 expression vector for F87A mutant haem domain; *lane 3*, pJM20 expression vector for F87A mutant intact P450 BM3.

Black *et al.*, (1994). The exceptions were that after cell lysis, using a French Press, the cell-free supernatant was subjected to ammonium sulphate precipitation collecting the 20-65% fraction and that the initial column purification involved a DEAE-sephadex column as opposed to a Q sepharose anion exchange column.

According to the original papers (Li *et al.*, 1991; Miles *et al.*, 1992), the concentrated samples of intact P450 BM3 obtained after the anion exchange step were to be purified by affinity isolation on a 2', 5'-adenosine diphosphate agarose column (2', 5'-ADP; 1.6cm id x 40cm). In keeping with this protocol, half the intact P450 BM3 protein sample (equivalent to 472.4mg) generated from the previous step was loaded on to a 2', 5'-ADP column equilibrated with low salt affinity buffer, it was washed with high salt affinity buffer before elution with 50mM 2'-adenosine monophosphate in high salt affinity buffer. The standard chromatography chart recorder trace indicated that there had been a large peak of material, which on examination was yellow in appearance and strongly absorbed at 280nm. This could not represent the intact P450 BM3, which normally appears orangey brown in colour. Also the affinity column had changed from white to pinky red in colour. The elution procedure was repeated a further two times such that finally, of the estimated 470mg of intact P450 BM3 loaded, only 50mg of protein was successfully reclaimed from the 2', 5'-ADP column. The yellow protein fractions exhibited a molecular weight of approximately 116kDa as observed by SDS-PAGE suggesting the eluted protein was the intact apoprotein with the haem moiety removed, most likely bound irreversibly to the column. In an attempt to regenerate the column, the 2', 5'-ADP agarose was washed with 0.1M Tris HCl, pH 8.5 with 0.5M NaCl then 0.1M sodium acetate, pH 4.0 followed by 2M guanidine HCl which failed to remove any more of the bound material.

As this method of separation appeared to be unsuccessful, it was abandoned and the alternative method as described in the methods section was developed. A HiLoad 26/10 Q sepharose column, attached to a Pharmacia FPLC system was chosen. This was used in preference to a Mono Q HR 10/10 anion exchange column used by others (Miles *et al.*, 1992). The HiLoad Q can be operated at flow rates of up 6mL/minute and large quantities of protein can be loaded, leading to rapid purification, though

probably at the cost of resolution. It was therefore possible to load the remaining 470mg of intact P450 BM3 obtained after the DEAE-sephadex on to the HiLoad Q column and purify it all using a single gradient. Figure 3.6 depicts the obtained elution profile of the 80 fractions collected during the 25mM to 450mM KCl salt gradient with regard to absorbance at 280nm and 418nm. The elution profile shows a large peak of protein, as indicated by the  $A_{280\text{nm}}$ , and haem absorbance, as indicated by the  $A_{418\text{nm}}$ , centring on fractions 48-52. Only fractions with an absorbance ratio at 418nm and 280nm ( $A_{418\text{nm}}/A_{280\text{nm}}$ ) greater than 0.7 were pooled. After the salt gradient, all coloured material was eluted from the column. Further elution with chaotropic agents failed to remove any additional proteins. Of the 470mg loaded, approximately 250mg of intact P450 BM3 was recovered from fractions 45 to 56 after dialysis into buffer A, before further purification on the sephacel S300 column. A large  $A_{280\text{nm}}$  and  $A_{418\text{nm}}$  peak was present in fractions 9 to 14. These fractions were pooled, concentrated using an Amicon concentrator and analysed by optical spectroscopy. The absorption spectra observed was identical to that of the haem domain. This concentrated sample of protein was subsequently analysed by SDS- PAGE and appeared to consist of a protein with the approximate molecular weight of 54kDa. This suggested that these fractions corresponded to haem domain.

Contrary to other reports (Li *et al.*, 1991; Miles *et al.*, 1992), all samples of protein required further purification by gel filtration using either a sephacel S300 column or a HiLoad 26/60 Superdex 200 column before they were considered sufficiently pure by SDS-PAGE analysis. Narhi *et al.* (1988) also found this step necessary for complete purification of P450 BM3 protein samples derived from *E. coli*. This resulted in homogenous proteins as shown electrophoretically by SDS-PAGE analysis visualised by coomassie blue staining (Example protein purification gels are shown in Figures 3.7 and 3.8) and by the proteins absorbance ratio of 418nm/280nm which were 0.719 for the intact P450 BM3 and 1.779 for its haem domain respectively. The samples of protein were considered to be of a high level of purity, as acceptable absorbance ratios are 0.7 for the intact P450 BM3 and 1.7 for its haem domain (A. W. Munro, Personal Communication).

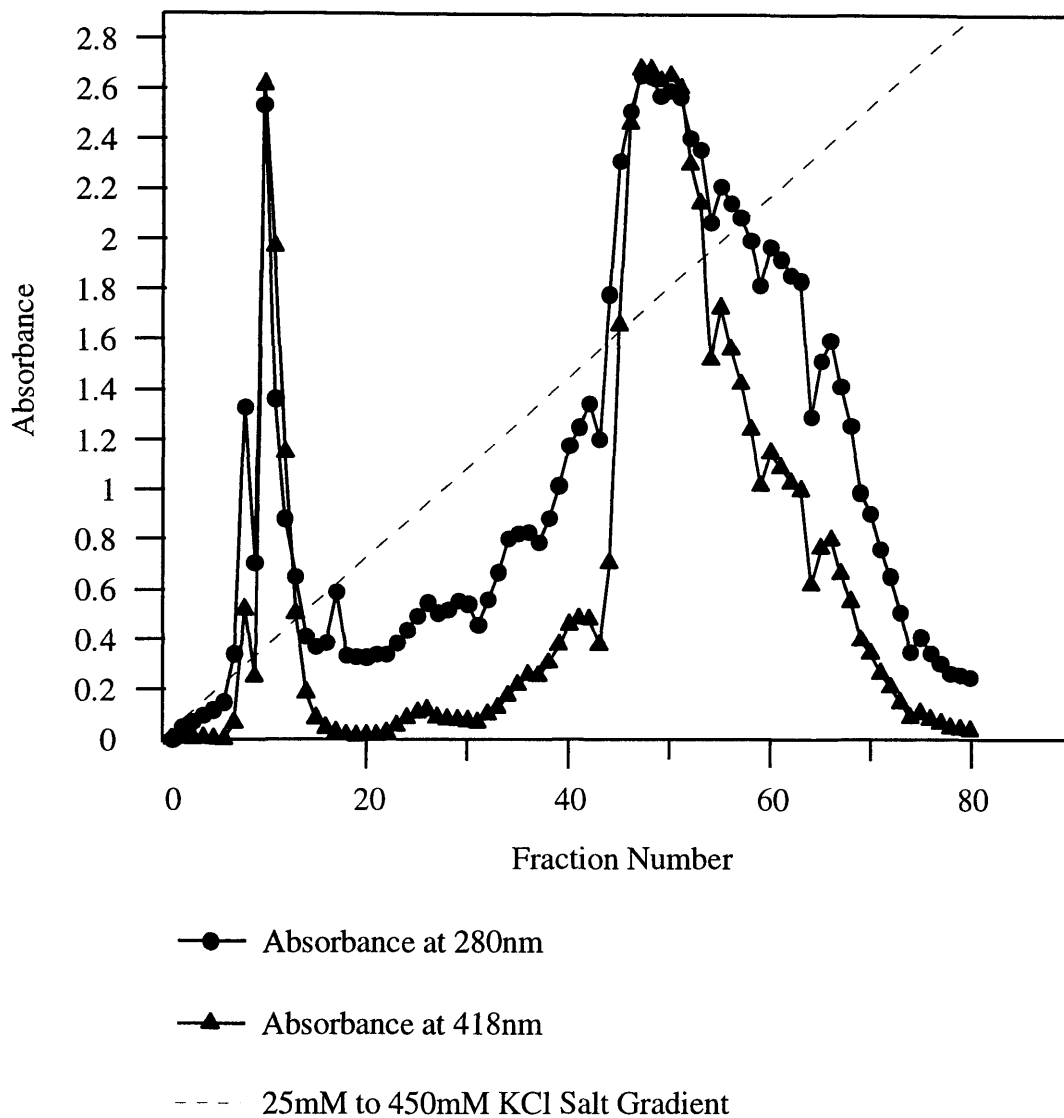


**Figure 3.6:** FPLC profile after loading P450 BM3 onto a HiLoad 26/10 Q sepharose column. 470mg of intact P450 BM3 was loaded onto a HiLoad Q sepharose column and eluted using a linear gradient of 25mM to 450mM KCl in FPLC buffer. 5mL fractions were collected. The absorbance at 280nm and 418nm was measured for each of the fractions, with the resulting profile above. Fraction number 45 to 56 were found to have an  $A_{418}/A_{280nm}$  ratio greater than 0.7 and were collected for further purification.

### 3.3.2 Mutant Protein Purification

The mutant intact P450 BM3 and the mutant haem domains were purified using the same procedure as developed for the wild type proteins, with one exception. Complete purification of the phenylalanine 87 to alanine (F87A) mutant proteins resulted in low, almost negligible yields of both the intact and haem domain enzymes. At the start of the purification it was apparent that the cell lysates for the F87A mutant proteins were paler than the normal red colour for the wild type enzyme. SDS-polyacrylamide gels of the cell lysates, obtained from the growth of colonies from LB agar plates in 2YT media, indicated that both proteins were expressed as a significant proportion of the total cell protein. Low yields of the pure protein may have occurred at some point during the purification procedure, due to either the action of proteases or to spontaneous degradation, though there is another more plausible explanation. The aromatic side chain of phenylalanine 87 (F87) lies perpendicular to the haem moiety in the three dimensional structure and its nearest atom is 5.66Å distance from the haem iron. The aromatic ring of the phenylalanine side chain may associate with the haem ensuring that it is positioned correctly within the substrate binding site and stabilising the ring such that it remains coordinated to cysteine 400 throughout purification. Removal of the aromatic ring by the F87A mutation increases the solvent accessible area in the substrate binding site immediately above the haem and this increased solvation may contribute to its loss. Thus it is possible that after expression of the F87A mutant intact P450 BM3 and its haem domain, difficulties in the retention/stabilisation of the haem moiety lead to loss of the haem moiety which resulted in protein unfolding such that the mutant enzymes could not be purified using the protocol described in the Material and Methods. Subsequent protein purifications of the F87A mutant P450 proteins were therefore performed in the presence of equimolar concentrations, as estimated by the absorbance at 418nm, of imidazole which was added immediately prior to cell lysis. This compound displaces the water molecule coordinated at the sixth position of the oxidised iron ( $\text{Fe}^{3+}$ ) and will form a stabilising adduct which can subsequently be removed by dialysis (McKnight *et al.*, 1993).

The total amount of pure protein obtained for the intact P450 BM3 and its haem domain varied for each of the mutations produced and the final amounts are represented in Table 3.1. The overall yields of the R47E and R47C mutant intact P450 BM3 and the R47E mutant haem domain are approximately the same as that for the wild type proteins. There is however one result that is lower than expected, that is the yield of 44.4 mg/L for the R47C mutant haem domain. This was due to loss of protein during the purification procedure, specifically when using the DEAE sephadex column.

**Table 3.1:** Concentration of pure intact P450 BM3 and its haem domain obtained after complete purification of the wild type and mutant proteins.

Protein	Total Yield (mg/L)	
	Intact P450 BM3	Haem domain
Wild Type	174.0	234.9
R47E Mutant	97.4	247.2
R47C Mutant	106.3	44.4
F87A Mutant	57.5	91.5

Table 3.2 lists the recovery for products of the arginine 47 to glutamic acid (R47E) mutation for both the intact P450 BM3 and its haem domain following each of the purification steps. The average harvest at 20.07 g wet weight of cells per litre of culture for both the wild type proteins and 14.33 g wet weight of cells per litre of culture for an average of all the mutant proteins were significantly higher than reported yields for the wild type protein of 8-9g/L (Kim and Fulco, 1983; Narhi and Fulco, 1986) and 13.2g/L (Black *et al.*, 1994).

The purity at each step was also estimated by calculating the  $A_{418}/A_{280nm}$  ratio. During the purification, some partial degradation of the intact P450 BM3 mutants was observed through a combination of loss of the haem moiety and proteolysis, however the majority of the degraded protein was removed during the first FPLC column. This

is in keeping with the observations by Yeom *et al.* (1995) that there is partial degradation of the mutant proteins during the purification procedure.

**Table 3.2:** Purification of recombinant intact P450 BM3 and its haem domain, both containing the R47E mutation.

	Intact P450 BM3			Haem domain		
	Yield		$A_{418}/A_{280nm}$ ratio	Yield		$A_{418}/A_{280nm}$ ratio
	mg/L <sup>a</sup>	%		mg/L <sup>a</sup>	%	
Wet weight cells (g/L)	14.6			14.5		
French press	389.1	100	0.072	404.4	100	0.161
(NH <sub>4</sub> ) <sub>2</sub> SO <sub>4</sub> precipitation	281.9	72.5	0.184	390.4	96.5	0.457
DEAE sephadex anion exchange	229.0	58.9	0.366	294.6	72.9	1.209
HiLoad Q (P450 BM3)	134.2	34.5	0.703	<sup>-b</sup>	<sup>-b</sup>	<sup>-b</sup>
Hydroxyapatite (haem domain)	<sup>-b</sup>	<sup>-b</sup>	<sup>-b</sup>	259.0	64.0	1.623
Sephacel S300/ Superdex 200	97.4	25.0	0.745	247.2	61.1	1.889

<sup>a</sup> The amount in milligrammes of protein present at each stage of the purification procedure obtained from 1L of growth culture.

<sup>b</sup> Column not used in purification procedure.

Samples from each stage in the purification procedure were removed and stored at 4°C. These samples and the purified, correctly folded proteins, as shown by their

absorption spectra, were analysed using an 8% SDS-polyacrylamide gel. Example gels for the purification are shown in Figures 3.7 and 3.8, representing purification of the arginine 47 to cysteine mutants of the intact P450 BM3 and its haem domain, respectively. The cytochrome P450 proteins, when compared to molecular weight markers, were shown to have molecular mass equivalent to the expected masses as calculated from the sequence and previously published estimates (Wen and Fulco, 1987; Li *et al.*, 1991; Miles *et al.*, 1992). The molecular masses were shown experimentally to be approximately 119kDa for intact P450 BM3 and 54kDa for its haem domain.

Figure 3.9 represents an SDS-polyacrylamide gel to verify the purity of all the intact P450 BM3 and haem domain proteins used in this body of work. There are apparent weak contamination bands corresponding to proteins of approximately 85 and 100kDa present in all samples of the 'pure' intact P450 BM3. Using an absorbance ratio of 0.7 to represent pure protein (A. W. Munro, Personal Communication), the samples of intact proteins used in this gel are between 85.4% and 97.9% pure as calculated from their  $A_{418\text{nm}}/A_{280\text{nm}}$  absorbance ratio. The use of protease inhibitors during the purification procedure suggests that these are more likely to be due to contaminating proteins which could not be separated during the protein purification rather than protein degradation products.

### **3.3.3 Incorporation of the P450 Haem**

For the purified wild type and R47E mutant proteins intact P450 BM3 and its haem domains, the specific content of the P450 haem was determined as described by Omura and Sato (1964). The results are depicted in Table 3.3. The values for the haem domain are somewhat lower than the theoretical value of 18.4 nmol/ng based on the molecular mass, at 89.8% for the wild type and 82.9% for the R47E mutant. As the haem domains are overexpressed as the major protein in *E. coli*, small shortfalls in the haem content may reflect difficulty for the cell in matching the rates of haem synthesis and incorporation to the high rate of protein production. The values for the intact P450 BM3 are in complete agreement, which contrasts with previously published

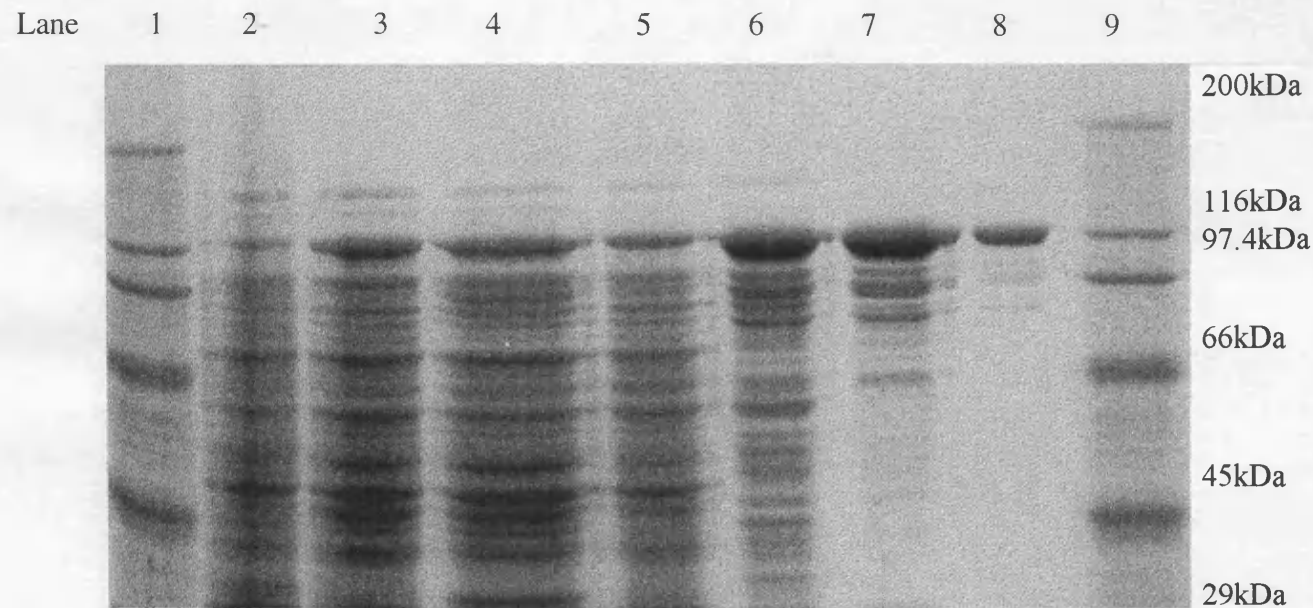


**Figure 3.7:** Electrophoretic analysis of various fractions from the purification of the R47C mutant of intact P450 BM3. Samples were subjected to SDS-PAGE with migration from top to bottom, using a 8% separating gel. *Lane 1 and 9*, molecular weight standard protein marker; *lane 2*, crude cell extract; *lane 3*, sample post French press; *lane 4*, supernatant post 25% ammonium sulphate precipitation ; *lane 5*, pellet post 60% ammonium sulphate precipitation; *lane 6*, sample post DEAE sephadex column; *lane 7*, sample post HiLoad Q column; *lane 8*, sample post Superdex 200.

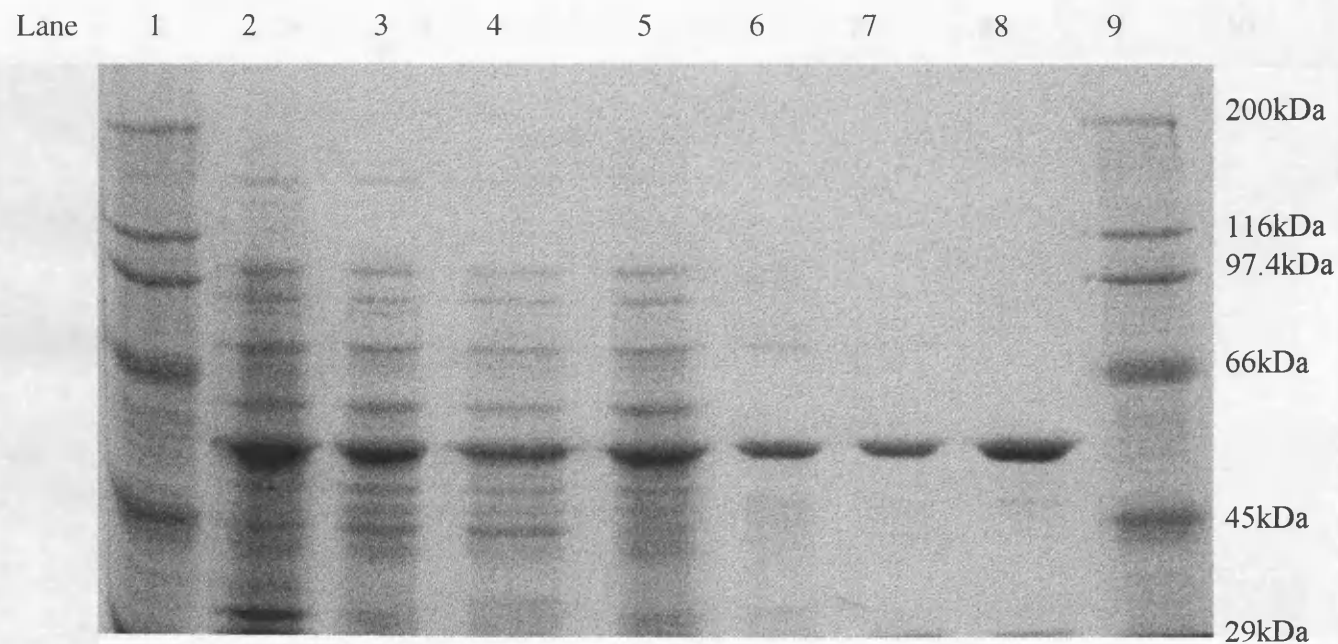


**Figure 3.8:** Electrophoretic analysis of various fractions from the purification of the R47C mutant of the haem domain of P450 BM3. Samples were subjected to SDS-PAGE with migration from top to bottom, using a 8% separating gel. *Lane 1 and 9*, molecular weight standard protein marker; *lane 2*, crude cell extract; *lane 3*, sample post French press; *lane 4*, supernatant post 25% ammonium sulphate precipitation; *lane 5*, pellet post 60% ammonium sulphate precipitation; *lane 6*, sample post DEAE sephadex column; *lane 7*, sample post ceramic hydroxyapatite Q column; *lane 8*, sample post Superdex 200.

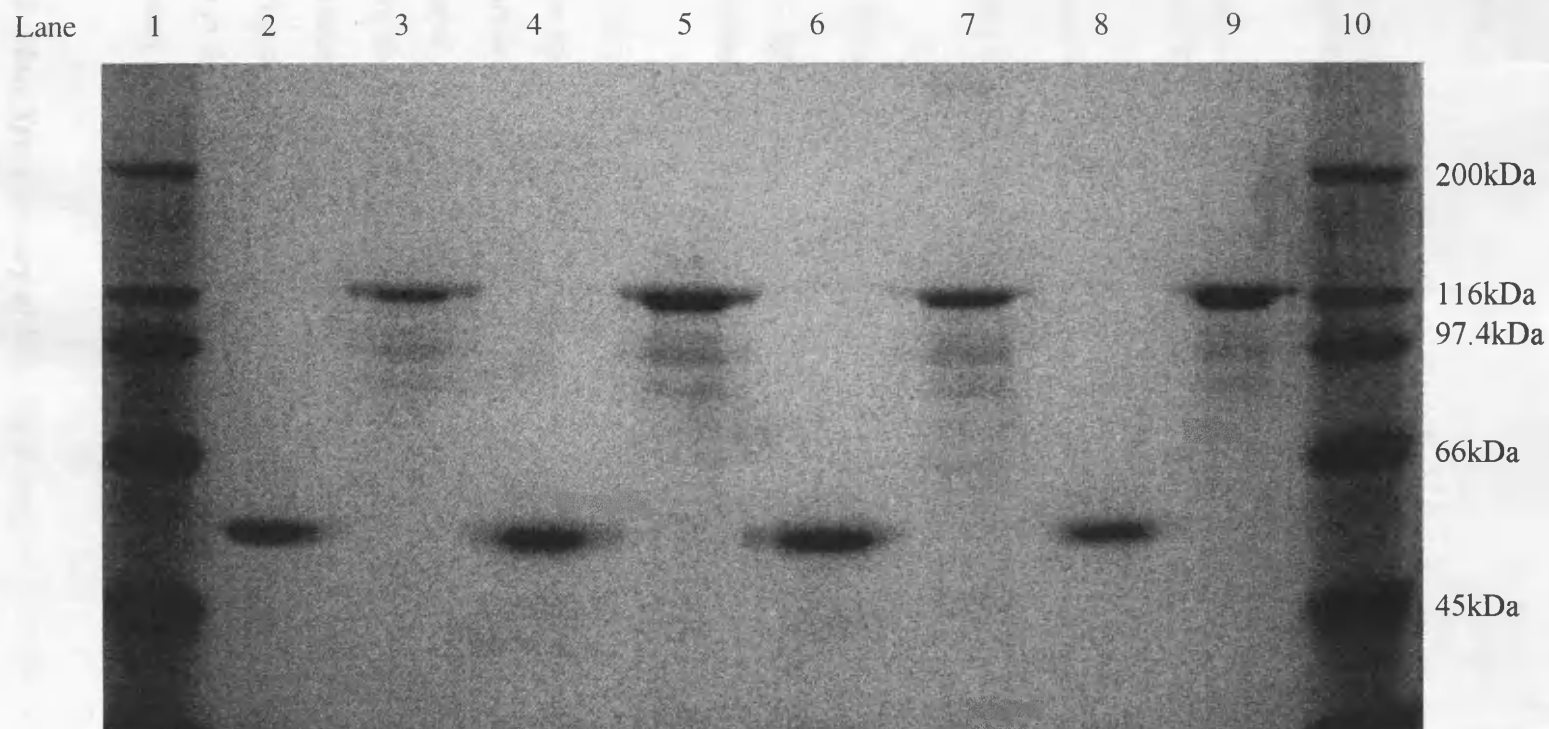


**Figure 3.9:** Electrophoretic analysis of all the wild type and mutant samples of intact P450 BM3 and its haem domain. Samples were subjected to SDS-PAGE with migration from top to bottom, using a 8% separating gel. *Lane 1 and 10*, molecular weight standard protein marker; *lane 2*, wild type haem domain; *lane 3*, wild type intact P450 BM3; *lane 4*, R47E mutant haem domain; *lane 5*, R47E mutant intact P450 BM3; *lane 6*, R47C mutant haem domain; *lane 7*, R47C mutant intact P450 BM3; *lane 8*, F87A mutant haem domain; *lane 9*, F87A mutant intact P450 BM3.

**Table 3.3:** The specific content of P450 haem for the wild type and R47E mutant intact P450 BM3 and haem domain.

Protein	Mutant	P450 Content (nmol/mg)	
		Obtained Value	Theoretical Value
Haem Domain	Wild Type	16.53	18.4
	R47E Mutant	15.26	18.4
Intact P450 BM3	Wild Type	8.40	8.4
	R47E Mutant	8.46	8.4

results (5.6nmol/mg, Miles *et al.*, 1992; 5.5nmol/mg, Boddupalli *et al.*, 1990).

### 3.4 Protein Characterisation

#### 3.4.1 Spectral Characterisation of the Wild Type and Mutant Intact P450 BM3 and its Haem Domain

All the recombinant proteins showed identical spectral features, which are represented by the spectra for the wild type protein in Figure 3.10. Figure 3.10a) shows the absorption spectra for the wild type haem domain. There are well resolved  $\alpha$  and  $\beta$  bands at 570 and 535nm respectively as well as a strong Soret peak at 418nm. Figure 3.10b) shows a typical spectrum of the intact enzyme with a Soret band at 418nm and an  $\alpha$  band at 567nm. The  $\beta$  band in the 525nm region is not well resolved, due to the overlap with a broad shoulder in the 440-490nm region. This shoulder, which is not seen in the spectra of other P450s, is due to the flavin prosthetic groups in the C-terminal reductase domain (Narhi and Fulco, 1986).

#### 3.4.2 Mass Spectrometry of Wild Type Intact P450 BM3 and its Haem Domain

Mass spectrometry was performed on the intact P450 BM3 and its haem domain where

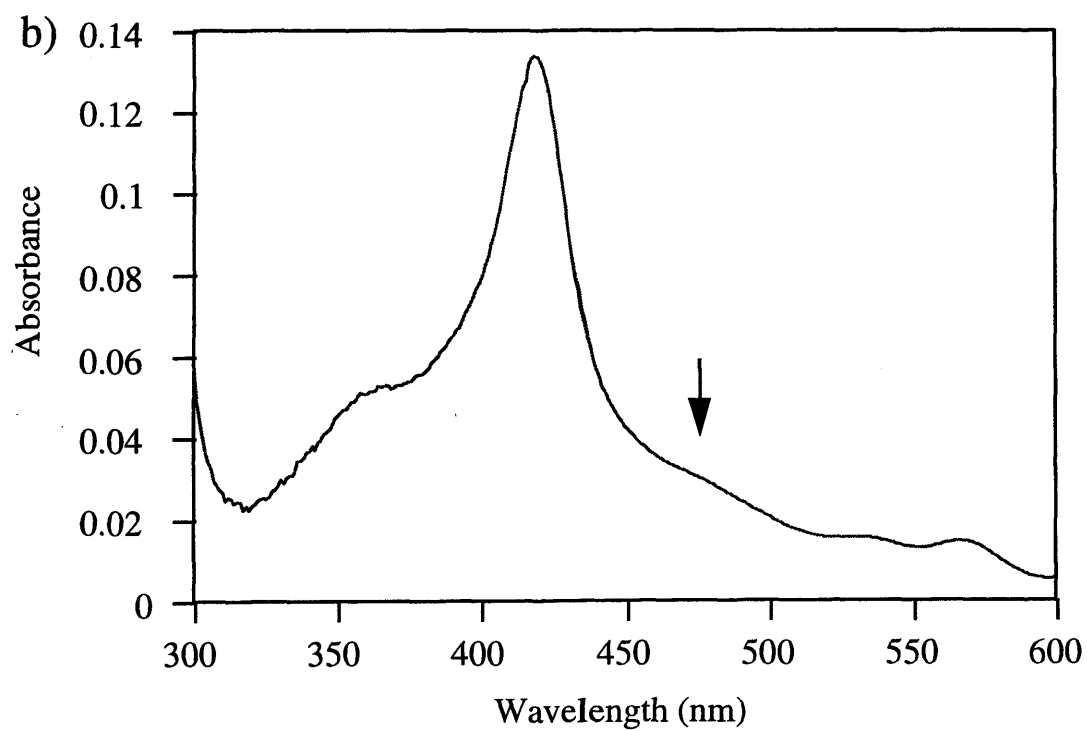
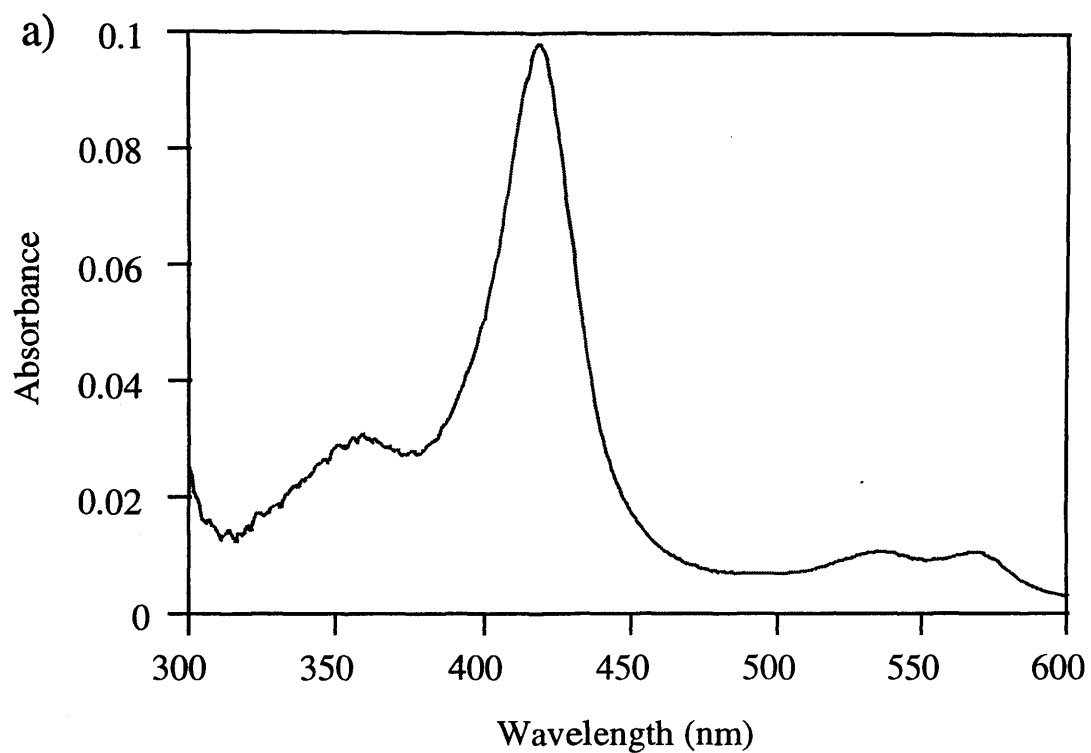


**Figure 3.10:** Absorption spectra of a) the wild type haem domain and b) the wild type intact P450 BM3. The arrow marks the position of the 440-490nm shoulder which indicates the presence of the flavin prosthetic groups.

samples used had undergone purification on HiLoad Q sepharose and ceramic hydroxyapatite respectively followed by gel filtration using either the standard chromatography sephacel S300 column or the FPLC. MALDI-TOF mass spectrometry was performed solely on the wild type intact P450 BM3, whereas Electrospray mass spectrometry (ES-MS) was performed on all proteins, including the wild type and mutants. The results for mass spectrometry of the wild type cytochromes are considered below, whereas the ES-MS results for the mutant enzymes are discussed in the relevant chapters.

#### ***3.4.2.1 MALDI-TOF Mass Spectrometry of the Wild Type Intact P450 BM3***

Matrix Assisted Laser Desorption Ionisation Time of Flight (MALDI-TOF) was developed in the late 1980s and allows the molecular weight determination of polar molecules in the mass range up to 100,000-200,000Da. In this technique, picomole amounts of the sample are embedded in either a liquid, for example glycerol, or a solid matrix, for example sinapinic acid, which is selected to strongly absorb laser light at the absorption band employed. Energy is transferred to the sample to create positively charged ions (Williams and Fleming, 1995). In the TOF mass spectrometer, ions are accelerated through a potential and drift down the tube toward the detector. If all the ions arrive at the beginning of the tube with the same energy, then those differing in mass will have different velocities. So for a tube of known length, the time of flight can be used to calculate the molecular mass. As the ions must be produced at an accurately known start time TOF analysers are mainly used with pulsed ionisation techniques (Wait, 1993).

The results obtained from the MALDI-TOF mass spectrum analysis gave an average mass of 119,401Da, with standard error of 175. This value is considerably higher than the estimated molecular weight of 117,651Da for the intact P450 BM3 apoprotein as calculated from its amino acid sequence. If the molecular weight of the holoenzyme is considered, the molecular weight would include the intact P450 BM3 protein without the N-terminal methionine (117,651Da), the haem moiety consisting of protoporphyrin IX (562.7Da) with co-ordinated iron atom (55.8Da) and the two flavin moieties in the

reductase domain of the protein, FAD (785.5Da) and FMN (456.3Da). This yields a combined total molecular weight of 119,511.3Da which is within the error limits of 0.1% for the result from the MALDI-TOF analysis showing that not only the haem but also the two noncovalently bound flavins are retained in MALDI-TOF MS.

#### ***3.4.2.2 Electrospray Mass Spectrometry of the Wild Type Intact P450 BM3***

Electrospray ionisation (ESI) refers to a small flow of liquid from a capillary needle where a potential difference is applied between the end of the capillary and an electrode nearby. Under these circumstances, the liquid leaving the capillary does not leave as a drop, but rather as spray or fine mist. The spray consists of highly charged liquid droplets that may be positively or negatively charged, depending on the sign of the voltage applied to the capillary. If this spray contains sample molecules, then sample molecule ions can be obtained by evaporation of the solvent. This is accomplished by passing a drying gas across the spray until the mutual repulsion of the multiply charged sample molecules is sufficient to overcome the forces holding the droplet together and Coulombic forces eject the charged sample molecules into the vapour phase. The residual charged particles are carried through a capillary into an ion analyser, in this instance a quadrupole mass spectrometer (Williams and Fleming, 1995).

The sample of intact P450 BM3 was subsequently analysed using electrospray ionisation sample analysis by mass spectrometry (ES-MS). The results obtained indicated a mass of 117,648Da, with standard error of 74Da. The intact P450 BM3 has a calculated molecular weight of 117,651Da for the protein expressed without the N-terminal methionine or 117,782Da for the protein expressed containing the N-terminal methionine. The observed molecular weight for this protein is clearly much closer to the calculated mass with the N-terminal methionine removed assuming there has been loss of all cofactors on electrospray ionisation.

#### ***3.4.2.3 Electrospray Mass Spectrometry of the Wild Type Haem Domain***

The results from the mass spectroscopic analysis of the haem domain were not so

straight forward. This protein was only analysed by ES-MS, which produced a series mass of 53,350Da with a standard error of 5Da. The measured value for the molecular weight of the haem domain does not agree with those calculated by various computer packages. Using the software provided on the mass spectrometer, the molecular weight for the haem domain was calculated from the amino acid sequence to be 53,855Da, where methionine represents the first amino acid residue and assuming all cofactors, in this protein only the haem moiety, had been removed. This means that in the case of the haem domains the measured mass is approximately 511 mass units less than that those calculated from the sequence. This would correspond to either three or four amino acid residues. The results of the N-terminal sequencing verify there are no residues missing from the N-terminus from both the wild type and mutant cytochrome P450 proteins, indicating that this discrepancy cannot be due to N-terminal digestion of the protein sample. At the C-terminal of the haem construct the predicted sequence is ....AKKVR (Ruettinger *et al.*, 1989). Removal of the last four residues would lead to a loss of 511 mass units. The mass spectrometry results do not allow us to distinguish between the removal of the last four residues (KKVR) from the C-terminal, with a calculated molecular mass of 53,346Da or removal of the last three residues (KVR) together with the N-terminal methionine with a calculated molecular mass of 53,342Da. For the wild type protein, it appears that the latter is the most likely as the N-terminal sequencing results did not detect any evidence of an N-terminal methionine. Whichever of the two possible scenarios has occurred, it appears that the haem domains are expressed as slightly C-terminally truncated proteins, presumably due to proteases present in *E. coli*.

### ***3.4.3 N-Terminal Sequencing of Both Wild Type and Mutant Proteins***

N-terminal sequencing was performed on all samples of wild type and mutant intact P450 BM3 and haem domain proteins. The N-terminal sequences were successfully obtained for the first 18 residues of all proteins. The wild type, F87A and R47C proteins possess identical amino acid sequences of:

Thr-Ile-Lys-Glu-Met-Pro-Gln-Pro-Lys-Thr-Phe-Gly-Glu-Leu-Lys-Asn-Leu-Pro

Whereas the R47E mutant intact and haem domain proteins had the N-terminal sequence of:

(Met)-Thr-Ile-Lys-Glu-Met-Pro-Gln-Pro-Lys-Thr-Phe-Gly-Glu-Leu-Lys-Asn-Leu-Pro

The protein sequences are identical to the sequence of intact P450 BM3 as published by Ruettinger *et al.* (1989). These results indicate that not all the recombinant genes produced proteins where the N-terminal methionine had been cleaved by post-translational modification.

### 3.5 Discussion

Attempts have been made to reconstitute the fatty acid hydroxylase activity associated with the intact P450 BM3 by mixing together the isolated flavoprotein domain and the haemprotein domain recovered after tryptic cleavage and domains made available using recombinant systems (Narhi and Fulco, 1987; Li *et al.*, 1991; Miles *et al.*, 1992; Boddupalli *et al.*, 1992; Munro *et al.*, 1994; Modi *et al.*, 1995a). The activity of the reconstituted systems reported varies markedly. Munro *et al.* (1994) found that assay mixtures containing the haem domain and the reductase gave an activity as measured by NADPH consumption equivalent to 0.1-0.3% of the intact enzyme activity of P450 BM3, but comparable to the specific activities of the reconstituted mammalian P450s (Guengerich, 1991). Modi *et al.* (1995a) also found that the maximum catalytic activity possible by mixing the two individual domains in a ratio of 1:12 for either domain was approximately 0.3% of that for the intact cytochrome P450 BM3 in complete agreement with the results of Munro *et al.* (1994). This is in contrast to Boddupalli *et al.* (1992) who reported an activity corresponding to 80% of the intact enzyme as measured by oxygen consumption. These results must be viewed with some caution as they did not consider the NADPH oxidase activity, exhibited by the reductase domain in the absence of an electron acceptor, and saturation kinetic behaviour was not demonstrated (Munro *et al.*, 1994). Even so, these results suggest that the natural fusion protein possesses some unique properties, such that within the

intact P450 BM3 the linker region plays an important role in “tethering” the two major domains such that they remain in close proximity so as to enhance the rate of electron transfer for efficient catalysis (Munro *et al.*, 1994; Murataliev and Feyereisen, 1996; Sevrioukova *et al.*, 1997). With this information in mind, it was considered essential that any site-directed mutagenesis was performed in both the intact P450 BM3 and its haem domain such that enzymatic activity could be measured using the intact system and the haem domain was available for other studies, including NMR and absorption spectroscopy.

Site-directed mutagenesis was performed using the Sculptor *in vitro* mutagenesis system, purchased from Amersham International plc. Although the desired mutations were obtained, the results were on the whole unsatisfactory for the reason detailed in the results section. If it were necessary to generate further mutant proteins, the site-directed mutagenesis protocols of choice would be either that described by Kunkel (1985) or the QuikChange site-directed mutagenesis system as described by Stratagene. The method described by Kunkel (1985) requires single stranded DNA (ssDNA) as the template. The ssDNA is prepared by growth using an *E. coli dut<sup>-</sup> ung<sup>-</sup>* strain. This strain is deficient in dUTPase (*dut<sup>-</sup>*) resulting in an increased pool of dUTP. Uracil that is incorporated into the DNA is not removed as this host strain is also uracil glycosylase deficient (*ung<sup>-</sup>*). The template DNA purified from this system contains uracil as opposed to thymine. When this uracil-containing template is applied to a site-directed mutagenesis protocol, the newly synthesised second strand of DNA will contain the desired mutation and no uracil. When this is transformed into a wild type (*ung<sup>+</sup>*) host cell, expression of the newly synthesised non-uracil-containing closed circular complementary strand will be more strongly favoured, resulting in a high efficiency of mutagenesis.

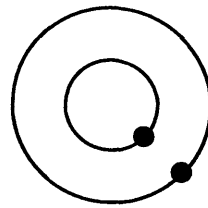
The QuikChange mutagenesis kit allows point mutations, amino acid substitution and insertion or deletion of single or multiple amino acids using double stranded DNA (dsDNA). This eliminates the need for subcloning and for ssDNA purification. The protocol differs from that for the Sculptor kit in that no unique restriction sites are required and the procedure is completed simply in four steps. The basic procedure

(Figure 3.11) utilises dsDNA vector containing the insert of interest and two synthetic oligonucleotide primers, complementary to opposite strands of the vector, containing the desired mutation. The oligonucleotide primers are annealed and extended by temperature cycling using the high fidelity *Pfu* DNA polymerase, generating mutant plasmids containing staggered nicks. The product is treated with *Dpn* I, an endonuclease which is specific for methylated and hemimethylated DNA, to digest the parental DNA template. DNA isolated from most *E. coli* strains are dam methylated which renders it susceptible to digestion by *Dpn* I. The nicked vector DNA containing the desired mutation is finally transformed into XL2-Blue, where the nicked DNA is repaired.

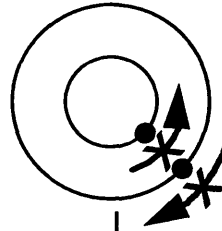
After purification of the F87A mutant of the intact P450 BM3, it was discovered that the sequence of the gene contained three other mutations that had been unknowingly incorporated resulting in the conversion of the amino acid residues tyrosine 429 and glutamate 430 to aspartate and lysine, respectively. Both these residues are located in a loop between the  $\beta$ -strands 3-3 and 4-1 which are part of a small  $\beta$ -domain situated near the C-terminal. The mutated side chains are depicted in Figure 3.12 using the x-ray crystal structure of the substrate-free P450 BM3 (Ravichandran *et al.*, 1993). This represents the F87A mutant haem domain with tyrosine 429 and glutamate 430 (a) as with the wild type protein and the same mutant enzyme now containing the aspartate 429 and lysine 430 mutations (b). It is evident from these representations that these residues are located near the surface of the protein and that amino acid side chains will interact with the solvent. Using the program GRASP (Nicholls and Honig, 1993) representations for the surface charge potentials were constructed for the two F87A mutant haem domains, with (b) and without (a) the additional substitutions at position 429 and 430 (Figure 3.13).

The DelPhi program was used to calculate the electrostatic potentials for both these F87A mutant proteins and is represented in Figure 3.13 with the molecules oriented in to represent the distal face. Comparison of Figure 3.13 (a) and (b) indicates there are no radical differences between the surfaces of the two F87A mutant haem domains. It is only when looking specifically at the surface in the immediate vicinity of residues 429

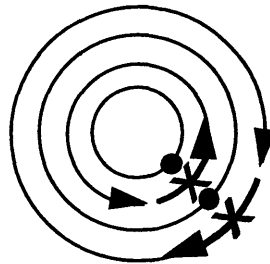
Gene in plasmid with target site ● for mutation



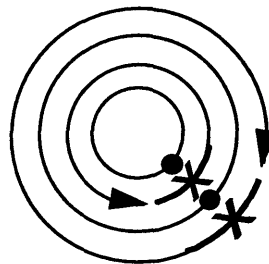
Denature plasmid and anneal primers containing the desired mutation X



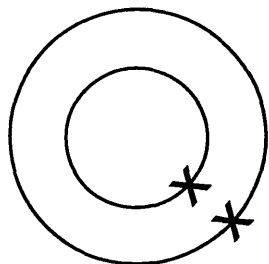
Temperature cycle to extend and incorporate mutation primers resulting in nicked circular strands



Digest methylated nonmutated parental DNA template



Transform the resulting annealed double stranded nicked DNA molecules



After transformation the XL2-Blue *E. coli* cell repairs the nicks in the plasmid

**Figure 3.11:** Schematic representation of the protocol for site-directed mutagenesis using the QuikChange site-directed mutagenesis system as described by Stratagene. (Taken from the Stratagene Protocol).

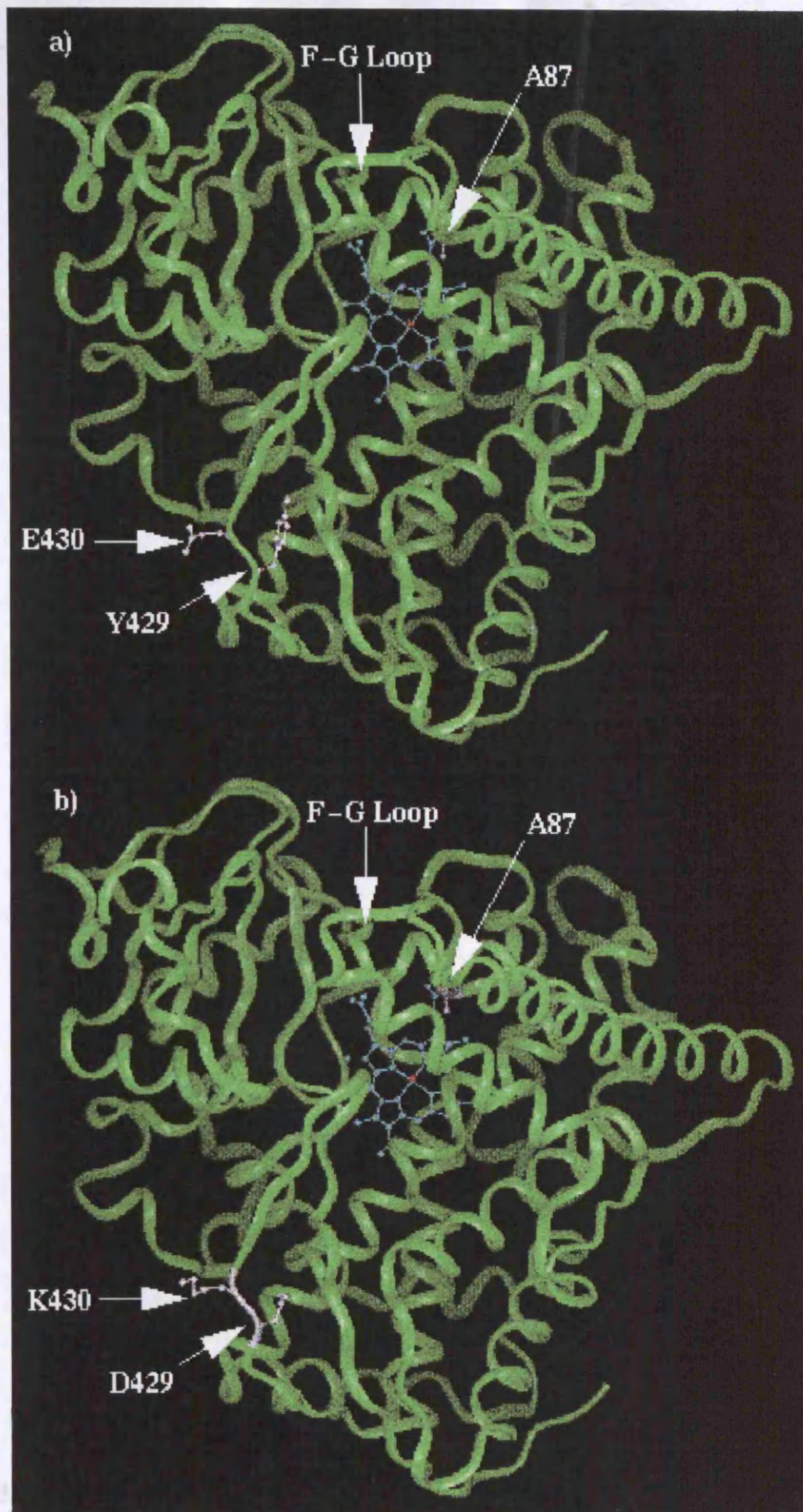


**Figure 3.12:** Ribbon diagrams of the haem domain of cytochrome P450 BM3 from *Bacillus megaterium* (Ravichandran *et al.*, 1993) containing the F87A mutation (a) and the additional spontaneous mutations of tyrosine 429 to aspartate and glutamate 430 to lysine (b). The F-G loop has been marked as well as the side chains at positions 429 and 430 in both structures.

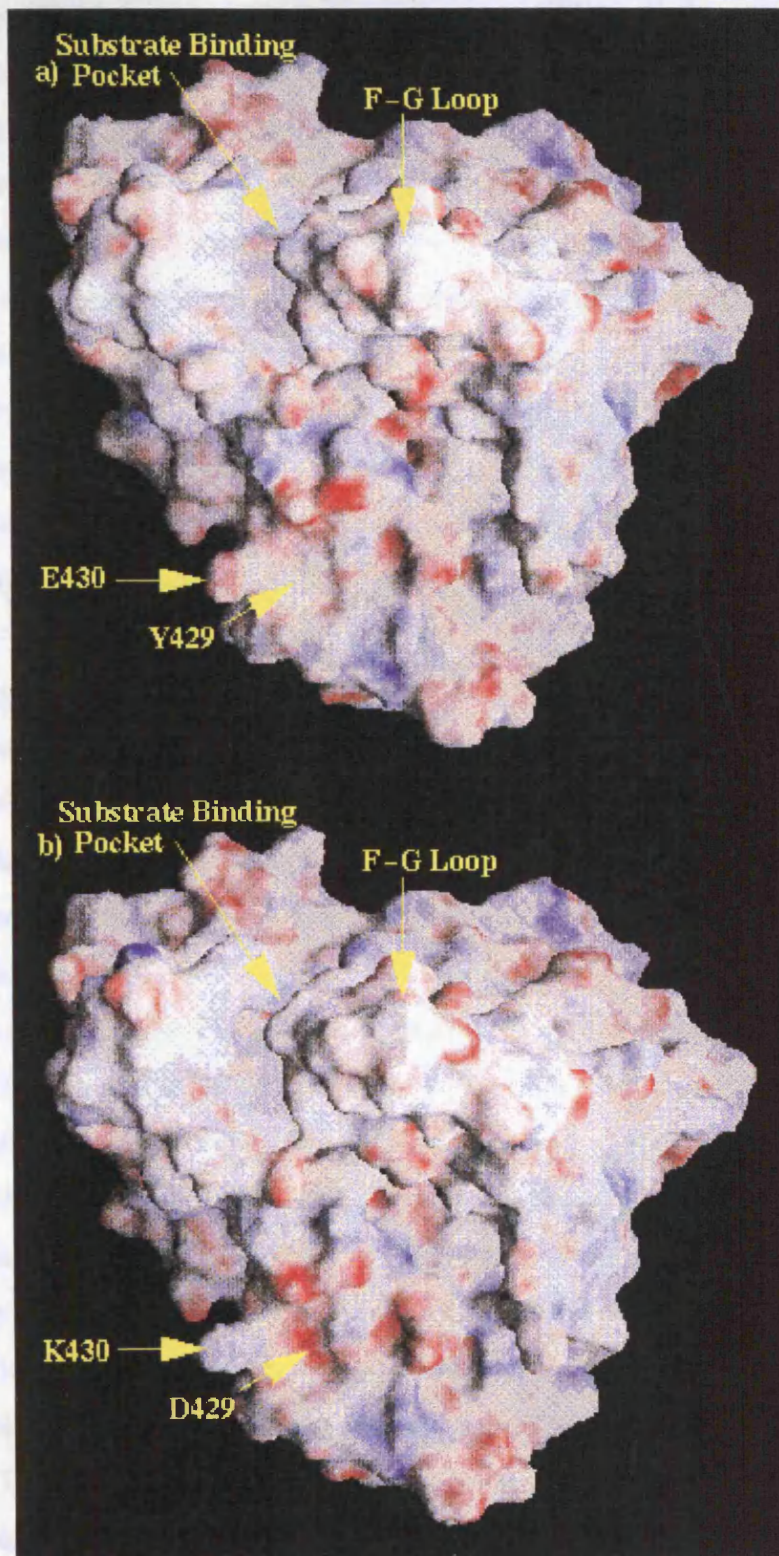


**Figure 3.13:** Electrostatic potentials at the molecular surface of the haem domain of cytochrome P450 BM3 containing the F87A mutation (a) and the additional spontaneous mutations of tyrosine 429 to aspartate and glutamate 430 to lysine (b). The F-G loop as well as the side chains at positions 429 and 430 have been identified in both structures. Surface points are colour coded from blue to red corresponding to positive to negative potential respectively, with neutral points coloured white.

and 430, located in the lower left-hand side of the diagrams, that the differences become apparent. These residues are located at the extreme edge of the haem domain, as far as possible from the haem binding site and far from the substrate binding pocket which is primarily defined by the F and G helices, as indicated in Figure 3.13. The side chain of residue 430 protrudes from the surface into the solvent whereas the side chain of residue 429 appears to lie more in the plane of the surface of the molecule. The substitutions at these positions have resulted in the addition of a negatively charged aspartate by the removal of the neutral tyrosine 429 and a change from the negatively charged glutamate to a positively charged lysine at position 430. Thus the overall effect of these mutations is that there has been a localised change in the surface charge potential by the addition of a positive charge.

Limited trypsin digestion of the intact P450 BM3 results in two domains that are readily separated from each other by HPLC on a DEAE-5PW column (Nahri and Fulco, 1987). It is theoretically possible to generate the two domains of the F87A mutant of the intact P450 BM3 and then isolate the haem domain containing the spontaneous mutations. Comparison could then be made between this haem domain and the recombinant haem domain generated and purified for the NMR studies which does not contain the substituted amino acids at positions 429 and 430. Referring to Figure 3.12, these mutations will not result in gross alteration to the molecular mass (a decrease of approximately 49Da) so there are likely to be no detectable effects on the rate of gel filtration by either of the F87A haem domains. The spontaneous mutations are not located either near to or within the substrate binding pocket and so are unlikely to have any effect on substrate binding. Unfortunately there does not exist a reliable reconstitution assay as discussed earlier in this chapter so it is impossible to accurately assess whether there is any difference in catalytic activity between the two F87A haem domains. The MacVector version 4.1.4 program was used to calculate the isoelectric point (pI) of the two F87A mutant haem domains. There does not appear to be a radical change in the pI, eliminating the possibility of detecting any difference by isoelectric focusing. Therefore, the conclusions drawn from the available evidence is that the spontaneous mutations will have had no effect on the overall structure of the haem domain and as a consequence will have no effect on the catalytic activity of the

F87A mutant. Ultimately this can only be proved by construction of the F87A mutant of the intact P450 BM3 which contains no spurious alterations.

During purification of the intact P450 BM3, there was evidence that the haem domain was also being produced, as indicated by the typical P450 absorption spectrum and the SDS-PAGE molecular weight estimate of 54kDa. This was probably due to proteolysis of the intact protein during storage. Whether the degradation occurred during cell growth, cell lysis or protein purification was not determined. It appears the addition of the protease inhibitors benzamidine hydrochloride and phenylmethanesulphonyl fluoride (PMSF) in all buffers could not prevent this from happening. There also appeared a tiny contamination band of approximately 65kDa on the SDS-PAGE gel of the entire purification procedure (Lane 7, Figure 3.7). This probably corresponded to the reductase domain which represents the other degradation product of the intact P450 BM3. Presumably this protein possesses the same properties that allows for the purification of the intact P450 BM3 using the HiLoad Q column. The results depicted in Table 3.1 suggest that after mutations to arginine 47, yields of pure protein are comparable to that of the wild type. However the mutation at position 87 in P450 BM3 which resulted in complete removal of an aromatic ring had a more profound effect. From the data the exact reason is unclear though it is likely to have resulted from a combination of effects. The paler cell lysates for the F87A mutant enzymes suggests that the proteins were expressed either at a lower level, which is unlikely as an identical expression system was used to that of the wild type enzyme, or that expression resulted in a mixed population of holo- and apo-protein. Thus ultimately poor protein expression at the cellular level would be responsible for the low yields. However, the SDS-polyacrylamide gel indicated that the mutant enzymes were expressed as a significant proportion of the total cell protein. Under these circumstances, if the phenylalanine ring plays a role in stabilising the haem moiety within the haem domain, haem depletion may occur during the purification procedure due to the unstable association of the haem moiety with the mutant enzyme.

The results obtained from N-terminal sequencing experiments indicated the wild type and mutant proteins all possess the same N-terminal sequence as published by

Ruettinger *et al.* (1989). They also indicated that the recombinant genes produced proteins, where not all of the N-terminal methionine had been cleaved by post-translational modification. The R47E mutant intact P450 BM3 and its haem domain were transformed into TG1, the host strain provided with the Sculptor *in vitro* mutagenesis system, for DNA manipulation, protein expression and protein purification. These proteins appeared to possess an N-terminal methionine. The wild type expression systems were obtained already transformed into the XL1-Blue *E. coli* strain and the other mutant expression vectors were transformed into XL1-Blue after the mutagenesis procedure. XL1-Blue contains the Tn10 gene on the F' plasmid which, together with the  $\beta$ -lactamase gene on the expression vector, allows selection using both the tetracycline and ampicillin antibiotics. Use of this host strain was necessary to avoid an ampicillin resistant contamination within the laboratory. The proteins obtained when expressed using the XL1-Blue strain did not retain the N-terminal methionine when sequenced. Nahri and Fulco (1988) used the *E. coli* strain JM103 and did not detect any N-terminal methionine. This suggests that the presence of the N-terminal methionine may be dependent on the *E. coli* host strain used.

The data from the SDS-PAGE analysis provide evidence that the purified proteins were of approximately the correct molecular weight as they electrophorised at positions equivalent to their calculated molecular mass according to the protein sequence (Ruettinger *et al.*, 1989). However this does not provide proof of structural integrity as the proteins are treated with SDS which acts as a chaotropic agent, denaturing the protein which would result in loss of the associated cofactors such as the haem moiety and the flavins, FAD and FMN. The absorption spectra of the enzymes can provide this information as the spectra is characteristically defined by the presence of the protein in association with its cofactors. The absorption spectra of the wild type and mutant proteins of both the P450 BM3 and its haem domain were identical, indicating all the proteins possessed identical structures where the cofactors were present and correctly bound, suggesting that the overall three dimensional structures in the mutant proteins was not sufficiently perturbed to disrupt the proper integration of the three prosthetic groups, that is, the haem, FAD and FMN moieties. When considering the mass spectroscopy results pertaining to the haem domain it is not surprising that to

date it had not been determined that the haem domain is purified in a truncated form. The N-terminus can be readily defined by protein sequencing, however it is no simple task to determine the C-terminus and from the sequence (Ruettinger *et al.*, 1989) there are several potential tryptic cleavage sites in the interdomain region which could lead to heterogeneity of this domain (Miles *et al.*, 1992).

It is essential that any sample that is to undergo mass spectrometry is of the highest possible quality. If it is not, there is a risk that the spectra produced will not be of the highest standard and thus may not convey the information required. Some of the spectra generated by the ES-MS were considered to be of inferior quality. This was probably due to the presence of small amounts of contaminating proteins in the sample, resulting in an over complicated mass spectrum. Even though the ES-MS spectrum for the wild type intact P450 BM3 was believed to be of poor quality the results appear to be extremely precise for this protein of relatively large mass, especially as a standard error of 0.1% for the calculated molecular weight is considered reasonable. When comparing the results obtained from both types of mass spectrometry, they suggest a fundamental difference between the two methods. When the intact cytochrome P450 undergoes mass spectroscopic analysis using electrospray ionisation only the apoprotein sample will “fly” and thus be detected, whereas when using the MALDI-TOF sampling device, the intact protein will “fly” with its associated cofactors, giving a combined calculated molecular weight.

## ***Chapter 4: The Arginine 47 to Glutamic Acid Mutation***

### ***4.1 Introduction***

Point mutation studies in cytochrome P450s have yielded important information and identified key individual residues which are responsible for divergent substrate specificity (Johnson *et al.*, 1992; He *et al.*, 1995). Most of these key residues were found to be clustered around sites that were mapped to amino acids that formed the substrate-binding site of P450 cam, the only P450 monooxygenase for which the x-ray crystal structure had been solved at the time (Johnson, 1992). With this in mind, the x-ray crystal structure of the haem domain of P450 BM3 (Ravichandran *et al.*, 1993) was examined with careful consideration to identify residues that appeared within the substrate binding pocket. This cavity is approximately 10Å in diameter and 20Å in length from the surface to the haem iron and was found to be lined with the side chains of hydrophobic amino acids or with the carbon backbone of the strands of the  $\beta$ 1 sheet. The only charged residue in the substrate binding site is arginine 47 which is located at the opening of the substrate access channel (Ravichandran *et al.*, 1993). Since fatty acids of approximately 20Å in length are the optimal substrates for this enzyme (Miura and Fulco, 1975) it was proposed that the carboxylate group of the fatty acid substrate would be anchored to arginine 47 and the fatty acid would then extend down the access channel to the haem at the active site. Methylation of the fatty acid substrate has been shown to completely abolish the oxidation of palmitate (Miura and Fulco, 1975) lending further support to this hypothesis. Arginine 47 was substituted with glutamate to investigate the contribution, if any, of a positively charged side chain at position 47 in P450 BM3 to the binding of the negatively charged fatty acid substrates.

### ***4.2 Protein Expression and Characterisation***

Arginine 47 was substituted by glutamate both in the intact P450 BM3 and in its haem domain. In both cases yields of the Arg47→Glu (R47E) mutant proteins were comparable to those of the wild type, in the range of 200-250 mg pure protein per litre of culture. All proteins were shown to be pure by existing as a single band on a

Coomassie blue stained SDS-PAGE gel and by their absorbance ratio of  $A_{418\text{nm}}/A_{280\text{nm}}$ ; 0.745 for the R47E mutant intact P450 BM3 and 1.889 for the R47E mutant haem domain. N-terminal sequencing indicated that the initial residues of both proteins were identical to that published by Ruettinger *et al.* (1989).

### 4.3 Electrospray Mass Spectroscopy

Mass spectroscopy is widely used to estimate the molecular weight of biological compounds, but here it has also been used to confirm the presence of the R47E mutation. The wild type and R47E mutant intact P450 BM3 and haem domain proteins were analysed using electrospray ionisation sample analysis for mass spectroscopy (ES-MS). The results are listed in Table 4.1 and the raw data for the R47E mutant proteins depicted in Figure 4.1. The calculated masses were calculated from the recombinant protein sequence (Ruettinger *et al.*, 1989) using the software on the mass spectrometer. It was assumed that all the cofactors, that is the haem moiety, FAD and FMN, had been removed.

**Table 4.1:** Molecular mass, measured by electrospray mass spectrometry, for wild type and R47E mutant intact P450 BM3.

Protein		Measured Mass <sup>a</sup>	Calculated Mass	
Intact enzyme	Wild Type	117,648 (±74)	117,782 <sup>b</sup>	117,651 <sup>c</sup>
	R47E Mutant	117,756 (±11)	117,755 <sup>b</sup>	117,623 <sup>c</sup>
Haem domain	Wild Type	53,350 (±5)	53,342 <sup>d</sup>	53,346 <sup>e</sup>
	R47E Mutant	53,330 (±13)	53,314 <sup>d</sup>	53,317 <sup>e</sup>

<sup>a</sup> The measured mass in Daltons (Da) obtained for the various proteins using ES-MS.

<sup>b</sup> Mass calculated with initial methionine still present.

<sup>c</sup> Mass calculated with initial methionine removed.

<sup>d</sup> Mass calculated with initial methionine and three C-terminal residues removed.

<sup>e</sup> Mass calculated with initial methionine present and four C-terminal residues removed.

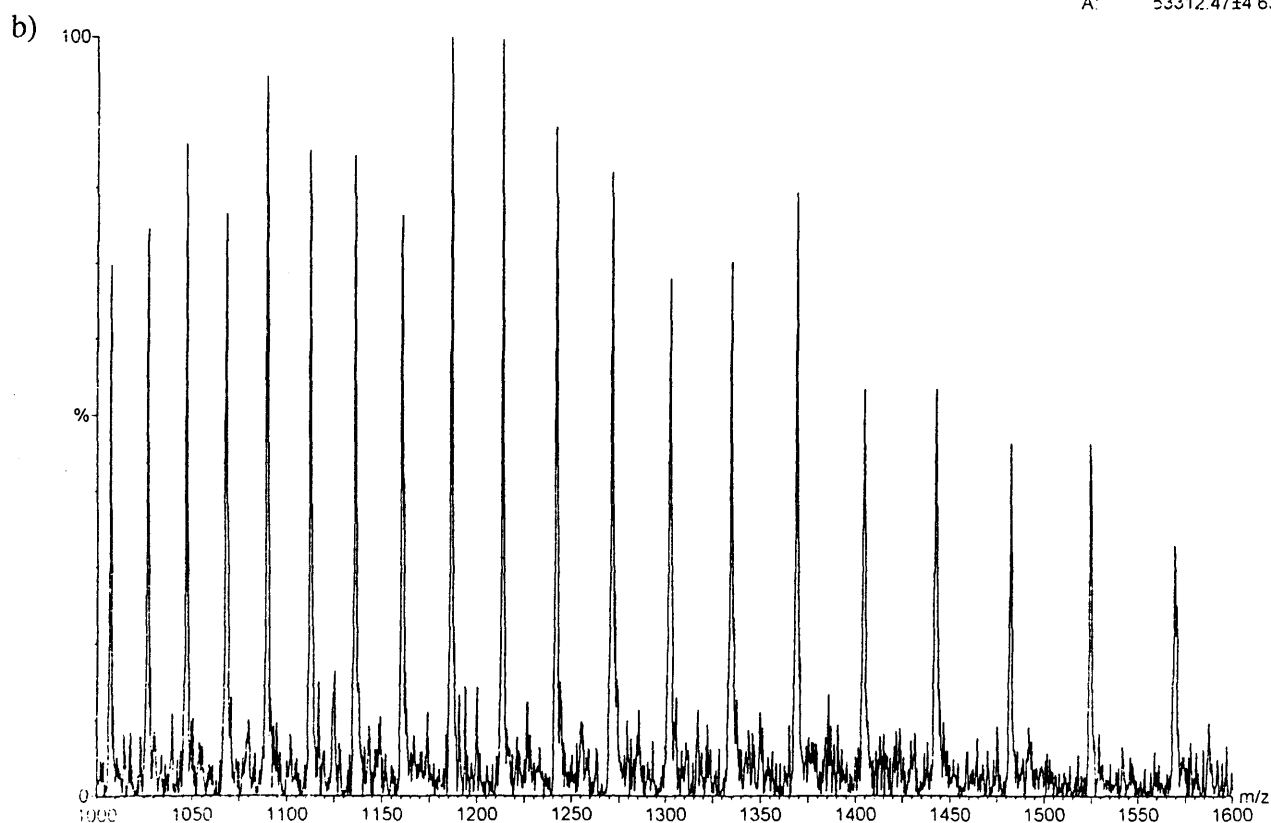
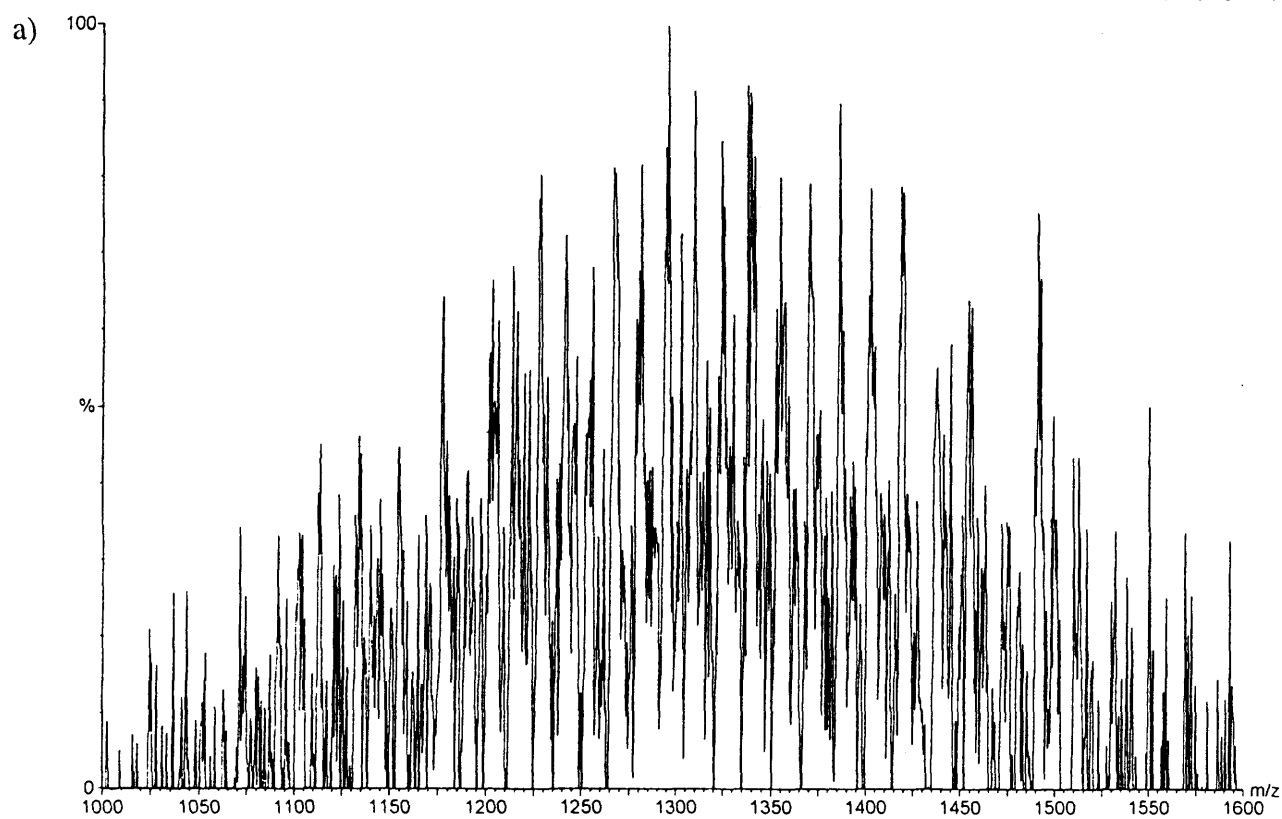


**Figure 4.1:** Data system enhanced raw data of the charge state envelopes for a) the R47E mutant intact P450 BM3 and b) the R47E mutant haem domain acquired in positive ion electrospray mass spectrometry.

The results obtained showed reasonable precision for the intact enzyme. They indicated a series mass of 117,648Da with standard error of 74Da for the wild type, with 117,756Da for the R47E mutant with standard error of 11Da. The result for the R47E mutant is in very good agreement with the calculated mass indicating the R47E mutant intact P450 BM3 was purified with the majority of the enzyme with the N-terminal methionine still present.

The measured mass for the R47E mutant haem domain was 53,330Da with standard error of 13Da as compared to 53,350Da for the wild type protein with standard error of 5Da. Neither of these values are in agreement with the calculated molecular mass for the 471 amino acid haem domain from P450 BM3: 53,856Da for the wild type protein and 53,829Da for the R47E mutation. Both proteins possess a measured mass which is less than expected, corresponding to the loss of either three or four amino acids as discussed in greater detail earlier in Chapter 3. These results show that mass spectrometry provides a sufficiently sensitive methodology such that it can be used to detect whether the proteins produced do indeed possess the desired mutation.

#### ***4.4 Optical Spectroscopy and Enzyme Assays***

##### ***4.4.1 Determination of the Catalytic Constant, $k_{cat}$ and the Michaelis Menten Constant $K_M$***

To obtain the catalytic constants,  $k_{cat}$  and  $K_M$ , the rates of hydroxylation of various saturated fatty acids and other potential substrates by P450 BM3 were determined as described in the Materials and Methods section. In the spectrophotometric assay (Matson *et al.*, 1977), the rate of substrate hydroxylation was determined indirectly by following the substrate-dependent consumption of NADPH from the absorbance at 340nm. All assays utilised electrophoretically homogenous P450 BM3 and were performed in duplicate at each substrate concentration.

The substrates described for P450 BM3 are long chain fatty acids, alcohols and amides and saturated or partially saturated fatty acids (Miura and Fulco, 1975; Ho and Fulco,

1976; Fulco, 1991). These are all long chain compounds which have a polar end of either carboxyl, hydroxyl or amido groups with a non polar end ( $\omega$  end) of either methyl or methylene groups (Li and Poulos, 1995). When choosing alternative substrates for the R47E mutant, where the positively charged arginine has been changed to negatively charged glutamic acid, these requirements were taken into consideration. As well as using saturated fatty acids, trimethylammonium (TMA) compounds were used as potential substrates for the R47E mutant. The R47E mutation and its possible interaction with the TMA compounds as a substrate, as well as the possible interaction of the wild type P450 BM3 and its fatty acid substrate have been diagrammatically represented in Figure 4.2. Data curves for the calculation of the steady state kinetic parameters  $k_{cat}$  and  $K_M$  are depicted in Figure 4.3 for both the wild type and R47E mutant P450 BM3 with all the substrates used.

The results from all kinetics measured by the spectrophotometric assay are represented in Table 4.2, where the results are given as means  $\pm$  standard deviations. For some of the compounds with high  $K_M$  values, the precision of the data was limited by the accessible range of substrate concentrations, in turn limited by micelle formation. This was especially relevant when considering the data relating to the wild type enzyme with the TMA compounds and the R47E mutant with the fatty acid substrates. In many cases the catalytic constants  $k_{cat}$  and  $K_M$  were estimated by extrapolation to a point beyond the end of the curve and were therefore prone to error. Ideally these experiments should be performed using saturating substrate concentration of approximately 5 times the  $K_M$ , with points concentrating on rates at low substrate concentrations and becoming more diverse as the substrate concentration increases. In the experiments detailed here, saturating substrate concentrations are never reached, resulting in high error. It should also be noted that the observed catalytic rates are in the  $10^{-1}$  AU/min range, which are close to the limits of the spectrophotometer used at  $10^{-4}$  AU/sec. A common solution to improve the catalytic rate is to increase to concentration of protein used. However, to ensure that the system obeys Michaelis Menten kinetics, the substrate concentration should always be in excess of the enzyme concentration. As substrate concentrations were limited by micelle formation, in most cases reported here it was not possible to increase the protein concentration and so the

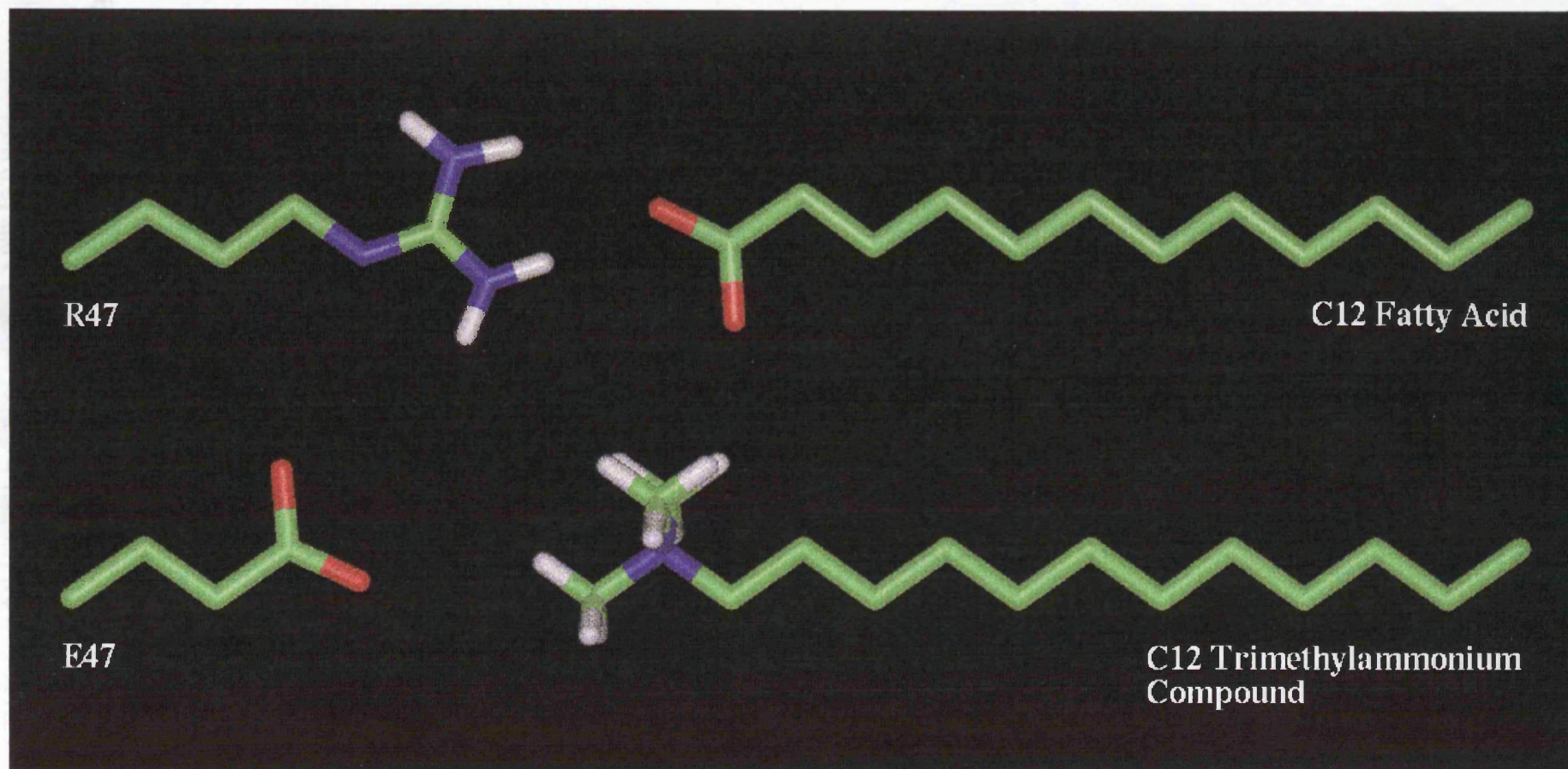
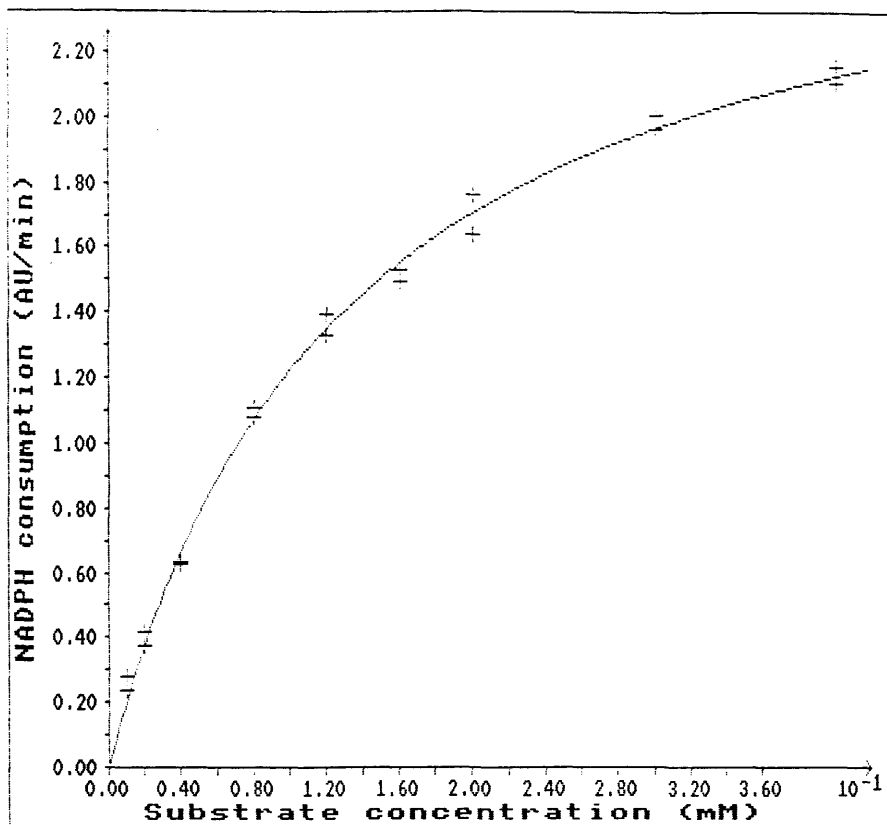


**Figure 4.2:** Diagrammatic representation of the possible interaction of wild type P450 BM3 and fatty acid substrate as well as the R47E mutation with the potential substrate, trimethylammonium compounds.

a)



b)

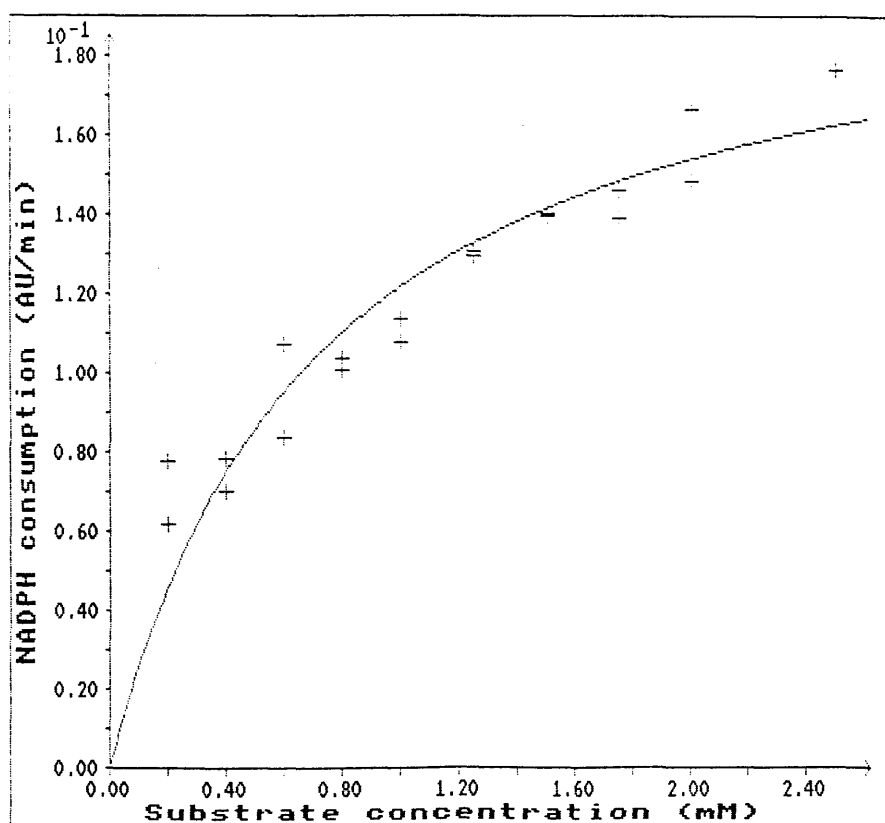
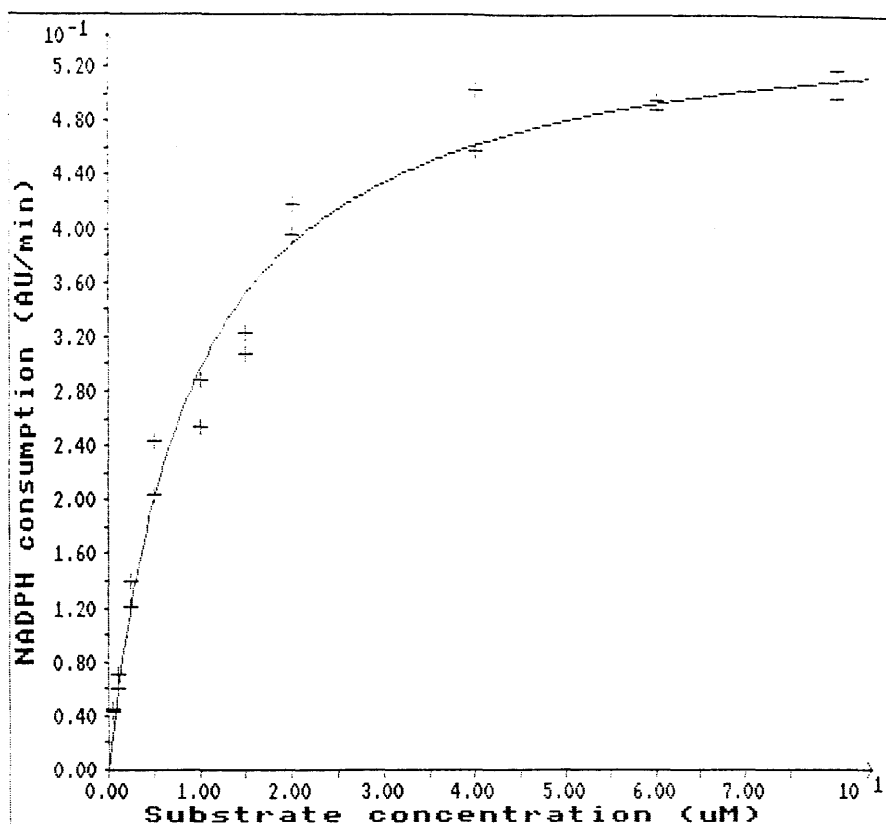


**Figure 4.3:** Data curves to show the effect of substrate concentration ( $S$ ) on the rate of reaction (AU/min) as measured by the NADPH consumption for the wild type P450 BM3 with the substrates lauric acid (a;  $k_{cat} = 24 \pm 0.5$ ,  $K_M = 130 \pm 6.8$ ) and C12 TMA (b;  $k_{cat} = 1.4 \pm 0.1$ ,  $K_M = 718 \pm 125$ )

c)



d)

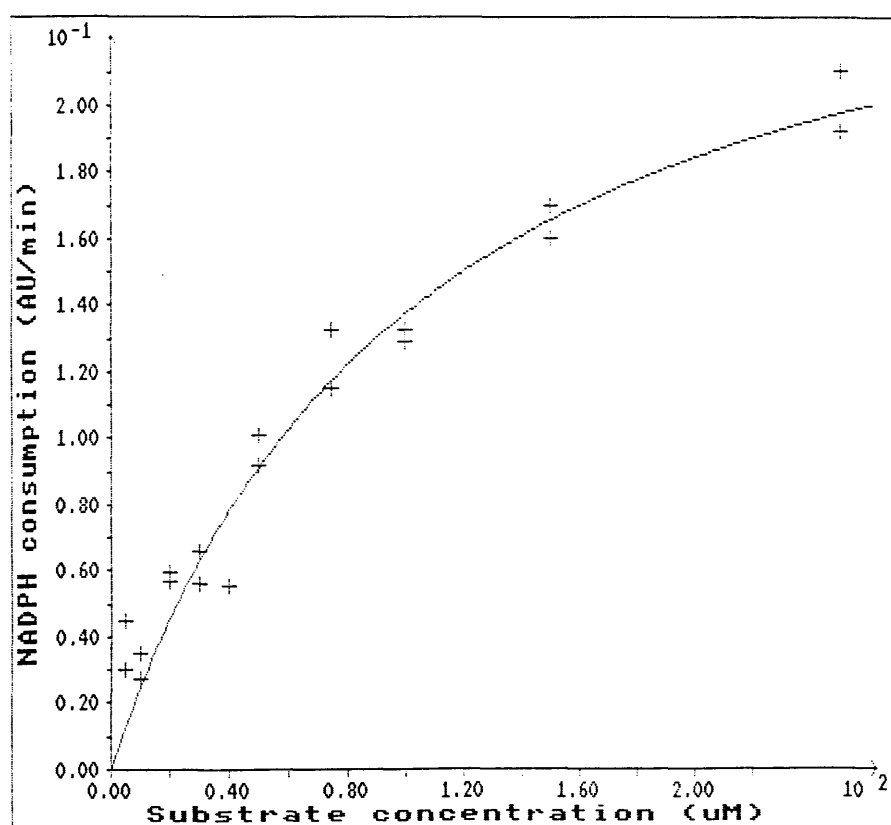


**Figure 4.3 (continued):** Data curves to show the effect of substrate concentration (S) on the rate of reaction (AU/min) as measured by the NADPH consumption for the wild type P450 BM3 with the substrates myristic acid (c;  $k_{\text{cat}} = 52 \pm 1.3$ ,  $K_M = 9.3 \pm 0.9$ ) and C14 TMA (d;  $k_{\text{cat}} = 2.4 \pm 0.2$ ,  $K_M = 103 \pm 18$ )

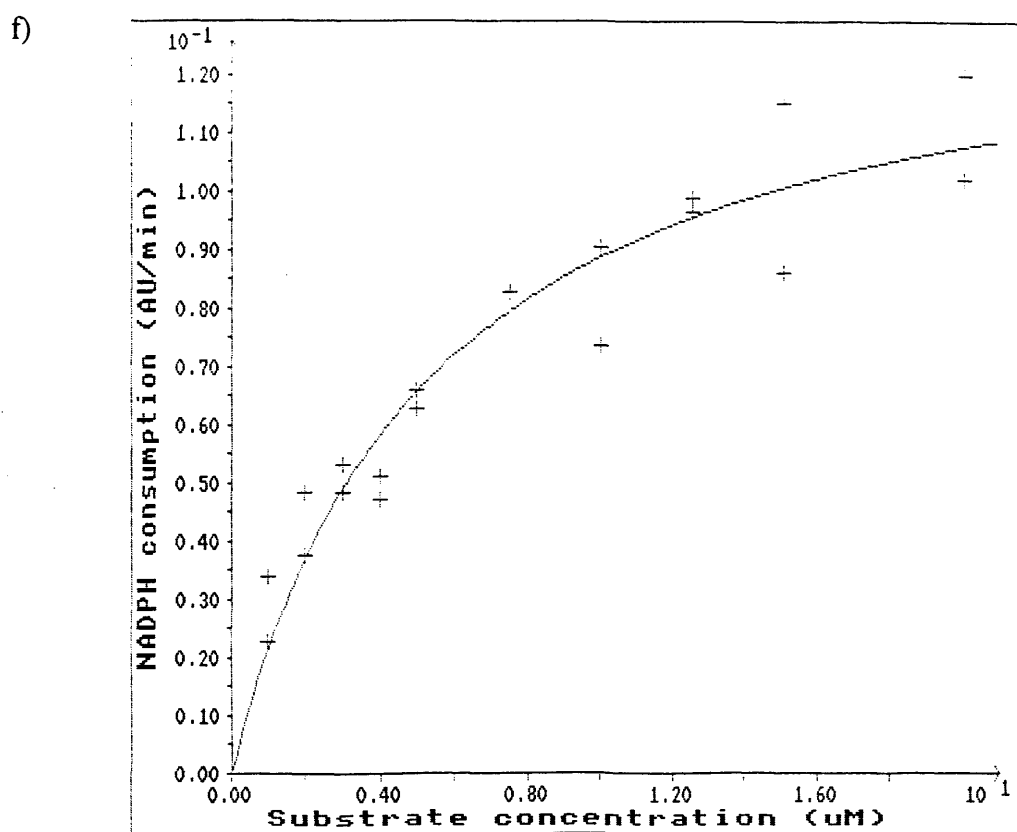
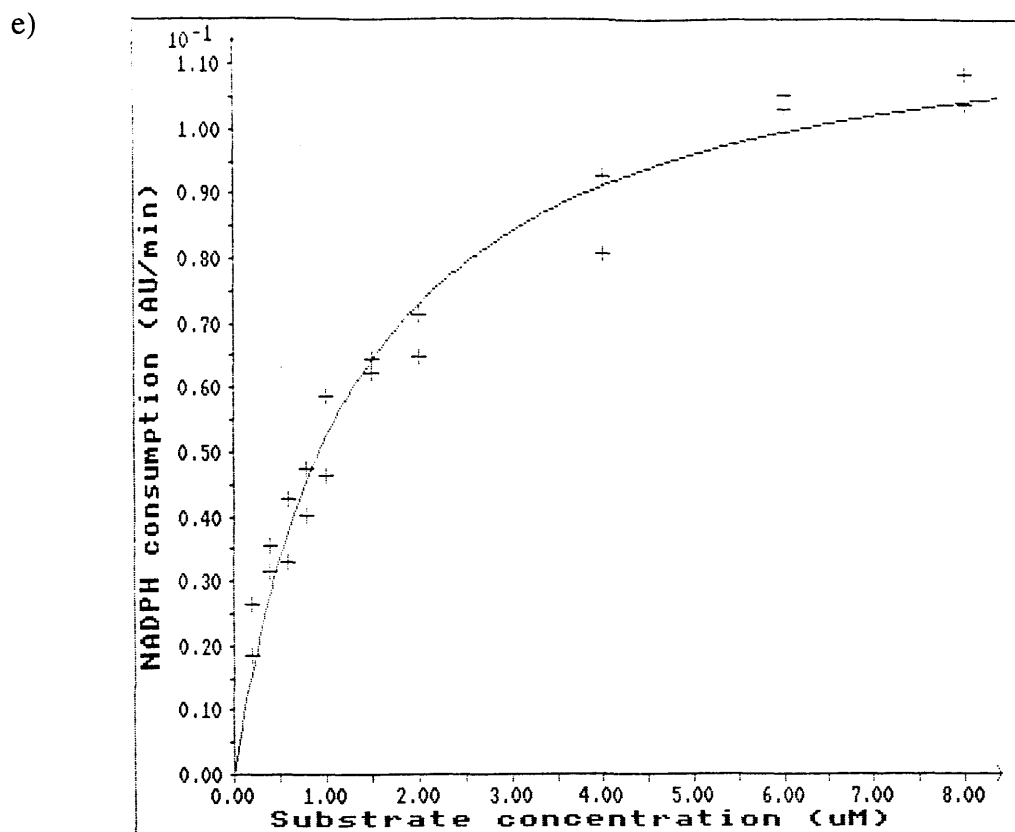
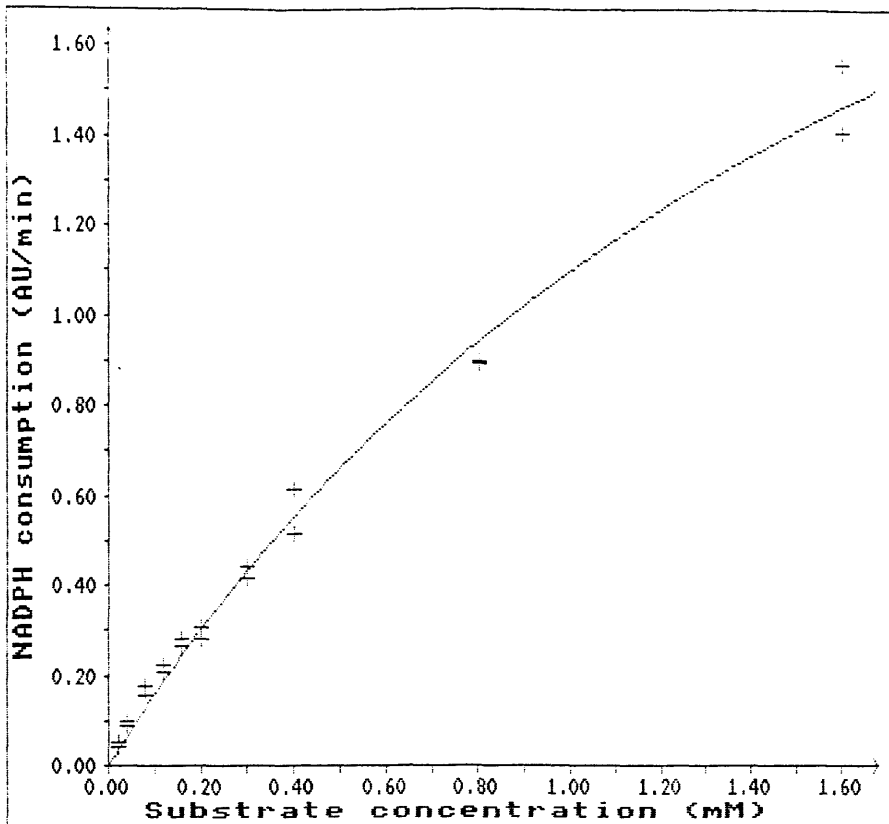


**Figure 4.3 (continued):** Data curves to show the effect of substrate concentration (S) on the rate of reaction (AU/min) as measured by the NADPH consumption for the wild type P450 BM3 with the substrates palmitic acid (e;  $k_{cat} = 66 \pm 2.4$ ,  $K_M = 1.3 \pm 0.1$ ) and C16 TMA (f;  $k_{cat} = 1.1 \pm 0.1$ ,  $K_M = 5.3 \pm 0.9$ )

g)



h)

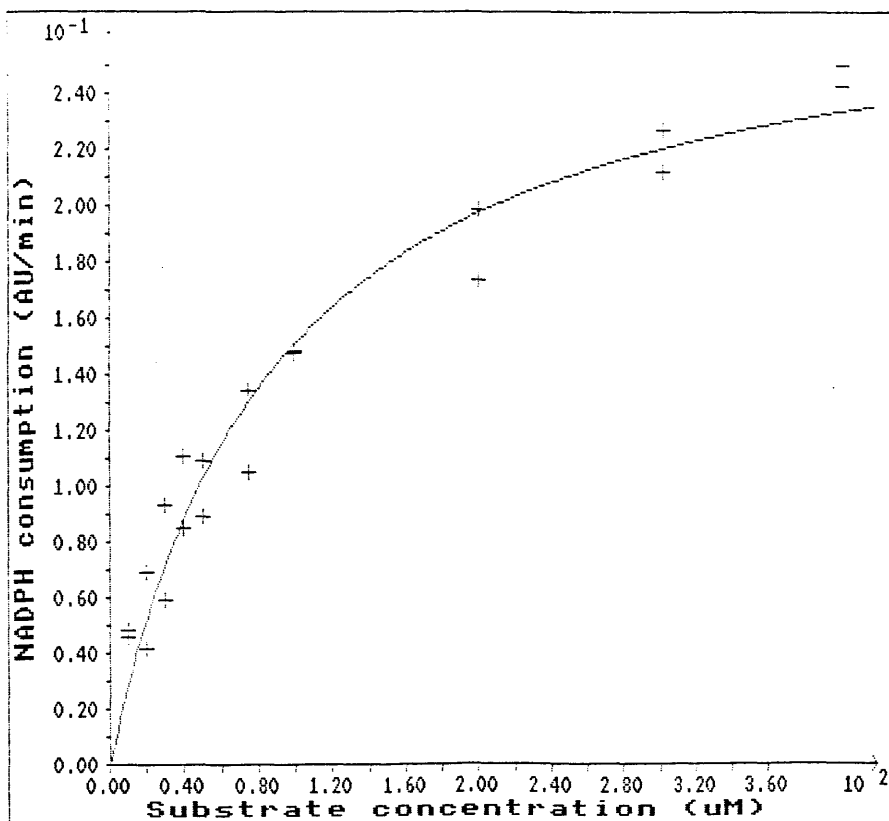
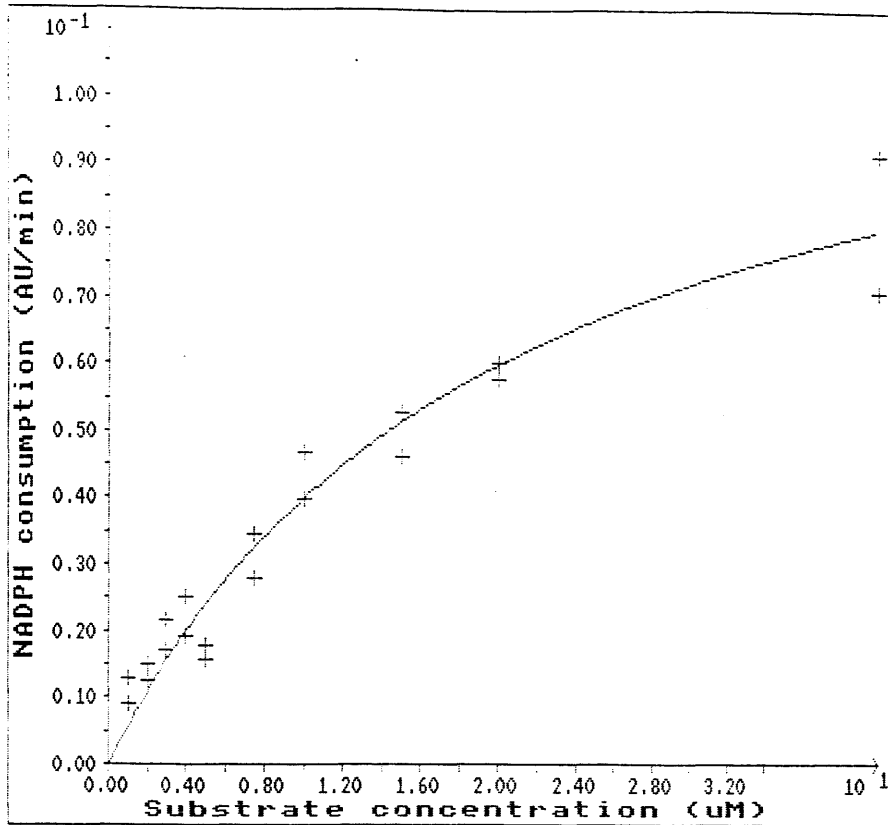


**Figure 4.3 (continued):** Data curves to show the effect of substrate concentration (S) on the rate of reaction (AU/min) as measured by the NADPH consumption for the R47E mutant P450 BM3 with the substrates lauric acid (g;  $k_{cat} = 29 \pm 2.3$ ,  $K_M = 1947 \pm 223$ ) and C12 TMA (h;  $k_{cat} = 2.5 \pm 0.1$ ,  $K_M = 89 \pm 11$ )

i)



j)

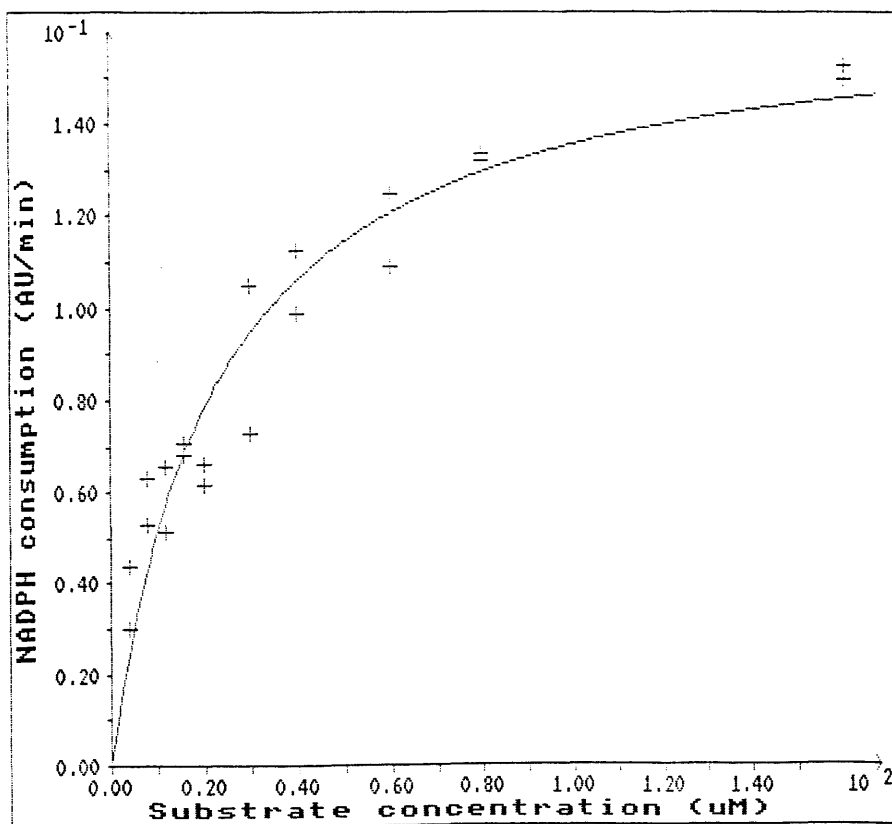
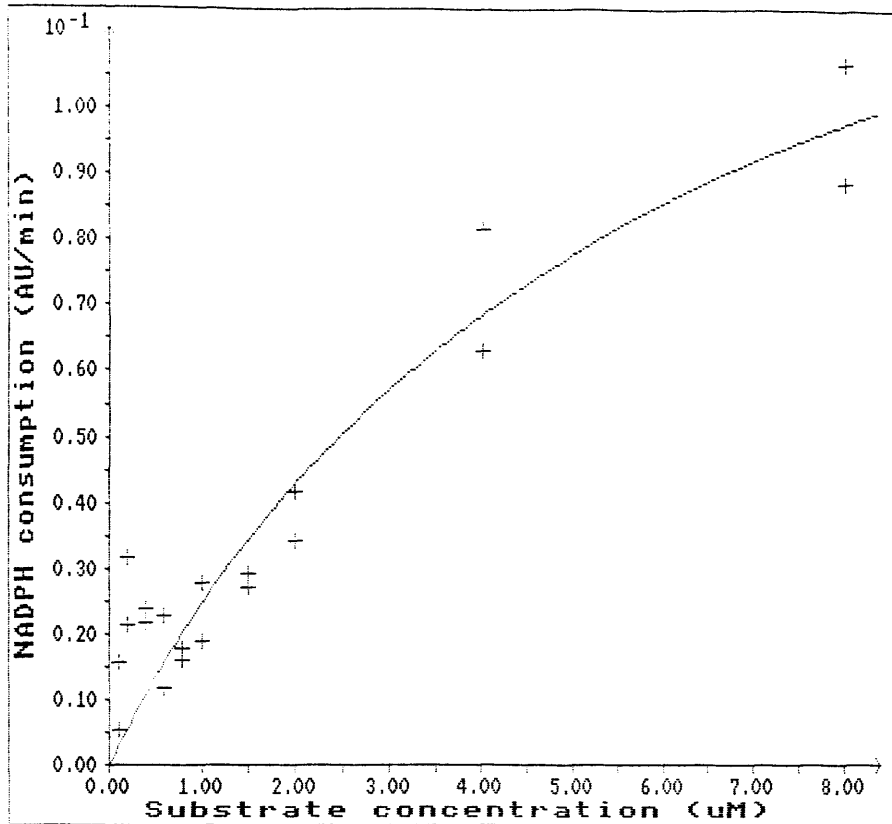


**Figure 4.3 (continued):** Data curves to show the effect of substrate concentration (S) on the rate of reaction (AU/min) as measured by the NADPH consumption for the R47E mutant P450 BM3 with the substrates myristic acid (i;  $k_{\text{cat}} = 6.6 \pm 0.7$ ,  $K_M = 20 \pm 3.7$ ) and C14 TMA (j;  $k_{\text{cat}} = 15 \pm 0.8$ ,  $K_M = 23 \pm 3.4$ )

k)



l)

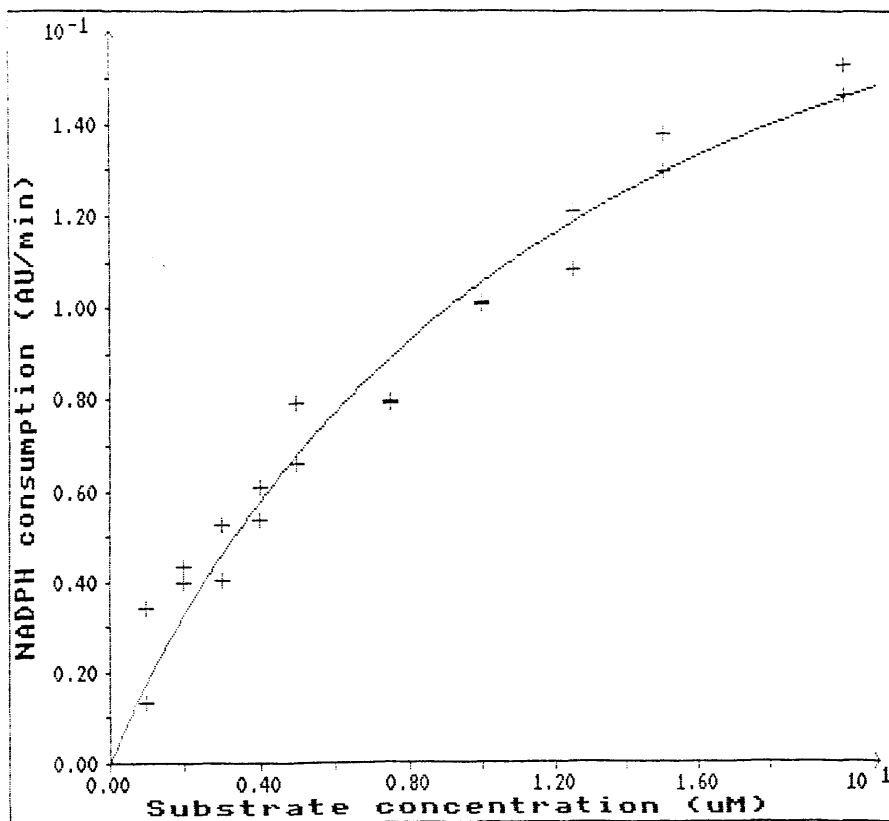


**Figure 4.3 (continued):** Data curves to show the effect of substrate concentration (S) on the rate of reaction (AU/min) as measured by the NADPH consumption for the R47E mutant P450 BM3 with the substrates palmitic acid (k;  $k_{\text{cat}} = 15 \pm 3.0$ ,  $K_M = 5.9 \pm 2.0$ ) and C16 TMA (l;  $k_{\text{cat}} = 22 \pm 1.8$ ,  $K_M = 12 \pm 2.0$ )

**Table 4.2:** Kinetic constants for the action of wild type and R47E intact cytochrome P450 BM3 for a series of saturated fatty acids and alkyl trimethylammonium compounds.

Enzyme	Wild Type			R47E Mutant			$k_{cat}/K_M$ Ratio
Substrate	$k_{cat}$ ( $s^{-1}$ ) <sup>a</sup>	$K_M$ ( $\mu M$ ) <sup>a</sup>	$k_{cat}/K_M$ ( $M^{-1}s^{-1}$ )	$k_{cat}$ ( $s^{-1}$ ) <sup>a</sup>	$K_M$ ( $\mu M$ ) <sup>a</sup>	$k_{cat}/K_M$ ( $M^{-1}s^{-1}$ )	Wild Type / Mutant
Fatty Acids							
C12: Laurate	26±3	136±4	1.9 x 10 <sup>5</sup>	29±6	2000±440	1.5 x 10 <sup>4</sup>	12.6
C14: Myristate	55±5	7±2	8.2 x 10 <sup>6</sup>	7.0±0.2	18±8	3.9 x 10 <sup>5</sup>	21.0
C16: Palmitate	81±17	1.4±0.1	6.0 x 10 <sup>7</sup>	12±5	4±3	3.0 x 10 <sup>6</sup>	20.0
Trimethylammonium compounds							
C12: Dodecyl	1.6±0.3	782±125	2.0 x 10 <sup>3</sup>	2.2±0.6	95±14	2.3 x 10 <sup>4</sup>	0.087
C14: Tetradecyl	2.2±0.4	87±34	2.5 x 10 <sup>4</sup>	15.1±0.8	23±3	6.6 x 10 <sup>5</sup>	0.038
C16: Hexadecyl	1.0±0.1	5.0±0.6	2.0 x 10 <sup>5</sup>	20±3	9±4	2.2 x 10 <sup>6</sup>	0.091

<sup>a</sup> Each constant was determined at 9 or 10 substrate concentrations, with at least 4 replicates at each concentration.

<sup>b</sup>  $k_{cat}/K_M$  refers to the specificity constant.

low catalytic rates were unavoidable. Other methods to increase the catalytic rate include increasing the temperature or use of organic solvents to increase substrate solubility. Both of these methods are valid for P450 BM3, however these would necessitate repeating all the kinetic experiments detailed in this thesis.

When considering just the results pertaining to the wild type enzyme using fatty acid substrates, all results obtained for the  $k_{\text{cat}}$  and  $K_{\text{M}}$  agree with those results already published (Narhi and Fulco, 1986; Fulco, 1991; Black *et al.* 1994). All  $K_{\text{M}}$  values are in the micromolar range, varying from 136 $\mu\text{M}$  for lauric acid to 1.4 $\mu\text{M}$  for palmitic acid, indicating that P450 BM3 has the highest affinity for the C16 fatty acid substrate. The order of substrate affinities are shown to be C16 > C14 > C12, which is in complete agreement with the order of activity for the saturated series, C15 = C16 > C14 > C17 > C13 > C18 > C12, as published originally by Miura and Fulco (1975). The rate of NADPH oxidation catalysed by P450 BM3 was also found to be dependent on the chain length of the fatty acid metabolised. As the chain length increases from C12 to C16,  $k_{\text{cat}}$  progressively increases as the  $K_{\text{M}}$  progressively decreases, such that the specificity constant,  $k_{\text{cat}}/K_{\text{M}}$  increases 300-fold. The calculated catalytic activity of the intact enzyme with lauric acid is low, compared to myristic acid and palmitic acid. The observed rate of reaction with palmitic acid at 81s<sup>-1</sup> was maximal and is somewhat greater than that for the C20 unsaturated fatty acid arachidonate (53s<sup>-1</sup>; Capdevila *et al.*, 1996). This is consistent with earlier observations (Miura and Fulco, 1975) and Narhi and Fulco (1986) who described a  $k_{\text{cat}}$  of 77s<sup>-1</sup> for palmitate.

If we were to consider just the results for the R47E P450 BM3 with the fatty acids as substrates, we can see that again the observed  $K_{\text{M}}$  values agree with the activity series of C15=C16 > C14 > C17 > C13 > C18 > C12 and are in the micromolar range, with the exception of lauric acid (C12). The behaviour of this protein with laurate as a substrate is somewhat different as the  $k_{\text{cat}}$  remains essentially unchanged relative to the wild type, whereas the  $K_{\text{M}}$  has increased substantially. This can probably be explained by an altered mode of binding of laurate to the mutant and is discussed later. For all fatty acid substrates the specificity constants are greater for the wild type than for the R47E P450 BM3. They indicate a 13- to 21-fold decrease in specificity toward the

fatty acid substrates in the R47E mutation.

Looking at the second half of Table 4.2, it can be seen that the three TMA compounds, dodecyl-, tetradecyl- and hexadecyl-trimethylammonium bromide (abbreviated to C12 TMA, C14 TMA and C16 TMA respectively) do act as substrates for both the wild type P450 BM3 and its R47E mutant. These compounds are relatively poor substrates for the wild type enzyme with  $k_{\text{cat}}$  values only 1-6% those of the fatty acids and  $K_M$  values 3- to 13-fold higher, leading to  $k_{\text{cat}}/K_M$  values 100- to 300-fold lower. These comparisons have been made using myristate and C14 TMA as examples. In terms of active site geometry, as discussed below, this may not be an exact comparison. As expected, the positively charged TMA compounds are much better substrates for the R47E mutant, as indicated by all the TMA specificity constants for the R47E mutant being greater than those for the wild type enzyme. In the case of C14 TMA, the  $k_{\text{cat}}/K_M$  is 26-fold greater with the mutant as compared to the wild type. The R47E enzyme also shows the same chain-length preference, C16>C14>C12, for the TMA compounds as the wild type does for the fatty acids. This is demonstrated by an increase in  $k_{\text{cat}}$  with a concomitant decrease in  $K_M$  as the substrate chain length increases.

C12 TMA shows the same anomalous behaviour as noted for the fatty acid of the same chain length, with no difference in the  $k_{\text{cat}}$  and a larger difference in the  $K_M$  between wild type and the R47E mutant enzyme. Overall,  $k_{\text{cat}}/K_M$  for the TMA compounds is 11- to 26-fold greater for the mutant.

#### **4.4.2 Substrate Binding**

##### **4.4.2.1 Substrate Binding by Optical Spectroscopy**

The purified wild type and R47E mutant proteins were purified in the ferric low spin state and showed spectra that were typical for cytochrome P450s (Figure 4.4). That is, the oxidised spectrum possessed well resolved  $\alpha$  and  $\beta$  bands at 570 and 535nm and a strong Soret band at 418nm, whilst after reduction by sodium dithionite and CO, the spectrum shows peaks at 547 and 448nm.

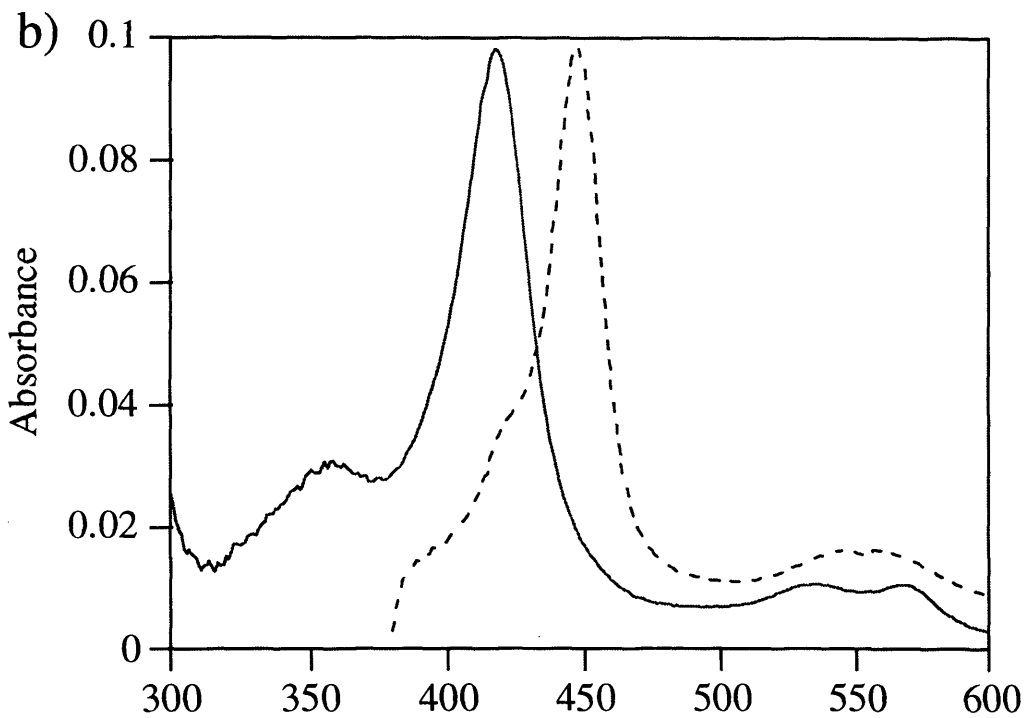
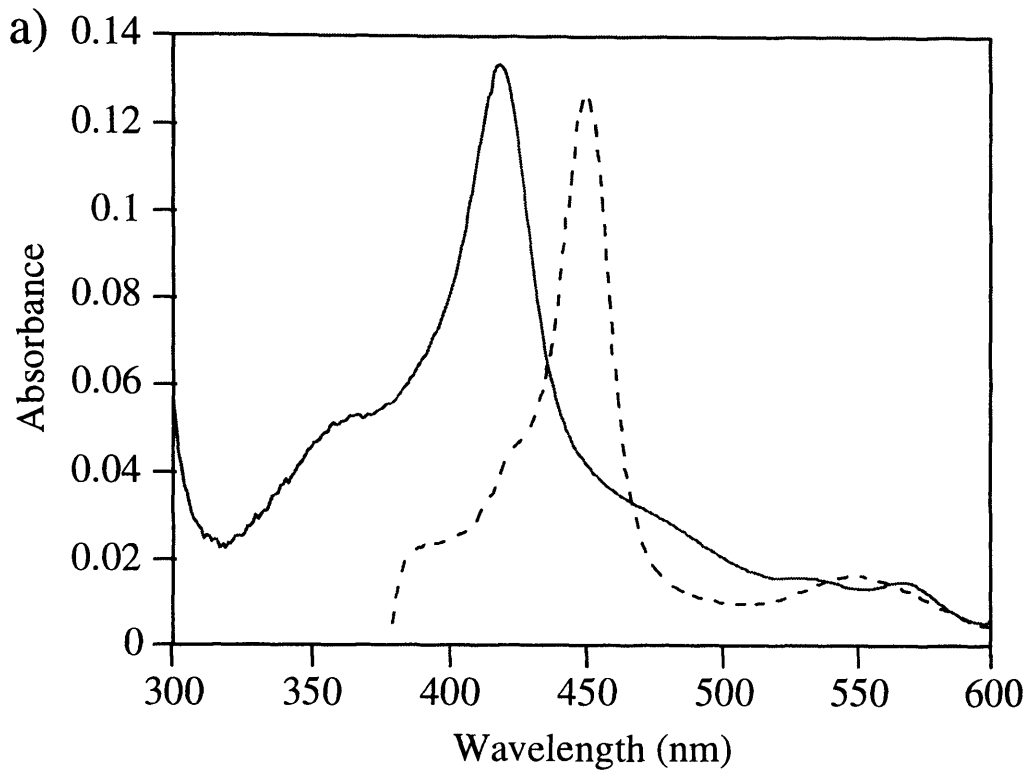


**Figure 4.4:** The absorption spectra for wild type intact cytochrome P450 BM3 (a) and its haem domain (b). The sample cuvette contained either  $1.35\mu\text{M}$  intact P450 BM3 or  $1.22\mu\text{M}$  haem domain. The spectrum with the solid line (—) is the oxidised form of the enzyme. The broken line (- - -) was taken after the sample was reduced by addition of sodium dithionite followed by saturation with CO.

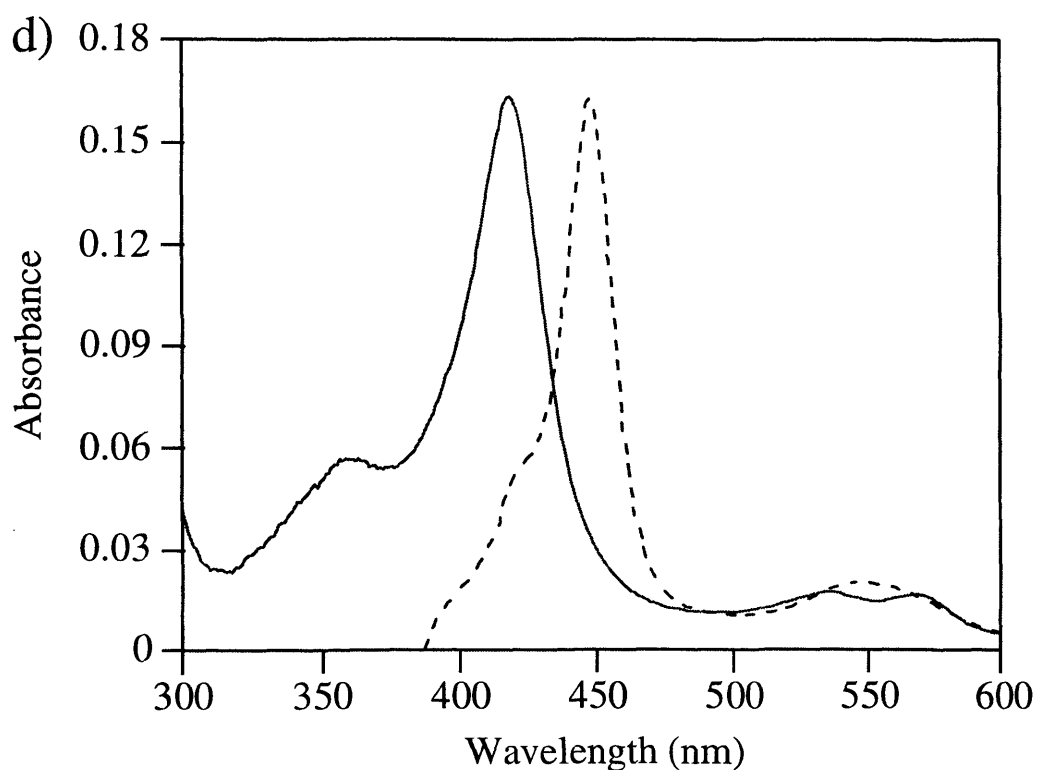
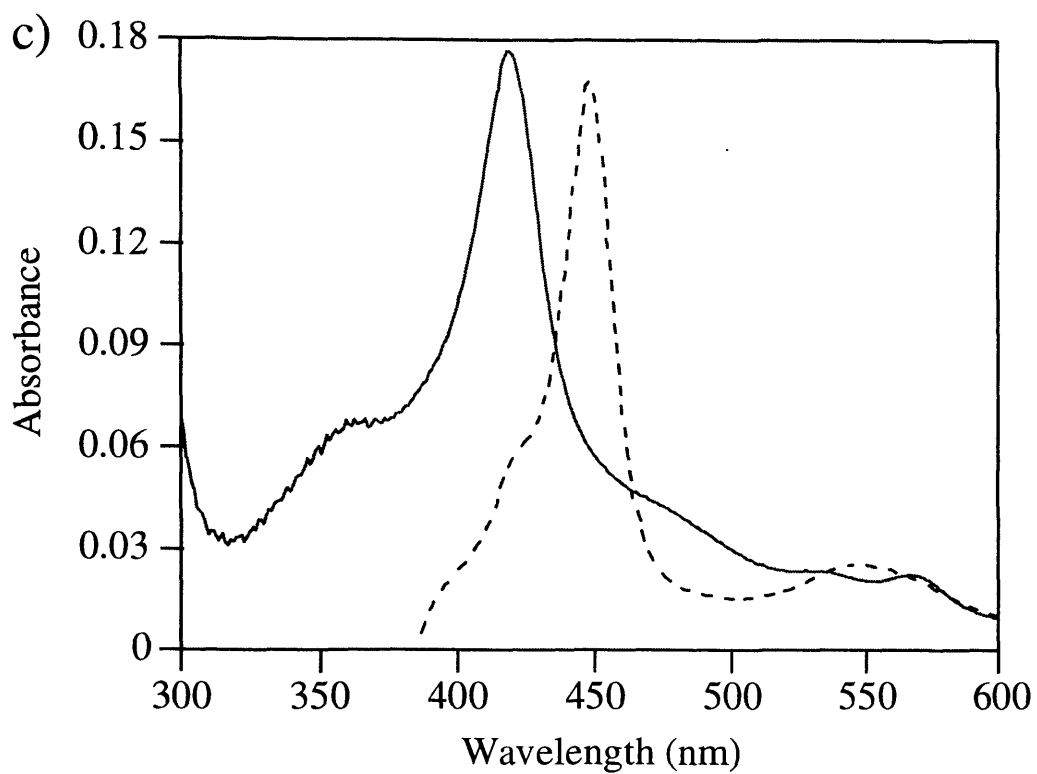


**Figure 4.4 (continued):** The absorption spectra for R47E mutant intact cytochrome P450 BM3 (c) and its haem domain (d). The sample cuvette contained either 1.41 $\mu$ M intact P450 BM3 or 1.34 $\mu$ M haem domain. The spectrum with the solid line (—) is the oxidised form of the enzyme. The broken line(- - -) was taken after the sample was reduced by addition of sodium dithionite followed by saturation with CO.

Figure 4.5 shows the electronic absorption spectra of the haem domains of the wild type and R47E mutant in the presence and absence of the substrates palmitate and C16 TMA. On addition of either substrate to the wild type protein a typical 'Type I' spectrum is produced, characterised by a decrease in the Soret band at 418nm with a simultaneous increase in the absorbance at 390 and 650nm (Figure 4.5a and b). The band at 650nm is characteristic of high spin ferric haem proteins (Falk, 1964). On closer inspection of the spectra from the wild type and R47E mutant with the C16 TMA as substrate it can be seen that there is a broadening of the peak at 650nm. There are three possible explanations for this effect: the haem moiety may be tilted in the substrate binding cavity, such that when this class of substrates binds the terminal methyl group interacts with the haem moiety in some way. It is more likely that the concentration of substrate required to produce the substrate binding spectra is above the critical micelle concentration and we are viewing the effect of micelles on the protein, or perhaps the most likely explanation is that we are observing light scattering by micelles.

Comparison of the substrate binding spectra for the wild type enzyme indicates that the terminal region of the natural fatty acid substrate and the trimethyl-ammonium compound bind in a similar way in the immediate vicinity of the haem moiety. In the case of the R47E mutant, binding of the C16 TMA leads to changes in the optical spectrum essentially identical to those seen in the wild type enzyme (Figure 4.5d). The concentration of palmitate which could be used was limited to 8 $\mu$ M due to micelle formation. This concentration was not sufficient to produce any clear changes in the absorption spectrum of the haem domain of the R47E mutant (Figure 4.5c). The difference in  $K_M$  for palmitate between wild type and R47E mutant enzyme is only approximately a factor of two (Table 4.2). The lack of effect of the 8 $\mu$ M palmitate on the absorption spectrum suggests that the difference in the  $K_d$  for the binding to the haem domain must be greater than this.

The equilibrium dissociation constant,  $K_d$ , for the binding of fatty acids to the wild type and of trimethylammonium compounds to the R47E mutant enzymes were calculated

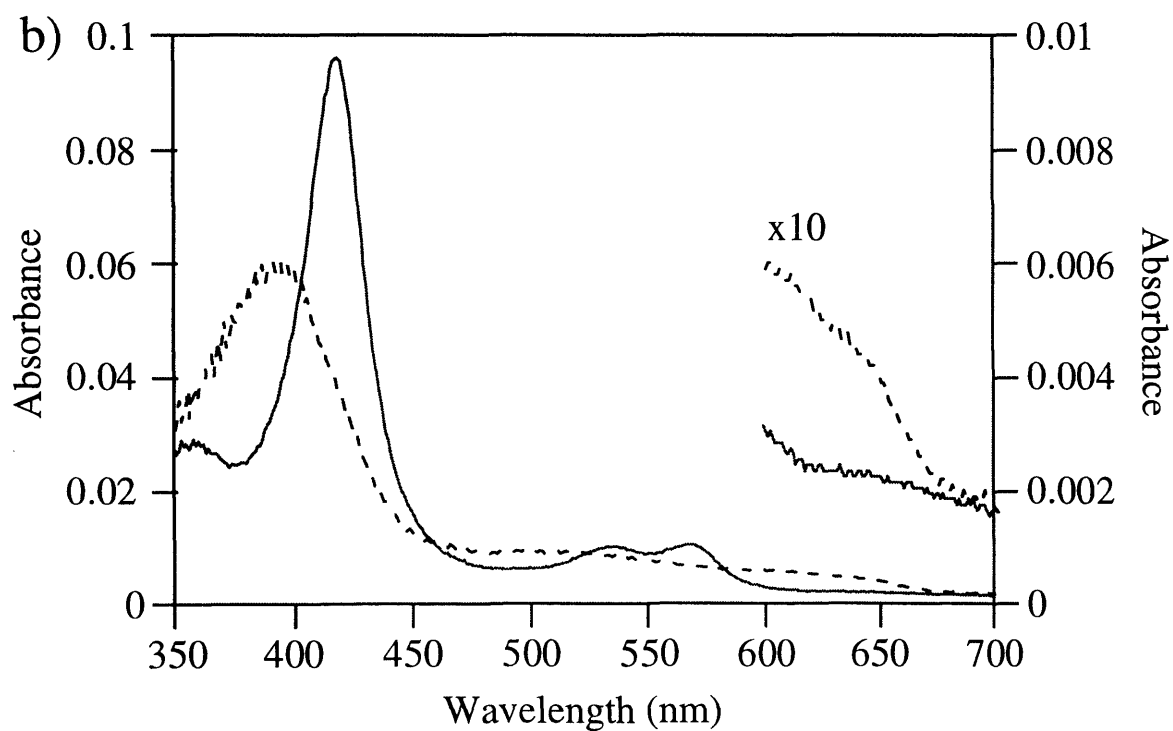
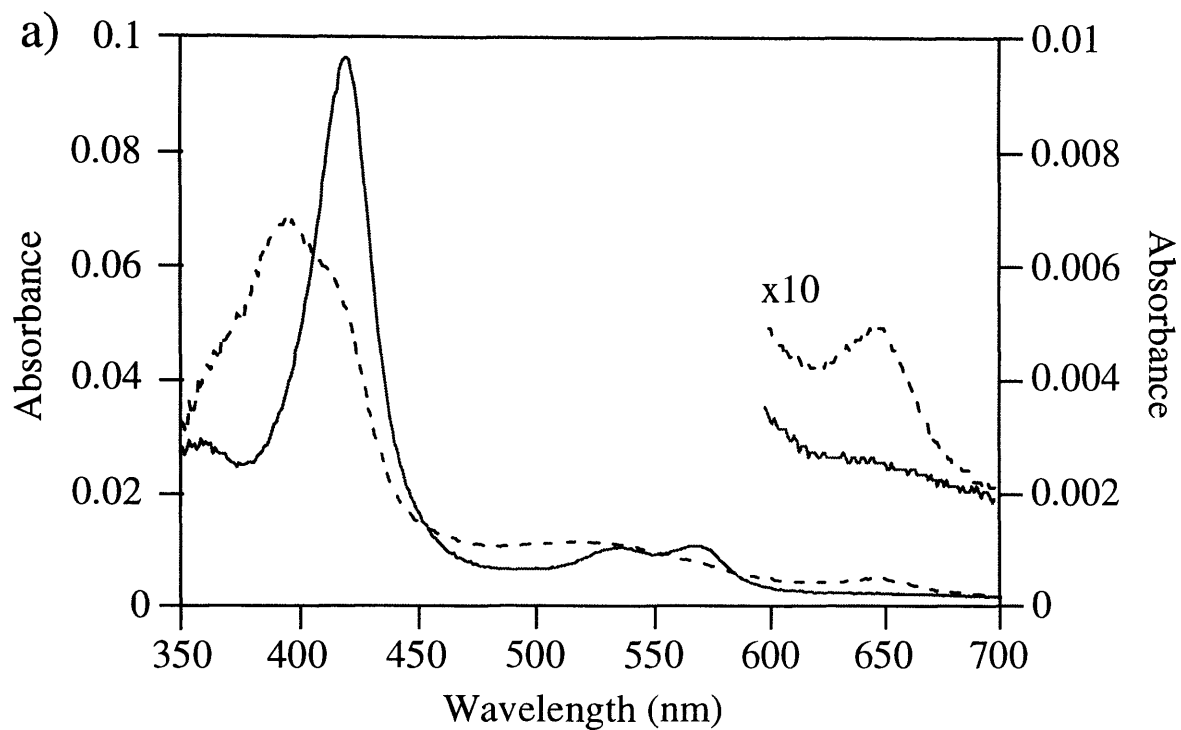


**Figure 4.5:** Absorption spectra of the wild type haem domain (1.22  $\mu\text{M}$ ) in the presence (---) and absence (—) of 8  $\mu\text{M}$  palmitate (a) and 0.8 mM C16 TMA (b).

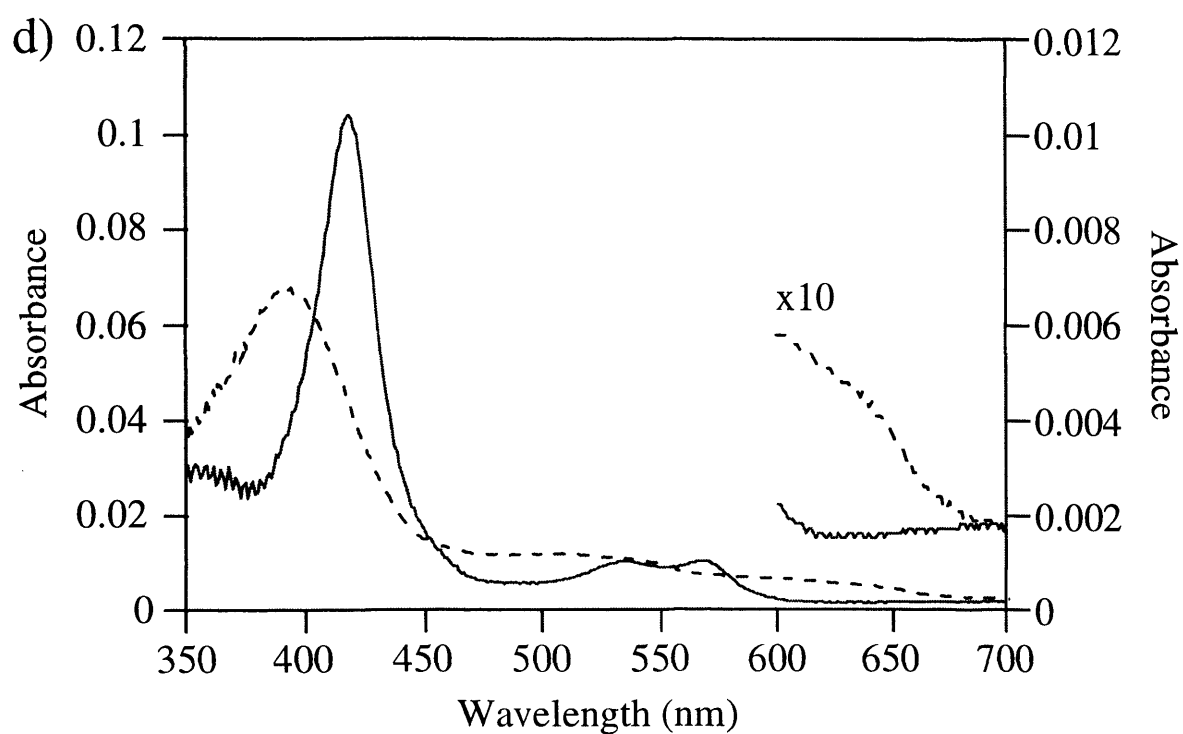
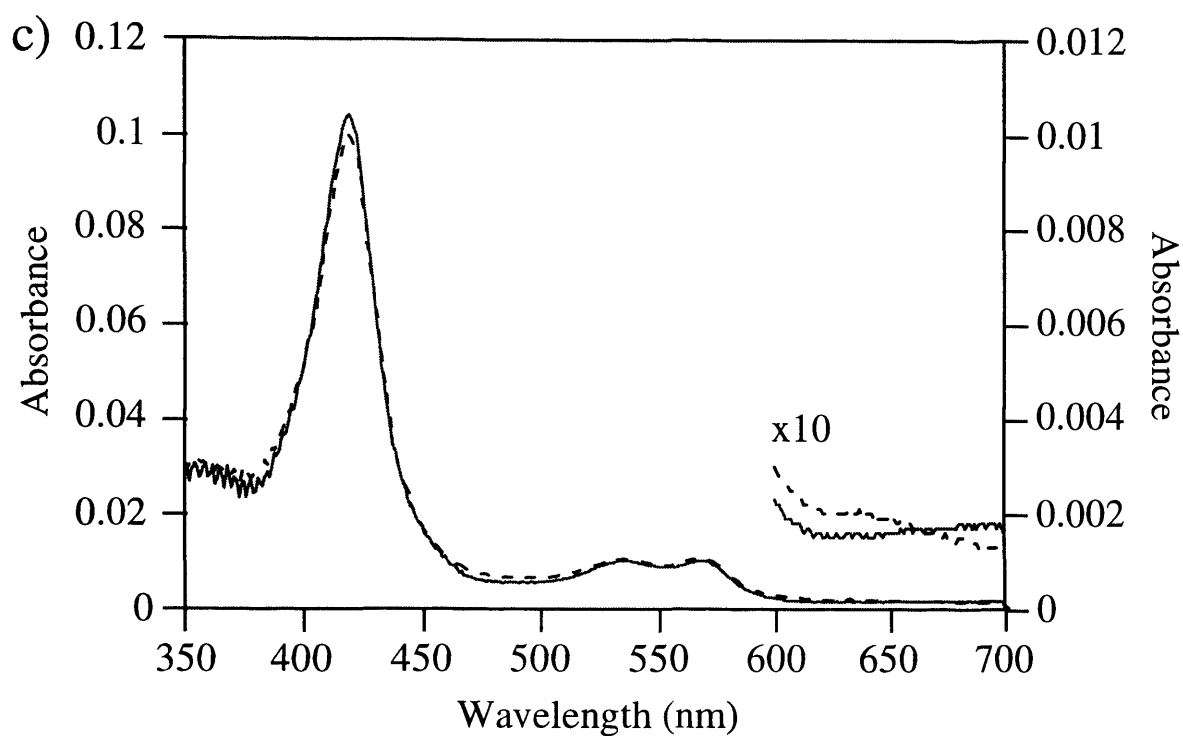


**Figure 4.5 (continued):** Absorption spectra of the R47E mutant haem domain ( $1.34\mu\text{M}$ ) in the presence (---) and absence (—) of  $8\mu\text{M}$  palmitate (c) and  $0.8\text{mM}$  C16 TMA (d).

from the concentration-dependence of the decrease in absorbance at 418nm and are given in Table 4.3. Selected data for the determination of  $K_d$  are represented in Figure 4.6. The values for the  $K_d$ s for the intact wild type protein range from 269 $\mu$ M for lauric acid (C12) 23.1 $\mu$ M for myristic acid (C14) to 5 $\mu$ M for palmitic acid (C16). The corresponding values for the haem domain were 626 $\mu$ M for lauric acid, 27.8 $\mu$ M for myristic acid and 8.1 $\mu$ M for palmitic acid. For both proteins, the lowest  $K_d$  was found for palmitic acid, the highest being for lauric acid. The  $K_d$  values follow the activity series C16> C14> C12 and are in agreement with the  $k_{cat}$  and  $K_M$  results, the C16 palmitic acid having the strongest association with the intact P450 BM3.

These results are mirrored by those obtained for the R47E mutant proteins with the trimethyl-ammonium compounds as substrates (Table 4.3). The  $K_d$  values for the intact R47E P450 BM3 range from 180 $\mu$ M for C12 TMA, 41 $\mu$ M for C14 TMA to 4.0 $\mu$ M for C16 TMA. The corresponding values for the haem domain were 245 $\mu$ M for the C12, 52.0 $\mu$ M for the C14 and 10.8 $\mu$ M for the C16, indicating that overall there has been an approximately 2-fold increase in binding of the TMA compounds as a result of the substitution of glutamate at position 47. C16 TMA showed the tightest binding with C12 TMA binding the weakest for both proteins. The obtained activity series C16>C14>C12 is in agreement with the  $k_{cat}$  and  $K_M$  results, suggesting that the C16 TMA has the strongest association with the R47E mutant P450 BM3.

#### **4.4.2.2 Binding of C12 Substrate Measured by Competition**

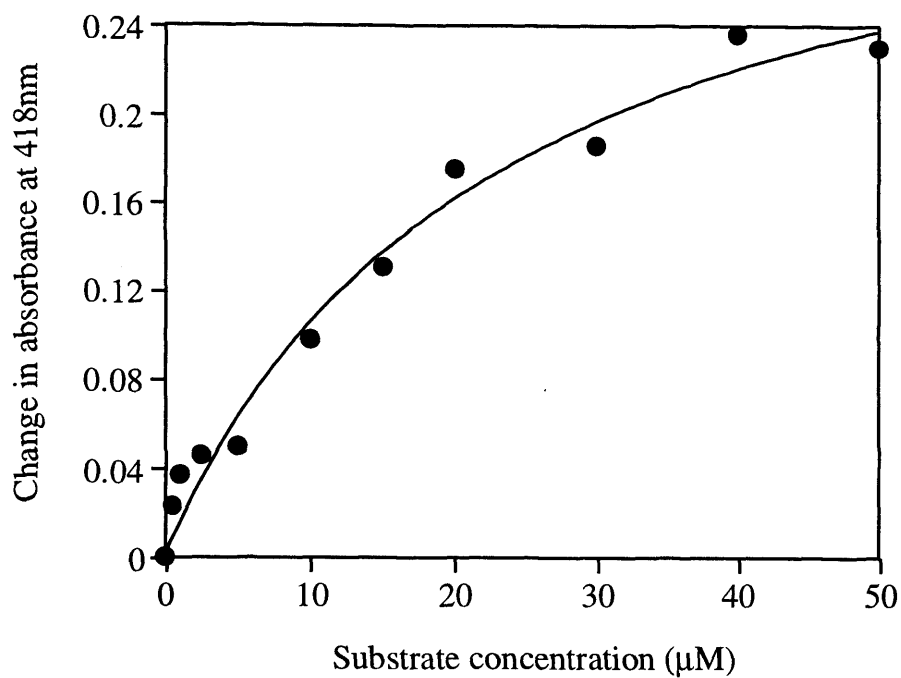
The binding of laurate to the R47E mutant and of C12 TMA to the wild type enzyme was too weak to be determined directly by the changes in the optical spectrum, as the overall change in absorbance at 418nm was too small which could lead to large errors. A different method was required and so the alternative method for determination of the  $K_d$  as described in the Materials and Methods section was used. In this instance, S1 represented the specific substrate of known  $K_d$  so that S2 represented the less appropriate substrate whose  $K_d$  was to be determined. In experimental terms this translated to the  $K_d$  determination for C12 TMA with the wild type haem domain in the presence of myristate and the  $K_d$  determination of laurate with the R47E mutant haem

**Table 4.3:** Equilibrium dissociation constants for wild type and R47E mutant P450 BM3.

Enzyme	Substrate		Method <sup>a</sup>	K <sub>d</sub> (M)		
				Intact Enzyme	Haem Domain Ferric State	Haem Domain Ferrous State
R47E Mutant	Fatty Acids	C12	NMR	nd	1.0 (±0.3) x 10 <sup>-2</sup>	3.6 (±0.3) x 10 <sup>-3</sup>
		C12	Optical, competition	nd	4.2 (±2) x 10 <sup>-3</sup>	nd
Wild Type	Fatty Acids	C12	NMR	nd	8.4 (±0.4) x 10 <sup>-4</sup>	7.9 (±1.6) x 10 <sup>-5</sup>
		C12	Optical	2.7 (±0.5) x 10 <sup>-4</sup>	6.3 (±1) x 10 <sup>-4</sup>	nd
		C14	Optical	2.3 (±0.6) x 10 <sup>-5</sup>	2.8 (±0.4) x 10 <sup>-5</sup>	nd
		C16	Optical	5.0 (±1.4) x 10 <sup>-6</sup>	8.0 (±3) x 10 <sup>-6</sup>	nd
R47E Mutant	Trimethylammonium compounds	C12	Optical	1.8 (±0.3) x 10 <sup>-4</sup>	2.5 (±0.5) x 10 <sup>-4</sup>	nd
		C14	Optical	4.1 (±0.7) x 10 <sup>-5</sup>	5.2 (±0.5) x 10 <sup>-5</sup>	nd
		C16	Optical	4.0 (±1.5) x 10 <sup>-6</sup>	1.1 (±0.3) x 10 <sup>-5</sup>	nd
Wild Type	Trimethylammonium compounds	C12	Optical, competition	nd	2.3 (±1) x 10 <sup>-3</sup>	nd

<sup>a</sup> NMR: from the concentration-dependence of the spin-lattice relaxation rate of the substrate protons; Optical: from the concentration-dependence of the absorbance at 418nm; Optical competition: from the effect of the C12 compound on the binding of a reference compound, the latter determined optically.  
nd not determined.

a)



b)

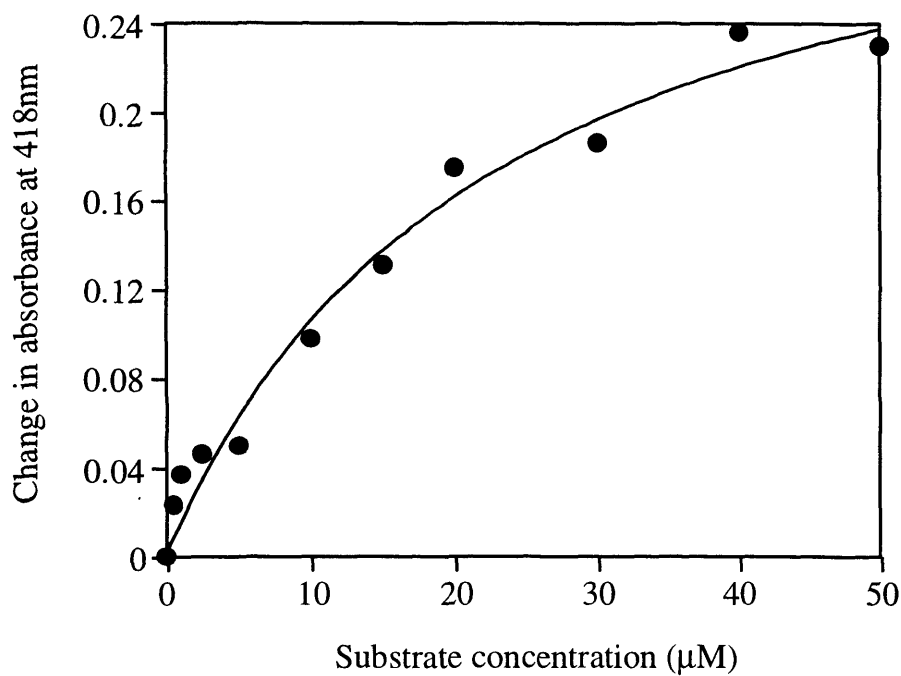
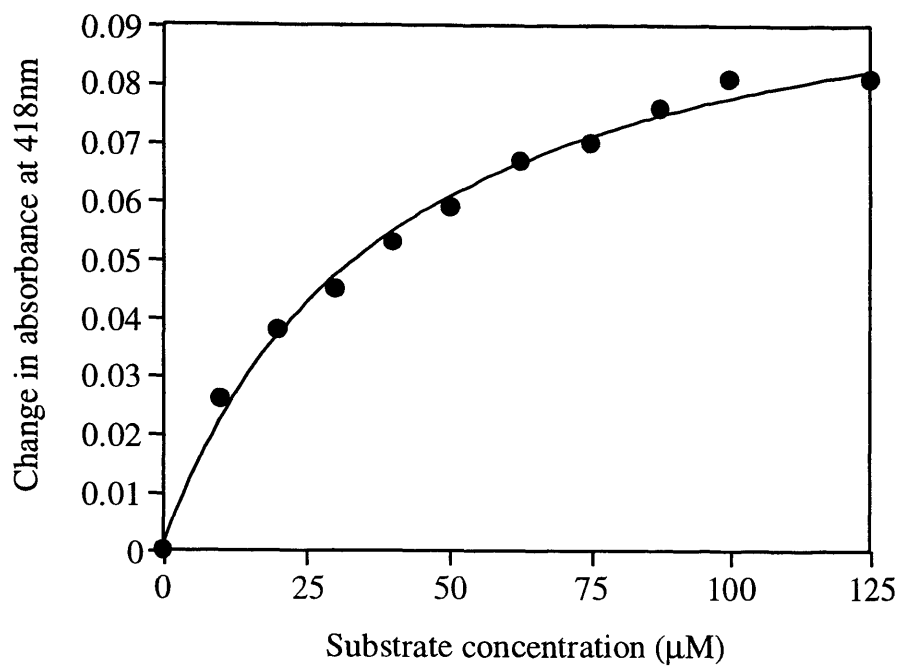


**Figure 4.6:** Data to represent the  $K_d$  determination for the C14 fatty acid, myristate with wild type intact P450 BM3 (a;  $K_d = 23 \pm 5.4$ ) and wild type haem domain (b;  $K_d = 29 \pm 3.3$ )

c)



d)

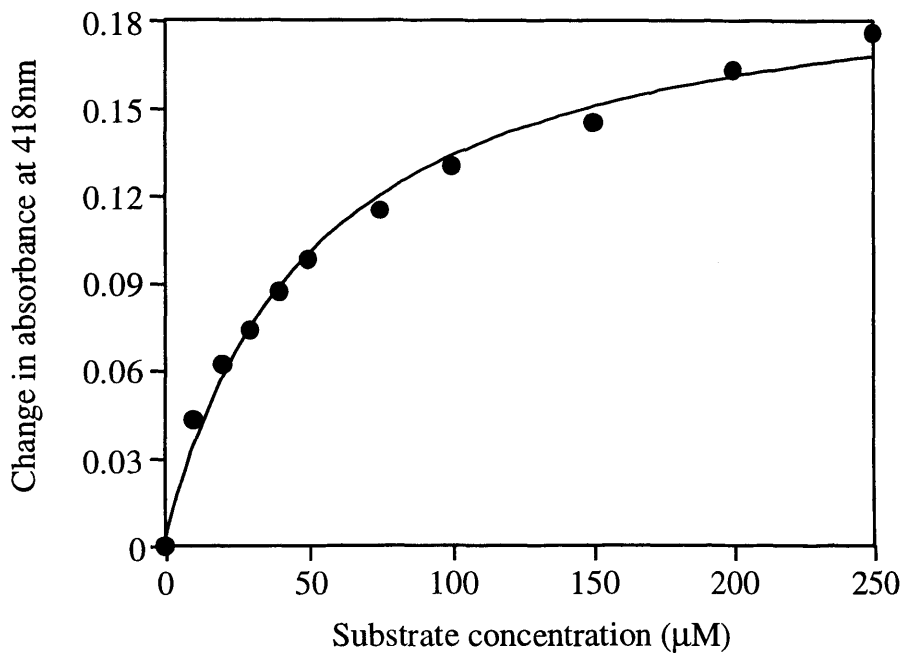
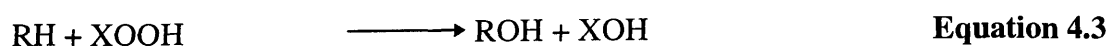
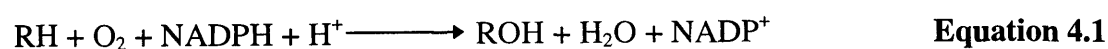


**Figure 4.6 (Continued):** Data to represent the  $K_d$  determination for the C14 trimethyl ammonium compound with R47E mutant intact P450 BM3 (c;  $K_d = 39 \pm 3.6$ ) and R47E mutant haem domain (d;  $K_d = 52 \pm 5.3$ )

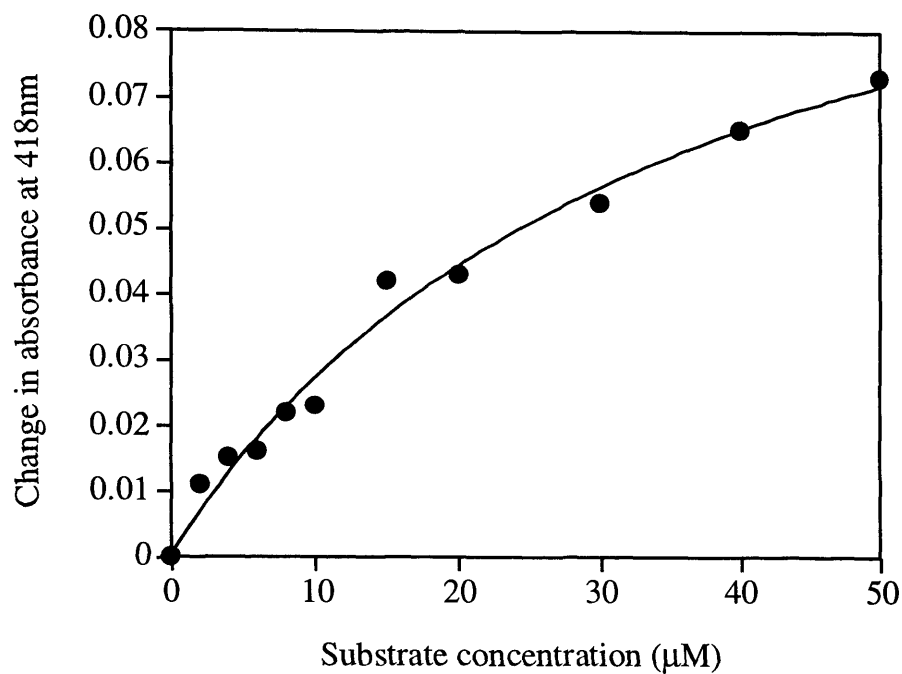
domain in the presence of C14 TMA. It was not possible to perform the  $K_d$  determinations for S1 in the presence of increasing concentrations of S2 as preliminary experiments indicated that either the critical micelle concentration for S1 was decreased in the presence of S2 or there was mixed micelle formation. The results given in Table 4.3 are therefore the results of a  $K_d$  determination from a single S2 concentration and are depicted in Figure 4.7. Approximate  $K_d$  estimates were obtained corresponding to 2.3mM for the wild type haem domain - C12 TMA interaction and 4.2mM for the R47E mutant haem domain - laurate interaction. An estimate of 10mM for the  $K_d$  of laurate binding to the R47E mutant haem domain was obtained from the NMR relaxation experiments described below. This result is in reasonable agreement with the result obtained by competition. The sum of the results in Table 4.3 regarding the C12 compounds suggest that the binding to the resting ferric state of the enzyme of a substrate possessing the same charge as the side chain of residue 47 is roughly ten-fold weaker than that of substrate having the opposite charge, which would be capable of making an ion pair interaction with the side chain functional group.

#### 4.4.3 Hydrogen Peroxide Formation

Since the earliest studies of liver microsomes, cytochrome P450 enzymes have been shown to be the main producers of reactive oxygen in the cell where hydrogen peroxide can be formed during drug metabolism (Gillette *et al.*, 1957). Subsequent studies by several groups revealed that cytochrome P450s catalyse monooxygenase (Eq. 4.1) but also oxidase (Eq. 4.2a, b, and c) and peroxidase (Eq. 4.3) reactions (Bernhardt, 1995):



a)



b)

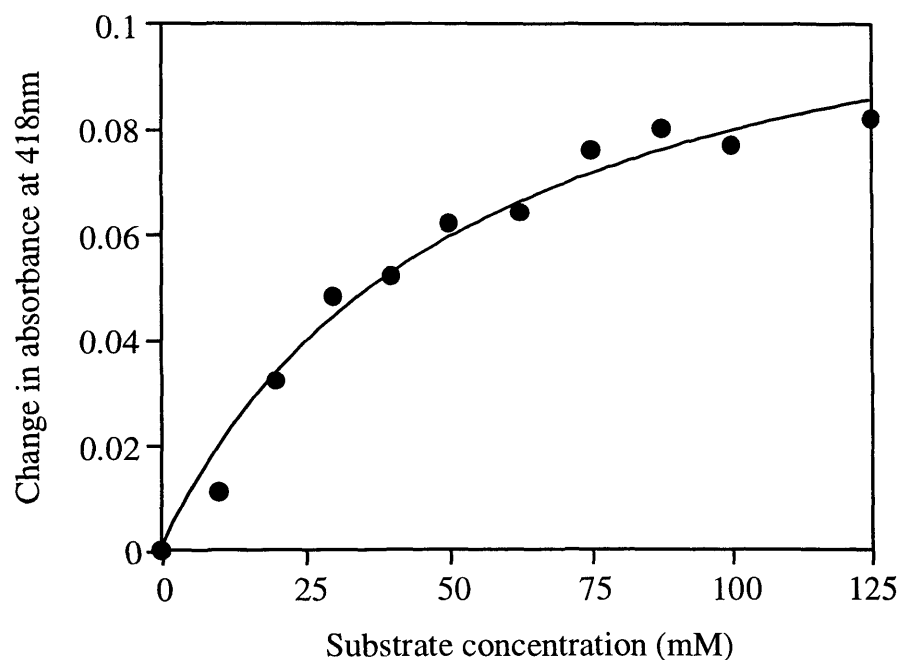


**Figure 4.7:** Data to represent the  $K_d$  determination by competition for myristic acid in the presence of 0.5mM C12 TMA with wild type haem domain (a;  $K_d = 35 \pm 6.3$ ) and for C14 TMA in the presence of 0.1mM lauric acid with the R47E mutant haem domain (b;  $K_d = 53 \pm 9.6$ )

As shown in Figure 1.2 in Chapter 1, it is possible for the cytochrome P450 catalytic cycle to become uncoupled such that the reactive ferryl oxygen species does not interact with the substrate to cause hydroxylation but reacts with water to produce hydrogen peroxide (Ortiz de Montellano, 1995a). A hydrogen peroxide assay was performed to monitor the amounts of hydrogen peroxide produced during catalysis in the presence of both classes of substrate. C12 substrates were chosen as it was known from the kinetic studies that these represented the poorest substrates and were therefore the most likely to result in an uncoupled reaction. The NADPH consumption assay was performed at the same time under identical conditions to allow direct comparison. The results are shown in Table 4.4. With both the wild type and R47E mutant intact P450 BM3 in the presence of laurate the hydrogen peroxide formation was less than  $10^{-5}$  mole peroxide formed per mole of NADPH consumed. That is, when the hydrogen peroxide formation is directly compared with the NADPH consumption, the ratio of hydrogen peroxide formed to NADPH consumed clearly indicates in all instances that hydrogen peroxide production is insignificant in comparison and therefore the reaction is tightly coupled.

**Table 4.4:** Determination of hydrogen peroxide using wild type and R47E mutant P450 BM3 with both 0.2mM C12 fatty acid (laurate) and 0.1mM C12 trimethylammonium compounds (C12 TMA) as substrate.

P450 BM3	Substrate	H <sub>2</sub> O <sub>2</sub> Production (mmol/min/mg)	NADPH Consumption (mmol/min/mg) <sup>a</sup>	Ratio
Wild Type	Laurate	$0.46 \times 10^{-5}$	0.41	$0.11 \times 10^{-4}$
	C12 TMA	$6.5 \times 10^{-5}$	0.16	$4.2 \times 10^{-4}$
R47E Mutant	Laurate	$4.44 \times 10^{-5}$	3.49	$0.13 \times 10^{-4}$
	C12 TMA	$7.4 \times 10^{-5}$	0.37	$2.0 \times 10^{-4}$

<sup>a</sup> NADPH consumption was performed under the same conditions as the hydrogen peroxide assay as detailed in the Materials and Methods section.

In the  $^1\text{H}$  NMR spectrum of the reaction mixture (Figure 4.9) the terminal methyl resonance of 11-hydroxylaurate appears as a well-resolved doublet at 1.19ppm, while the corresponding resonances of 9- and 10- hydroxylaurate appear as two closely spaced triplets at approximately 0.9ppm (Oliver *et al.*, 1997a). The spectra in Figure 4.9 demonstrate the formation of 9-, 10- and 11-hydroxylaurate in approximately the same ratios by both the wild type and mutant enzyme. It is thus clear that the R47E mutant of P450 BM3 is also capable of hydroxylating saturated fatty acids effectively.

For both the mutant and particularly, the wild type enzyme the peroxide production was somewhat greater with C12 TMA than with laurate, but was still less than  $10^{-3}$  moles peroxide per mole of NADPH consumed.  $^1\text{H}$  NMR spectroscopy of the reaction mixtures (Figure 4.10) showed that both enzymes catalysed hydroxylation of C12 TMA at the  $\omega$ -1,  $\omega$ -2 and  $\omega$ -3 positions in approximately the same ratios as the wild type.

#### 4.4.4 Oxygen Consumption

Oxygen consumption was measured in a Clark type oxygen electrode vessel as described in the Materials and Methods for both the wild type and mutant intact P450 BM3 with lauric acid and C12 TMA as substrate and representative traces of results are shown in Figure 4.8. The classic catalytic reaction dictates that NADPH and oxygen should be consumed in equimolar amounts. The obtained experimental results for oxygen consumption were compared with NADPH consumption rates obtained previously using the spectrophotometric assay and therefore determination of NADPH consumption and oxygen consumption rate were not performed simultaneously. These results are represented in Table 4.5.

For the wild type and R47E mutant enzyme with both the fatty acid and the C12 trimethylammonium compound as substrates, the ratio of oxygen consumption to NADPH consumption was satisfactorily in the same order, indicating that equivalent concentrations of oxygen and NADPH are consumed.

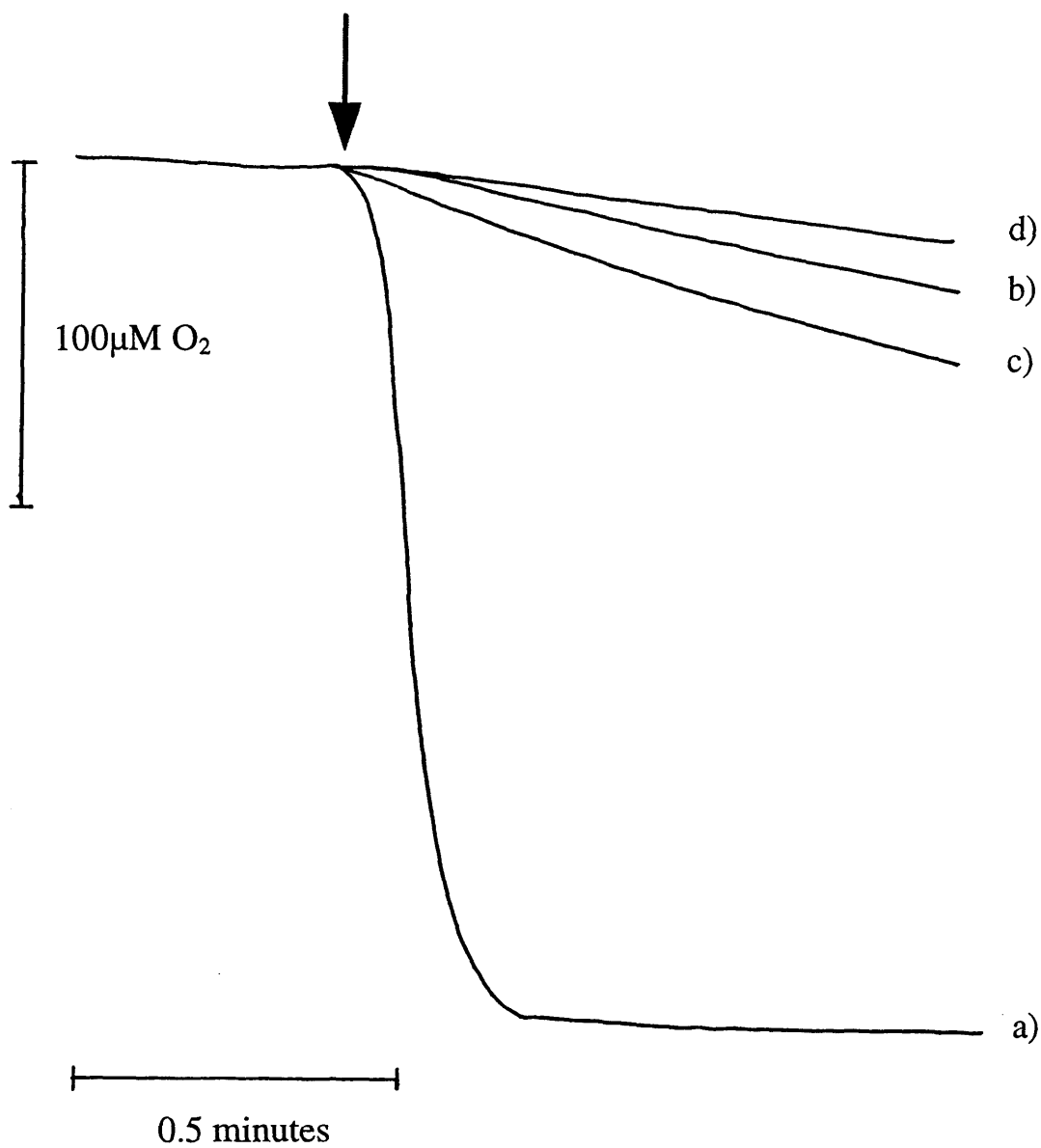


**Figure 4.8:** Oxygen consumption was measured in a Clark type oxygen electrode vessel as described in the Materials and Methods for both the wild type P450 BM3 (83.8 $\mu$ M) with 0.4mM lauric acid (a) and 0.2mM C12 TMA (b) as substrate and R47E mutant P450 BM3 (57.3 $\mu$ M) with 0.4mM lauric acid (c) and 0.2mM C12 TMA (d) as substrate. Substrate and NADPH were preincubated in the vessel and the reaction was initiated by addition of enzyme as indicated by the vertical arrow.

**Table 4.5:** Determination of Oxygen Consumption using wild type and R47E mutant P450 BM3 using both C12 substrates, 0.4mM laurate and 0.2mM C12 TMA.

P450 BM3	Substrate	O <sub>2</sub> Consumption (mmol/min/mg)	NADPH Consumption (mmol/min/mg) <sup>a</sup>	Ratio
Wild Type	Laurate	14.3	13.4	1.07
	C12 TMA	2.16	2.18	0.99
R47E Mutant	Laurate	1.30	1.33	0.98
	C12 TMA	0.49	0.52	0.94

<sup>a</sup> The values for the NADPH consumption used were those obtained in the presence of 0.1M phosphate at pH 8.

#### 4.5 NMR Spectroscopy

NMR spectroscopy was used to measure the paramagnetic relaxation effects on the protons of the substrate molecule to obtain estimates of distances between the individual protons of the bound substrate and the haem iron (Modi *et al.*, 1995b). The substrates used were laurate and its analogue 12-bromolaurate, a good substrate which has a better resolved NMR spectrum allowing the positions of the C10 and C11 methylene groups (the sites of hydroxylation) to be determined. The relaxation times and the derived distances are given in Table 4.6, where they are compared with the wild type enzyme previously published (Modi *et al.*, 1995b; Modi *et al.*, 1996b). In the initial ferric complex, the protons for the terminal methyl group are significantly closer in the R47E mutant haem domain (6.05Å) than in the wild type haem domain (7.6Å). On reduction of the complex to the ferrous state, there is a structural change which leads to substantial movement of the substrate towards the haem (Modi *et al.*, 1996b) into a position of hydroxylation at the active site. This movement is also in evidence with this mutant domain. In the ferrous complex the difference in position of the laurate terminal methyl group is much smaller at about 0.2Å and is only marginally

**Table 4.6:** Paramagnetic relaxation times and iron-proton distances for laurate and 12-bromolaurate binding to the haem domain of the wild type and R47E mutant cytochrome P450 BM3.

Protein	Substrate	Parameter	C10 -CH <sub>2</sub> -	C11 -CH <sub>2</sub> -	C12 -CH <sub>2</sub> X <sup>a</sup>
Ferric State <sup>b</sup>					
R47E Mutant	Laurate	T <sub>1,M</sub> (ms)	- <sup>d</sup>	- <sup>d</sup>	0.43±0.03
		r (Å)	- <sup>d</sup>	- <sup>d</sup>	6.05±0.1
Wild Type <sup>c</sup>		r (Å)	- <sup>d</sup>	- <sup>d</sup>	7.6±0.3
Ferrous State <sup>b</sup>					
R47E Mutant	Laurate	T <sub>1,M</sub> (ms)	- <sup>d</sup>	- <sup>d</sup>	5.30±0.20
		r (Å)	- <sup>d</sup>	- <sup>d</sup>	4.89±0.02
Wild Type <sup>c</sup>		r (Å)	- <sup>d</sup>	- <sup>d</sup>	5.1±0.2
R47E Mutant	12-Bromo-laurate	T <sub>1,M</sub> (ms)	0.17±0.01	0.26±0.01	5.10±0.10
		r (Å)	2.75±0.03	2.95±0.02	4.85±0.02
Wild Type <sup>c</sup>		r (Å)	3.0±0.1	3.1±0.1	5.1±0.1

<sup>a</sup> X=H or Br.

<sup>b</sup> Relaxation measurements on the ferric state were carried out at 200MHz and those on the ferrous state at 600MHz.

<sup>c</sup> Data from Modi *et al.* 1995b, Modi *et al.* 1996b.

<sup>d</sup> Resonance not resolved.

significant. Similar observations were made with 12-bromolaurate, where the methyl group is in a similar position in the ferrous complexes of the wild type and mutant haem domains. These results suggest that in the ferric R47E mutant, the negatively charged fatty acid substrate may be bound closer to the haem moiety through an unfavourable interaction with the negatively charged side chain of the glutamic acid residue now at position 47. In the ferrous complex, the importance of the side chain at position 47 is diminished as any effect on binding is reduced.

The relaxation experiments also provide estimates for the equilibrium dissociation constant,  $K_d$ , for the binding of laurate in the ferric and ferrous state and these are included in Table 4.3. In the ferric state, laurate binds weakly to both proteins, though at 10mM, binding to the R47E haem domain is 12-fold weaker than the wild type protein. As noted previously (Modi *et al.*, 1996b), substrate binding is significantly stronger for the ferrous enzyme and is comparable to the kinetically determined  $K_M$ . In the ferrous state, laurate binds 45-fold more weakly to the R47E mutant than the wild type protein at 3.6mM and 79 $\mu$ M respectively, representing a significantly larger difference than that seen in the ferric enzyme.

NMR spectroscopy was also used to determine whether production of the hydroxylated products had taken place and the nature of the products produced. A reaction mixture containing substrate, NADPH (in 0.1M phosphate made up with 99.96%  $D_2O$ , pH\*8) and enzyme made was incubated at room temperature. A 1D proton NMR spectra was measured after 16 hours (Figure 4.9 and 4.10). The peaks for the distinguishable carbon protons have been labelled. With lauric acid as substrate, the major product has  $\omega$ -1 hydroxylation, 11-hydroxylaurate. Here the terminal methyl triplet is converted to a doublet and shifts downfield closer to the large methylene peak. For both the wild type and R47E mutant this doublet is present at approximately 1.2ppm indicating  $\omega$ -1 hydroxylation has taken place. When looking at Figure 4.9 representing the catalysis of C12 TMA in the presence of wild type and R47E mutant protein the doublet is also present again suggesting  $\omega$ -1 hydroxylation has taken place.

# **SPECIAL NOTE**

**This item is tightly bound  
and while every effort has  
been made to reproduce the  
centres force would result  
in damage.**

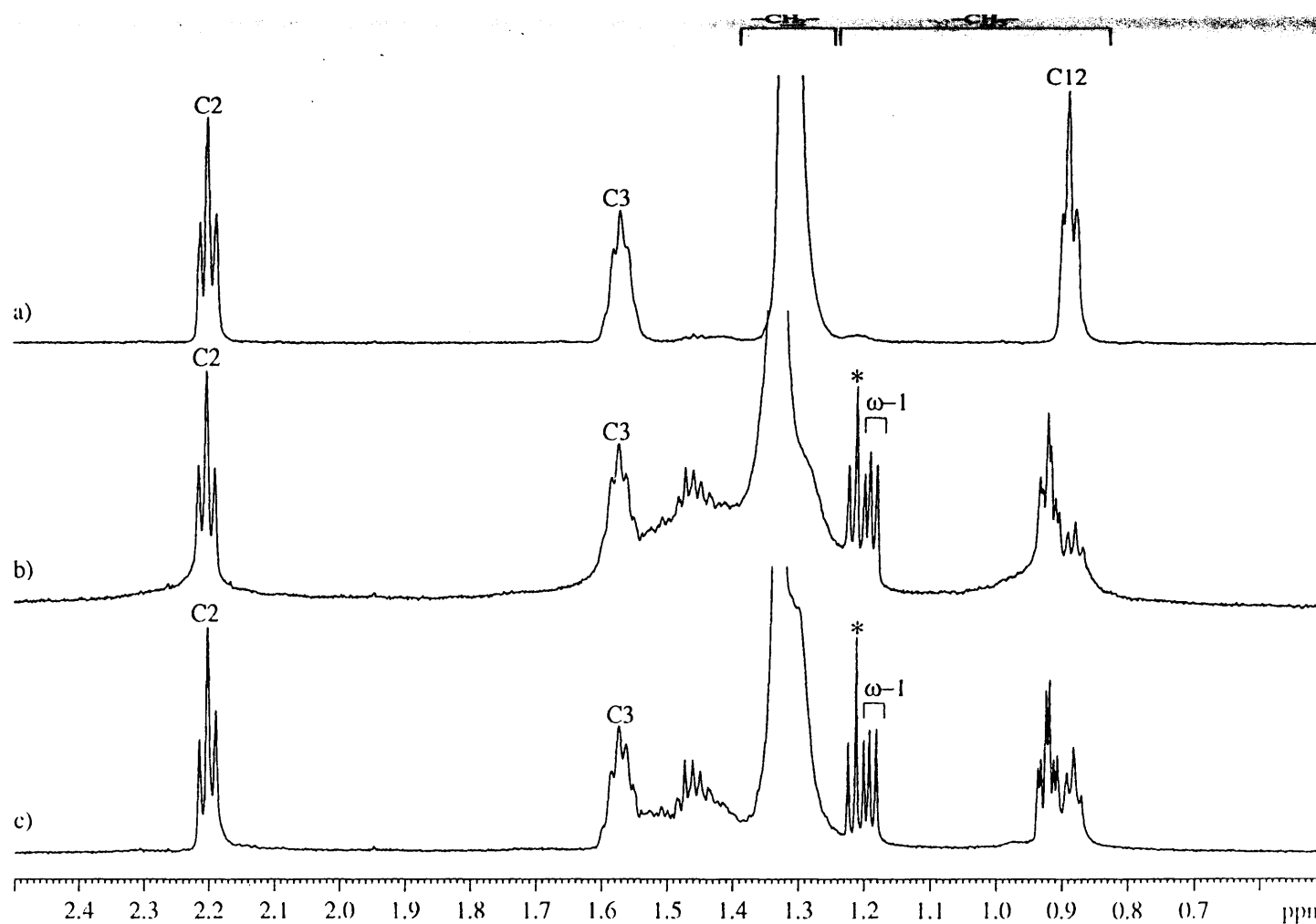


**Figure 4.9:** 600MHz proton NMR spectra of the reaction mixtures from incubation of laurate with (b) wild type and (c) R47E mutant P450 BM3. The spectrum of laurate (a) is included as a reference. The reaction mixture contained 10 $\mu$ M enzyme, 2mM laurate and 2mM NADPH in 0.1M phosphate, pH\*8.0 and were incubated for 24 hours at room temperature followed by 3 days at 4°C to ensure that the reaction had gone to completion. The doublet from the methyl resonance of the product hydroxylated at the  $\omega$ -1 position is marked. The asterisk indicates a doublet resonance from NADPH.

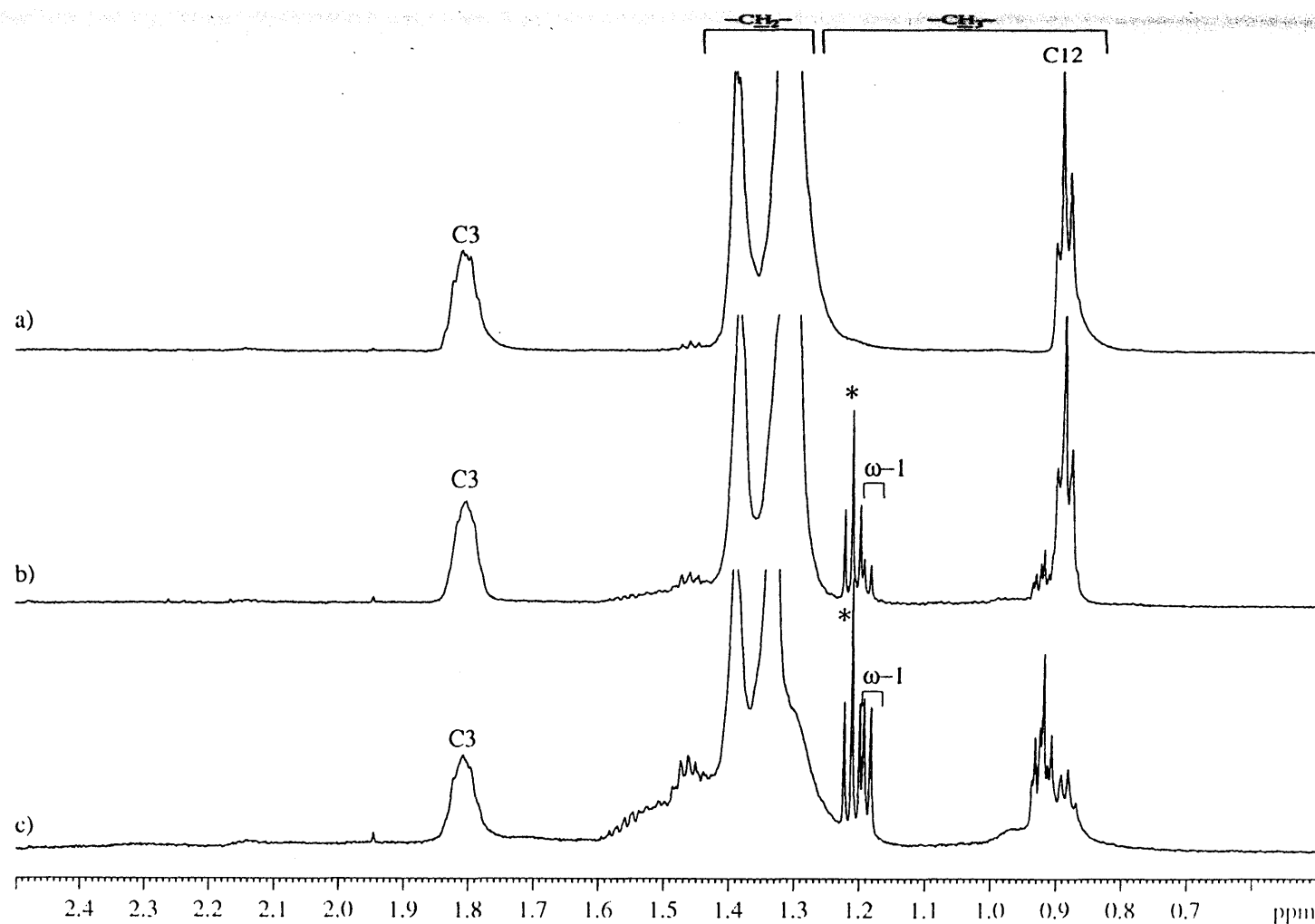


**Figure 4.10:** 600MHz proton NMR spectra of the reaction mixtures from incubation of C12 TMA with (b) wild type and (c) R47E mutant P450 BM3. The spectrum of laurate (a) is included as a reference. The reaction mixture contained 10 $\mu$ M enzyme, 2mM laurate and 2mM NADPH in 0.1M phosphate, pH\*8.0 and were incubated for 24 hours at room temperature followed by 3 days at 4 $^{\circ}$ C to ensure that the reaction had gone to completion. The doublet from the methyl resonance of the product hydroxylated at the  $\omega$ -1 position is marked. The asterisk indicates a doublet resonance from NADPH.

## 4.6 Discussion

P450 BM3 interacts with a broad spectrum of substrates, though this monooxygenase shows a marked preference for saturated fatty acids specifically of C12 to C18 in chain length (Miura and Fulco, 1975; Ho and Fulco, 1976; Fulco, 1991). To explain observed differences in hydroxylation for the various fatty acids by P450 BM3 it was originally hypothesised that the enzyme contained three sites essential for catalytic activity: two binding sites capable of interaction with the methyl and carboxylate groups of the fatty acid substrate and an active site to perform the hydroxylation reaction (Miura and Fulco, 1975). After the publication of the x-ray crystal structure of the haem domain (Ravichandran *et al.*, 1993), these binding sites were proposed to be centred around two residues within the protein: arginine 47, whose guanidinium group provides a polar binding site which could interact with the substrates carboxylate and whose flexibility would be necessary for the hydroxylation of fatty acids of various lengths, and phenylalanine 87, the aromatic side chain of which contributes to the formation of a hydrophobic pocket which could be involved in sequestration of the terminal methyl of the saturated fatty acid and thus protecting it from hydroxylation. The C15 and C16 fatty acids, which exhibited the highest  $k_{cat}$  values, would interact optimally with all three sites resulting in hydroxylation at the fastest rate. Paramagnetic relaxation experiments have been used in conjunction with the crystal structure to construct an approximate model for the binding of lauric acid to the oxidised enzyme and reduced enzyme (Modi *et al.*, 1995b; Modi *et al.*, 1996b). This substrate binding model indicates that the alkyl chain of laurate is only just long enough to extend from arginine 47 to the position close to the haem required for hydroxylation at the  $\omega$ -1,  $\omega$ -2 and  $\omega$ -3 positions (Modi *et al.*, 1996b). It also shows that in the ferric form of the haem domain, lauric acid is distant from both the iron in the haem moiety and the guanidinium group of the arginine 47 side chain, which may indicate why it is relatively unsuitable as a substrate for P450 BM3. This suggests that the substrate must adopt a fully extended conformation for interaction with all three sites within the substrate binding domain in order for hydroxylation to occur, ultimately resulting in a reduced rate of reaction (Miura and Fulco, 1975; Boddupalli *et al.*, 1992b). The existence of these postulated sites has been born out with the recent

publication of the x-ray crystal structure of the haem domain of P450 BM3 complexed with the substrate palmitoleic acid (Li and Poulos, 1997) and this is discussed in more detail later.

When viewing the data in Table 4.2 above it can be seen that after the substitution of arginine 47 by glutamate in cytochrome P450 BM3 (the R47E mutation) there has been a switch in the substrate specificity, such that the mutant protein displays a greater preference for the trimethylammonium compounds as opposed to the original saturated fatty acid for substrates. Results from both the hydrogen peroxide assay and the oxygen consumption assays indicate that catalytic reaction with the wild type and mutant enzyme using either fatty acids or TMA compounds as substrates is tightly coupled, such that the NADPH and O<sub>2</sub> consumed is not used to produce H<sub>2</sub>O<sub>2</sub> excessively or “extra” water (Gorsky *et al.*, 1984; Atkins and Sligar, 1987; Ortiz de Montellano, 1995a). On comparison of the ratios of the specificity constant,  $k_{cat}/K_M$ , of the C16 fatty acid and TMA compound for both the wild type and mutant proteins, the ratios obtained are 232 for the wild type and 0.8 for the R47E mutant P450 BM3. Put another way, the wild type enzyme is approximately 300-fold more active against the fatty acids than against the trimethylammonium compound, while the R47E mutant shows a very similar activity against both, having a  $k_{cat}$  as high as 19s<sup>-1</sup> for hydroxylation of the C16 TMA. These results are mirrored with the results for the C14 substrates. The change in charge state from positive to negative of the amino acid side chain at position 47 has essentially reciprocal effects on the activity of the enzyme towards the two different, oppositely charged, groups of substrates. For the fatty acids, the  $k_{cat}/K_M$  values of the wild type enzyme are 14- to 21-fold higher than those of the mutant, while for the TMA compounds the  $k_{cat}/K_M$  values are 12- to 26-fold higher for the mutant than the wild type. Similarly the binding constants for the fatty acids to the wild type enzyme are generally closely comparable to those for the TMA compounds to the R47E mutant. Exact comparisons are difficult to make in view of the differences in length between the arginine and glutamate side chains and between fatty acids and the alkyl trimethylammonium compounds. A glutamate side chain is two bonds (ca. 2.3Å) shorter than an arginine, although the difference in the effective positions of the charges will be slightly less than this. At the same time, recalling that

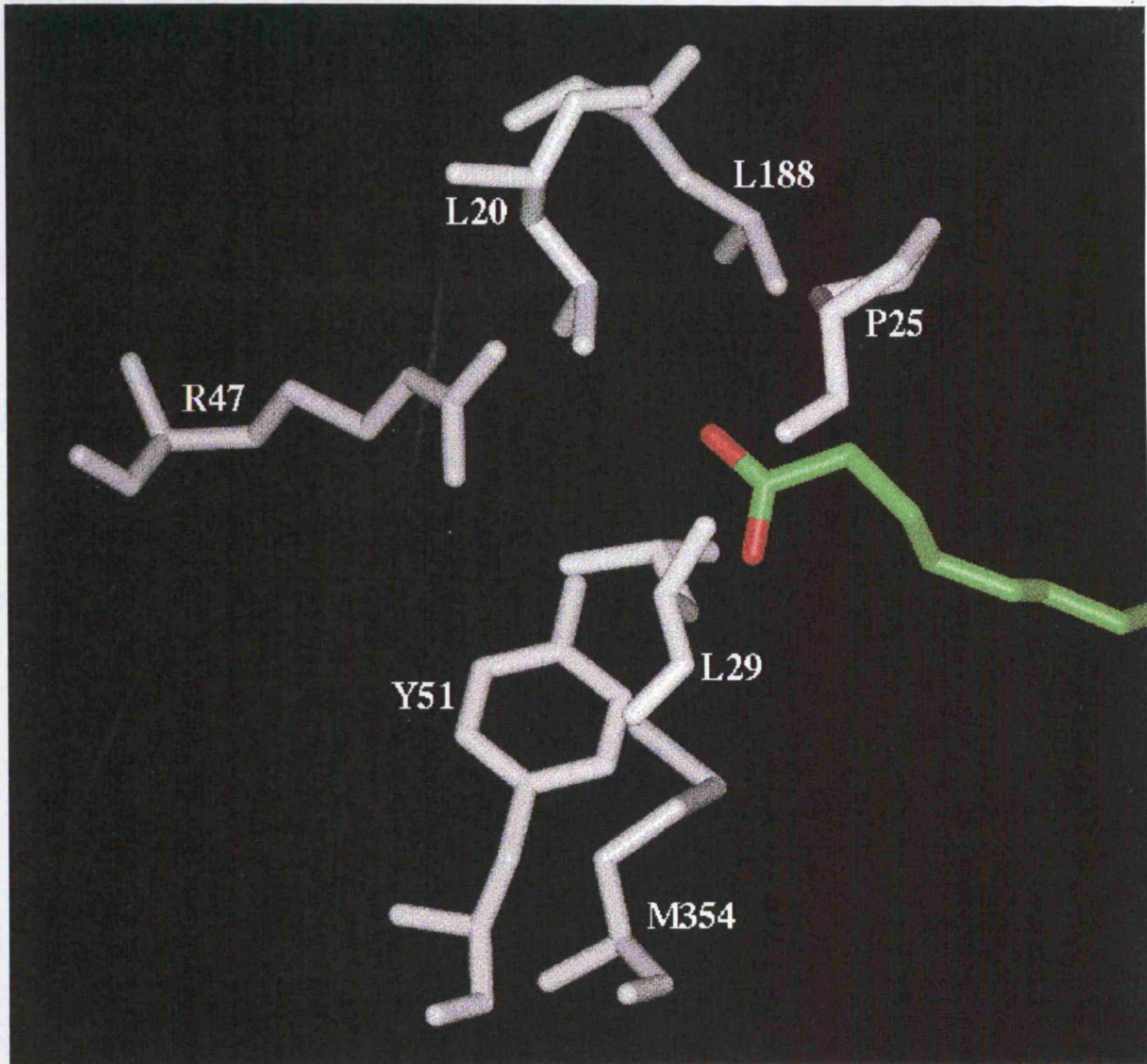
the charge of a trimethyl ammonium group is very largely delocalised over the N-methyl groups a C12 TMA compound is effectively one bond longer than a C12 fatty acid. For an illustration of this point refer to Figure 4.2.

It is not surprising that trimethylammonium compounds can act as substrates for both the R47E mutant P450 BM3 and the wild type protein, where the bulky trimethylammonium head group is accommodated within the substrate binding site which has been demonstrated to be a channel approximately 8Å to 10Å in diameter and 20Å in length suggesting a long funnel shape. Molecular modelling experiments involving the docking of C14 myristic acid into the substrate binding channel suggested that the active site cleft undergoes considerable motion upon substrate binding (Li and Poulos, 1995) opening to at least 14.7Å width (Paulsen and Ornstein, 1995). This acceptance of compounds, which contain large functional groups increasing that substrates bulk, has been observed with other fatty acid metabolising cytochrome P450s, notably those from the  $\omega/\omega-1$  hydroxylating Family 4 enzymes. Alterman *et al.* (1995) also observed in a P450 4A1/ NADPH cytochrome P450 reductase fusion protein that modifications adjacent to the carboxylic acid group of lauric acid, such as  $\alpha,\alpha$ -dimethylation, were well tolerated.

The R47E mutant is clearly still a reasonably effective fatty acid hydroxylase, forming the same products as the wild type in essentially the same ratios, at maximum rates less than an order of magnitude slower. This is in marked contrast to the previous report (Graham-Lorence *et al.*, 1994) specifying a lack of substrate binding with the C16 fatty acid palmitate and a recent report (Graham-Lorence *et al.*, 1997) that this mutant is catalytically inactive towards arachidonic acid and eicosapentaenoic acid and their methyl esters. Since arachidonic acid is epoxidised by P450 BM3 at the 14, 15 ( $\omega-5$ ,  $\omega-6$ ) positions (Capdevila *et al.*, 1996), it must be able to bind differently in the active site from the saturated fatty acids which are hydroxylated at the  $\omega-1$ ,  $\omega-2$  and  $\omega-3$  positions. Nonetheless, it is surprising that a difference in binding near the haem should lead to such a difference in the importance of the arginine 47 side chain, some 15Å away.

The differences in catalytic activity between the wild type and mutant enzymes towards the two classes of substrates are smaller than would be expected for the conversion of a significant electrostatic attraction between the substrate and the enzyme into an electrostatic repulsion. In terms of binding, direct comparisons can only be made for the C12 compounds, where the affinity for a substrate having the same charge as residue 47 is only approximately ten times weaker than that for a substrate having the opposite charge. These observations, which suggest that arginine 47 does not make a major contribution to substrate binding, can be understood in the light of the very recently published crystal structure of the complex of the ferric state of the enzyme with palmitoleic acid (Li and Poulos, 1997). Figure 4.11 shows the environment of the carboxylate group of the palmitoleic acid bound to the haem domain of cytochrome P450 BM3. Only those side chains that are within 7Å of the carboxylate group of the substrate have been illustrated. Arginine 47 is among a group of residues, which also includes leucine 20, proline 25, leucine 29 and tyrosine 51, identified within the substrate binding pocket that interact with the polar end of the substrate (Li and Poulos, 1995). Of particular interest are arginine 47 and tyrosine 51. The side chain of arginine 47 appears to be very flexible even in the complex, but is positioned so as to be able to form an ion-pair with the carboxylate. In addition, the carboxylate is capable of forming a second hydrogen bond to the phenolic hydroxyl of tyrosine 51 to strengthen substrate binding and support hydroxylation. Assuming that the two classes of substrates bind similarly to the wild type and mutant enzymes (see below), this structure indicates two possible reasons for the modest effect of a “mis-match” of charge between residue 47 and substrate. First, from the crystal structures of both the substrate-free and substrate-bound P450 BM3 haem domain we know that the amino acid side chain at position 47 is not well resolved, suggesting that it is highly mobile (Ravichandran *et al.*, 1993; Li and Poulos, 1997). The flexibility, possibly together with the large gating of the substrate binding pocket of P450 BM3, will allow, for example, movement of the substituted glutamyl side chain within the substrate binding site to move away from the carboxylate of a fatty acid. At the same time, tyrosine 51 will continue to provide a favourable interaction. Its hydroxyl group will act as a hydrogen donor to the carboxylate anion of fatty acid substrates, thus supporting fatty acid hydroxylation in the absence of the guanidinium group as in the R47E mutation, and will also be able to contribute a favourable interaction between its electronegative

oxygen and the...  
instant enzyme



likely to have...  
the fatty acids...  
laurate (Table 4.1)...  
substrate...  
towards the iron...  
movement of laurate...

**Figure 4.11:** The environment of the substrate carboxylate in the crystal structure (Li and Poulos, 1997) of the complex of palmitoleic acid with the ferric state of the haem domain of cytochrome P450 BM3.

oxygen and the cation of trimethylammonium substrates with both the wild type and mutant enzymes.

It is clear that both the initial binding of the substrate (Modi *et al.*, 1995b; Li and Poulos, 1997) and subsequent steps in the catalytic cycle (Modi *et al.*, 1996b; Oliver *et al.*, 1997a) involve structural changes in the enzyme. The changes in the optical absorption spectra of the haem on substrate binding to cytochromes P450 have been attributed (Dawson, 1988; Sarisalani, 1991) to a change in spin state of the haem iron from low ( $S = 1/2$ ) to high spin ( $S = 5/2$ ) accompanied by the expulsion of the water molecule from the sixth coordination position of the iron. In the case of P450 BM3, the expulsion of the coordinated water must result from the structural change accompanying substrate binding, since the substrate binds to the ferric form of the enzyme at some distance from the iron (Modi *et al.*, 1995b; Li and Poulos, 1997; see also Table 4.6) and cannot displace the water directly. Where they can be measured, the changes in the optical absorption spectra of the haem on the binding of fatty acids and alkyl trimethylammonium compounds to wild type and R47E mutant enzyme are closely similar, indicating that a similar structural change is induced by substrate binding in each case. The exception is the observed optical absorption spectra of the haem on the binding of fatty acids to the R47E mutant. The spectrum indicates that fatty acid substrate binding is seriously affected by this mutation and may account for previous reports that claimed the R47E mutation was not catalytically active as addition of palmitate did not produce a typical "Type I" binding spectra consisting of a decrease in absorbance from 418nm with concomitant increase at 390nm (Graham-Lorence *et al.*, 1994). This lack of change in the substrate binding spectra was more likely to have resulted from the radical increase in equilibrium dissociation constants of the fatty acids after the mutation as typified by that calculated for the C12 substrate, laurate (Table 4.3). The next step in the catalytic cycle, the reduction of the enzyme-substrate complex, is accompanied by a marked movement of the bound substrate towards the iron, into position for hydroxylation (Modi *et al.*, 1996b); a very similar movement of laurate occurs on reduction of its complex with the haem domain of the R47E mutant, again emphasising the similarity in behaviour of the mutant and wild type enzymes.

The R47E mutation produces an increase in  $K_M$  for fatty acids and a decrease in  $K_M$  for trimethylammonium compounds which, though quite small in all cases, is noticeably less for the C14 and C16 compounds (less than 4-fold) than for the C12 compounds (13- to 15-fold). One would expect a proportionally larger contribution of the electrostatic interaction to the overall binding affinity of compounds with shorter alkyl chains, and hence weaker hydrophobic interactions. As mentioned previously, it is known that laurate (C12) represents the shortest fatty acid substrate for P450 BM3 (Miura and Fulco, 1975) and its alkyl chain has been shown to be only just long enough to extend from arginine 47 to the position close to the haem required for hydroxylation at the  $\omega$ -1,  $\omega$ -2 and  $\omega$ -3 positions (see Modi *et al.*, 1996b). Using this information, it is thus possible that the binding of laurate to the wild type enzyme is a balance between optimising the interactions of the carboxylate with arginine 47 and tyrosine 51 and those of the alkyl chain with the hydrophobic remainder of the binding site. When the interaction with the arginine is abolished (indeed made repulsive) in the R47E mutant, the optimum hydrophobic interactions may lead to a different mode of binding. Support for this comes from the paramagnetic relaxation experiments, which show that laurate does bind differently to the R47E mutant than to the wild type enzyme in the ferric form of the complex, the methyl group of laurate binding 1.5Å closer to the iron in the mutant. With the longer alkyl chains of palmitate and myristate, it may be possible to simultaneously optimise both the electrostatic and the hydrophobic interactions so that little or no change in the mode of binding takes place on the substitution of arginine 47. Similar arguments apply to the binding of the trimethyl-ammonium compounds to the R47E mutant.

One might question the validity of the arguments presented as some of the results obtained rely on the use of the haem domain as opposed to the intact P450 BM3, for example, to obtain certain equilibrium binding constants and in the NMR paramagnetic relaxation experiments. The reaction of cytochrome P450s with phenylhydrazines is a well documented method for the investigation of the active site (For a review see Ortiz de Montellano, 1995 and references therein). This results in the formation of phenyl-iron, where further treatment with potassium ferricyanide shifts the phenyl group from

the iron to the porphyrin nitrogens. Acidification and extraction of the ferricyanide-treated enzymes yields a different mixture of the four possible N-phenylprotoporphyrin IX regioisomers which are specific for the active site topology of the cytochrome P450 under investigation. The ratios of the regioisomers with the phenyl ring on pyrrole rings B, A, C and D are 2:10:2:1 for P450 BM3 and 2:9:2:1 for its haem domain showing that presence of the reductase does not significantly perturb the active site topology of cytochrome P450 BM3 (Tuck *et al.*, 1992) and therefore the estimation of active site parameters using the isolated haem domain are pertinent for the intact protein.

The results reported here thus show that arginine 47 does play a role in the binding of the carboxylate group of fatty acid substrates to cytochrome P450 BM3, though this is not quantitatively a dominant one. This is in good agreement with the conclusions drawn very recently from the crystal structure of an enzyme-substrate complex (Li and Poulos, 1997). Additionally, the phenomenon illustrated here, where a single amino acid can significantly alter the substrate specificity of an enzyme, is not without precedent. Investigations into the roles of individual amino acids in determining the specific activity of cytochrome P450 enzymes showed that the mouse P450 2a4 and P450 2a5 differed by only 11 residues within their 494 amino acids. Changing phenylalanine 209 to leucine is sufficient to convert the specificity of coumarin 7-hydroxylase (P450 2a5) to steroid 15 $\alpha$ -hydroxylase (P450 2a4). This experiment dramatically demonstrates that a single amino acid residue can control the enzymatic specificity of a specific form of P450 (Lindberg and Negishi, 1989). The single point mutation of leucine 209 to alanine resulted in decreased catalytic activity towards androstenedione with concomitant increase in activity towards progesterone for cytochrome P450 2B1 (Szklarz *et al.*, 1995). And finally, the fatty acid hydroxylase P450 2C2 which shows absolutely no catalytic activity towards steroids, yet after a single substitution of valine for serine 473 exhibits progesterone 21-hydroxylase activity (Ramarao and Kemper, 1995).

## ***Chapter 5: Arginine 47 to Cysteine Mutation***

### ***5.1 Introduction***

Site-directed mutagenesis (SDM) allows the mechanistic enzymologist to replace selectively any amino acid in an enzyme of interest and as such, is one of the most powerful techniques available for understanding the molecular basis for protein functions as well as creating novel proteins for practical applications. For many millions of years, proteins have been constructed using the same building blocks and this provides the major limitation for SDM, in that the target amino acid can only be replaced by one of the 20 naturally occurring amino acids. An aspartate to glutamate or asparagine to glutamine mutation are examples of homologous mutation where the amino acid side chains differ in length and volume, although possess similar chemical properties. With other amino acids the properties of the target amino acid, such as hydrogen bonding for a tyrosine to phenylalanine mutation or side chain length for a lysine to arginine mutation, have to be altered to find the most appropriate replacement (Schindler and Viola, 1996). For some mechanistically important amino acids, such as histidine, even though no structurally similar replacements are available, asparagine and glutamine are often used to maintain hydrogen-bonding (Plapp, 1995).

This limitation in the number of replacement amino acids has been recognised and several approaches have been developed in an attempt to overcome the restrictions. Unnatural amino acids have been introduced through the use of chemically aminoacylated transfer RNA molecules. SDM is used to convert the codon for the target amino acid into the amber codon TAG which is not recognised by any of the common transfer RNAs involved in protein synthesis. A suppressor transfer RNA which recognises the amber nonsense codon and is then chemically aminoacylated with the desired unnatural amino acid and introduced into an *in vitro* transcription/translation system to allow incorporation of the unnatural amino acid at the desired site (Ellman *et al.*, 1991). Though the potential for this suppressor method is great, there are associated synthetic challenges as well as high costs which restrict its implementation.

Prior to the development of mutagenesis techniques, chemical modification was the method of choice for producing variants of a chosen native protein. Early this century, modifications were carried out largely to gain understanding of the chemical composition of proteins. Later, this approach became useful to study protein function. As knowledge of protein structure grew, the modification studies became more sophisticated, such that carefully designed reagents were used to probe the reaction mechanisms and to detect the changes in protein conformation that accompany function (Means and Feeney, 1971). For enzymes where the gene has not yet been fully characterised, chemical modification remains a useful alternative to site-directed mutagenesis in conducting structure/function investigations (Hirasawa and Knaff, 1993). For many amino acids, these methods usually suffer from a lack of specificity and/or incomplete modification. In contrast, cysteine modification reagents are numerous, specific and generally go to completion due to the intrinsic reactivity of the thiol (-SH) group (Brocklehurst, 1979; Wynn and Richards, 1993). The thiol side chain functional groups of cysteine residues are extremely reactive with many reagents, including most alkylating agents, heavy metal ions and are easily oxidised by mild oxidising agents (Brocklehurst, 1979). This, together with a relatively low abundance of cysteine, results in modification at one or a few sites in a protein.

The methods of SDM and chemical modification can be combined to allow the site-specific alteration of any amino acids in a protein by a straight forward procedure. This takes advantage of the chemical reactivity of thiol groups by allowing the selective modification of a cysteine that has been substituted for the functional group of interest by SDM. At the same time, the shortcomings of each individual method are overcome: the limited availability of analogues for SDM and limited specificity in chemical modification studies. In these investigations, the arginine 47 to cysteine variant of the both the intact P450 BM3 and its haem domain were produced to further explore the role of the amino acid side chain at position 47. These mutants lack the flexible and positively charged protruding side chain and have a single cysteine residue introduced in the upper region of the substrate binding pocket near the surface of the protein molecule, away from the catalytic centre. Chemical modifications were then performed

to specifically alter this cysteine to glutamic acid “analogues” using either iodoacetic acid or iodopropionic acid and these unnatural amino acid side chains are depicted in Figure 5.1. This figure emphasises the differences between the naturally occurring amino acids and the “analogues”, in that both the S-carboxymethyl and S-carboxyethyl cysteine 47 derivatives will be longer than the glutamate 47 substitution they are attempting to mimic.

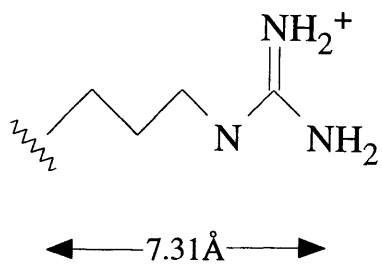
## 5.2 Protein Expression and Characterisation

Arginine 47 was substituted by cysteine in both the intact P450 BM3 and in its haem domain. As before, the gene was completely sequenced to confirm the presence of the desired mutation and to ensure no spurious mutations were present. In both cases yields of the Arg47→Cys (R47C) mutant proteins were less than that of the wild type, in the range of 50-100 mg pure protein per litre of culture, due to accidental loss of protein during the purification procedure. All proteins were shown to be pure by existing as a single band on a Coomassie blue stained SDS-PAGE gel and by their absorbance ratio of  $A_{418\text{nm}}/A_{280\text{nm}}$ ; 0.688 for the R47C mutant intact P450 BM3 and 1.629 for the R47C mutant haem domain.

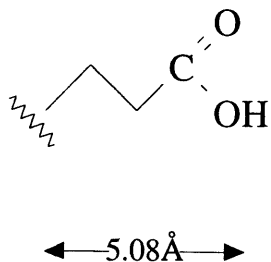
## 5.3 Electrospray Mass Spectroscopy

Mass spectroscopy was used to estimate the molecular weight of the R47C mutant enzymes to confirm at the protein level that the desired mutation had taken place. The results are given in Table 5.1. The calculated masses were calculated from the recombinant protein sequence (Ruettinger *et al.*, 1989) using the software on the mass spectrometer, assuming all cofactors had been removed.

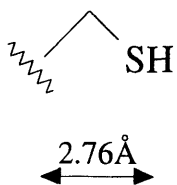
The results obtained showed reasonable precision for the intact enzyme, indicating a series mass of 117,593Da with standard error of 15Da for the R47C mutant of the intact P450 BM3. The result for the R47C mutant is in very good agreement with the calculated mass indicating the R47C mutant intact P450 BM3 was purified with the majority of the enzyme with the N-terminal methionine removed unlike the R47E



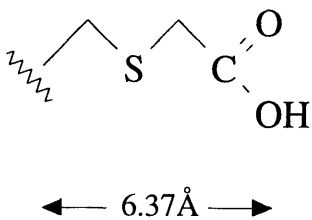
Arginine



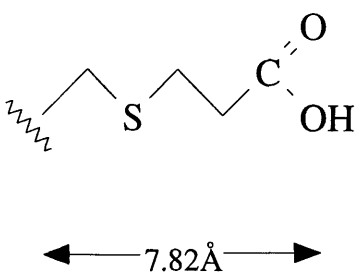
Glutamic Acid



Cysteine



Cysteine + Iodoacetic Acid



Cysteine + Iodopropionic Acid

**Figure 5.1:** Structures of arginine, glutamic acid, cysteine and modified cysteines. The structures are shown in the extended formation starting from the C $\alpha$  position.

mutant where the proteins were purified with the N-terminal methionine still present. The measured mass for the R47C mutant haem domain was 53,293Da with standard error of 4Da as compared to 53,350Da for the wild type protein with standard error of 5Da. Neither of these values are in agreement with the calculated molecular mass for the 471 amino acid haem domain from P450 BM3, 53,856Da for the wild type protein and 53,802Da for the R47C mutation. Both proteins possess a measured mass which is less than expected, corresponding to the loss of either three or four amino acids as discussed in Chapter 3. These results confirm that the R47C substitution, and only that substitution is present, in the mutant proteins.

**Table 5.1:** Molecular mass, measured by electrospray mass spectrometry, for wild type and R47C mutant intact P450 BM3.

Protein		Measured Mass <sup>a</sup>	Calculated Mass	
Intact enzyme	Wild Type	117,648 (±74)	117,782 <sup>b</sup>	117,651 <sup>c</sup>
	R47C Mutant	117,593 (±15)	117,729 <sup>b</sup>	117,597 <sup>c</sup>
Haem domain	Wild Type	53,350 (±5)	53,342 <sup>d</sup>	53,346 <sup>e</sup>
	R47C Mutant	53,293 (±4)	53,287 <sup>d</sup>	53,291 <sup>e</sup>

<sup>a</sup> From ES-MS.

<sup>b</sup> Mass calculated with initial methionine still present.

<sup>c</sup> Mass calculated with initial methionine removed.

<sup>d</sup> Mass calculated with initial methionine and three C-terminal residues removed.

<sup>e</sup> Mass calculated with initial methionine still present and four C-terminal residues removed.

#### 5.4 Determination of the Number of Free Thiols

The Ellman assay (Figure 5.2; Ellman, 1957) was used to measure the number of free thiols present in the both the wild type and R47C mutant intact P450 BM3 and its

haem domain as described in the Materials and Methods section. This assay measures the nitrothiobenzoate (NTB) released on reaction of a thiol with 5,5'- dithionitrobenzoic acid (DTNB). The results described in Table 5.2 show that neither the wild type intact P450 BM3 nor its haem domain, in their native state reacted with the Ellman reagent, DTNB, indicating that none of the cysteine side chain thiols are accessible to this reagent.

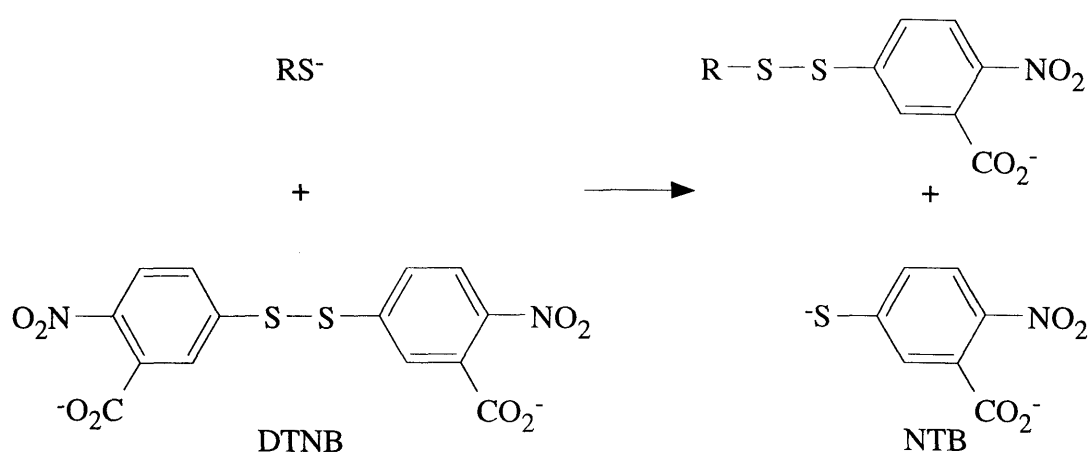


**Figure 5.2:** The reaction of thiol groups with Ellman reagent, DTNB

On repeating the Ellman assay in the presence of 6M GdmCl, three and nine cysteines in the wild type haem domain and intact P450 BM3 respectively were available for reaction with the DTNB. This is in complete agreement with the predicted number of cysteines for the intact P450 BM3 and its P450 domain (Ruettinger *et al.*, 1989; Li *et al.*, 1991; Miles *et al.*, 1992). These results indicate that all the cysteine amino acid side chains are buried in the native protein. When the assay was performed on the R47C mutant enzymes, neither protein exhibited accessible thiol side chains in the native state, though in the presence of 6M GdmCl approximately 10 cysteines were detected in the intact R47C mutant and four in the R47C mutant haem domain. The numbers of thiols in each of the proteins are in complete agreement with the predicted number from the published sequences (Ruettinger *et al.*, 1989; Li *et al.*, 1991; Miles *et al.*, 1992), together with the extra cysteine introduced at position 47 by SDM.

**Table 5.2:** Number of free thiols determined in the wild type and R47C mutant P450 BM3 and its haem domain.

Protein	Number of Free Thiols	
	Buffer <sup>a</sup>	6M Guanidinium HCl <sup>b</sup>
Wild Type Haem Domain	0	3.0
Wild Type Intact P450 BM3	0	9.0
R47C Mutant Haem Domain	0	3.8
R47C Mutant Intact P450 BM3	0	9.9

<sup>a</sup> 0.1M phosphate buffer, at pH 8.

<sup>b</sup> 0.1M phosphate buffer, at pH 8 containing 6M guanidinium hydrochloride.

These results were unusual, in that, we had expected to detect the thiol group incorporated by SDM using the native enzyme. As the additional cysteine residue is located at the open end of the substrate binding pocket in close proximity to the molecular surface of the protein, it was expected that this amino acid side chain would be accessible to solvent. These results are perhaps not quite so unreasonable if one considers that some double ring compounds have been found not to act as substrates for the wild type P450 BM3, including those depicted in Figure 5.3.

Neither (p-toluoyl)benzoic acid or 4-ethyl-4-biphenyl-carboxylic acid (Figure 5.3) produced the classical cytochrome P450 Type I binding spectra, involving a decrease in the Soret peak at 418nm with concomitant increase in absorbance at 390nm, or produced a detectable catalytic activity, as evidenced by NADPH consumption when mixed with the wild type P450 BM3 (A. N. J. Shaw, Unpublished Results).

Comparison of these compounds with DTNB (Figure 5.3) indicates that all these compounds have a common structure consisting of two aromatic rings with an ionisable group attached. Energy minimisation and molecular dynamic simulations of P450 BM3 in the absence of substrate suggest that the active-site cleft can undergo

substantial conformational changes such that the mouth region of the cleft can widen significantly allowing access to the wide range of structures that can act as substrates (Li and Poulos, 1995; Paulsen and Ornstein, 1995). The results from the DTNB assay detailed in Table 5.2 however, suggest that this movement of the substrate access channel is insufficient to allow influx of the Ellman reagent and therefore it seems unlikely that the substrate binding site is capable of binding the type of compound depicted in Figure 5.3.

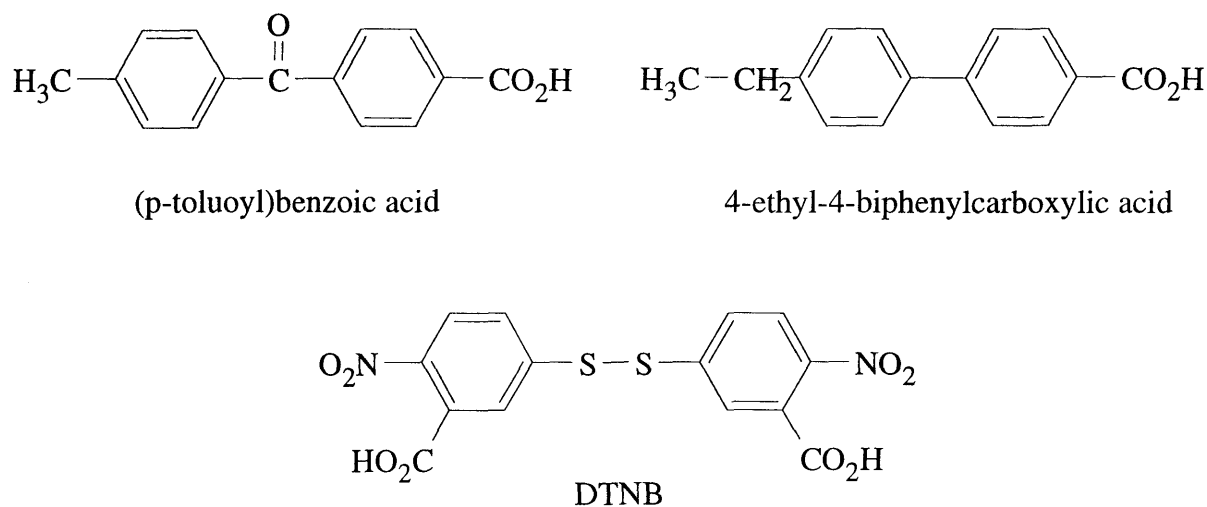
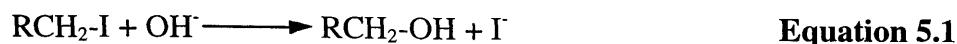


**Figure 5.3:** Chemical structure of (p-toluoyl)benzoic acid and 4-ethyl-4-biphenylcarboxylic acid, which have been found not to act as substrates for the wild type P450 BM3 (A. N. J. Shaw, Unpublished Results). The structure of 5,5-dithionitrobenzoic acid (DTNB) has been included for the purpose of comparison.

### 5.5 Chemical Modification

The R47C mutant intact P450 BM3 and its haem domain were modified using two reagents which both contained a carboxylate group to mimic the functionality of a glutamate residue. The iodoacetate-modified cysteine residue resembles the glutamate side chain though it is 1.29Å longer whereas the length of the amino acid side chain at position 47 after the iodopropionate modification closely resembles that of arginine with 0.51Å difference. Solutions of the modifying haloacids were made up

immediately prior to use as they are subject to slow hydrolysis under alkaline conditions as depicted in Equation 5.1 (Means and Feeney, 1971).



Of the several nucleophilic groups (thiol, imidazole, thioether, amine) found in proteins that react with haloacids, thiols are the most reactive under almost all conditions.

Reaction of the substituted cysteine in the mutated P450 BM3 with these reagents leads to a nucleophilic displacement and the formation of adducts (Equation 5.2).



Reactivity will increase with pH, as the anion is the reactive species. To prevent unwanted reactions with amino groups a pH near neutrality compatible with physiological activity is desirable. The pH optimum for chemical modification with haloacids is therefore between pH 6 and pH 8.5, though there is some reaction specificity outside of this pH range (Means and Feeney, 1971). Therefore chemical modifications were performed at pH 8, as additionally under these conditions the protein was stable. Chemical modification was accomplished at room temperature. When establishing the ideal conditions for chemical modification 160 $\mu$ M of the haem domain protein was used, whereas in the final experiments with the intact enzyme an 80 $\mu$ M solution of protein was found to be convenient.

### ***5.5.1 Determination of the Optimum Conditions for Chemical Modification with Iodoacetate***

Before catalytic analysis of the chemically modified R47C mutant proteins could begin, the ideal conditions for that chemical modification had to be established. The Ellman assay results indicated there were four and ten cysteines in the haem domain and the intact R47C mutant P450 BM3 respectively, though none of these reacted with DTNB in the native protein. It was originally intended to monitor the extent of enzyme modification by each haloacid using Ellman reagent in the presence of 6M guanidinium

hydrochloride, as DTNB did not appear to react with cysteine 47 in the native protein. Initial experiments using this method produced inconsistent results, possibly due to a cross reaction of unreacted excess  $\beta$ -mercaptoethanol with DTNB, yielding the coloured NTB ion. This thiol reagent was used to stop the reaction and could not be completely removed by gel filtration. It was therefore decided to use ES-MS to establish whether chemical modification had occurred, as the data generated was consistent and the presence of any contaminating small molecules not removed by dialysis during sample preparation would not affect the final results. However, there were limitations in that consistent ES-MS data for the intact R47C mutant P450 BM3 had been difficult to obtain due to its high molecular weight and so chemical modification could only be followed accurately for the R47C mutant haem domain.

Chemical modification was performed on the R47C mutant haem domain using final concentrations of iodoacetate ranging from 0.2 to 20mM at room temperature for up to 60 minutes. The reaction was stopped using  $\beta$ -mercaptoethanol (at twice the concentration of iodoacetate) with the excess reagents being removed by gel filtration. After extensive dialysis in EM water the samples of chemically modified proteins were sent for ES-MS. The ES-MS spectra obtained clearly showed whether chemical modifications had occurred. If a chemically modified species was present, an additional peak in the spectrum with a molecular weight approximately 70Da greater than that corresponding to the unmodified R47C mutant haem domain. This could represent the additional molecular weight for either the carboxymethyl ( $-\text{CH}_2\text{CO}_2^-$  at 58Da) or its sodium salt ( $-\text{CH}_2\text{CO}_2\text{Na}$  at 81Da). In all the ES-MS spectra obtained no evidence was detected of additional protein peaks with greater additional molecular mass that would indicate that more than one modification had not taken place.

The spectra obtained from ES-MS were further analysed to estimate the extent of modification by calculating the area under the peaks corresponding to unmodified and modified protein. The results for the modification of the R47C mutant haem domain with iodoacetate are shown in Figure 5.4. The optimum conditions were considered to be 5mM iodoacetate incubated at room temperature for 60 minutes, quenched with 10mM  $\beta$ -mercaptoethanol. The concentration of modifying agent present represented

an approximately 32-fold excess with respect to the concentration of protein. As the concentration of R47C mutant intact P450 BM3 used was  $80\mu\text{M}$ , as opposed to  $160\mu\text{M}$  R47C mutant haem domain, the concentration of iodoacetate and  $\beta$ -mercaptoethanol used were halved to ensure that the final modification conditions were identical for both the haem domain trials and the intact protein used in kinetic analysis.

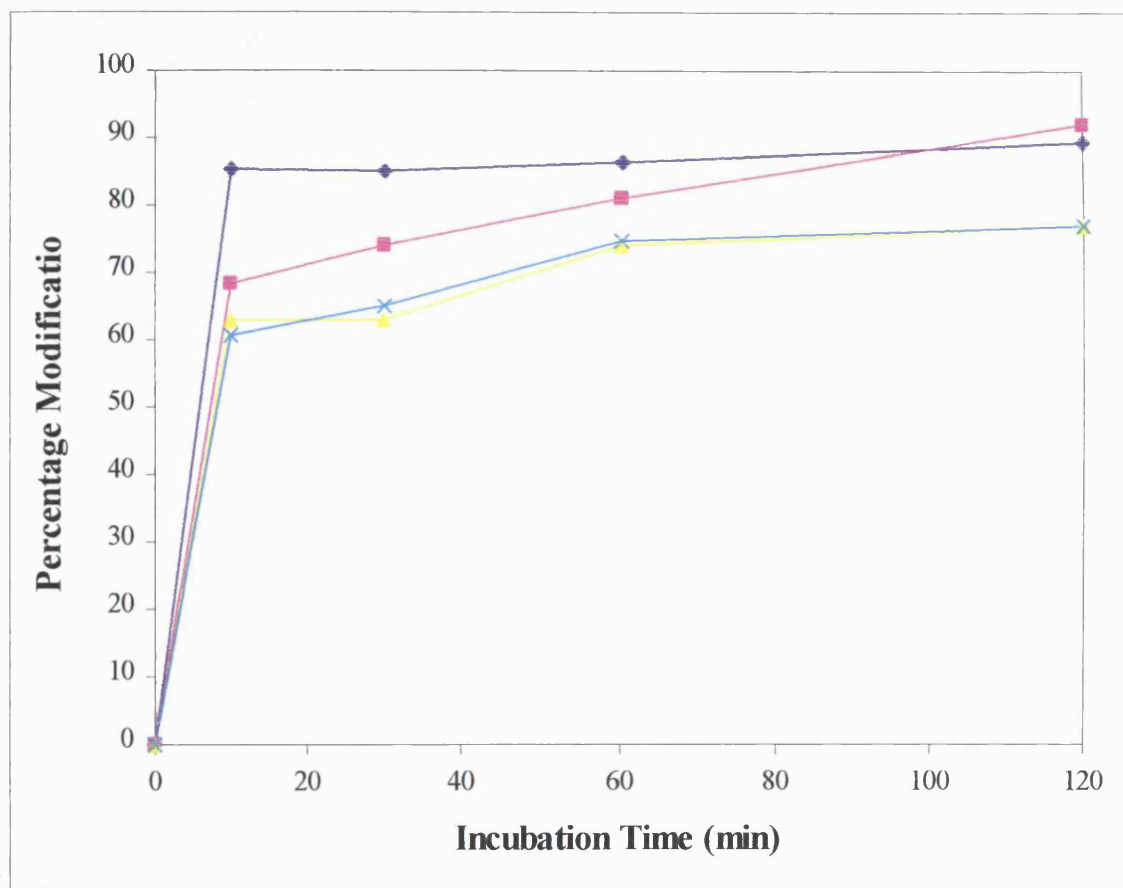


**Figure 5.4:** Percentage chemical modification of the R47C mutant haem domain with the modifying reagent iodoacetate, measured at differing incubation times. The extent of chemical modification was determined using reaction solutions containing  $160\mu\text{M}$  protein in  $0.1\text{M}$  phosphate buffer pH 8.0. Varying concentrations of iodoacetate, represented by ◆  $0.2\mu\text{M}$ , ■  $1\mu\text{M}$ , ▲  $2\mu\text{M}$ , ×  $5\mu\text{M}$ , ★  $10\mu\text{M}$ , ●  $15\mu\text{M}$ , and +  $20\mu\text{M}$ , were added and incubated at room temperature for the specified length of time. The proportion of unmodified to modified R47C mutant haem domain was determined by electrospray mass spectrometry. No evidence of chemical modification was detected using  $0.2$  and  $1\mu\text{M}$  concentrations of iodoacetate.

### ***5.5.2 Determination of the Optimum Conditions for Chemical Modification with Iodopropionate***

The experiments to determine the optimum conditions for the chemical modification of the R47C mutant haem domain by iodopropionate were performed after those for iodoacetate. It was considered inappropriate to use concentrations of modifying agent ranging from 0.2 to 2mM due to the relatively poor percentage modification obtained when using iodoacetate. Instead, it was decided to include an additional incubation time at 120 minutes to ascertain whether the larger iodopropionate would necessitate a longer incubation period. The ES-MS spectra obtained clearly indicated chemical modifications had occurred. In all the measured spectra, an additional peak was present with a molecular weight of approximately 72Da greater than that of the unmodified R47C mutant haem domain, representing the additional molecular weight for the propionate group ( $-\text{CH}_2\text{CH}_2\text{CO}_2^-$ ). As with the ES-MS spectra from the modifications with iodoacetate, there was no evidence of additional protein peaks with greater molecular mass, indicating chemical modification had occurred at a single cysteine residue side chain within the haem domain. The results for the chemical modification of the R47C mutant haem domain with iodopropionate are depicted in Figure 5.5. This data shows that the optimal conditions for modification using iodopropionate are identical to those for iodoacetate: 5mM iodopropionate incubated at room temperature for 60 minutes followed by quenching with 10mM  $\beta$ -mercaptoethanol, suggesting the presence of an additional methylene group did not significantly alter its reactivity with the additional thiol in the R47C mutant.

### ***5.5.3 Control of Chemical Modification***

Chemical modification was performed on the wild type haem domain and the intact P450 BM3 to ascertain whether there were any inadvertent reactions at cysteine residues other than the substituted 47. The wild type proteins were incubated with 2mM solutions of both iodoacetate and iodopropionate for 1 hour at room temperature. The chemically modified haem domain was examined using ES-MS. No

chemical modification was detected with either reagent, confirming the results obtained from the DTNB assay, excluding the possibility that unwanted chemical modification could occur at any of the three cysteine residues within the wild type haem domain.

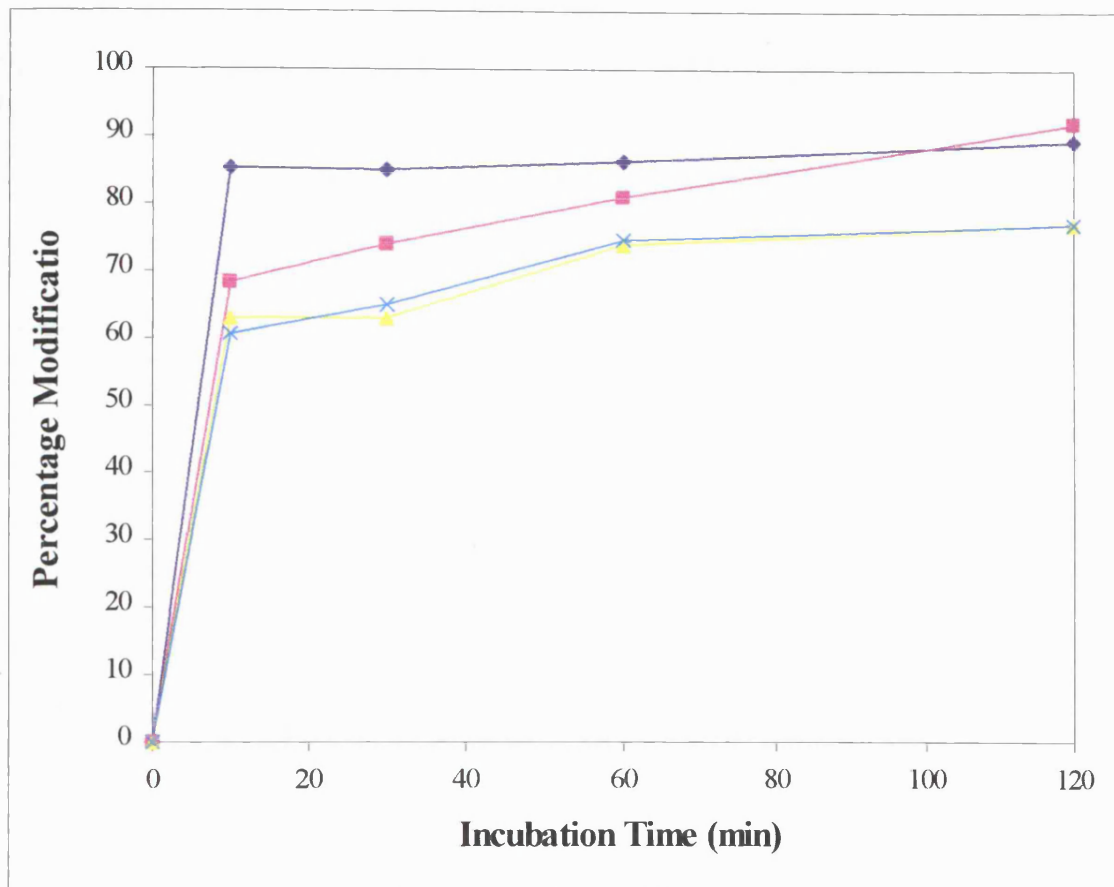


**Figure 5.5:** Percentage chemical modification of the R47C mutant haem domain with the modifying reagent iodopropionate, measured at differing incubation times. The extent of chemical modification was determined using reaction solutions containing 160 μM protein in 0.1M phosphate buffer pH 8.0. Varying concentrations of iodopropionate, represented by ◆ 5 μM, ■ 10 μM, ▲ 15 μM and × 20 μM were added and incubated at room temperature for the specified length of time. The proportion of unmodified to modified R47C mutant haem domain was determined by electrospray mass spectrometry.

ES-MS was not possible for the wild type intact P450 BM3. The haem domain data does not indicate any chemical modification using either haloacid, therefore the effect of modification on the six cysteine residues within the reductase domain was monitored indirectly by measuring the catalytic activity of the “modified wild type intact protein” using laurate as substrate and the results are depicted in Table 5.3.

**Table 5.3:** Kinetic constant for the wild type intact P450 BM3 before and after chemical modification using the haloacids, iodoacetate and iodopropionate, with laurate as substrate

Protein	$k_{cat}$	$K_M$	$k_{cat}/K_M$
Wild Type	26.4±3	136±4	1.9 x 10 <sup>5</sup>
Wild Type + Iodoacetate	27.7±3	135±21	2.0 x 10 <sup>5</sup>
Wild Type + Iodopropionate	34.9±6	201±7	1.8 x 10 <sup>5</sup>

After chemical modification with iodoacetate there does not appear to be any difference in any of the steady state kinetic parameters. This is not the case for the wild type enzyme incubated with iodopropionate. The  $k_{cat}$  appears to remain constant though there is a slight increase in the  $K_M$ . Overall there does not appear to be any significant change in the specificity constant,  $k_{cat}/K_M$ .

#### **5.5.4 Structural Integrity of Chemically Modified Enzymes**

The chemically modified proteins were analysed by SDS-PAGE which is shown in Figure 5.6. The data shows that when compared to the control unmodified R47C mutant intact P450 BM3 there was no significant change in the electrophoretic mobility of the chemically modified R47C mutant enzyme when modified with either iodoacetate or iodopropionate. A single band was observed in all lanes suggesting that no protein degradation occurred during the modification procedure.

### **5.6 Optical Spectroscopy and Enzyme Assays**

#### **5.6.1 Determination of the Catalytic Constant, $k_{cat}$ and the Michaelis Menten Constant $K_M$**

The rates of hydroxylation for the R47C mutant P450 BM3 and its iodoacetate and iodopropionate modified analogues were determined using the NADPH consumption

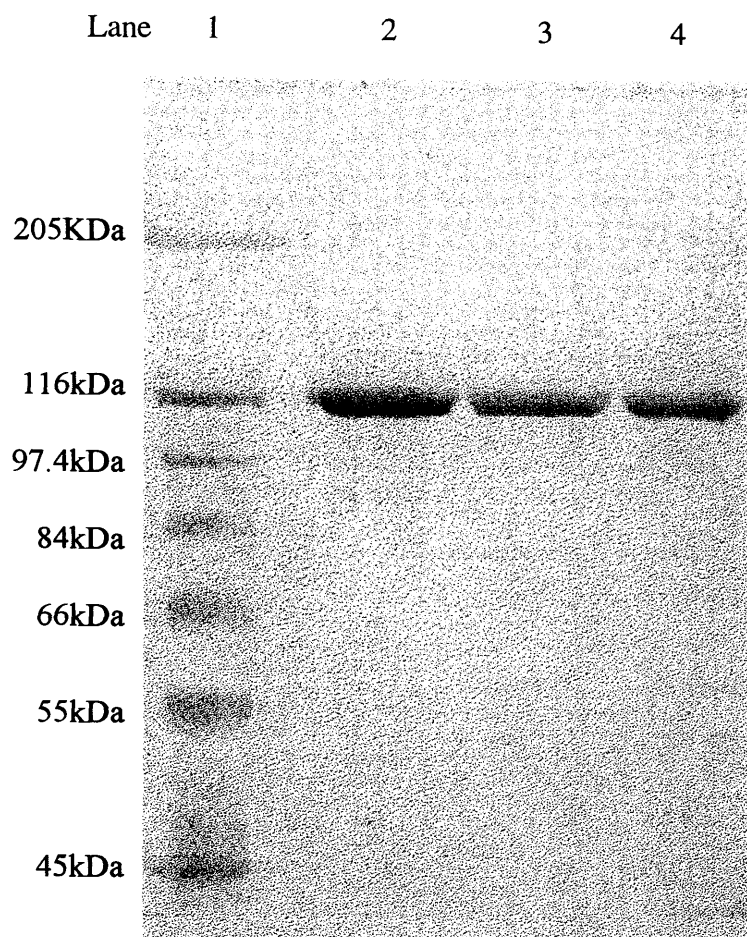


**Figure 5.6:** Electrophoretic analysis of control R47C mutant intact P450 BM3 and samples of this protein chemically modified with either iodoacetic acid or iodopropionic acid. Samples were subjected to SDS-PAGE with migration from top to bottom, using a 8% separating gel. *Lane 1*, molecular weight standard protein marker; *lane 2*, R47C mutant intact P450 BM3; *lane 3*, R47C mutant intact P450 BM3 modified with iodoacetate and *lane 4*, R47C mutant intact P450 BM3 modified with iodopropionate.

assay (Matson *et al.*, 1977). As with the R47E mutant, where the positively charged arginine has been changed to negatively charged glutamic acid, the modification with these haloacids resulted in negatively charged side chains at position 47. For this reason it was considered that the only suitable fatty acid substrate would be laurate, due to its lower affinity with the wild type P450 BM3 protein and its higher solubility in comparison with the other fatty acid substrates, myristate and palmitate, whereas the trimethylammonium (TMA) compounds would represent the more appropriate group of substrates.

The results from kinetics measured by the spectrophotometric assay are represented in Table 5.4, where the results are given as means  $\pm$  standard deviations. Data curves for the calculation of the steady state kinetic parameters  $k_{cat}$  and  $K_M$  are depicted in Figure 5.7 represented by those for the R47C mutant P450 BM3 with laurate (a) and C12 TMA as substrates (b). As with the kinetic results obtained for the R47E mutant P450 BM3, for some of the compounds with high  $K_M$  values, the precision of the data was limited by the accessible range of substrate concentrations, in turn limited by micelle formation and the experiments were performed under the same constraints as discussed in Chapter 4. When considering the results for the unmodified R47C mutant P450 BM3, all  $K_M$  values are in the micromolar range, varying from 534 $\mu$ M for lauric acid and 186 $\mu$ M for C12 TMA to 28 $\mu$ M for C16 TMA, indicating that the mutant has the highest affinity for the C16 TMA. The order of substrate affinities are shown to be C16>C14>C12, in complete agreement with the order of activity for the saturated series of fatty acid substrates with the wild type (Miura and Fulco, 1975). The rate of NADPH oxidation catalysed by the mutant P450 BM3 was also found to be dependent on the substrate chain length. As the chain length increases from C12 to C16,  $k_{cat}$  progressively increases as the  $K_M$  progressively decreases, such that the specificity constant,  $k_{cat}/K_M$  increases 50-fold. This increase in specificity constant is not as dramatic as that for the wild type protein with the fatty acids as substrates which exhibited a 300-fold increase (Oliver *et al.*, 1997b). The calculated catalytic activity of the R47C mutant intact enzyme with lauric acid is high, compared to the activities for the TMA compounds. This could be due to the effective removal of any side chain at position 47 by the incorporation of a cysteine residue, instead of either an arginine or glutamate and is discussed later.

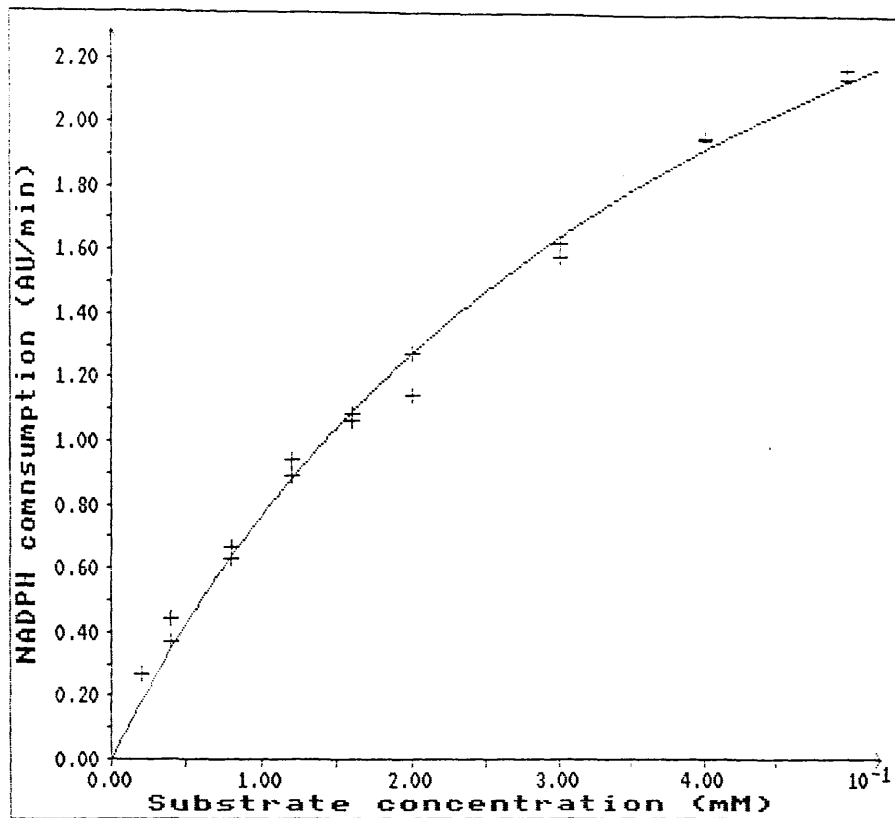
**Table 5.4:** Kinetic constants for the action of wild type and R47C intact cytochrome P450 BM3 for a series of saturated fatty acids and alkyl trimethylammonium compounds.

Protein	Parameter <sup>a</sup>	Substrate			
		Fatty Acid	Trimethylammonium compound		
		Laurate	C12 TMA	C14 TMA	C16 TMA
Wild Type	$k_{cat}$ ( $s^{-1}$ )	26±3	1.6±0.3	2.2±0.4	1.0±0.1
	$K_M$ ( $\mu M$ )	136±4	782±125	87±34	5.0±0.6
	$k_{cat}/K_M$ ( $M^{-1}s^{-1}$ )	$1.9 \times 10^5$	$2.0 \times 10^3$	$2.5 \times 10^4$	$2.0 \times 10^5$
R47E Mutant	$k_{cat}$ ( $s^{-1}$ )	29±6	2.2±0.6	15.1±0.8	20±3
	$K_M$ ( $\mu M$ )	2000±440	95±14	23±3	9±4
	$k_{cat}/K_M$ ( $M^{-1}s^{-1}$ )	$1.5 \times 10^4$	$2.2 \times 10^4$	$6.6 \times 10^5$	$2.2 \times 10^6$
	$k_{cat}/K_M$ wt/mut. <sup>b</sup>	12.6	0.087	0.038	0.091
R47C Mutant	$k_{cat}$ ( $s^{-1}$ )	38±6	1.1±0.02	9.0±0.5	9.3±1.8
	$K_M$ ( $\mu M$ )	534±110	186±12	70±3	28±9
	$k_{cat}/K_M$ ( $M^{-1}s^{-1}$ )	$7.0 \times 10^4$	$6.1 \times 10^3$	$1.3 \times 10^5$	$3.3 \times 10^5$
	$k_{cat}/K_M$ wt/mut. <sup>b</sup>	2.7	0.328	0.192	0.606
Cys47 S-carboxymethyl	$k_{cat}$ ( $s^{-1}$ )	23±2.3	1.1±0.1	6.4±0.2	7.3±1.5
	$K_M$ ( $\mu M$ )	310±31	141±14	21±1.1	13.1±2.9
	$k_{cat}/K_M$ ( $M^{-1}s^{-1}$ )	$7.2 \times 10^4$	$7.7 \times 10^3$	$3.1 \times 10^5$	$5.5 \times 10^5$
	$k_{cat}/K_M$ wt/mut. <sup>b</sup>	2.6	0.260	0.081	0.364
Cys47 S-carboxyethyl	$k_{cat}$ ( $s^{-1}$ )	35±0.9	1.0±0.02	11±0.1	9.2±0.7
	$K_M$ ( $\mu M$ )	356±15	171±12	60±1.0	22±3
	$k_{cat}/K_M$ ( $M^{-1}s^{-1}$ )	$1.0 \times 10^5$	$5.9 \times 10^3$	$1.8 \times 10^5$	$4.2 \times 10^5$
	$k_{cat}/K_M$ wt/mut. <sup>b</sup>	1.9	0.338	0.139	0.476

<sup>a</sup> From rates measured at 9 or 10 substrate concentrations, with at least 4 replicates at each concentration.

<sup>b</sup> The ratio of  $k_{cat}/K_M$  wt/mut. refers to the ratio of the specificity constant for the wild type to that of the mutant before or after chemical modification.

a)



b)

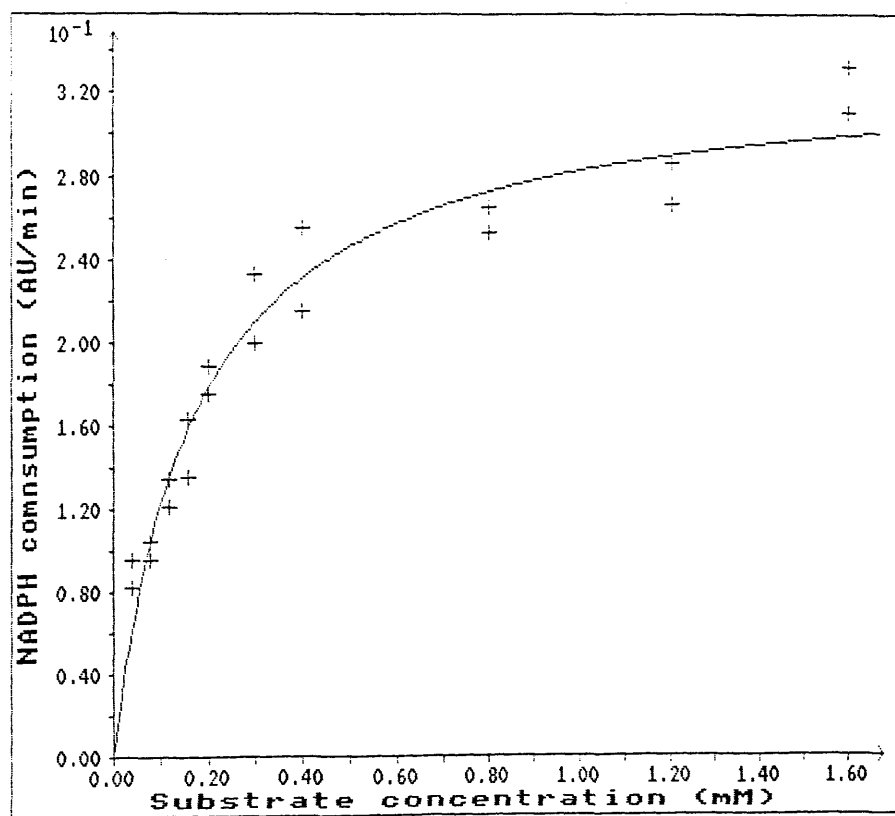


**Figure 5.7:** Typical data to show the effect of substrate concentration ( $S$ ) on the rate of reaction (AU/min) as measured by the NADPH consumption for the R47C mutant P450 BM3 with the substrates lauric acid (a) and C12 TMA (b).

On comparison of the results for the R47C P450 BM3 with those for the wild type and R47E mutant P450 BM3, it can be seen that the observed values for the specificity constant appear to be midway between the two latter proteins. That is, for example, the R47C mutant protein when laurate is used as a substrate, the  $k_{cat}$  remains essentially unchanged, whereas the  $K_M$  has increased relative to the wild type enzyme but decreased relative to the R47E mutant P450 BM3. This phenomena is reversed when considering the C12 TMA compounds as substrates, that is the  $K_M$  decreased relative to the wild type enzyme whereas an increase relative to the R47E mutant P450 BM3 was seen. For the fatty acid substrate the specificity constant is greater for the wild type than for the R47C P450 BM3, indicating a 3-fold decrease in specificity toward the fatty acid substrates in the R47C mutation, however this specificity constant represents a 5-fold increase in specificity towards the fatty acid laurate with respect to the R47E mutation. When considering the TMA compounds the situation is reversed, such that on comparison with the wild type P450 BM3 the results indicate a 3-fold increase in specificity toward the TMA compounds as substrates in the R47C mutation, but a 4-fold decrease in specificity with respect to the results for the R47E mutation.

Looking at the lower half of Table 5.4, it can be seen that the three TMA compounds do act as substrates for the R47C mutant P450 BM3 modified with either iodoacetate or iodopropionate. Both the negatively charged fatty acid laurate and the positively charged TMA compounds act as substrates for the modified R47C mutants, with the TMA compounds being much better substrates as indicated by all the TMA specificity constants for the R47C mutants being greater than those for the wild type enzyme, but not as high as those for the R47E mutant.

Considering the results for the modified proteins with laurate as substrate, the  $K_M$ s are greater than that for the wild type (approximately 2-fold) though significantly less than that for the R47E mutant (approximately 4-fold). Combined with the results for the unmodified R47C intact P450 BM3 these data suggest that the catalytic activity towards negatively charged substrates is not significantly perturbed by the absence of any functional group at position 47 or indeed chemical modification to include a

negatively charged side chain. The results for the TMA compounds present a different picture. There does not appear to be a significant difference between the  $k_{cat}$ s for the modified R47C mutant P450 BM3 and that of the unmodified mutant enzyme. This would suggest any contribution by the unnatural amino acid side chains at residue 47 formed after thiol modification does not result in any alteration to the overall catalytic mechanism. This is not the case however when considering the observed  $K_M$ s. Use of the haloacid iodoacetate for modification results in  $K_M$  values that bear a strikingly close resemblance to those obtained for the R47E mutant cytochrome P450. Whereas those obtained after chemical modification using iodopropionate, though less than those for the wild type protein more closely resemble those obtained for the unmodified R47C mutant P450 BM3. In the case of the iodoacetate modified P450 BM3 the  $k_{cat}/K_M$  ranges from approximately a 125% to 240% increase with the thiol modified mutant as compared to the unmodified mutant, where the specificity constant range for the iodopropionate modified enzyme represents a 97% to 138% increase. As a result, it can be said that the catalytic activity of the iodoacetate modified R47C mutant P450 BM3 more closely resembles that of the R47E mutant P450 BM3 and therefore must have more structural elements in common. The modified R47C enzymes also show the same chain-length preference, C16>C14>C12, for the TMA compounds as the wild type does for the fatty acids and the R47E and R47C mutant proteins do for the TMA compounds. This is demonstrated by a decrease in the specificity constants due to a decrease in  $K_M$  as the chain length increases despite there being no significant change in the  $k_{cat}$  values.

### **5.6.2 Substrate Binding**

The purified R47C mutant proteins were purified in the ferric low spin state and their spectra, as well as those for the proteins chemically modified with the haloacids were typical for cytochrome P450s (Figure 5.8). That is, the oxidised spectrum possessed well resolved  $\alpha$  and  $\beta$  bands at 570 and 535nm and a strong Soret band at 418nm, whilst after reduction by sodium dithionite and CO, the spectrum shows peaks at 547 and 448nm. As with the R47E mutation, the substitution of a cysteine residue does not appear to have had any effect on the electronic structure of the haem, as reflected

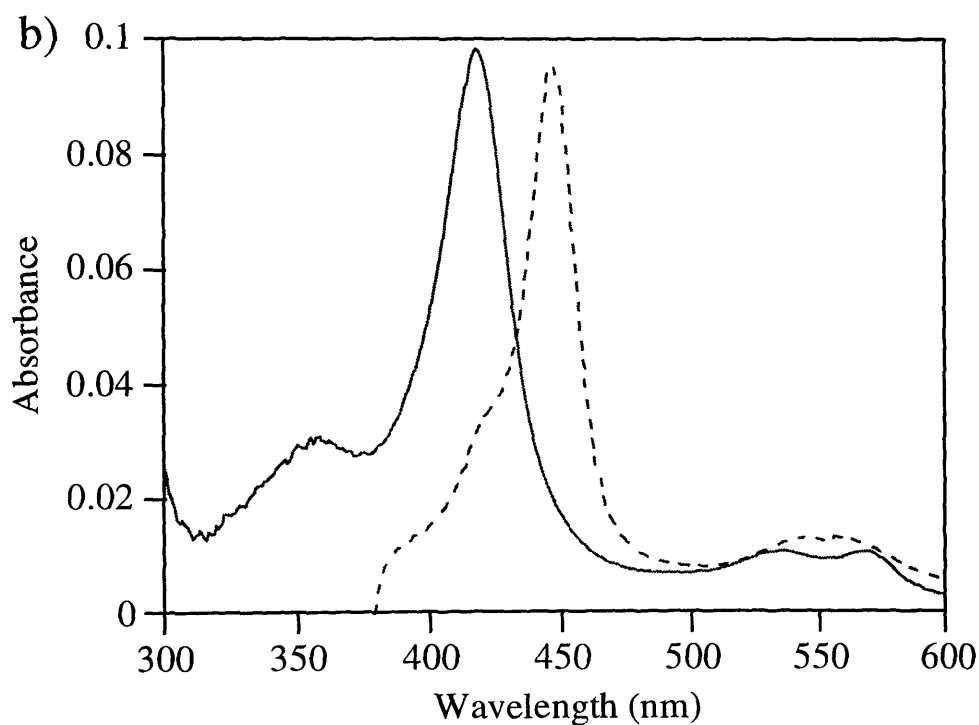
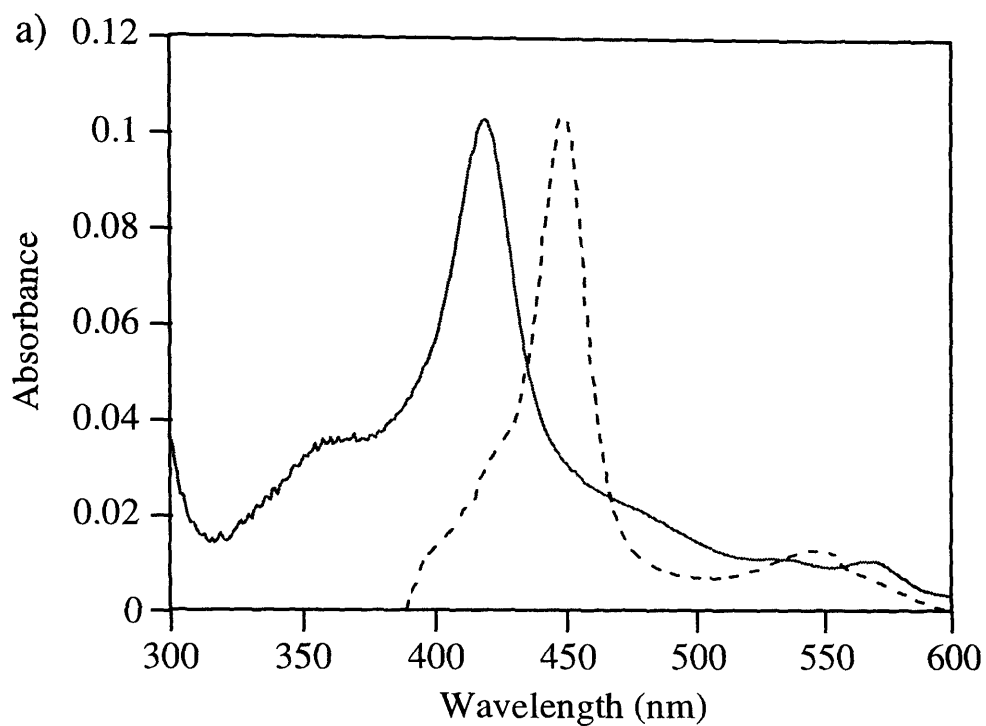


**Figure 5.8:** The absorption spectra for R47C mutant intact cytochrome P450 BM3 (a) and its haem domain (b). The sample cuvette contained either 2.42 $\mu$ M intact P450 BM3 or 3.29 $\mu$ M haem domain. The spectrum with the solid line (—) is the oxidised form of the enzyme. The broken line (- - -) was taken after the sample was reduced by addition of sodium dithionite followed by saturation with CO.

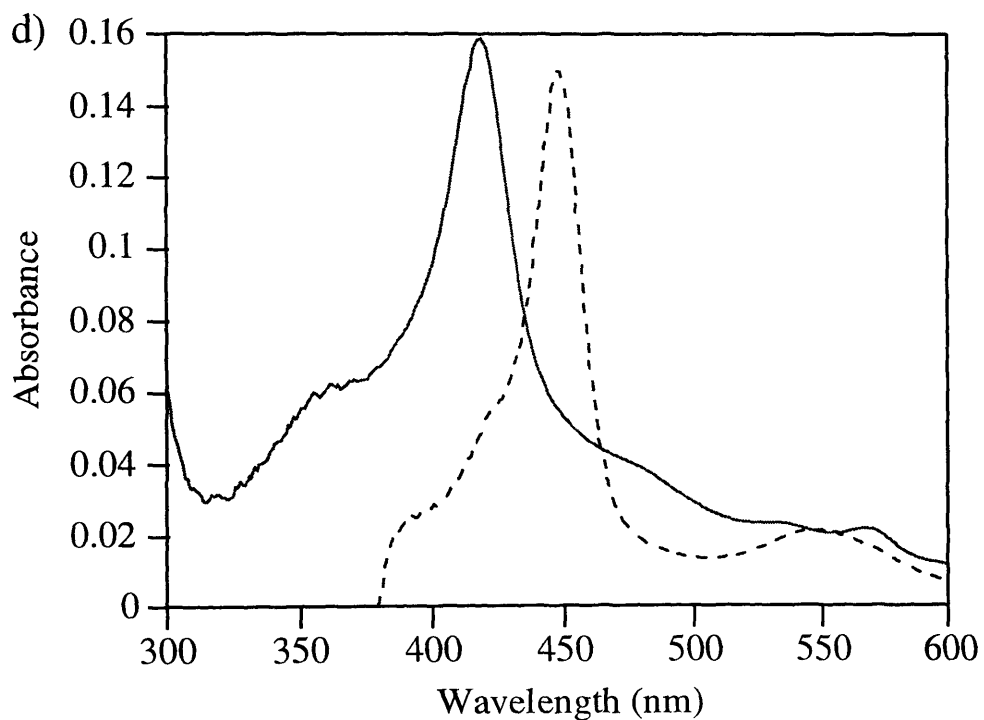
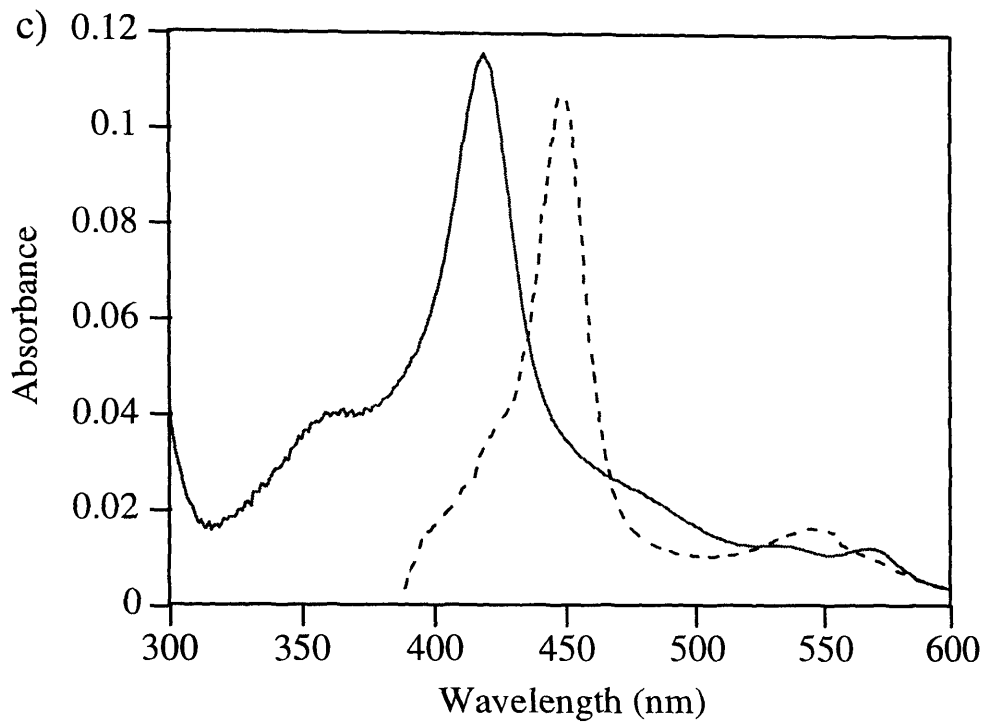


**Figure 5.8 (continued):** The absorption spectra for R47C mutant intact cytochrome P450 BM3 after chemical modification with iodoacetate (c) and iodoacetate (c) and iodopropionate (d). The sample cuvette contained  $2.13\mu\text{M}$  protein in (c) and  $1.91\mu\text{M}$  protein in (d). The spectrum with the solid line (—) is the oxidised form of the enzyme. The broken line (- - -) was taken after the sample was reduced by addition of sodium dithionite followed by saturation with CO.

in its optical spectrum.

Electronic absorption spectra were obtained for the R47C mutant, before and after chemical modification with iodoacetate and iodopropionate, in the presence and absence of the substrates laurate and C12 TMA, typified by those for the Cys47 S-carboxyethyl protein in Figure 5.9. Addition of either substrate to the R47C mutant protein produced a typical 'Type I' spectrum characterised by a decrease in the Soret band at 418nm with a simultaneous increase in the absorbance at 390 and 650nm. On closer inspection of the spectra from the R47C mutants with the C12 TMA as substrate it can be seen that there is a broadening of the peak at 650nm. As with the R47E mutant substrate binding spectra with the C16 TMA compound, this could be due to either the haem moiety being tilted in the substrate binding cavity or we are viewing the effect of micelles on the protein.

These spectra indicate that the fatty acid substrate and the trimethylammonium compound bind to the R47C enzyme in a similar way before and after chemical modification. The concentration of laurate which could be used was limited to 2mM due to micelle formation. The substrate-bound spectra for the R47C mutants were obtained after incubation for 30 minutes, where no further change in absorbance was monitored. This substrate concentration was not sufficient to produce complete conversion of the Soret peak at 418nm to a peak indicative of substrate binding at an absorbance at 390nm with any of the R47C mutant proteins, though it was evident that substrate binding was clearly taking place due to the increase in absorbance at 650nm (Figure 5.9a). This is similar to the situation with the R47E mutant haem domain where the concentration of palmitate used was not sufficient to produce any clear changes in the absorption spectrum (Chapter 4; Figure 4.4c). The observed effect of the 2mM laurate on the absorption spectrum suggests that again there must be a significant difference between the  $K_M$  and the  $K_d$  for the binding to the unmodified and modified intact R47C.

The equilibrium dissociation constant,  $K_d$ , for the binding of trimethylammonium compounds to the R47C mutant P450 BM3, before and after chemical modification

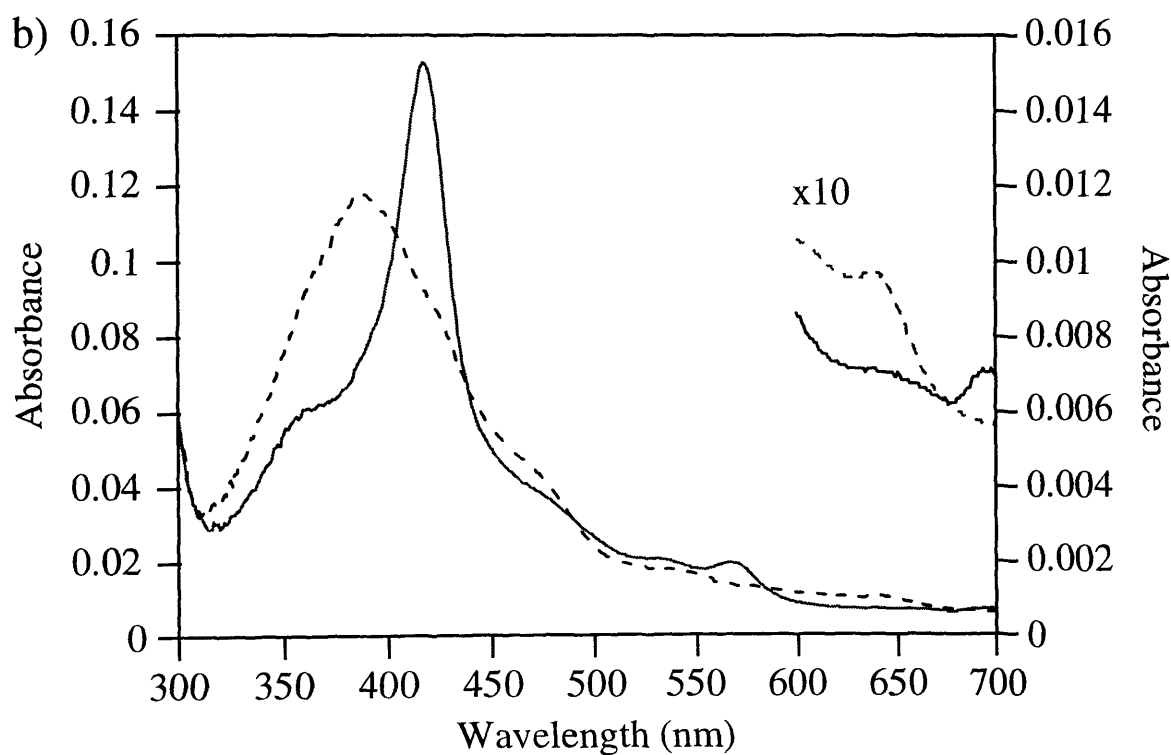
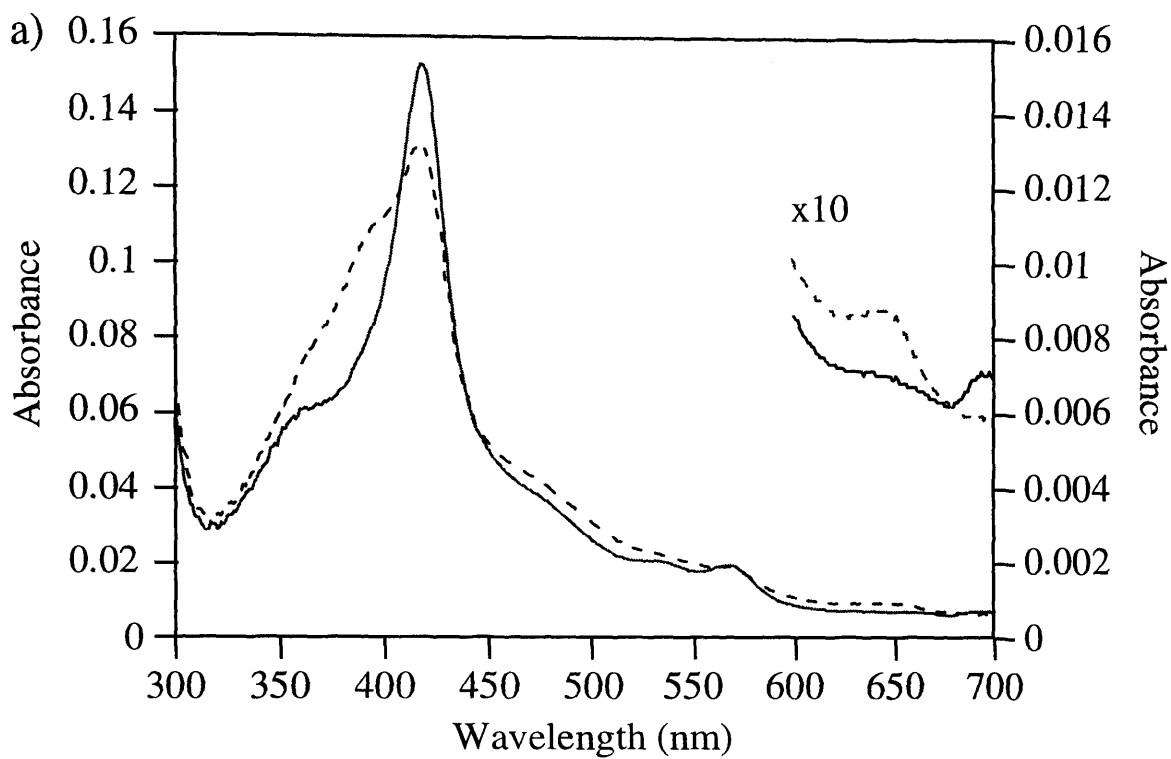


**Figure 5.9:** Absorption spectra of the R47C mutant P450 BM3 ( $1.91\mu\text{M}$ ) after modification with iodopropionate in the presence (-----) and absence (——) of 2mM laurate (a) and 10mM C12 TMA (b).

with iodoacetate and iodopropionate, were calculated from the decrease in absorbance at 418nm and the results are given below in Table 5.5. The corresponding dissociation constants for the R47E mutant enzyme are also given. The values for the  $K_d$ s for the R47C protein range from 870 $\mu$ M for C12 TMA, 196 $\mu$ M for C14 TMA to 6.9 $\mu$ M for C16 TMA. The maximum  $K_d$  was found for C16 TMA, the lowest being for C12 TMA.

**Table 5.5:** Equilibrium dissociation constants for wild type and R47E mutant P450 BM3.

Enzyme	Substrate $K_d$ Values( $\mu$ M)		
	C12 TMA	C14 TMA	C16 TMA
R47E Mutant	180 $\pm$ 26.7	41 $\pm$ 7	4.0 $\pm$ 1.5
R47C Mutant	870 $\pm$ 478	196 $\pm$ 21	6.9 $\pm$ 2.7
Cys 47 S-carboxymethyl	329 $\pm$ 82	52 $\pm$ 0.1	2.3 $\pm$ 0.6
Cys 47 S-carboxyethyl	985 $\pm$ 321	113 $\pm$ 28	4.8 $\pm$ 2.3

All the R47C mutant P450 BM3 values are higher than those for the R47E variant suggesting that binding of the TMA compounds is weaker in the absence of the negatively charged side chain at residue 47. The  $K_d$ s follow the activity series C16>C14>C12 in agreement with the  $k_{cat}$  and  $K_M$  results, suggesting that C16 TMA has the strongest association with the intact R47C mutant as for the R47E mutant enzyme. The unmodified R47C results are mirrored by those for the protein after chemical modification with the haloacids, iodoacetate and iodopropionate (Table 5.5). The  $K_d$  values for the iodoacetate modified R47C P450 BM3 range from 329 $\mu$ M for C12 TMA, 52 $\mu$ M for C14 TMA to 2.3 $\mu$ M for C16 TMA. The corresponding values for the iodopropionate modified R47C enzyme range from 985 $\mu$ M for C12, 113 $\mu$ M for C14 to 4.8 $\mu$ M for C16. C16 TMA showed the tightest binding with C12 TMA binding

the weakest for both proteins. The  $K_d$ s for the iodoacetate modified protein most closely resembled those from the R47E mutant P450 BM3. The iodopropionate were similar to the unmodified R47C mutant, suggesting that binding of the TMA compounds must be similar in the absence and presence of propionate group within the substrate binding pocket. Again, the obtained activity series C16>C14>C12 is in agreement with the  $k_{cat}$  and  $K_M$  results, suggesting that the C16 TMA has the strongest association with the modified R47C mutant P450 BM3.

## 5.7 Discussion

Within the three dimensional structure of a given protein certain residues may exhibit reactivities that are different to the expected due to their specific microenvironment. These particular residues are usually involved in biological function and because of this unique reactivity can be selectively modified, thereby facilitating structure-function studies. Therefore before making functional deductions regarding the effects of performing chemical modifications on a protein, it is important that the specificity of the reagent employed is understood, as well as any effects on protein structure. Keeping this information in mind and considering the other methods available today for the investigation of the structure/function relationship of proteins, one immediately will suggest the method of site-directed mutagenesis, which can be utilised to explore the role of individual amino acid residues in substrate binding and catalysis in several different ways. The most obvious substitution involves replacing a residue like arginine with one that lacks charge and/or length of side chain. A more informative method uses mutagenesis to replace an amino acid with one that retains a functional group, such as cysteine, so that chemical modification can be used to attempt to “rescue” activity by adding back chemical fragments that have functional groups. With this method charge requirements, as well as length of side chain can be investigated. The first application of this method was in the study of the function of a lysine residue in the reaction catalysed by ribulosebisphosphate carboxylase/oxygenase from *Rhodospirillum rubrum*. Cysteine substitutions of the active site lysines abolished catalytic activity which was partially recovered by treatment of the cysteine mutants with 2-bromoethylamine due to selective aminoethylation of the thiol group (Smith and

Hartman, 1988). In the present study, the function of an active site arginine has been explored using haloacidic compounds.

The reactivity of the thiol (-SH) side chain functional groups of cysteine residues are extremely reactive with haloacids under almost all conditions. This makes it possible to employ an extremely wide range of conditions, satisfying any requirements of the protein and still obtaining selective reaction. Within the experiments detailed here, a model system containing the thiol group has been used to evaluate the reactivity of a series of amino acid analogue reagents that have been chosen to react with protein cysteinyl residues. The reagent conditions were varied to discover the optimal conditions for the R47C mutant cytochrome P450 BM3 modification. These optimal conditions are a compromise between the conditions which produce the fastest rates of reaction and those that will adversely affect the enzyme under investigation. As P450 proteins function at physiological pH, it is unlikely that this class of enzymes will exhibit any adverse side effects if modification occurs at pH values of approximately 8, however other proteins may be particularly sensitive to high pH.

From the x-ray crystal structure of both the substrate-free and substrate-bound haem domain of P450 BM3 (Ravichandran *et al.*, 1993; Li and Poulos, 1997) it is known that the three cysteines present do not form any disulphide linkages. Although the disulphide content of the P450 BM3 reductase domain is not known, it is unlikely that there are any linking the two domains as they readily dissociate when P450 BM3 is cleaved with trypsin (Narhi and Fulco, 1987). The accessibility and reactivity of any thiols is of important consideration when performing chemical modification upon a wild type protein or one which has had a thiol group introduced by SDM. Unless the introduced thiol is the only free thiol, or at least the most reactive thiol in the protein it is necessary to protect any other essential thiols before modification. Evidence from the DTNB assay and ES-MS of the wild type haem domain indicate there are no freely accessible cysteine residues and none of the residues are chemically modified, suggesting that the most reactive thiol in the cysteine mutant proteins will be the additional thiol introduced into the substrate binding pocket. However, the slight increase in  $K_M$  after treatment of the wild type protein with iodopropionate suggests

that chemical modification may have occurred at any of the six cysteine residues within the reductase domain. As the catalytic activity has not been affected, any modification resulted solely in an altered mode of binding, not affecting the transfer of the reducing equivalents required for the monooxygenation of the fatty acid substrate. It must be emphasised that this effect is slight as the overall specificity constant has not been significantly altered. The additional modification may also have occurred when using iodoacetate, however this haloacid is shorter by one methylene and the additional steric bulk resulting from this potential modification may have been insufficient to affect the kinetic parameters.

Comparison of both the sodium dithionite/CO binding spectra and the substrate binding spectra for the wild type P450 BM3 and the R47C mutant, as well as the proteins chemically modified with either iodoacetate or iodopropionate indicate that no significant differences are present. These indicate that the haem moiety is successfully incorporated in all of these proteins and its immediate environment is identical. The data from the SDS-PAGE analysis indicates that after treatment with the haloacids there are no obvious changes in the electrophoretic mobility of the proteins through either addition from chemical modification or through degradation of the protein due to the experimental conditions used. These, together with the presence of catalytic activity, suggests that the overall protein secondary structure is intact and that the structure of the substrate binding pocket has not been seriously perturbed by the removal of the positively charged side chain at position 47, and the subsequent introduction of a negatively charged side chain.

Given that it was originally postulated that the guanidinium side chain of arginine 47 was necessary for interaction with the fatty acid substrate carboxylate group, one of the more surprising results of this series of experiments was that the R47C mutant P450 BM3, in the absence of a substantial charged amino acid side chain at position 47, was still capable of acting as an efficient fatty acid hydroxylase, as well as catalysing the hydroxylation of the trimethylammonium compounds. This finding correlates well with those obtained for the R47E mutation discussed in the previous chapter, together with the evidence obtained from the substrate-bound x-ray crystal data published recently

highlighting the importance of tyrosine 51 (Li and Poulos, 1997). It should be noted that the catalytic activity, as measured by  $k_{\text{cat}}$ , was greater in the variant enzyme for the fatty acid laurate rather than the trimethylammonium compounds, by a factor of 35. It is conceivable that incorporation of a smaller amino acid functionality at position 47 resulted in the removal of any possible steric hindrance due to the presence of a large side chain positioned at the opening of the substrate binding site. Also, under the experimental conditions used the thiol group would be neutral eliminating any charged residues within the substrate binding site. The removal of potential negative interactions between the ionisable side chains, of either the guanidinium group of arginine or the carboxylate of glutamate, at residue 47 may also have had the effect of enhancing accessibility and subsequent binding of either class of potential substrates, in the fatty acids and the trimethylammonium compounds.

After chemical modification of the R47C mutant P450 BM3 with either iodoacetate or iodopropionate, the resulting proteins were still catalytically active, suggesting that the process of chemical modification did not in itself lead to any gross changes in any of the residues involved in the catalytic activity (within the substrate active site of the haem domain or the electron transfer pathway of the reductase domain) which would have been indicated by inactivation of the enzymes. The mutant enzyme modified with iodoacetate showed decreased  $K_M$  values, though decreased  $k_{\text{cat}}$  values relative to the unmodified R47C mutant protein, this phenomenon was not so apparent for the iodopropionate modified R47C protein. The  $K_M$  values obtained for the trimethylammonium compounds with the iodoacetate modified R47C mutant most closely reflected those obtained for the R47E mutant P450 BM3. Again, the increase in specificity towards the trimethylammonium compounds for the Cys 47 S-carboxymethyl P450 BM3, but not the Cys 47 S-carboxyethyl P450 BM3, was reflected in the values for the equilibrium binding constant  $K_d$ , indicating that the introduction of the acidic charged side chain at position 47 has enhanced the binding of cationic substrates. In general, the differences obtained for the iodopropionate modified R47C mutant P450 BM3 are small and as such can not be considered significant. Prior to experimentation, it had been hypothesised that the catalytic activities of the modified proteins with both classes of substrate would reflect those of

the R47E mutant P450 BM3. However, the obtained catalytic activities represented only a percentage of those expected. These results can be compared to those obtained in the similar studies of Smith and Hartman (1988) where only approximately 20-60% of the wild type catalytic activity was recovered, after aminoethylation of mutant cysteine residues to recover active site lysines. There is good correlation between the  $K_d$  values and those of the  $k_{cat}/K_m$  and therefore indicates that there may be little wrong with the obtained values for  $k_{cat}$  and  $K_m$  for the modified R47C mutant P450 BM3. There are, however, two possible explanations for any observed or imagined discrepancies. The side chain of cysteine is the equivalent of two atoms long (-CH<sub>2</sub>SH). Chemical modification reactions with the haloacid reagents examined resulted in unnatural amino acid analogues that were one and two atoms longer when modified with iodoacetate and iodopropionate respectively, than the naturally occurring glutamate that they were attempting to mimic. In addition, the resulting amino acid side chains will both contain sulphur as one of the extra atoms, as depicted in Figure 5.1. The length of the side chain and the inclusion of a carbon-sulphur-carbon chain within the chemically modified protein emphasises the possible requirements for the side chain charge, volume and length at residue 47 to ensure proper positioning of the substrates in the active site, which ultimately may be a determinant in catalysis. Mutagenesis studies using triosephosphate isomerase, substituting glutamate 165 with aspartate, indicated that the positioning of the functionality at the active site of the enzyme needs to be quite precise if the full catalytic potency is to be realised (Knowles, 1991).

A second possible explanation for the obtained catalytic activity concerns the extent of chemical modification and may also explain the data obtained from the control experiments. There are six cysteines in the reductase domain of P450 BM3 at positions 569, 773, 810, 879, 936 and 999. Using the sequence alignment published by Porter (1991) these correspond to leucine 173, serine 394, leucine 437, arginine 506, cysteine 566 and cysteine 630 of rat cytochrome P450 reductase, for which the x-ray crystal structure is now available (rCPR: Wang *et al.*, 1997). Cys 569 (rCPR Leu 173) is located in  $\beta$ -strand 4, Cys 773 (rCPR Ser 394) is located in a loop between the I and J helices, Cys 810 (rCPR Leu 437) is located in a loop between the L and M helices,

Cys 879 (rCPR Arg 506) is located in a loop between the N helix and  $\beta$ -strand 16 and Cys 936 (rCPR Cys 566) is located in  $\beta$ -strand 4 which forms part of the FMN binding site (Wang *et al.*, 1997). A sequence alignment of the NADPH-binding regions of key members of the NADPH-cytochrome P450 reductase (CPR) family (Figure 5.10) suggest that they all contain a highly conserved cysteine residue, corresponding to cysteine 999 in P450 BM3 (Fulco 1991; Wang *et al.*, 1997). As this cysteine is located in the NADPH binding regions it may be more susceptible to chemical modification.

NADPH Pyrophosphate			
NADP(H) Binding Region	CPR	<b>527</b>	VIMVGPGTGIAPFMGFIQER
	NOS	<b>1244</b>	CILVGPGTGIAPFRSFWQQR
	BM3	<b>898</b>	LIMVGPGTGVAPFRGFVQAR
	SR	<b>454</b>	VIMIGPGTGIAPFRAFMQQR
	FNR	<b>220</b>	IIMLGTGTGIAPFRSFLWKM
NADPH Adenine			
NADP(H) Binding Region	CPR	<b>599</b>	AHKVYVQHLLKRDR . EHLWKLIEGGAHYV <b>CGDARN</b> MAKDV
	NOS	<b>1318</b>	RPKKYVQDVLQEQLAESVYRALKEQGGHIYV <b>CGDV</b> . TMAADV
	BM3	<b>970</b>	QPKTYVQHVMEQDG . KKLIELLDQG . AHFYI <b>CGDGSQ</b> MAPAV
	SR	<b>522</b>	KEKVYVQDKLREQG . AELWRWINDG . AHIYV <b>CGDANR</b> MAKDV
	FNR	<b>297</b>	GEKMYIQTRMAQYA . VELWEMLKKDNTYFY <b>M</b> GLK . GMEKGI

**Figure 5.10:** Sequence line-up for NADPH-binding regions of key members of the NADPH-cytochrome P450 reductase (CPR) family. The proteins are: CPR, rat cytochrome P450 reductase; NOS, rat neuronal nitric oxide synthase; BM3, cytochrome P450 BM3; SR, *E. coli* sulphite reductase; FDX, *D. vulgaris* flavodoxin; and FNR, *Spinacia oleracea* ferredoxin-NADP<sup>+</sup> reductase. The numbering is for the first amino acid of each region of the given protein. The conserved cysteine residue in the NADP(H) binding site is highlighted within the box. Adapted from Wang *et al.* (1997).

Thiol modification of the protease solubilised NADPH-cytochrome P450 reductase at the critical thiol group in the cosubstrate binding site affected the  $K_M$  for NADPH but not the  $V_{max}$  for the cytochrome *c* reduction. However, in the presence of NADPH one of the cysteinyl groups is protected from modification (Lumper *et al.*, 1980). This

paper presents direct evidence that the modification at this essential cysteinyl residue affects the attachment of the cosubstrate by steric hindrance and electrostatic interactions of the group introduced with the NADPH binding site. If there is random additional modification of cysteine residues within the reductase domain this would account for the altered  $K_M$  and  $k_{cat}$  values within the wild type and R47C mutant proteins respectively after incubation with iodopropionate. Digestion of the intact enzyme using either proteases or cyanogen bromide treatment to form peptides, with subsequent purification by gel filtration and either reverse phase or anion exchange HPLC, followed by peptide sequencing would determine exactly where chemical modification has occurred as well as the number of modified thiol groups. Also, to remove any suspicion that Cys 999 is implicated in the reduction in  $k_{cat}$  after chemical modification of the intact R47C mutants, the thiol reaction with the haloacids could be performed in the presence of either NADPH,  $NADP^+$  or an NADPH analogue which would protect the thiol group of the cysteine side chain in the cofactor binding pocket. Shorter incubation times would reduce the possibility of any spurious chemical mutations that may occur at the more inaccessible residues, though at the cost of maximising the extent of chemical modification at the target cysteine (See Figures 5.4 and 5.5).

The data presented here for the unmodified R47C mutant and after modification with iodoacetate and iodopropionate, in conjunction with the results obtained from the R47E mutant P450 BM3, indicates that residue 47 cannot be solely responsible for the effective binding of the naturally occurring fatty acid substrates, or indeed the binding of the unnatural trimethylammonium compounds in the presence of a glutamyl side chain. Any role that the positively charged arginine 47 guanidinium group plays in the binding of the negatively charged fatty acid carboxylate can only be minor at best, as catalysis is not significantly perturbed by the absence of any functional group or indeed chemical modification to include a negatively charged side chain. In the absence of the positively charged guanidinium group the only residues in close proximity ( $5\text{\AA}$ ) to the fatty acid carboxylate are leucine 25, proline 25 leucine 29 and tyrosine 51 with leucine 188 and methionine 354 within  $7\text{\AA}$  (Chapter 4; Figure 4.8). Of these only tyrosine 51 is capable of providing a favourable interaction to facilitate orientation and subsequent

binding within the substrate binding site of P450 BM3.

This system where SDM is combined with chemical modification could be used to produce structural analogues of several different amino acids. This methodology builds on the model system proposed by Schindler and Viola (1996) and the work performed by Dhalla *et al.* (1994). Schindler and Viola (1996) showed that a reaction mixture containing acetylcysteamine on reaction with primary and secondary haloalcohols generated analogues of serine and threonine, reaction with haloacids produced glutamate analogues and haloamides lead to glutamine-like structures. Treatment with alkyl halides generated methionine homologues and haloamines generated lysine analogues (Schindler and Viola, 1996). In addition to introducing the functional groups of naturally occurring amino acids, new functionalities were also introduced by this method and the various reagents used are summarised in Table 5.6.

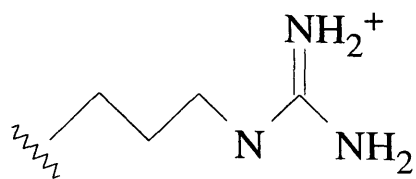
**Table 5.6:** Reagents used to synthesis unnatural amino acid analogues. Adapted from Schindler and Viola (1996)

Analogue of Amino Acid	Reagent	Product (R) <sup>a</sup>
Serine	2-Bromoethanol	-CH <sub>2</sub> CH <sub>2</sub> OH
Methionine	Iodomethane	-CH <sub>3</sub>
Methionine	Bromoethane	-CH <sub>2</sub> CH <sub>3</sub>
Lysine	2-Bromoethylamine	-CH <sub>2</sub> CH <sub>2</sub> NH <sub>3</sub> <sup>+</sup>
Tyrosine	4-Fluorobenzyl chloride	-CH <sub>2</sub> C <sub>6</sub> H <sub>4</sub> F
Tyrosine	4-Aminobenzyl chloride	-CH <sub>2</sub> C <sub>6</sub> H <sub>4</sub> NH <sub>2</sub>
Glutamate	2-Chloroethanephosphonate	-CH <sub>2</sub> CH <sub>2</sub> PO <sub>3</sub> <sup>-2</sup>
Glutamate	2-Chloronitroethane	-CH <sub>2</sub> CH <sub>2</sub> NO <sub>2</sub> <sup>-</sup>

<sup>a</sup> General structure of acetylcysteamine analogues: H<sub>3</sub>C•CO•NH•CH<sub>2</sub>CH<sub>2</sub>-S-R

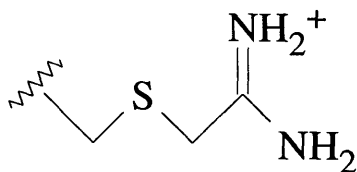
This paper also detailed nine different structural analogue reagents designed for the substitution of histidine, which is one of the most important acid-base catalysts in enzymes, though this amino acid side chain has not been implicated in the reaction cycle of the cytochrome P450s. This approach combines the absolute site specificity of SDM and the ability to introduce a wide range of structural analogues by chemical modification. This approach has already been successfully used by Dhalla *et al.* (1994) in the regeneration of catalytic activity of active site mutants of glutamine synthetase. SDM was used to replace an arginine with a cysteine resulting in substantial loss of activity. Chemical modification was used to “rescue” activity by adding back chemical fragments to mimic the original amino acid. The reagents used to create arginine analogues were either 2-chloroacetamide or 2,2'-dithiobis(acetamide) (Figure 5.11). These compounds could prove important in establishing the validity of the thiol modifications experiments performed on the R47C mutant of P450 BM3. Both chloroacetamide and dithiobis(acetamide) could be utilised to recover the wild type P450 BM3 catalytic activity and thus indicate the extent to which the chemical modification procedure affects the kinetic parameters  $k_{cat}$  and  $K_M$ . Unfortunately as seen in Figure 5.10 the modified side chains would possess different characteristics to the natural arginine as they would contain either one or two sulphur atoms, resulting in differing side chain lengths, 6.60Å for chloroacetamide and 8.28Å for dithiobis(acetamide) as opposed to 7.31Å for arginine. If, however, chloropropionitrile is used in preference to chloroacetonitrile in the synthesis of 2-chloroacetamide (Schaefer and Peters, 1961) the synthesis would result in the production of 2-chloropropionamide. If this were then used in chemical modification of a cysteine residue, the resulting unnatural amino acid chain would contain the minimum of sulphur atoms and the overall length at 7.87Å would most closely resemble that of arginine (Figure 5.11).

The potential to investigate the properties of amino acid side chains in positions of interest using this combined approach of site-directed mutagenesis and chemical modification is enormous, not only for the cytochrome P450 field, but also for other proteins in general. Studies discussed in Chapters 4 and 6 have shown that a single



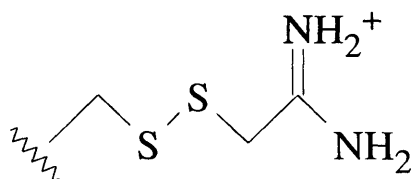
7.31Å

Arginine



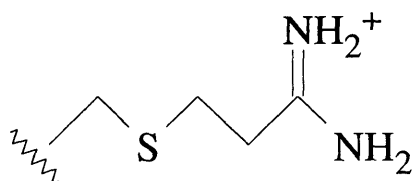
6.60Å

Cysteine + Chloroacetamide  
Reaction I



8.28Å

Cysteine + Dithiobis(acetamide)  
Reaction II



7.87Å

Cysteine + Chloropropamide  
Reaction III

**Figure 5.11:** Structures of arginine and modified cysteines. The structures are shown in the extended conformation starting from the C $\alpha$  position and the measurements calculated using InsightII (Biosym Technologies). The groups attached to the cysteines are named according to the molecules that were used as modifying agents (Adapted from Dhalla *et al.* 1994).

amino acid can influence the substrate specificity and regioselectivity in the P450 enzymes (Lindberg and Negishi, 1989; Fukuda *et al.*, 1994; Ramarao and Kemper, 1995; Szklarz *et al.*, 1995; Curnow *et al.*, 1997). The introduction of a cysteine residue at a key position within the substrate access channel/substrate binding pocket provides a focus for a “chemical cassette system” where potentially chemical modification can be used to incorporate reagents to produce semi-synthetic side chains to either mimic the naturally occurring amino acids and or produce an “amino acid” with a novel side chain structure. This procedure could modify the structure within an amino acid side chain by adjusting the position of a functional group, to alter the properties of an amino acid side chain by changing the reactive functional group, or to alter the location of a functional side chain within the protein structure, resulting in the radical expansion of the catalytic ability of a single enzyme. This method could also introduce specific reporter groups that could be used for structural probes, not only at the site of the specific residue of interest, but also extensively throughout the protein. Examples include isotopically labelled probes such as  $^{19}\text{F}$ ,  $^{31}\text{P}$ ,  $^{15}\text{N}$  and  $^{13}\text{C}$  which are used extensively in NMR, fluorescent probes and the inclusion of heavy atoms to aid X-ray crystallography (Brocklehurst, 1979; Schindler and Viola, 1996).

## Chapter 6: The Phenylalanine 87 to Alanine Mutation

### 6.1 Introduction

It is now appreciated that fatty acid hydroxylases are widespread in nature, being present in mammals (Björkhem and Danielsson, 1970; Okita *et al.*, 1981; Hardwick *et al.*, 1987; Fukuda *et al.*, 1994), plants (Salaün *et al.*, 1989), fungi (Nakayama *et al.*, 1996), yeast (Scheller *et al.*, 1996) and bacteria (Miura and Fulco, 1975). A number of different P450 enzymes catalyse the  $\omega$ - and/or  $\omega$ -1 hydroxylation of fatty acids, prostaglandins, leukotrienes and related compounds, for example, P450 2B1, P450 2C2 and P450 2E1 all catalyse the  $\omega$ -1 hydroxylation of lauric acid, where P450 2E1 also catalyses  $\omega$  and  $\omega$ -2 hydroxylation to a lesser extent. Terminal hydroxylation of fatty acids and related compounds is catalysed primarily by the highly homologous (66-98%) Family 4 P450 enzymes, which appear to form little if any ( $\omega$ -1)-hydroxy metabolites (Bambal and Hanzlik, 1996).

P450 BM3 from *Bacillus megaterium* and P450 foxy from *Fusarium oxysporum* appear to be unique in that they preferentially catalyse the subterminal hydroxylation of long chain fatty acids in the  $\omega$ -1,  $\omega$ -2 and  $\omega$ -3 position, while most other hydroxylases of the mixed function oxidase type act on the terminal methyl group ( $\omega$ -oxidation) or less often, on the  $\omega$ -1 position (Miura and Fulco, 1975; Shoun *et al.*, 1985). In the initial complex of the substrate with the enzyme, in the ferric state, the substrate laurate binds some way from the haem, but on reduction of the enzyme it moves closer such that the observed hydroxylation at the  $\omega$ -1,  $\omega$ -2 and  $\omega$ -3 positions is now possible (Modi *et al.*, 1996b).

The aromatic ring of phenylalanine 87 is positioned perpendicular to the haem moiety and is in close contact on its distal side. The model of substrate binding in the ferrous intermediate (Modi *et al.*, 1996b) is consistent with the suggestion that the structure of P450 BM3 actively suppresses oxidation of the terminal carbon atom and that this residue may play an important role in the regiospecificity of the enzyme by sequestering the substrate terminal carbon into a lipophilic pocket at the end of the

substrate binding site, such that it is not accessible to the ferryl oxygen at the haem (Ravichandran *et al.*, 1993; Shirane *et al.*, 1993). Recently Capdevila *et al.* (1996) have reported that P450 BM3 metabolises arachidonic acid stereoselectively to the 18(*R*)-hydroxy and 14(*S*), 15(*R*)-epoxy derivatives and presented a model for the binding of this substrate to the enzyme in which Phe 87 is proposed to play an important role in controlling the modes of binding which lead to two different products.

## **6.2 Protein Expression and Purification**

Phenylalanine 87 was substituted by alanine both in the intact P450 BM3 and in its haem domain. The gene sequencing of the mutant intact P450 BM3 has been discussed fully in Chapter 3, Section 3.2.3 and that chapters discussion section. Some modifications to the purification protocol were necessary and these were that imidazole was added prior to cell lysis to stabilise haem incorporation and the final purification column for both the F87A mutant proteins was a HiLoad Superdex S200 FPLC column. Pure protein yields for the Phe87→Ala (F87A) mutant proteins were between 50-100mg per litre of culture, which was significantly less than that for the wild type proteins which were in the range of 200-250 mg pure protein per litre of culture. All proteins were shown to be pure by existing as a single band on a Coomassie blue stained SDS-PAGE gel and by their absorbance ratio of  $A_{418nm}/A_{280nm}$ ; 0.597 for the F87A mutant intact P450 BM3 and 1.679 for the F87A mutant haem domain. N-terminal sequencing indicated that the initial residues of both proteins was identical to that published by Ruettinger *et al.* (1989).

## **6.3 Electrospray Mass Spectroscopy**

Mass spectroscopy is widely used to estimate the molecular weight of biological compounds, but here it has also been used to confirm the presence of the F87A mutation. The F87A mutant intact P450 BM3 and haem domain proteins were analysed using electrospray ionisation sample analysis for mass spectroscopy (ES-MS). The results are listed in Table 6.1. The calculated masses were calculated from the

recombinant protein sequence (Ruettinger *et al.*, 1989) using the software on the mass spectrometer, assuming all cofactors had been removed.

**Table 6.1:** Molecular mass, measured by electrospray mass spectrometry, for wild type and F87A mutant intact P450 BM3.

Protein		Measured Mass <sup>a</sup>	Calculated Mass	
Intact enzyme	Wild Type	117,648 (±74)	117,782 <sup>b</sup>	117,651 <sup>c</sup>
	F87A Mutant	117,608 (±61)	117,706 <sup>b</sup>	117,574 <sup>c</sup>
			117,657 <sup>bf</sup>	117,525 <sup>cf</sup>
Haem domain	Wild Type	53,350 (±5)	53,342 <sup>d</sup>	53,346 <sup>e</sup>
	F87A Mutant	53,280 (±11)	53,268 <sup>d</sup>	53,264 <sup>e</sup>

<sup>a</sup> The measured mass represents the molecular weight, in Daltons (Da) obtained for the various proteins using ES-MS.

<sup>b</sup> Mass calculated with initial methionine still present.

<sup>c</sup> Mass calculated with initial methionine removed.

<sup>d</sup> Mass calculated with initial methionine and three C-terminal residues removed.

<sup>e</sup> Mass calculated with initial methionine still present and four C-terminal residues removed.

<sup>f</sup> Mass calculated with spontaneous mutations at residues 429 and 430.

The results obtained showed reasonable precision for the intact enzyme, indicating a series mass of 117,608Da with standard error of 61Da for F87A mutant of the intact P450 BM3. Despite a greater standard error with this enzyme than those for the other intact P450 BM3 mutant proteins, the result for this enzyme is still in good agreement with the calculated mass indicating the presence of the desired mutation. The results from the N-terminal sequencing indicate that the intact mutant protein was purified with the majority of the enzyme with the N-terminal methionine removed unlike the R47E mutant where both the proteins were purified with the N-terminal methionine

still present. Taking this into consideration, the measured mass more closely resembles that for the F87A mutant protein in the absence of any of the spontaneous mutations at residue 429 and 430. These are described in greater detail in Chapter 3, Section 3.2.3. This indicates that the data obtained from the molecular mass determination for the intact F87A P450 BM3 does not appear to support the presence of the “extra” mutations.

The measured mass for the F87A mutant haem domain was 53,280Da with standard error of 11Da as compared to 53,350Da for the wild type protein with standard error of 5Da. Neither of these values are in agreement with the calculated molecular mass for the 471 amino acid haem domain from P450 BM3, 53,856Da for the wild type protein and 53,782Da for the F87A mutation. Both proteins possess a measured mass which is less than expected, corresponding to the loss of either three or four amino acids as discussed in Chapter 3. The measured mass for the F87A haem domain does not correspond exactly to the calculated molecular mass, however as the obtained value was within 5Da, the data was considered sufficiently accurate as the overall standard error for the technique is 0.1% of the total mass, equivalent to 53Da for this mutant protein. These results show that mass spectrometry provides a sufficiently sensitive method to detect whether the F87A mutant proteins produced do indeed possess the desired change.

## ***6.4 Optical Spectroscopy and Enzyme Assays***

### ***6.4.1 Substrate Binding***

The purified F87A mutant intact P450 BM3 and its haem domain were purified in the ferric low spin state and showed the typical P450 type spectra (Figure 6.1). The spectra of the proteins in the oxidised state showed well resolved  $\alpha$  and  $\beta$  bands at 570 and 535nm and a strong Soret band at 418nm. After reduction with sodium dithionite and CO, the spectra shows characteristic peaks at 547 and 448nm. A closely similar spectra was obtained for the F87A mutant intact P450 BM3 which contained an additional peak around 450 to 470nm which is indicative of the presence of the flavins (Narhi and Fulco, 1988). In both spectra an absence of a band at 420nm in the sodium

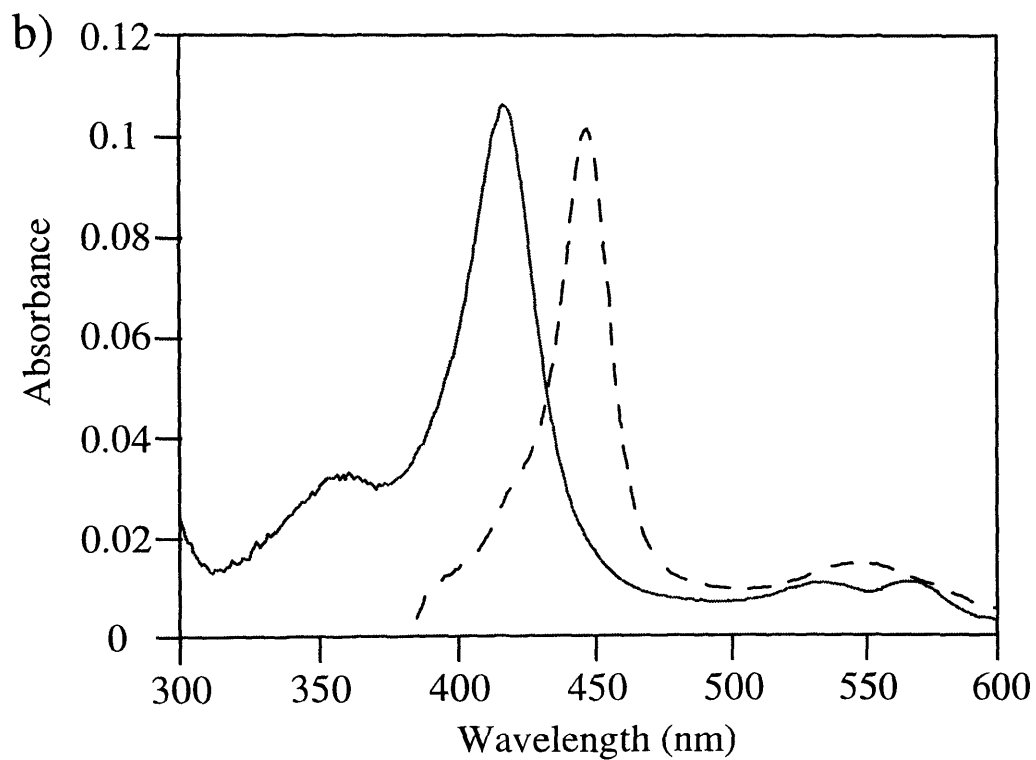
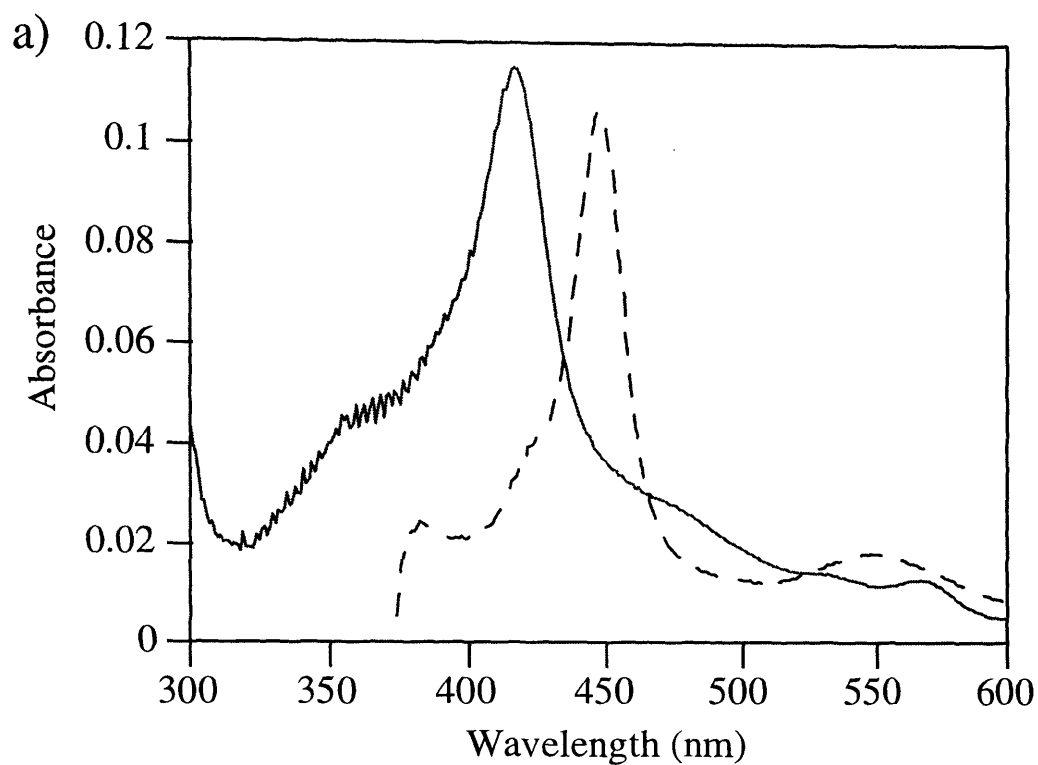
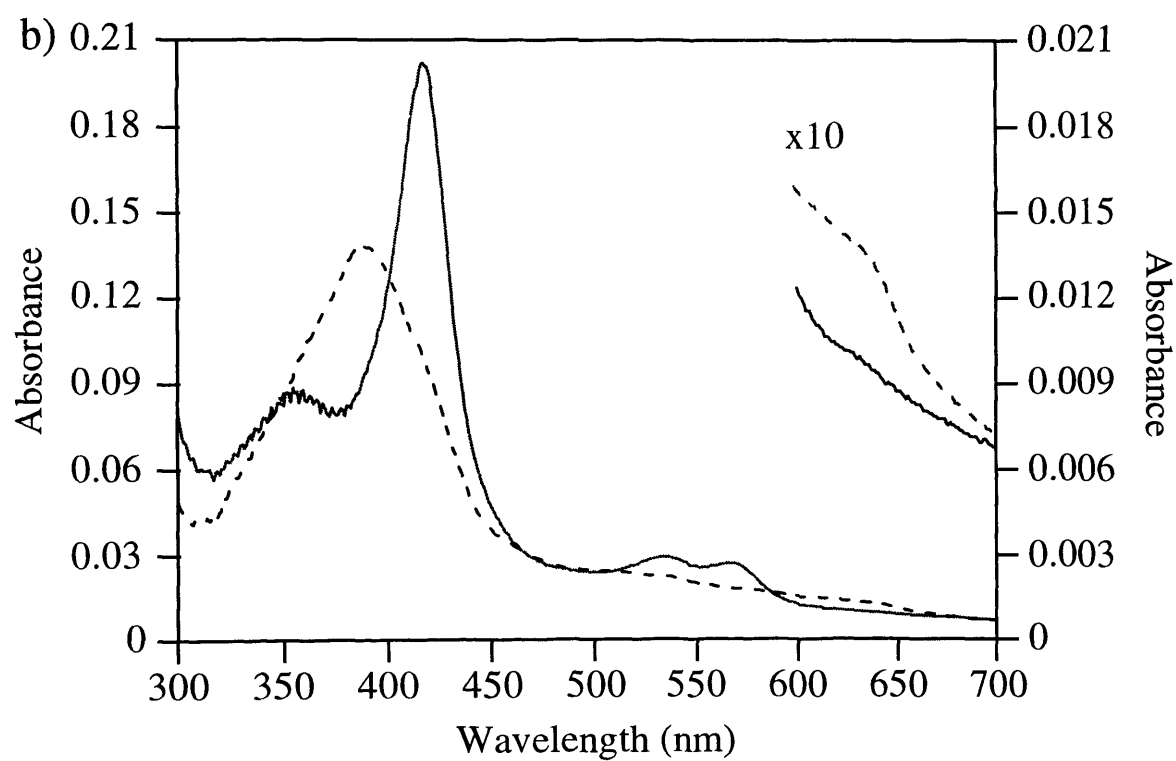
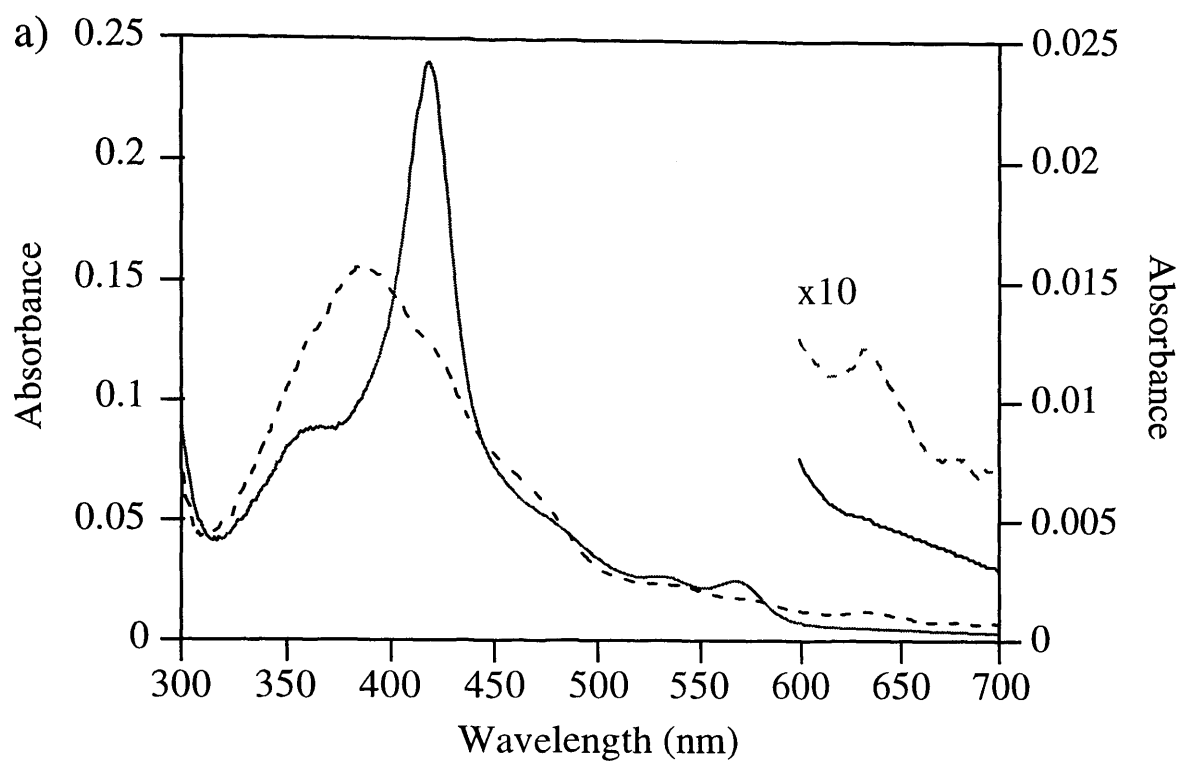


**Figure 6.1:** The absorption spectra for F87A mutant intact cytochrome P450 BM3 (a) and its haem domain (b). The sample cuvette contained either  $1.20\mu\text{M}$  intact P450 BM3 or  $1.36\mu\text{M}$  haem domain. The spectrum with the solid line (—) is the oxidised form of the enzyme. The broken line (- - -) was taken after the sample was reduced by addition of sodium dithionite followed by saturation with CO.

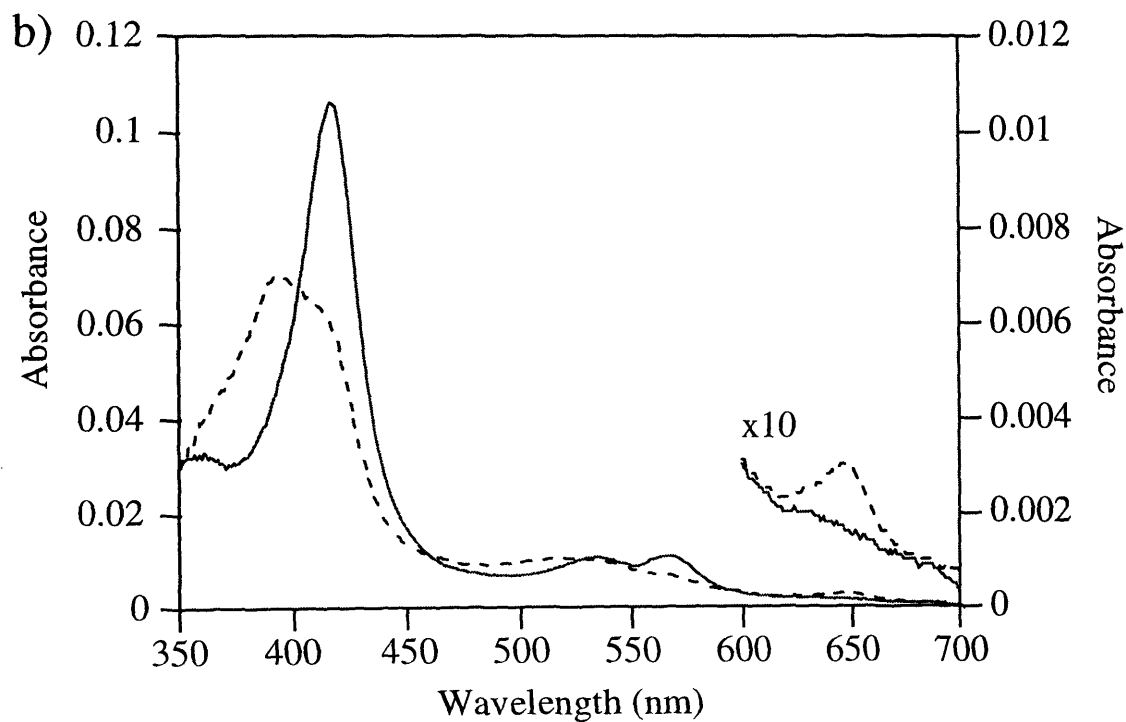
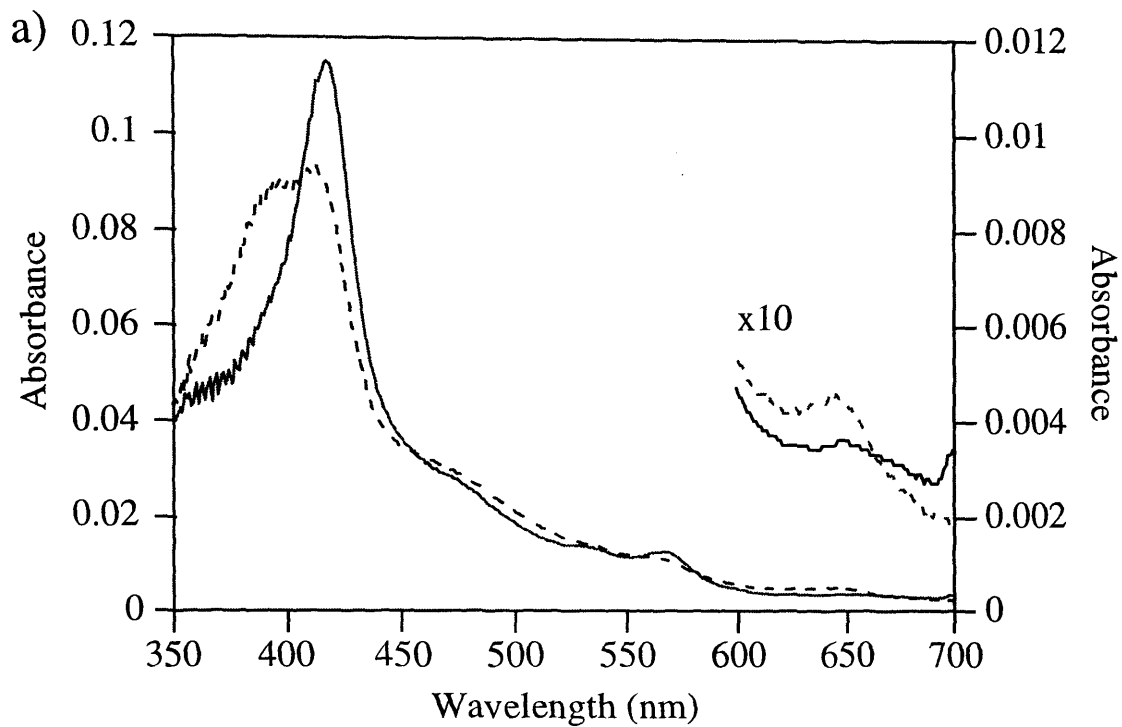
dithionite-CO complex of the reduced enzyme indicates there is no inactive P450 in the preparation (Modi *et al.*, 1995a). Comparison with the wild type spectra (see Chapter 4, Figure 4.3a and b) shows that the F87A mutants of the intact P450 BM3 and its haem domain were purified in the low spin hexacoordinated state, were capable of being reduced in the presence of sodium dithionite and CO and thus represent active cytochrome P450 enzymes. They also suggest that although the phenylalanine side-chain forms close van der Waals interactions with the haem (Ravichandran *et al.*, 1993), substitution by an alanine does not significantly affect the electronic structure of the haem as reflected in its optical spectrum.

Figure 6.2 shows a comparison between the electronic absorption spectra of the wild type and F87A mutant proteins in the presence and absence of the fatty acid substrate, lauric acid. On addition of substrate a typical type I spectrum is produced characterised by a decrease in the Soret band at 418nm and the  $\alpha$  and  $\beta$  bands at 570 and 535nm respectively, with a simultaneous increase in the absorbance at 390 and 650nm. The change in spectrum at saturating laurate concentrations is consistent with a complete spin-state conversion as seen with the wild type enzyme (Modi *et al.*, 1995b).

The equilibrium dissociation constants,  $K_d$ , were calculated from the decrease in absorbance at 418nm and the values obtained are detailed in Table 6.1. The  $K_d$ s obtained for the F87A mutant haem domain and intact P450 BM3 were 140 $\mu$ M and 103 $\mu$ M respectively when using lauric acid as substrate. These compare with values of 840 $\mu$ M and 270 $\mu$ M obtained for the wild type haem domain and intact P450 BM3 respectively. As with the wild type data, the F87A mutant intact P450 BM3 enzyme has a slightly lower  $K_d$  than that of the mutant haem domain. The dissociation constants for both the F87A mutant proteins have decreased significantly from those of the corresponding wild type enzymes indicating that an increase of between 2.6- and 6-fold in substrate affinity for this fatty acid substrate is observed after the F87A substitution.



**Figure 6.2:** Absorption spectra of the wild type intact P450 BM3(a; 2.50 $\mu$ M) and haem domain (b; 2.13 $\mu$ M) in the presence (-----) and absence (————) of 2mM lauric acid as substrate.



**Figure 6.2:** Absorption spectra of the F87A mutant intact P450 BM3(c; 1.20 μM) and haem domain (d; 1.36 μM) in the presence (-----) and absence (————) of 0.6 mM lauric acid as substrate.

**Table 6.1:** Laurate binding and hydroxylation by the wild type and F87A mutant P450 BM3 and its haem domain.

Protein	$K_d$ ( $\mu\text{M}$ ) <sup>a</sup>	$k_{\text{cat}}$ ( $\text{sec}^{-1}$ ) <sup>b</sup>	$K_M$ ( $\mu\text{M}$ ) <sup>b</sup>	$k_{\text{cat}}/K_M$ <sup>c</sup> ( $\text{M}^{-1}\text{s}^{-1}$ )
Wild type P450 BM3	270±47	26.1±1	136±3	0.19 x 10 <sup>5</sup>
Wild type Haem domain	840±40			
F87A Mutant P450 BM3	103±53	24.5±4	167±50	0.15 x 10 <sup>5</sup>
F87A Mutant Haem domain	140±44			

<sup>a</sup> The dissociation constants refer to binding to the ferric state of the enzyme.

<sup>b</sup> Each constant was determined at 9 or 10 substrate concentrations, with at least 4 replicates at each concentration.

<sup>c</sup>  $k_{\text{cat}}/K_M$  refers to the specificity constant.

#### 6.4.2 Determination of the Catalytic Constant, $k_{\text{cat}}$ and the Michaelis Menten Constant $K_M$

The NADPH consumption assay (Matson *et al.*, 1977) was used to determine the catalytic rate constants for the wild type and F87A mutant P450 BM3. Sodium laurate was chosen as the sole substrate as it is the most soluble fatty acid substrate and its products of hydroxylation are known not to undergo further oxidation unlike longer fatty acids such as palmitic acid (Boddupalli *et al.*, 1990).

The results from kinetics measured by the spectrophotometric assay are represented in Table 6.1, where the results are given as means ± standard deviations. A typical data curve for the calculation of the steady state kinetic parameters  $k_{\text{cat}}$  and  $K_M$  is depicted in Figure 6.3 for F87A mutant P450 BM3 using laurate as substrate. The results for the F87A mutant are very similar to those obtained for the wild type protein. The values of 26.1 $\text{sec}^{-1}$  for the wild type P450 BM3 and 24.5  $\text{sec}^{-1}$  F87A mutant P450

BM3 for the catalytic activity can be considered virtually identical. The  $K_M$  for the fatty acid laurate, which may reflect binding to the reduced state rather than the resting state of the enzyme (Modi *et al.*, 1996b), were essentially the same with values of 136 $\mu$ M for the wild type protein and 167 $\mu$ M for the F87A mutant protein as the margin of error for the F87A mutant protein allowed some overlap.

### 6.4.3 Hydrogen Peroxide Formation

Use of substrate analogues, active site mutations or mutations that give rise to hydration of the active site may alter the catalytic reaction such that the ferryl-oxygen species will react with water to produce hydrogen peroxide in an uncoupled reaction. The substitution at position 87 introduced a change in close proximity to the catalytic centre at the haem. Therefore the hydrogen peroxide formation assay was performed to assess the coupling of NADPH consumption to substrate hydroxylation in the F87A mutant of P450 BM3 and the results are represented in Table 6.2.

**Table 6.2:** Determination of hydrogen peroxide production using 0.2mM lauric acid as substrate to assess the coupling of the catalytic reaction.

P450 BM3	H <sub>2</sub> O <sub>2</sub> Production (mmol/min/mg)	NADPH Consumption (mmol/min/mg) <sup>a</sup>	Ratio <sup>b</sup>
Wild type	0.46 x 10 <sup>-5</sup>	0.41	1.1 x 10 <sup>-5</sup>
F87A Mutant	1.36 x 10 <sup>-5</sup>	1.34	1.0 x 10 <sup>-5</sup>

<sup>a</sup> NADPH consumption was performed using the same conditions as the hydrogen peroxide assay as detailed in the results section.

<sup>b</sup> The ratio represents the production of hydrogen peroxide in relation to the NADPH consumed.

The production of hydrogen peroxide for the F87A mutant P450 BM3 was in the same order of magnitude as that obtained for the wild type protein. When comparing the

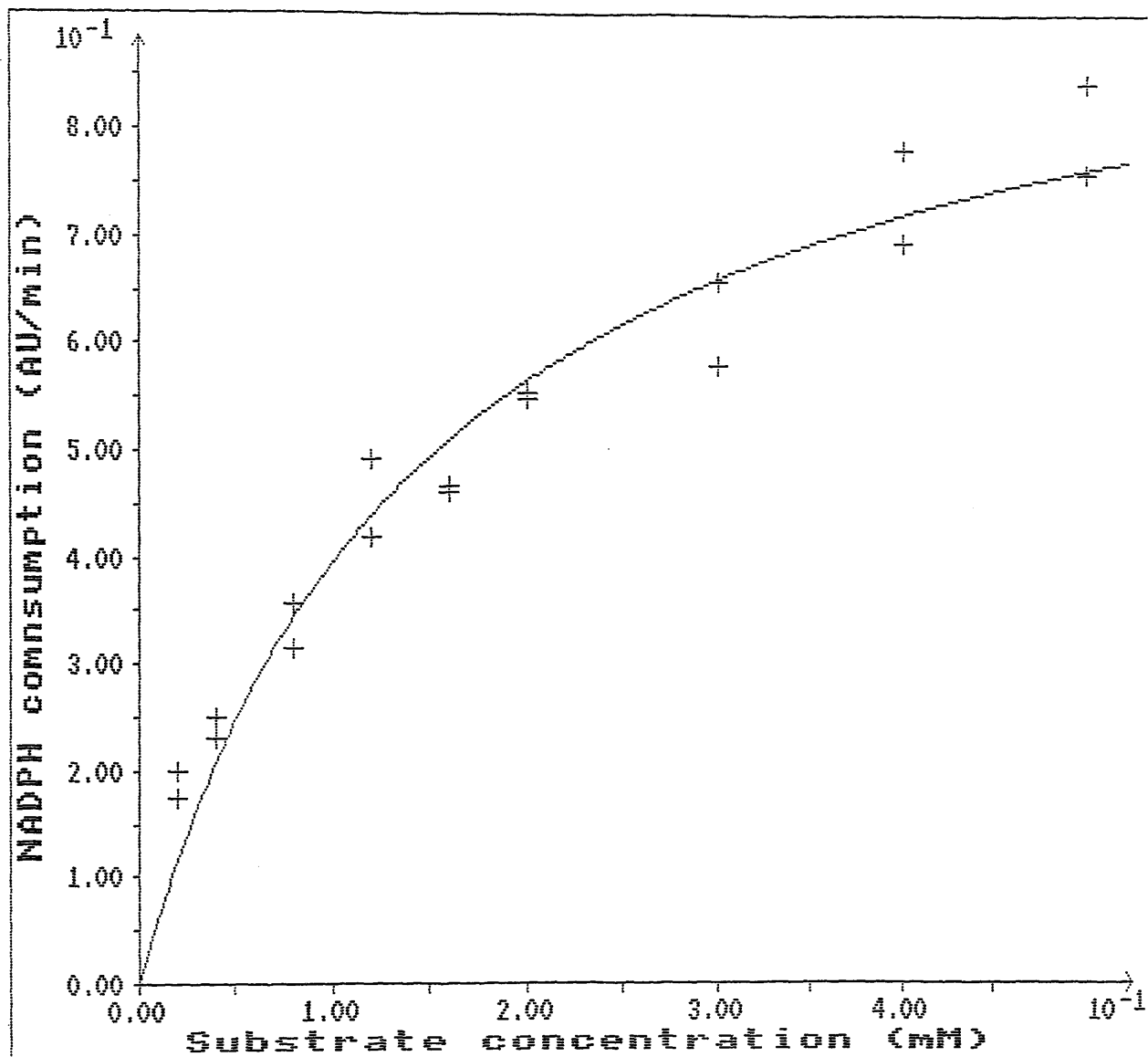


**Figure 6.3:** Typical data to show the effect of substrate concentration (S) on the rate of reaction (AU/min) as measured by the NADPH consumption for the F87A mutant P450 BM3 with the substrates lauric acid.

production of hydrogen peroxide with the consumption of NADPH, the resulting ratio was approximately  $10^{-5}$  for both proteins indicating that the quantity of hydrogen peroxide produced during the catalytic reaction is insignificant in relation to the quantity of NADPH consumed suggesting that there is little uncoupling of the catalytic reaction.

## **6.5 Identification of Products of Hydroxylation from the F87A mutant P450 BM3**

### **6.5.1 HPLC Purification of Products of Hydroxylation**

The difference in the position of the terminal methyl group suggested that the mutant might, unlike the wild type, hydroxylate the substrate at this position. Therefore, the products of hydroxylation were identified and quantified using laurate as substrate. To initially confirm the presence of terminal hydroxylation products for the fatty acid substrate lauric acid, the catalytic reaction was performed using an excess of lauric acid and a NADPH regenerating system for 3 hours at room temperature, the products of hydroxylation extracted with ethyl acetate and separated by reverse phase HPLC. All the resulting fractions were dried under nitrogen at room temperature and only those fractions which contained any residue were examined by  $^1\text{H}$  NMR spectroscopy; fractions 17, 19, 44 and 45 for the wild type and fractions 14, 17, 19, 44 and 45 minutes for the F87A mutant protein, where the fraction number represents the retention time in minutes. The  $^1\text{H}$  NMR spectra of laurate and the HPLC purified lauric acid products of hydroxylation from the reaction using the F87A mutant of P450 BM3 are represented in Figure 6.4, using the invariant  $\text{C}(2)\text{H}_2$  resonance as a standard.

Figure 6.4a) represents the spectra of the excess lauric acid substrate which eluted in fractions 44 and 45 for both proteins. The resonance for the  $-\text{C}(12)\text{H}_3$  or terminal ( $\omega$ ) methyl appears upfield at approximately 0.7 to 0.9 ppm and there are no resonances between the C4-C11 (internal methylenes) and the C3 methylene. Figure 6.4b) represents a product of hydroxylation with a retention time of 14 minutes that was unique to the F87A mutant as the fraction 14 from the HPLC purified products of hydroxylation using the wild type protein contained no residue. The  $-\text{C}(12)\text{H}_3$  resonance has disappeared whereas a clear triplet has appeared downfield in the region

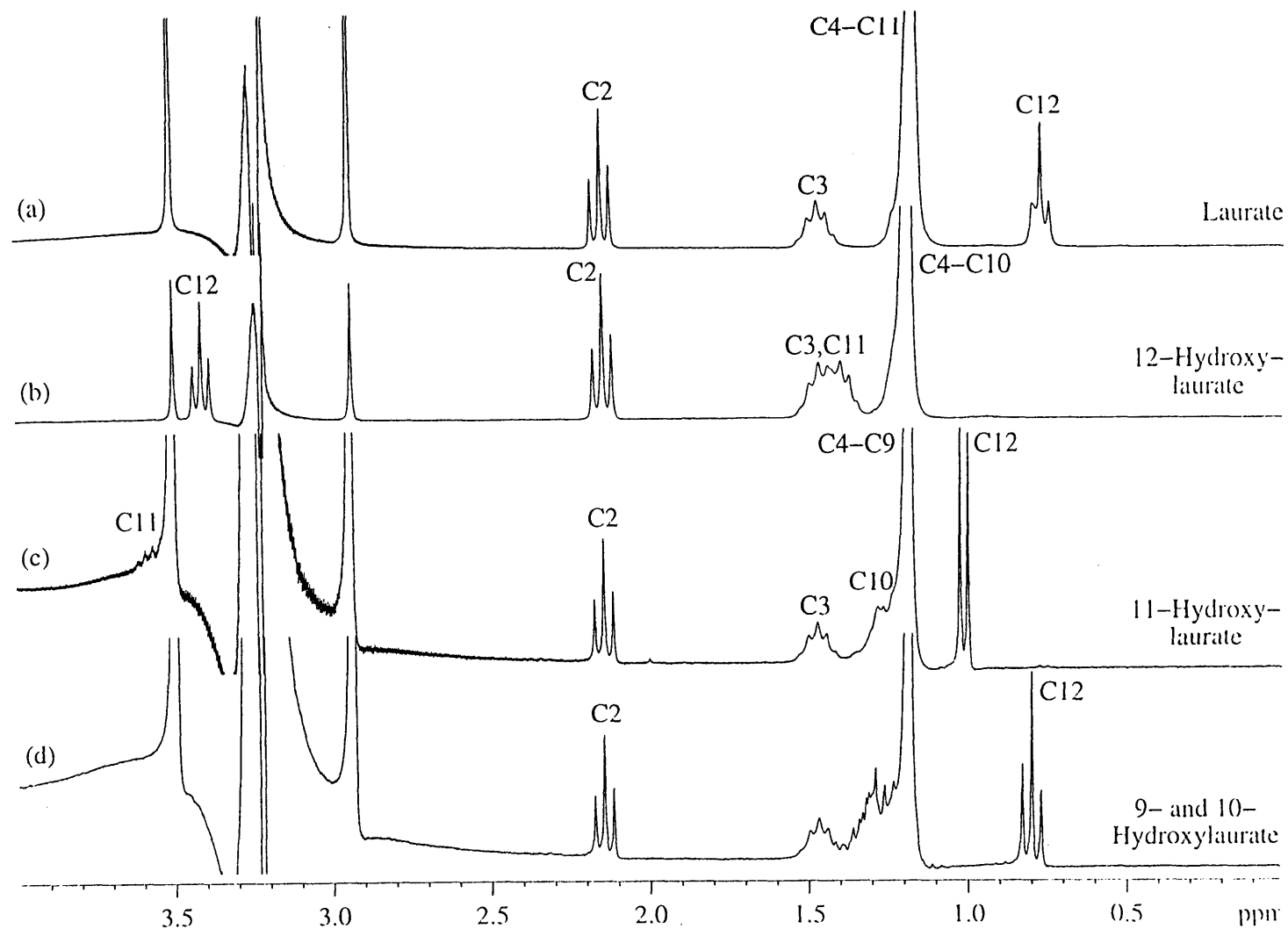


**Figure 6.4:** 250MHz  $^1\text{H}$  NMR spectra ( $\text{CD}_3\text{OD}$ , 300K) of the HPLC-purified products of enzymatic hydroxylation from lauric acid. (a) Lauric acid substrate, (b) 12-hydroxylauric acid, (c) 11-hydroxylauric acid and (d) mixture of 9- and 10-hydroxylauric acid (not separated under the HPLC conditions used). Resonance assignments are indicated on the spectra.

of 3.3 to 3.5 ppm and represents  $-C(12)H_2OH$ , the terminally hydroxylated C12 of laurate. The  $\omega$ -1 hydroxylated product was eluted in fraction 17 and is represented in Figure 6.4c). The disappearance of the  $-C(12)H_3$  triplet at approximately 0.8 ppm is coupled with the appearance of a doublet in the region of 0.9 to 1.1 ppm and other resonance between 1.2 and 1.4 ppm representing the  $-C(10)H_2-$  due to the presence of  $-C(11)HOH-$ . Finally, Figure 6.4d) represents a combination of the  $\omega$ -2 and  $\omega$ -3 hydroxylated products that coeluted in fraction 19, manifested by the appearance of resonances between 1.2 and 1.4 ppm. The  $^1H$  NMR spectra of the fractions 17, 19 and 44/45 from HPLC separation of the lauric acid products of hydroxylation using wild type P450 BM3 gave similar results to those from the corresponding fractions from the F87A mutant protein.

The spectra in Figure 6.4 representing all the products of hydroxylation of lauric acid using F87A mutant P450 BM3, have been displayed such that they can be directly compared and each of the NMR experiments were performed under identical conditions making it possible to integrate invariant  $-C(2)H_2-$  resonance to calculate the relative abundance of each product of hydroxylation. For the wild type enzyme acting on laurate, a 0:30:70 ratio of  $\omega$ : $\omega$ -1: $\omega$ -2/ $\omega$ -3 hydroxylated products, compares favourably with the previously published ratio of 36:30:34 representing  $\omega$ -1: $\omega$ -2: $\omega$ -3 products of hydroxylation where all the products of hydroxylation are present in approximately equal ratios (Miura and Fulco, 1975), with no detectable  $\omega$ -hydroxylated product being observed. In contrast, a product ratio of 85:8:7 was calculated for the HPLC purified products from the F87A mutant, where the major product is  $\omega$ -hydroxylated and represents 85% of the total product, with very little production of either the  $\omega$ -1,  $\omega$ -2 or  $\omega$ -3. The F87A mutant hydroxylated laurate and myristate almost entirely (>90%) at the  $\omega$  position in the complete reaction mixtures.

These retention times obtained in these experiments differ to those obtained when measuring the lauric acid metabolism using either lung microsomes, liver microsomes or purified proteins (Okita *et al.*, 1991). The retention times were 15 minutes and 13 minutes as opposed to 14 minutes and 17 minutes for the  $\omega$  hydroxylated and  $\omega$ -1 hydroxylated products respectively. The elution conditions were subtly different in

that a different make of column was used, but more importantly, the products were eluted using gradient of 62% aqueous 0.2% acetic acid in methanol increasing to 100% aqueous 0.2% acetic acid, thus increasing the polarity of the solvent, which may account for the  $\omega$ -hydroxylated product eluting after that of the  $\omega$ -1 hydroxylated product.

### **6.5.2 1D Proton NMR of Complete Reaction Mixtures for both the Wild Type and F87A Mutant P450 BM3**

In order to obtain an accurate quantitation of the relative amounts of each product formed, the  $^1\text{H}$  NMR spectra of the reaction mixtures were integrated. Figure 6.5 shows the spectra of the reaction mixture after incubation of wild type and F87A mutant P450 BM3 with laurate and NADPH. Protons geminal to the hydroxyl group appear at 3.5 to 3.9 ppm; a clear triplet from the  $-\text{C}(12)\text{H}_2\text{OH}$  of  $\omega$ -hydroxylaurate appears at 3.57 ppm in the incubation with the F87A mutant enzyme (Figure 6.5b) but not in that of the wild type (Figure 6.5a). The region 0.8 to 1.2 ppm contains resonances from the  $-\text{C}(12)\text{H}_3$  in the substrate and in the  $\omega$ -1,  $\omega$ -2 and  $\omega$ -3 hydroxylated products. These resonances are very clear in Figure 6.5a but appear weak in Figure 6.5b showing that the F87A mutant produces only very small amounts of these products. Resonances from methylene protons vicinal to a secondary hydroxyl group appear at 1.3 to 1.5 ppm in Figure 6.5a, but are clearly absent in Figure 6.5b. The resonance from the  $\text{C}(11)\text{-H}_2$  of  $\omega$ -hydroxylaurate appears at 1.51 ppm in Figure 6.5b, coincident with that of the invariant  $\text{C}(3)\text{H}_2$ . The chemical shifts for the various protons in Figures 6.4 and 6.5 vary due to the solvent used.

### **6.6 NMR Spectroscopy**

In order to make a structural comparison of substrate binding to the wild type and F87A mutant enzyme, NMR spectroscopy was used to obtain estimates of distances between the individual protons of the bound substrate and the haem iron in the haem domain of the enzyme from the paramagnetic relaxation effects of the iron on the substrate protons (Modi *et al.*, 1995b). These experiments were performed using both

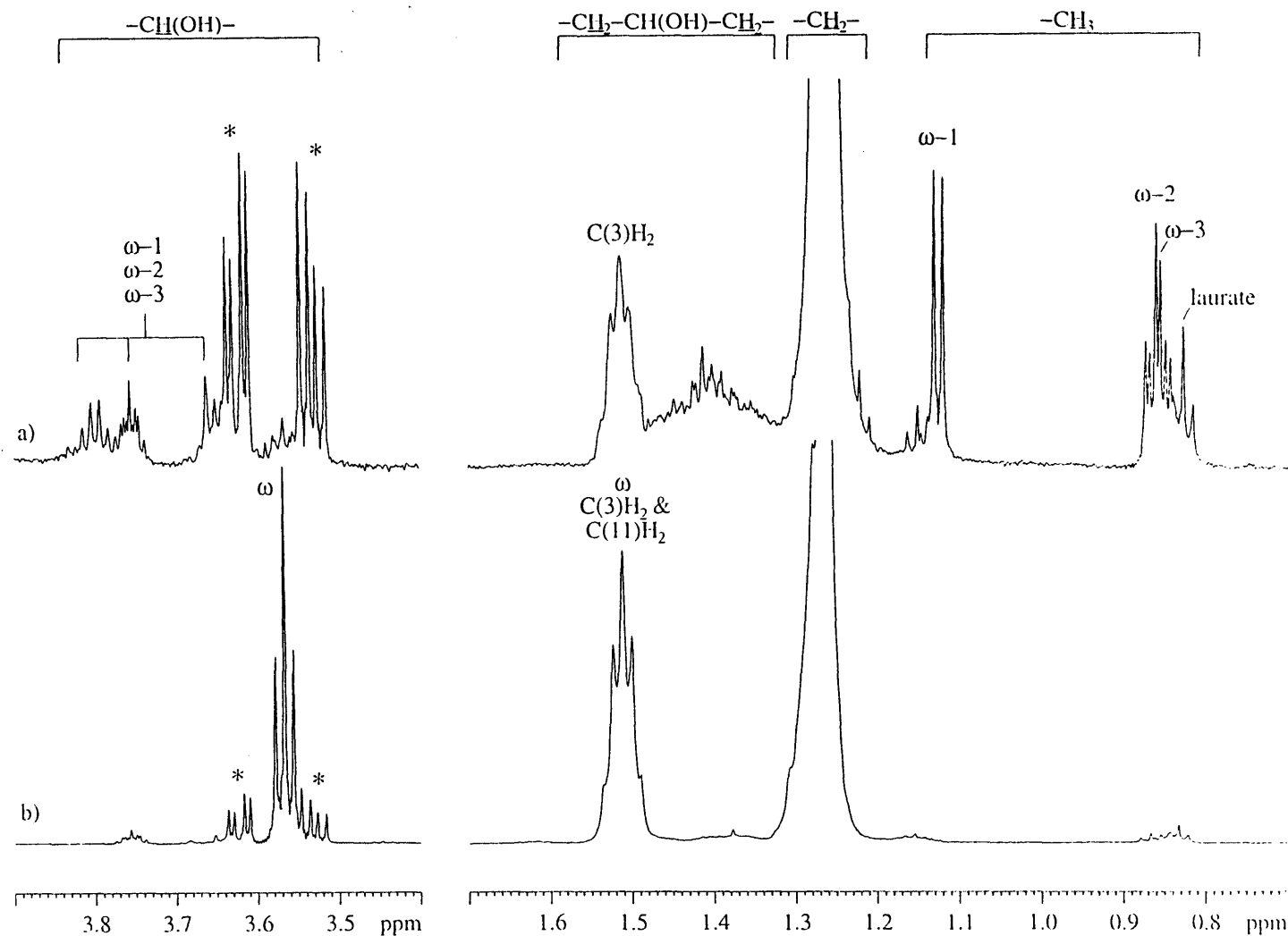


**Figure 6.5:** 600 MHz <sup>1</sup>H NMR spectra of the reaction mixtures from incubations of (a) wild type and (b) F87A mutant P450 BM3 (each at 0.2 μM) with 1 mM laurate and 1 mM NADPH. The intensities of the spectra were normalised using the invariant resonance of the C2 protons (2.20 ppm). Resonance assignments are indicated on the spectra: signals from  $\text{NADP}^+$  at 3.52 and 3.62 ppm are indicated by asterisks.

laurate and 12-bromolaurate as substrates, as the latter has a very similar  $k_{\text{cat}}$  and  $K_{\text{M}}$  to laurate, which suggests it is as good a substrate for P450 BM3, and possesses a better resolved 1D proton NMR spectrum (Modi *et al.*, 1995b). The necessary controls to ensure rapid exchange of the substrate between the bound and free states, to correct for diamagnetic contributions to relaxation, and to determine the relevant correlation times were carried out as described in detail by Modi *et al.* (1995b). The correlation time was estimated using two methods: the frequency dependence of  $R_{1,\text{P}}$  and the ratio of  $T_1/T_2$ , over the range of 250-600MHz. Values of  $2.3 (\pm 0.1) \times 10^{-10}$ s for the ferric state and  $3.8 (\pm 0.4) \times 10^{-12}$ s for the ferrous state were obtained and these are identical to those previously determined for the wild type enzyme (Modi *et al.*, 1995b, Modi *et al.*, 1996b). As the correlation time values were shorter for the reduced versus the oxidised protein, only the paramagnetic contribution to the relaxation for the C10 to C12 protons were observed (Modi *et al.*, 1996b).

The paramagnetic contributions to the relaxation times of the bound substrate and the derived iron proton distances are given in Table 6.3, where the distances are compared with those previously published for the wild type comparison (Modi *et al.*, 1995b; Modi *et al.*, 1996b). The initial enzyme-substrate complex is formed with the ferric state of the enzyme. In this complex the substrate is relatively distant from the haem, and thus also from the residue phenylalanine 87. The closest approach is that of the terminal methyl group, whose protons are 7.6-7.8Å from the haem iron whereas the C2 methylene protons are furthest away at 16.3-16.9Å (Modi *et al.*, 1995b). These results indicate that the position and orientation of both laurate and 12-bromolaurate bound to the ferric state of the F87A mutant are essentially the same as for the wild type enzyme (Table 6.3).

The next intermediate in the catalytic cycle is the ferrous enzyme-substrate complex, formed by the transfer of one electron from the reductase. Modi *et al.* (1996b) showed that this reduction is accompanied by a substantial movement of the substrate (and presumably a structural change of the protein), such that the  $\omega$ -1 and  $\omega$ -2 methylene groups move some 6Å closer to the iron, into a position appropriate for hydroxylation. The terminal ( $\omega$ ) methyl, which is not hydroxylated by the wild type enzyme, is 5.1Å from the iron in the ferrous intermediate of the wild type enzyme

**Table 6.3:** Paramagnetic relaxation times and distances of substrate protons from the haem iron in the haem domain of wild type and F87A mutant P450 BM3 from *Bacillus megaterium*.

Substrate	Protein	Parameter	C2 -OOCCH <sub>2</sub> -	C3 -CH <sub>2</sub> -	C10 -CH <sub>2</sub> -	C11 -CH <sub>2</sub> -	C12 -CH <sub>2</sub> X <sup>a</sup>
Ferric State <sup>b</sup>							
Laurate	F87A Mutant	T <sub>1,M</sub> (ms)	130±2	80±3	- <sup>d</sup>	- <sup>d</sup>	1.29±0.03
		r (Å)	16.3±0.2	15.6±0.2	- <sup>d</sup>	- <sup>d</sup>	7.8±0.3
	Wild Type <sup>c</sup>	r (Å)	16.5±0.2	15.4±0.3	- <sup>d</sup>	- <sup>d</sup>	7.6±0.3
Bromolaurate	F87A Mutant	T <sub>1,M</sub> (ms)	128±1	78±1	3.1±0.1	2.23±0.08	1.18±0.06
		r (Å)	16.9±0.1	15.5±0.1	9.1±0.2	8.6±0.2	7.7±0.2
	Wild Type <sup>c</sup>	r (Å)	16.3±0.2	15.1±0.3	9.4±0.2	8.9±0.2	7.8±0.2
Ferrous State <sup>b</sup>							
Laurate	F87A Mutant	T <sub>1,M</sub> (ms)	- <sup>e</sup>	- <sup>e</sup>	- <sup>d</sup>	- <sup>d</sup>	0.43±0.1
		r (Å)	- <sup>e</sup>	- <sup>e</sup>	- <sup>d</sup>	- <sup>d</sup>	3.15±0.6
	Wild Type <sup>c</sup>	r (Å)	- <sup>e</sup>	- <sup>e</sup>	- <sup>d</sup>	- <sup>d</sup>	5.1±0.2
Bromolaurate	F87A Mutant	T <sub>1,M</sub> (ms)	- <sup>e</sup>	- <sup>e</sup>	0.25±0.05	0.38±0.1	0.40±0.05
		r (Å)	- <sup>e</sup>	- <sup>e</sup>	2.9±0.06	3.1±0.07	3.1±0.05
	Wild Type <sup>c</sup>	r (Å)	- <sup>e</sup>	- <sup>e</sup>	3.0±0.1	3.1±0.1	5.1±0.1

<sup>a</sup> X=H or Br, <sup>b</sup> Resonance not resolved, <sup>c</sup> data from Modi *et al.* (1995b, 1996b), <sup>d</sup> resonance not resolved

<sup>e</sup> insufficient paramagnetic contribution to relaxation for a distance to be estimated.

(Table 6.3) and is close to Phe 87 in our model of the complex (Figure 6.6). In the complex of the ferrous state of the F87A mutant, the positions of the  $\omega$ -1 and  $\omega$ -2 methylenes are unaffected, at approximately 3.0Å from the haem iron, which suggests that both these groups are in such a position that they can undergo hydroxylation. However, additionally the terminal methyl group is now clearly closer to the iron than in the wild type enzyme (3.1Å versus 5.1Å; Table 6.3 and Figure 6.6). Thus, this amino acid substitution has no effect on substrate binding in the initial enzyme-substrate complex but does significantly alter the conformation of the bound substrate in the subsequent catalytic intermediate. Measurements of the paramagnetic relaxation effects on the protons of the substrate molecule can also be used to provide an estimate of the equilibrium dissociation constants,  $K_d$ . The values obtained for both laurate and 12-bromolaurate binding to the haem domain of the F87A mutant are shown in Table 6.4 with those for the wild type protein for comparison.

**Table 6.4:** Equilibrium dissociation constant,  $K_d$ , estimated from paramagnetic relaxation experiments with both laurate and 12-bromolaurate as substrate for the wild type and F87A mutant haem domains in the ferric and ferrous states.

Haem domain	Substrate	$K_d$ ( $\mu$ M)		
		Optical Ferric State	NMR Ferric State	NMR Ferrous State
Wild Type	Laurate	840±40	840±40	100±15
	Bromolaurate		890±50	150±16
F87A Mutant	Laurate	140±44	567±29	79±16
	Bromolaurate		623±90	147±16

The  $K_d$  determinations for the F87A mutant haem domain generated by optical spectroscopy are approximately 4-fold greater than those generated using NMR methods, whereas the  $K_d$  values for the wild type haem domain for both these methods are identical. The  $K_d$  values obtained from the paramagnetic relaxation experiments

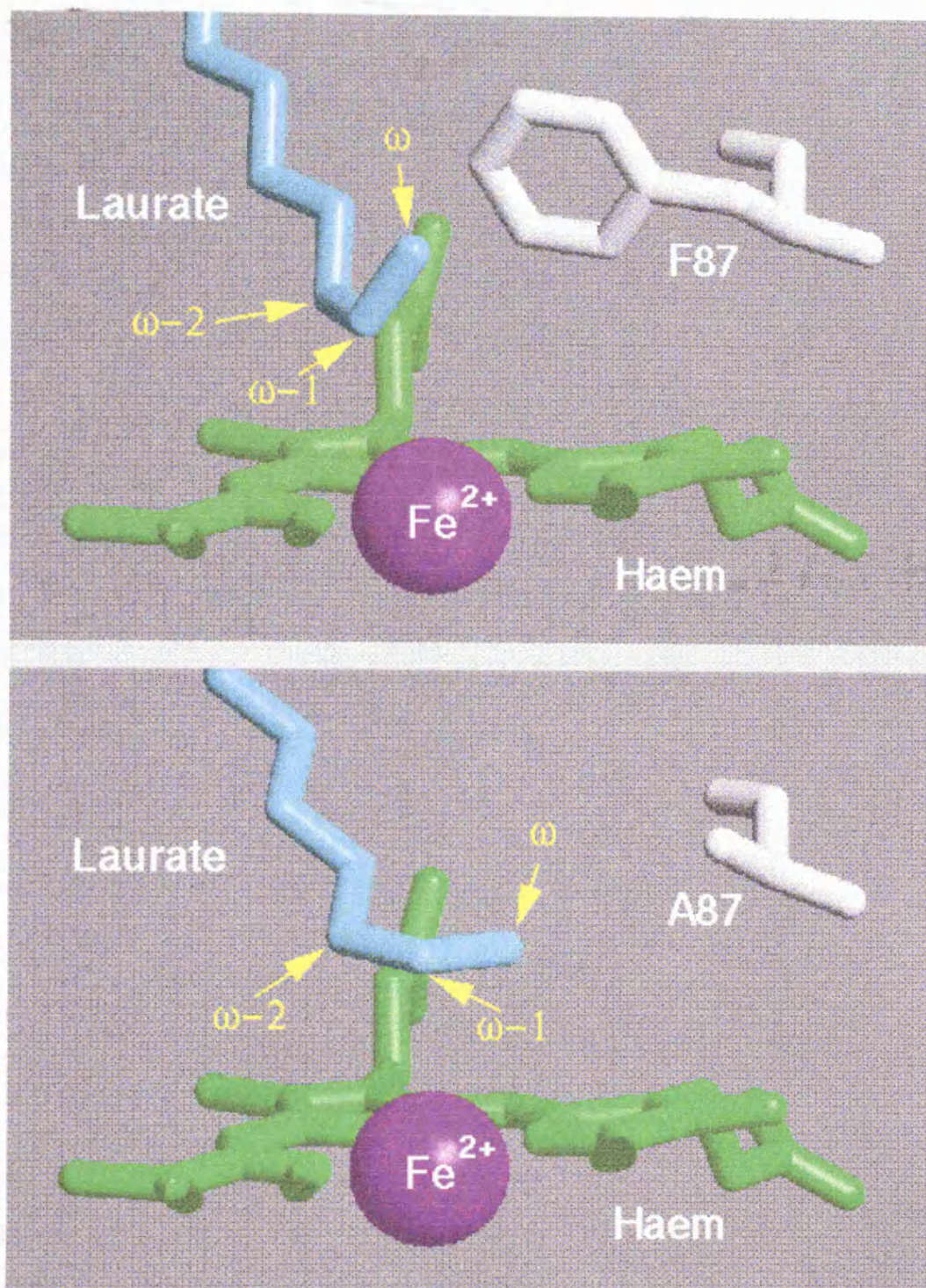


**Figure 6.6:** Model of the binding of laurate to the wild type (top) and F87A mutant (bottom) cytochrome P450 BM3 in the ferrous state of the complex. The substrate was docked into the crystal structure of the haem domain of the enzyme on the basis of iron-proton distance constraints derived from the paramagnetic relaxation experiments (Table 6.3). In the absence of detailed structural information on the ferrous state of the enzyme-substrate complex, these structures should be regarded only as an indication of the position and orientation of the substrate in the binding site of the wild type and mutant enzymes (Oliver *et al.*, 1997).

are in the range of 567-890 $\mu$ M for both the wild type and F87A mutant haem domains in the ferric state, whereas these same proteins have  $K_d$ s in the region of 79-150 $\mu$ M in their ferrous state. The  $K_d$ s for the binding of laurate to the haem domain in the ferrous state are of the same magnitude as the  $K_M$  results depicted in Table 6.2. As such, they support the theory suggested in Modi *et al.*, (1996b) that the  $K_M$  is a reflection of the affinity of the fatty acid substrate for the reduced form of the enzyme as opposed to the low spin, hexacoordinated resting enzyme.

## 6.7 Discussion

The regiospecificity of wild type P450 BM3 is such that it can efficiently catalyse the  $\omega$ -1,  $\omega$ -2 and  $\omega$ -3 of medium chain fatty acids and so it appears that the enzyme catalyses the thermodynamically favoured oxidation of the internal methylene group rather than the terminal methyl group. This is due to the relative strengths of the C-H bonds, which decrease in strength in the order primary > secondary > tertiary with bond energies of 98.0, 94.5 and 91.0 kcal/mol respectively. These indicate that it is thermodynamically more difficult to insert an oxygen into the C-H bond of a terminal methyl group than the adjacent methylene group (Ortiz de Montellano *et al.*, 1992). This is not however the deciding factor, as the regiospecificity is actively determined by the enzyme. For example, substrates having terminal double or triple bonds, which are intrinsically more reactive are hydroxylated by P450 BM3 almost exclusively at the  $\omega$ -2 position with no more than a trace of oxidation of the terminal  $\pi$  bond (Shirane *et al.*, 1993). This led Shirane *et al.* (1993) to suggest that the structure of P450 BM3 actively suppresses oxidation of the terminal carbon atom by sequestering the substrate terminal carbon into a lipophilic pocket at the end of the substrate binding site, such that only the methylene is accessible to the ferryl oxygen at the haem.

Cytochrome P450 BM3 does not terminally hydroxylate fatty acids, in contrast to most other fatty acid hydroxylases which act on the terminal ( $\omega$ ) methyl group of the alkyl chain and usually to a lesser extent on the  $\omega$ -1 position. The  $\omega$ -hydroxylases are historically important as they were the first cytochrome P450 to have been solubilised and partially purified (Lu and Coon, 1968). The genes for several of the  $\omega$ -

hydroxylases have been cloned, including the gene for the Family 4 cytochrome P450 4A1 from rat liver (Hardwick *et al.*, 1987), which represents the best characterised of this family of enzymes. This enzyme is a 58 kDa protein that represents approximately 1-2% of the cytochrome P450 in uninduced rat liver microsomes and 16-30% after induction with clofibrate (CaJacob *et al.*, 1988). Members of the Family 4 P450s, especially P450 4A members such as P450 4A1, and the Family 2 fatty acid  $\omega$ -hydroxylases, including P450 2B1, have overcome the terminal hydroxylation chemical barrier and are known to hydroxylate lauric acid in ratios of 94:6 and 89:11 respectively for  $\omega$ : $\omega$ -1 hydroxylation. They are also capable of catalysing the hydroxylation of other hydrophobic compounds, such as other fatty acids, prostaglandins and leukotrienes in a substrate and regiospecific manner (CaJacob *et al.*, 1988; Alterman *et al.*, 1995).

Despite  $\omega$ -hydroxylation being one of the first catalytic reactions to be linked to microsomal P450's, very little is known as to how the Family 4 P450's can discern fatty acids of different lengths and select only the least reactive end of a long flexible molecule to attack. It was originally thought that the active site consisted of a carboxyl-recognition site located at the opposite end of a hydrophobic channel from the haem moiety where oxygen activation and transfer take place. Here the polar group of the substrate would be anchored such that the  $\omega$  terminal methyl group could reach the oxoiron ferryl moiety more easily than the otherwise more reactive  $\omega$ -1 methylene group (Ellin *et al.*, 1973). This method of substrate orientation has been implicated for a number of proteins that bind fatty acids, including P450 BM3, P450 2C2 and intestinal fatty acid binding protein (Miura and Fulco, 1975; Sacchettini *et al.*, 1989; Fukuda *et al.*, 1994). CaJacob *et al.* (1988) have suggested an alternative hypothesis, where reaction control is exerted by structuring the active site so that only the terminal methyl group can reach the ferryl group of the haem moiety so that  $\omega$ -1 hydroxylation is suppressed. Using P450 4A1 as an example, with substrates of longer carbon chain length than C12 laurate, a small increase in  $\omega$ -1 hydroxylation is observed but as the chain length increases  $\omega$ -2/ $\omega$ -3 hydroxylation never appears and the absolute quantity of  $\omega$ -1 hydroxylation never becomes large (Bambal and Hanzlik, 1996). This indicates that the vicinity of the haem moiety is insufficient to accommodate the extra

methylene groups of >C12 fatty acids and therefore, they are arranged along the region between the polar group recognition site and the ferryl moiety. The factors determining the steric reach of the substrate toward the ferryl-oxygen group as a determinant of hydroxylation regioselectivity were investigated using 11-methylaurate and 11-dimethylaurate as a substrate (Alterman *et al.*, 1995; Bambal and Hanzlik, 1996). These experiments indicated that if steric hindrance is responsible for limiting  $\omega$ -1 hydroxylation of longer fatty acids by P450 4A1, it must be delicately arranged to accommodate the extra bulk presented by these substrates which exhibit only  $\omega$  hydroxylation (Alterman *et al.*, 1995; Bambal and Hanzlik, 1996). Mutagenesis studies by Fukuda *et al.* (1994) to investigate how P450 2E1 and P450 2C2 recognised their fatty acid substrates and selected the position of hydroxylation further confused the issue by suggesting that control of regioselectivity could be due to either substrate interactions or the topology of the active site. Their results indicated that the conserved threonine in each of these proteins plays an important, but different role. In P450 2E1 it was postulated that the  $\gamma$ -methyl group of Thr303 interacts with the substrate in the relatively broad substrate pocket to limit hydroxylation to primarily the  $\omega$ -1 position, whereas that of Thr301 of P450 2C2 works on the substrate to restrict severely its possible movement within the substrate pocket such that  $\omega$ -1 carbon atoms of C9 to C13 fatty acids can be accommodated.

Initial molecular modelling experiments, using the substrate-free crystal structure of the haem domain of P450 BM3, showed that phenylalanine 87, isoleucine 263 and threonine 268 were all capable of making possible contacts with the terminal methyl of a fatty acid substrate (Li and Poulos, 1995). Phe87 resides on a loop between the B' and C  $\alpha$ -helices and its phenyl ring is positioned above the pyrrole C ring and therefore partially blocks access to the haem (Ravichandran *et al.*, 1993). The publication of the substrate-bound complex gave a clearer picture (Li and Poulos, 1997). On binding of the substrate, palmitoleic acid, Phe87 rotates from a position nearly perpendicular to the haem in the substrate-free structure to a more parallel position which more effectively blocks the terminal methyl group from the approach to the haem. The terminal methyl group of the substrate is therefore 'stuck' in the hydrophobic patch formed by Leu75, Leu78, Ile263, Ala264 and Phe87 (Li and Poulos, 1997). This

structure confirmed the hypothesis that the side chain of F87 forms a hydrophobic pocket into which the terminal methyl of the fatty acid substrate is sequestered and thus protected from terminal hydroxylation as suggested by Miura and Fulco (1975) and Ravichandran *et al.* (1993), explaining why P450 BM3 never hydroxylates in the  $\omega$ -terminal methyl group of fatty acid substrates.

The haem domain of P450 BM3 shares little identity with other microbial P450's, at approximately 15%, but is reported to possess 25% identity and 40% similarity in its amino acid sequence to P450 4A1 (Ruettinger *et al.*, 1989) and as such it is considered that the catalytic activities of P450 BM3 are analogous to the numerous mammalian microsomal fatty acid hydroxylases. The sequence alignments published by Hasemann *et al.* (1995) and Lewis (1995) were combined to compare P450 BM3 with the Family 4 cytochromes P450s 4A1, 4A4 and 4A11 to investigate the sequence homology in the region surrounding Phe87 and the results are depicted in Figure 6.7. The previously published sequence alignments (Hasemann *et al.*, 1995; Modi *et al.*, 1996a) and that featured in Figure 6.7 show that most mammalian P450's possess a phenylalanine at the equivalent position to Phe87 in P450 BM3 whereas P450s 2D6 and 3A4 as well as P450s 4A1 4A4 and 4A11 possess sterically smaller hydrophobic residues such as leucine or isoleucine.

	XSS	$\alpha\alpha\alpha$	$\alpha\alpha\alpha\alpha\alpha$
P450 BM3		FAG DGL <b>F</b> TSWTHEKNWK	
P450 4A1		WIGYGL <b>L</b> LLNG	QPWF
P450 4A4		WIGYGL <b>L</b> LLDG	QTWF
P450 4A11		WIGYGL <b>L</b> LLNG	QTWF

**Figure 6.7:** Sequence alignment between P450 BM3 with the Family 4 (CYP4) cytochromes P450s 4A1, 4A4 and 4A11. XSS represents the x-ray crystal structure for the haem domain of P450 BM3 as determined by Ravichandran *et al.* (1993). The sequences displayed for the CYP4 sequences are those that aligned with residue numbers 81 to 97 of P450 BM3. Adapted from Hasemann *et al.* (1995) and Lewis (1995).

Using the atomic coordinates for the substrate-free haem domain of wild type P450 BM3, a model was constructed for the solvent accessible surface at the enzymes substrate access channel (Ravichandran *et al.*, 1993; Figure 6.8a). The aromatic side chain of Phe87 occupies a substantial portion of the access channel volume distal to the haem which markedly reduces accessibility of the substrate to the haem and thus increases substrate binding rigidity. The volume of the substrate binding region appears to be conical in shape, such that its base is facing the opening of the channel at the surface of the molecule with the other end pointing towards the haem iron. A similarly constructed model for the F87A mutant is illustrated in Figure 6.8b. Replacement of the Phe87 with alanine eliminates the steric effects of the aromatic side chain in the vicinity of the haem and increases substrate accessibility to this area. From this depiction it is clearly evident that the F87A mutation results in significant expansion of the volume available for substrate binding near the haem moiety and has little or no effect at the opposite end at the surface opening of the access channel. Comparing the wild type and F87A mutant substrate binding regions, after the F87A substitution this area is approximately cylindrical as opposed to conical in shape. Exactly how this opening is positioned above the pyrrole rings of the haem moiety could be determined by following the formation of aryl iron complexes in the active site of the F87A mutant of P450 BM3 and its haem domain as described by Ortiz de Montellano, (1995b), as there is space above the haem moiety which is capable of accommodating pyridine (Modi *et al.*, 1995b). P450 BM3, with Phe87 located perpendicular to the haem moiety above pyrrole ring C, was shown to be open above pyrrole ring A and to a lesser extent rings B and C (Tuck *et al.*, 1992). This is in contrast to the mammalian P450's which are open above rings A and D. This method has also been successfully used to demonstrate the significant alteration in the active site after mutation of Phe87 to alanine in P450 cam which resulted in an opening above the pyrrole ring D, reducing the proportion of the pyrrole ring D isomer in favour of the pyrrole ring A isomer as opposed to open above pyrrole ring D and partly open above pyrrole ring C (Tuck *et al.*, 1993). These experiments would show if there was any gross change in the active site that may be responsible for the altered binding of the terminal methyl end of the fatty acid substrate. Inspection of the x-ray crystal structure of the substrate-free P450 BM3 suggests that the F87A mutation result in an opening above both pyrrole rings A and C. It would be interesting to compare this

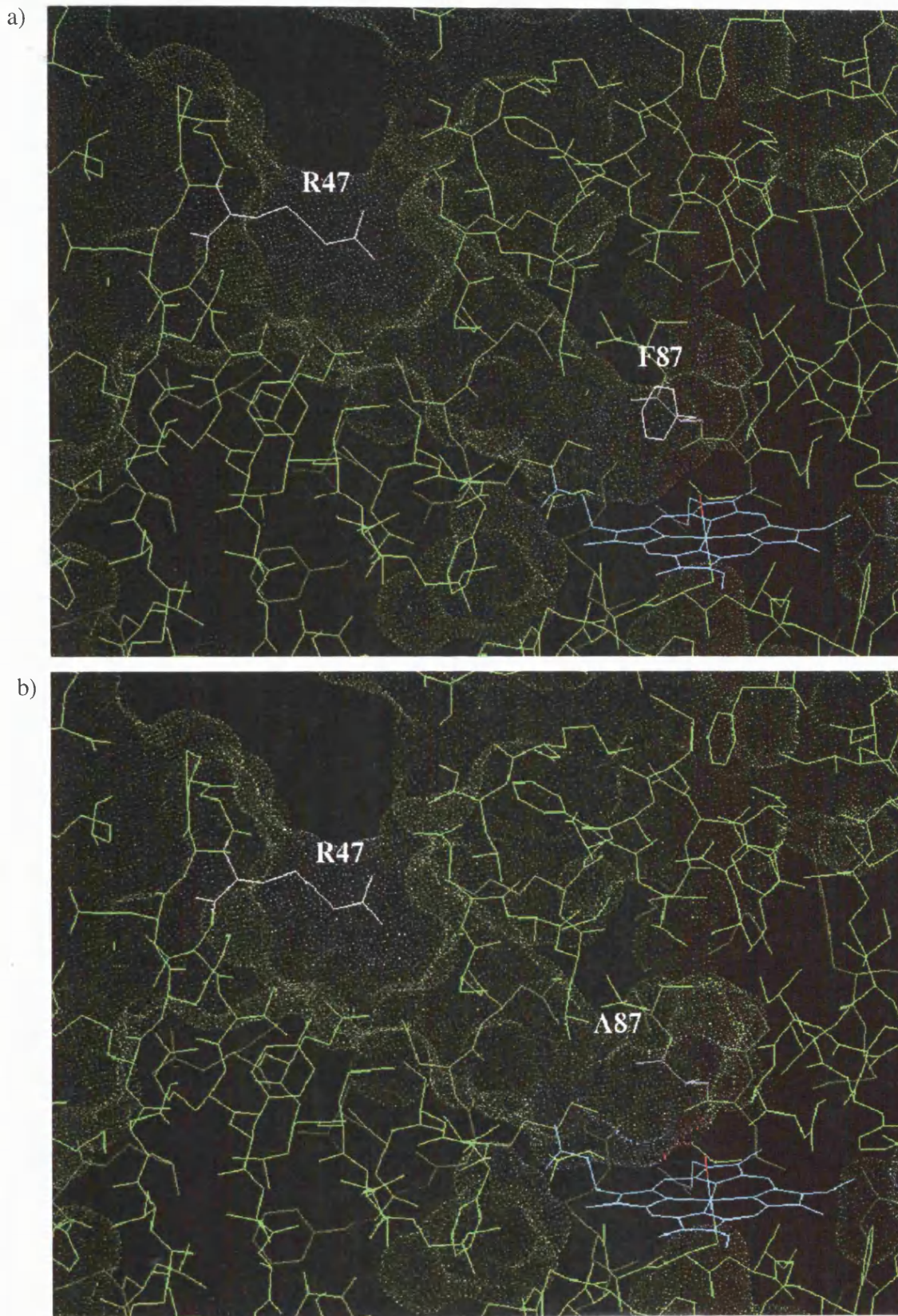


**Figure 6.8:** Solvent accessible surfaces in the substrate binding region of wild type P450 BM3 (a) and its F87A mutant (b). The x-ray structure for the wild type P450 BM3 was used to construct both models (Ravichandran *et al.*, 1993). The residues at positions 47 and 87 have been highlighted in white.

with members of the Family 4 enzymes of which none have as yet been investigated by this method. Use of either this method or x-ray crystallography with the F87A mutant haem domain would be instrumental in determining whether any other residues were implicated in the binding of the terminal methyl of the wild type protein as in the substrate-bound form of the x-ray crystal the terminal methyl is in close proximity to the amino acid side chains of valine 78, leucine 181, isoleucine 263 and alanine 264 (Li and Poulos, 1997).

It is still unclear how a single point mutation can result in the alteration of the regioselectivity as the overall structure of the active site of the protein should remain the same as there has only been a single substitution within the enzyme. Stereo- and regio-selectivity of hydroxylation is achieved by a combination of the protein orientating the substrate such that the correct carbon atom is held close to the highly reactive ferryl atom (Poulos, 1996) and the relative strengths of the C-H bonds within the substrate molecule (Ortiz de Montellano *et al.*, 1992). This suggests that the tertiary structures of the cytochrome P450s are far more conserved than the primary structure as a single point mutation can alter the position on the substrate where the catalytic reaction is performed. The mutagenesis studies on P450 2E1 and P450 2C2 mentioned earlier illustrated a change in the distribution of the hydroxy analogues due to the mutation of the conserved threonine to serine though no alteration in regioselectivity or substrate specificity was observed (Fukuda *et al.*, 1994). Since the 1980's cloning studies showed that some mammalian P450's from the same family differed only by a few amino acids and that mutagenesis of these residues had a profound effect on catalytic activity. Lindberg and Negishi (1989) demonstrated that a single amino acid substitution converted coumarin hydroxylase P450 2A5 to 15 $\alpha$  hydroxylase activity of P450 2A4. Also, full aldosterone synthetic capacity was conferred on the steroid 11 $\beta$ -hydroxylase P450 11B1 enzyme containing the P450 11B2 residues after the serine 288 to glycine and valine 320 to alanine mutations (Curnow *et al.*, 1997). These experiments showed that substitution of a catalytic activity to that of another member of the same cytochrome P450 subfamily was possible, whereas the transformation of P450 BM3 to a  $\omega$ -hydroxylase signifies a conversion to a completely different family of P450 enzymes.

The F87A substitution which would result in an opening up of the substrate binding site close to the haem moiety has very little effect on the overall catalytic efficiency of the enzyme. There is no change in the catalytic activity towards the C12 fatty acid substrate, laurate, which represents the worst substrate for the wild type enzyme as measured by  $k_{\text{cat}}/K_M$  values (Table 6.1). This, together with the comparable results for the substrate proton-iron distances for both the wild type and F87A mutant protein, suggests that the amino acid residue side chain at position 87 plays no part in the orientation or subsequent binding of the substrate. It is likely that this role being fulfilled by the residue side chains at the outer end of the substrate binding pocket in the proximity of Arg47, as in the wild type enzyme. Despite this F87A mutation producing neither gross alteration in substrate specificity or binding, the substitution may have increased the availability of solvent protons in the active site. Raag *et al.* (1991) concluded from analysis of the structures of P450 cam and its T252A variant that the increase in active site solvation was responsible for the uncoupling of the catalytic reaction. A hydrogen peroxide formation assay was therefore performed on this mutant and the results indicate that there was no increase in  $\text{H}_2\text{O}_2$  production indicating that the catalytic reaction in the F87A enzyme was as tightly coupled as in the wild type protein. It therefore seems likely that the role played by Phe87 to facilitate tight coupling between electron transfer, oxygen reduction and activation and hydroxylation of the substrate is a minor one.

The  $K_{\text{d}}$ s obtained for the F87A mutant using optical spectroscopy and NMR relaxation measurements appear to give conflicting results. The former results do not support the hypothesis that the  $K_{\text{d}}$  reflects the binding of the substrate to the enzyme in the ferric oxidised state and the  $K_M$  reflects the binding of the substrate to the enzyme in the ferrous reduced state, as the  $K_{\text{d}}$ s obtained with the F87A mutant most closely resemble the  $K_M$  values. Mutation of phenylalanine to alanine may result in more than one binding conformation for the substrate laurate in the binding site due to the removal of the bulky side chain at position 87. It is possible that with the NMR relaxation measurements for the substrate-iron distances, only the closest approach for the substrate protons to the haem iron are measured and from this single approach the

$K_d$  is determined, whereas for the  $K_d$  determination by optical spectroscopy a sum of binding constants are measured resulting a smaller  $K_d$ . In general terms, the decrease in  $K_d$  for laurate with the F87A mutant suggests the lauric acid now fits the active site uniquely well. These results also show that both proteins in the ferrous state have a reduced affinity with bromolaurate, where binding is approximately 2/3 that of the substrate laurate. This suggests that previous experiments, limited to investigation of the ferric enzyme, were unable to show the effect that the substantial additional bulk of a bromine atom had on substrate binding (Modi *et al.*, 1995a).

In the present case, a point mutation of phenylalanine 87 to alanine has affected the regioselectivity of P450 BM3 by converting the enzyme from one which specifically suppresses hydroxylation at the  $\omega$  position of the fatty acid substrate to one that specifically favours hydroxylation at this chemically less favourable position. The mode of suppression is not entirely clear. The results presented here suggest that the aromatic side chain of Phe87 plays a pivotal role in the sequestration of the  $\omega$ -terminal methyl group thus protecting it from hydroxylation. Graham-Lorence *et al.* (1997) concluded from experiments using a Phe87 to valine mutation that regiospecificity in the hydroxylation of arachidonate and its substrate analogues results predominantly from freedom of longitudinal displacement and not from oxygen chemistries and/or unique binding properties. Either way, the profound change in regioselectivity has not arisen from a simple repositioning of the substrate in the initial enzyme-substrate complex, as the estimated distances between the substrate protons and the haem iron as measured using the paramagnetic relaxation effects on the haem iron suggest that the substrate is bound to the F87A mutant haem domain in an identical manner to that of the wild type protein. The fatty acid substrate adopts an extended conformation with its carboxylate positioned in close proximity to the flexible side chain of arginine 47 (R47) consistent with the suggestion of ion pair formation between the guanidinium group and the substrate carboxylate (Ravichandran *et al.*, 1993). There is a clear difference in substrate orientation in the next, reduced, intermediate, but even in this intermediate, the iron-proton distances, which are essentially equal for the  $\omega$ ,  $\omega-1$  and  $\omega-2$  carbons (Table 6.3 and Figure 6.6), do not explain the observer preference for  $\omega$ -hydroxylation in the mutant. With the F87A mutant P450 BM3 a significant decrease

in the proportion of  $\omega$ -1,  $\omega$ -2 and  $\omega$ -3 hydroxylation is observed, suggesting that these methylenes, as in P450 4A1, must be accommodated close proximity to the ferryl moiety in such a way as to be protected from hydroxylation. Energy minimisation and molecular dynamic simulations of P450 BM3 in the absence of substrate suggest that the active-site cleft can undergo substantial conformational changes (Li and Poulos, 1995; Paulsen and Ornstein, 1995). These conformational changes are thought to be important for enzyme function and the selective nature of substrate binding to P450's may be the primary determinant of regio- and stereo-selectivity (Oguri *et al.*, 1994). The movement of the bound substrate on reduction of the protein (Modi *et al.*, 1996b) provides indirect evidence for a structural change accompanying the transfer of the first electron in the catalytic cycle. The comparison of the substrate position in the reduced F87A enzyme with the observed regiospecificity suggests that, in order to account for the almost exclusive  $\omega$ -hydroxylation, additional structural changes in subsequent steps must be postulated. There appears to be a progressive adaptation of the active site of cytochrome P450 BM3 through the catalytic cycle, which goes beyond the expected accommodation of the changing structure of the haem in successive intermediates, to a series of progressive changes in the position and orientation of the substrate. In this enzyme, and perhaps in others the regiospecificity of catalysis is not simply determined by the geometry of the initial enzyme-substrate complex but a series of structural changes extending through much of the catalytic cycle.

## ***Chapter 7: General Discussion***

Site-directed mutagenesis (SDM) can be used to provide an empirical means of ascertaining which of the differences in amino acid sequence that occur between P450 enzymes contribute to distinct substrate specificities. The rationale for these experiments rests on the idea that only a few of these differences are likely to govern catalytic specificity, and that the structural integration of different residues in related enzymes occurs without disruption of overall topology. In this approach, the selection of the mutations performed was guided by the published x-ray crystal structure for cytochrome P450 BM3 from *Bacillus megaterium*. The aim was to identify amino acid substitutions that would confer the capacity to catalyse a different reaction, either a novel process or that of another known P450 enzyme. Thus the experiments performed were postulated to have a positive end-point. By contrast, many SDM studies have been designed to test the role of specific residues in catalysis selected on the basis of both the structure of the enzyme and existing hypothesis regarding catalytic mechanisms. Often, the impaired function of the mutant for some aspect of catalysis (the negative end-point) is interpreted as confirming a role for the original amino acid side chain in enzyme function. However, inactivation may reflect alternative possibilities (Johnson, 1992).

The molecular basis for the diverse substrate specificities of individual members of the cytochrome P450 superfamily is currently a question of great interest. Using the cytochrome P450 2C family as an example, comparisons of the protein sequences has shown that highly similar P450s exhibit quite different substrate selectivities, whereas enzymes that differ greatly in amino acid sequence can catalyse the same reaction with similar efficiencies. At the same time, these structurally dissimilar enzymes all catalyse the same reaction involving the reduction of molecular oxygen to an oxidant that will readily react with xenobiotics. This suggests that P450 structures can readily accommodate genetic changes in ways that affect substrate metabolism without disrupting the fundamental capacity of P450s to reduce molecular oxygen to a form reactive with a wide variety of organic chemicals (Johnson, 1992; Johnson *et al.*, 1992). Studies with site-directed mutants and hybrid enzymes have yielded important

information regarding the role of individual amino acid residues (Lindberg and Negishi, 1989; Johnson, 1992; He *et al.*, 1992). From these studies it was discovered, unsurprisingly, that within the P450 superfamily the molecular framework is in place such that a single amino acid change can lead to the loss or acquisition of one of several substrate specificities displayed by another P450 enzyme.

Until 1993 no three dimensional structure was reported for the mammalian cytochrome P450s so models were based on the sequence alignments with the bacterial P450 cam (Poulos *et al.*, 1985; Poulos *et al.*, 1987). Modelling studies of the various cytochrome P450s included P450 1A1 (Zvelebil *et al.*, 1991), P450 2C2 (Ramarao and Kemper, 1995) and P450 2D6 (Koymans *et al.*, 1992) used structural information of this enzyme. Models based on the P450 cam are not reliable for a number of fundamental reasons: 1) All the modelled P450s have very low sequence identity (15-20% for the mammalian P450s and less than 25% for the bacterial ones) with the P450 cam sequence. This low level of sequence homology makes it extremely difficult to make reliable sequence alignments, especially at the N-terminal of mammalian enzymes, and without a reliable sequence alignment it is not possible to derive structural information for a target protein. 2) The studies assume that the binding site architecture of P450 cam is conserved. Homology modelling using P450 cam did however reveal putative substrate recognition sites (Zvelebil *et al.*, 1991; Gotoh, 1992) and it is these putative regions which can tolerate great change without disrupting the overall topology of the enzyme. A comparison was made between P450 cam structure and the subsequently determined crystal structures of three other bacterial cytochrome P450s; P450 BM3 (Ravichandran *et al.*, 1993), P450 terp (Hasemann *et al.*, 1994) and P450 eryF (Cupp-Vickery and Poulos, 1995), while also considering a sequence alignment of these isoenzymes (Introduction, Figure 1.7). These results clearly indicate both sequence and spacial variability for the residues in the substrate binding region such that key residues are located on topological elements lacking extensive secondary structure demonstrating that the binding site of any P450 is the most variable region of the protein, so that genetic variation may occur without extensive disruption of the overall topology of the enzyme. It is likely that these features are also conserved in the

mammalian enzymes explaining the catalytic diversity seen for the mammalian enzymes (Johnson, 1992; Cupp-Vickery and Poulos, 1995; Hasemann *et al.*, 1995).

These comparisons also indicate that P450 BM3 appears to be the best template for modelling the mammalian enzymes, as it is the only prokaryotic member of the Class II cytochrome P450s and is known to possess a higher sequence homology to the mammalian enzymes than the other bacterial enzymes. The models of cytochrome P450s using this enzyme as a template are detailed in the Introduction, Section 1.6.4. Some of the models constructed (Amarneh *et al.*, 1993; Lewis, 1995; Lewis and Lake, 1995; de Groot *et al.*, 1996) have already been used to identify residues which potentially reside within the substrate binding site and therefore targeting them for mutagenesis studies. These examples all serve to reiterate that a thorough understanding of the structure function relationship of P450 BM3 is very important when attempting to derive homology models of the mammalian enzymes on the basis of the P450 BM3 structure (Ravichandran *et al.*, 1993).

It is therefore important that the interaction of the substrate with the cytochromes P450 active site be delineated and roles of key amino acid residues in determining the specific activity identified. The work described in this thesis has gone a long way to describe the individual roles of the two residues highlighted by the x-ray crystal structure and demonstrated their importance with regard to substrate orientation and binding. All the changes in catalytic outcome and/or reaction rates reported in this thesis are the consequence of single amino acid replacements: at position 47 (Arg47→Glu mutant; Oliver *et al.*, 1997b and Arg47→Cys mutant), located at the opening of the substrate binding pocket, resulting in a change in substrate specificity and position 87 (Phe87→Ala mutant; Oliver *et al.*, 1997a), in the vicinity of the haem prosthetic group, which demonstrated an alteration in regioselectivity of catalysis. Furthermore, these substitution-dependent changes appear to take place in the absence of major protein and/or active site structural modifications. The results reported here (Oliver *et al.*, 1997a and b) together with recent experiments by others (Lindberg and Negishi, 1989; Johnson, 1992; Johnson *et al.*, 1992; Szklarz *et al.*, 1995; Negishi *et al.*, 1996; Curnow *et al.*, 1997) indicate that substrate selectivity and catalytic outcome can

be critically dependent on the chemical nature of unique residues located in a finite, more or less predictable, area of the protein active site and support the hypothesis that the appropriate combination of substitutions at a few key residues can be used in a predictable fashion to confer new activities on P450 enzymes. Thus, the nature of the reaction products is controlled not simply by the chemical properties of the oxidant species, but by active site binding and the resulting spatial orientation of acceptor bond within the substrate molecule with respect to the haem-bound reactive oxygen. These studies are beginning to provide a molecular description of active site determinants for regio- and stereo-selective metabolism in different P450 isoforms (Negishi *et al.*, 1996). These studies also contribute to a further understanding of the molecular basis of the catalytic versatility of these functionally diverse but structurally homologous proteins.

At the inception of this work, the first question posed on initial consideration of the x-ray crystal structure of P450 BM3 was the importance of the arginyl side chain at position 47 with regard to substrate orientation, substrate binding and subsequent catalytic activity. Arginine residues frequently serve as positively charged recognition sites for negatively charged substrates and anionic cofactors in enzyme active sites (Riordan *et al.*, 1977). For example, the structures of fatty acid binding protein (FABP)-fatty acid complexes (Sacchettini *et al.*, 1989) reveal that in addition to interactions between the fatty acid chain and hydrophobic amino acids, FABP possesses an interior cavity where the negatively charged carboxylate of the fatty acid participates in an electrostatic interaction with the positively charged guanidinium moiety of arginine 106 (Sacchettini *et al.*, 1989; Börchers and Spener, 1993). The role of this arginine (Arg106) was investigated by reciprocal mutagenesis studies using cellular retinol binding protein (CRBP; Cheng *et al.*, 1991; Jakoby *et al.*, 1993). CRBP possesses 31% sequence identity to FABP, does not bind fatty acids and has a glutamine residue in the position corresponding to Arg109 of FABP (Jakoby *et al.*, 1993). These studies (Cheng *et al.*, 1991; Jakoby *et al.*, 1993) indicated that the presence or absence of this key arginine is an important determinant of ligand binding specificity and affinity for these proteins, due to the ion-pair electrostatic interactions (Cheng *et al.*, 1991). The FABP and CRBP reciprocal mutagenesis experiments (Cheng *et al.*, 1991; Jakoby *et al.*, 1993) provide clear parallels with the pattern of

substrate affinity observed here for the wild type P450 BM3 and its R47E and R47C variants. In the x-ray crystal structure of the substrate bound haem domain of P450 BM3 (Li and Poulos, 1997), the guanidinium group of arginine 47 is positioned such that it is capable of forming hydrogen bonds/ion pairs with the fatty acid substrate carboxylate. Substitution of a negatively charged residue at position 47 (R47E mutant) results in a 12.7 fold decrease in  $k_{\text{cat}}/K_M$  for the fatty acid substrates and the effective elimination of any amino acid side chain in the R47C mutant caused the  $k_{\text{cat}}/K_M$  to decrease by 2.7 fold. Both these mutations however still display catalytic activity towards the fatty acid substrates, where the steady state kinetic parameters for laurate (C12),  $k_{\text{cat}}$  remains the same with increases in both the  $K_M$  and  $K_d$ . It therefore appears that like FABP and CRBP, the interaction of the arginyl guanidinium group of the wild type P450 BM3 and the fatty acid carboxylate is involved in fatty acid binding, whereas in the Arg47 mutants, another residue present within the lining of the binding cavity must be instrumental in the binding and subsequent catalytic activity towards this class of substrates. Owing to the conformational differences observed between the substrate-free (Ravichandran *et al.*, 1993) and the substrate-bound (Li and Poulos, 1997) structures of P450 BM3, tyrosine 51 as well as arginine 47 is in a position to form hydrogen bonds/ion pairs with the fatty acid carboxylate (Figure 7.1). The aromatic side chain of this tyrosine residue appears to be well ordered within the crystal structure of the complex and makes a direct hydrogen bond to the carboxylate. This is in contrast to arginine 47 which, as in the substrate-free structure, is still ill-defined. The results obtained from the arginine 47 mutagenesis studies indicate that binding of the fatty acid substrate laurate is decreased approximately 12-fold after the inverse substitution of a positively charged arginine with that of the negatively charged glutamate and the catalytic activity of the R47C mutant suggests that in Arg47 mutants involving the removal of the charged side chain will result in a smaller decrease in fatty acid binding. This implies that the overall contribution of the guanidinium group to the overall binding energy, through for example electrostatic interactions, must be relatively small and that other forces such as hydrophobic interactions must play a larger role. These results confirm the hypothesis by Li and Poulos (1997) that, while the arginine 47-substrate interactions may be important for the orientation of the substrate within the substrate binding pocket, these interactions are likely to be flexible,

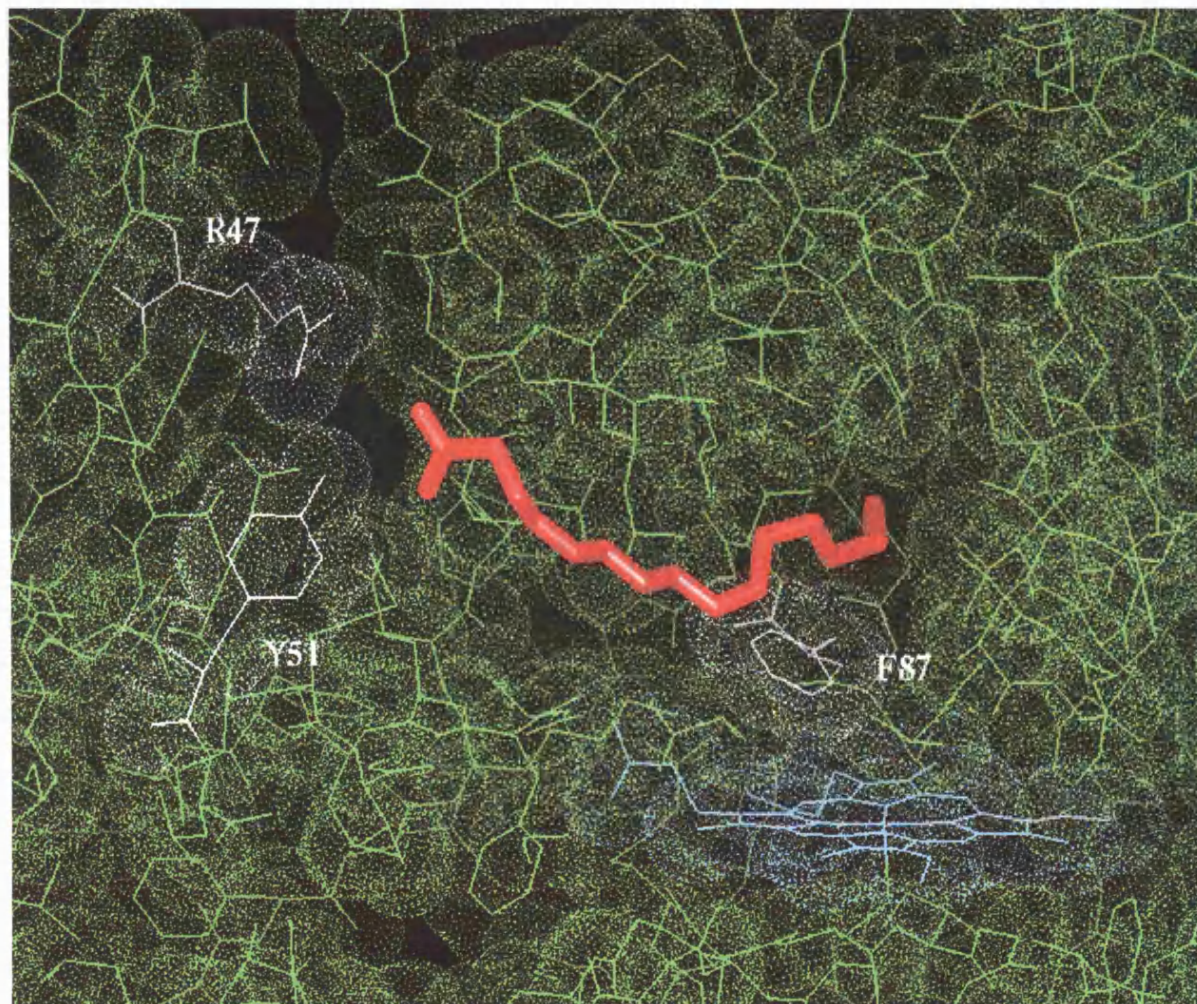


**Figure 7.1:** Van der Waals surface of the substrate binding pocket of the haem domain of P450 BM3 from *Bacillus megaterium* in the presence of the bound substrate, palmitoleic acid (Li and Poulos, 1997). The residue side chains for arginine 47, tyrosine 51 and phenylalanine 87 have been highlighted.

transient and not very critical for substrate binding.

The work on the F87A mutant P450 BM3 presented in this thesis confirm the absolute requirement for the aromatic side chain of phenylalanine at position 87 for the prevention of terminal methyl hydroxylation (Oliver *et al.*, 1997), though the relative chemical reactivity of the internal methylene C-H bond versus the terminal methyl C-H bond may also play an important role. Energy minimisation studies (Capdevila *et al.*, 1996) and the later x-ray crystal structure of the substrate-bound enzyme (Li and Poulos, 1997) indicate that phenylalanine 87 rotates from a position near the perpendicular to the haem in the substrate-free structure (Ravichandran *et al.*, 1993) to a more parallel position in the substrate-complex (Introduction, Figure 1.10). The substrate terminal methyl group is therefore stuck in a hydrophobic patch formed by leucine 75, leucine 78, isoleucine 263, alanine 264 and phenylalanine 87 (Li and Poulos, 1997). This is discussed in more detail in Chapter 6. Considering all the data presented involving the broad substrate specificity and regioselectivity of the wild type P450 BM3 and its mutants implies that the active site of this enzyme is quite flexible.

A wide range of experimental techniques, as detailed in Chapter 2 and the successive results chapters, have already been used to obtain an understanding of the roles of the individual residues within the substrate binding pocket of P450 BM3. Future work could involve either these methods, applied to produce further information from the wild type and existing mutant enzymes, or introducing novel substitutions and procedures. First, let us consider arginine 47 and the mutants pertaining to it. A simple, though crude experiment to investigate the importance of the presence of an arginyl guanidinium group would be chemical modification using butandione in the presence of 50mM borate, which is known to be specific for this residue (Figure 7.2; Means and Feeney, 1971; Riordan *et al.*, 1977), which could immediately demonstrate any contribution to catalytic function. The usefulness of this experiment is limited as it is known that arginine residues are present on the surface of the haem domain and so would therefore be susceptible to any chemical modification. It would also be essential to perform this reaction in the dark as this reagent has been implicated in the photo-catalysed destruction of amino acids and photooxidation of anionic cofactors such as

NADH and NADPH (Riog and Kennedy, 1992). Under these circumstances, site-directed mutagenesis offers far more possibilities. Substitution of arginine 47 with amino acids that possess bulky side chains, such as phenylalanine, tryptophan and tyrosine could be performed to investigate the accessibility of the substrate binding pocket. The incorporated aromatic side chain could either act as 'hinged lid' within the substrate access channel or may completely inhibit substrate binding through steric hindrance. An arginine 47 to tyrosine substitution may also augment binding of negatively charge substrates in comparison to the R47C mutant. The combined results from site-directed mutagenesis, to phenylalanine, tyrosine or tryptophan representing the three largest side amino acid side chains, and chemical modification experiments could provide information as to the limitations of the substrate binding pocket, in that what size of residue located at the opening of the substrate binding pocket is necessary to allow binding?

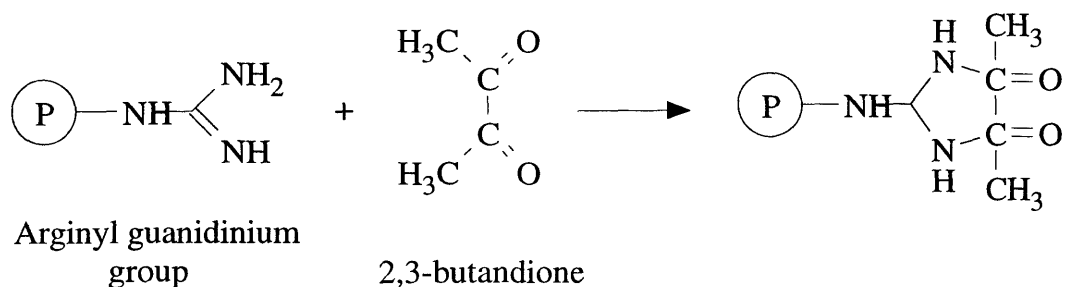


**Figure 7.2:** Chemical reaction of the guanidinium group with the chemical modifying agent, 2,3-butanedione, where P represents the remainder of the protein molecule.

The startling conclusion from Chapter 6 is that the single mutation from phenylalanine 87 to alanine resulted in a dramatic change in regioselectivity of the hydroxylation reaction. Thus, this substituted P450 BM3 protein now performs the catalytic reaction in a similar, if not identical manner to Family 4 cytochrome P450s. The Class II mammalian enzymes are rarely available in large quantities as there are difficulties in heterologous expression in either bacterial or insect cells of the intact protein, and so it may be advantageous to use this complete, soluble, bacterial mutant protein to investigate the as yet, unknown requirements for the terminal hydroxylation reaction. This mutant P450 BM3 may not be sufficiently similar to the Family 4 enzymes to act

as a complete model, and as such may need further refinement. If this expression system is to be used in such a capacity, it will be necessary to replicate experiments that have previously used the wild type P450 BM3, as well as those already performed on proteins that catalyse this highly specific reaction. Unsaturated fatty acids, such as 11-dodecenoic acid, 12-tridecenoic acid and 10-undecynoic acid, can be used to further study regioselectivity and the consequences of that specificity by the mechanism based inactivation of the enzyme (CaJacob *et al.*, 1988; Shirane *et al.*, 1993). Terminal hydroxylation of terminal acetylenes can result in inactivation of the P450 enzyme due to N-alkylation of the haem moiety (Figure 7.3; CaJacob *et al.*, 1988).

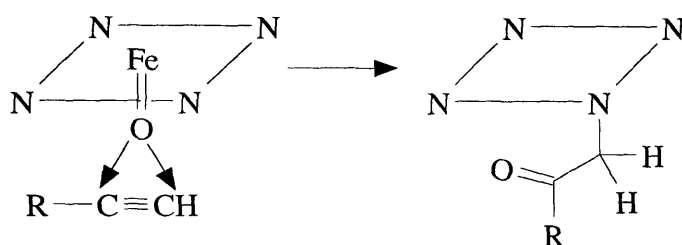


**Figure 7.3:** Inactivation of P450 enzymes by N-alkylation using terminal acetylenes. Adapted from CaJacob *et al.* (1988).

Alternative substrates could include the following compounds: 11-methylaurate and 11-dimethylaurate to ascertain whether the enlarged F87A mutant active site can accommodate steric bulk and monitor the degree of freedom of the terminal methyl groups (Alterman *et al.*, 1995; Bambal and Hanzlik, 1996), 10-dodecenoic acid, a substrate with increased molecular rigidity and 9-phenylnonanoic acid to investigate whether compounds possessing a bulky  $\omega$ -terminal group are susceptible to hydroxylation (Bambal and Hanzlik, 1996). Work has already been initiated using the 11-phenoxyundecanoic acid, which has been discovered to be a substrate for P450 BM3 (A. N. J. Shaw, Unpublished results). Further studies could incorporate laurate analogues that contain a rigid phenylene unit at various points along the chain to investigate bulk and rigidity in the midsection of the substrate (Bambal and Hanzlik, 1996). Longer chain substrate derivatives, of at least 15 carbon atoms which are preferentially hydroxylated at the  $\omega$ -2 by the wild type P450 BM3 as opposed to the  $\omega$ -1 position for C12-C13, must also be used to determine whether regioselectivity is

governed by steric constraints of the protein at the active site or by steric reach controlled by the interactions of the substrate carboxylate. Using the sequence alignment depicted in Chapter 6; Figure 6.7, other Phe87 mutants containing either valine, leucine or isoleucine at this position could be prepared to investigate the tolerance of terminal hydroxylation to increased steric bulk in the immediate vicinity of the active site.

The most unexpected discovery was that arginine 47 is ultimately not that important for catalytic activity and that it is likely that tyrosine 51 plays a far more important role. Either site-directed mutagenesis or chemical modification can be used to investigate the contribution of this residue to the hydroxylation reaction. If chemical modification is to be performed, using for example the acylating reagent N-acetylimidazole, the appropriate control experiments must be performed as tyrosyl side chains are known to be exposed on the surface of the haem domain of P450 BM3. The obvious substitution would be tyrosine 51 to phenylalanine (Y51F) as this removes the ionisable group, while almost maintaining the volume of this aromatic side chain. Investigations should include this single mutant as well as double mutants with arginine 47. Using the Arg47 mutants generated for this thesis, a Y51F R47C double mutant would determine the role of Tyr51 with regard to fatty acid binding and its subsequent hydroxylase activity. Whereas a Y51F R47E double mutant may show an increase in catalytic activity towards the trimethylammonium compounds due to the effective removal of any potential negative interactions between the tyrosyl side chain and the trimethylammonium group. Trypsinolysis studies of P450 BM3 (Narhi and Fulco, 1987) indicated additional cleavage sites at lysine 10 and lysine 16 as well as the lysine 472. It has been postulated that the former lysines are an essential component of a substrate recognition or docking site as removal of these residues disrupted substrate binding (Narhi and Fulco, 1987). Again, site-directed mutagenesis would be extremely useful in determining the contribution to substrate binding of these residues. Substitution could involve either hydrophobic residues to eliminate any electrostatic interaction or negatively charged residues to enhance binding of positively charged substrates, both of which are of interest with the R47E mutation.

Finally, mutagenesis could also be used for the site-specific incorporation of unnatural amino acids, as discussed in Chapter 5, at positions 47, 51 and 87 of P450 BM3- the residues of interest with regard substrate binding. The effect of different functional groups incorporated either onto by chemical modification or instead of the existing amino acid side chains using synthesised unnatural amino acids could provide valuable insights into the structure function relationship of this family of proteins.

In conclusion, the site-directed mutagenesis experiments on residues arginine 47 and phenylalanine 87 of cytochrome P450 BM3 from *Bacillus megaterium* suggest that this cytochrome provides an excellent model to further investigate geometrical topologies and functional roles of these and other key residues within the substrate binding pocket and active site. The results indicate that the pocket structure of this P450 is geometrically flexible and can be altered by single amino acid mutations at key positions so as to properly accommodate various molecules, consequently this enzyme exhibit versatility in its activity. These experiments provide further information essential to the overall understanding of the underlying principles that regulate this flexible pocket and will provide ways to predict the metabolism by other P450s of environmental chemicals and to assess human susceptibility to them as well as increasing the researchers ability to 'tailor' the catalytic activity of this and other cytochrome P450s for such applications as organic synthesis and bioremediation.

## ***Appendix***

All solutions, when possible, were made using double distilled water (EM water) provided by an Elga Ltd. Maxima Ultra Pure Water system.

### ***A1 Reagent Solutions***

**Agarose Gels for DNA analysis.** All DNA agarose gels consisted of a 1% agarose solution containing sufficient 10mg/mL ethidium bromide to give a final concentration of 1µg/mL.

**Affinity Buffer (10x Stock Solution).** 20.882g dipotassium hydrogen orthophosphate, 1.157g potassium dihydrogen orthophosphate, 1.566g benzamidine HCl, 0.309g DTT and 0.058g EDTA were diluted to 1 litre with EM water. 100mL of stock solution was diluted to 1 litre and 3mL 20mg/mL PMSF added to give a solution containing 10mM potassium phosphate at pH 7.7, 1mM benzamidine HCl, 0.2mM DTT, 0.02mM EDTA and 60µg/mL PMSF.

**Affinity Buffer High Salt (2x Stock Solution).** 83.529g dipotassium hydrogen orthophosphate, 4.627g potassium dihydrogen orthophosphate, 0.313g benzamidine HCl, 0.062g DTT and 0.234g EDTA were diluted to 1 litre with EM water. 100mL of stock solution was diluted to 1 litre and 3mL 20mg/mL PMSF added to give a solution containing 200mM potassium phosphate at pH 7.7, 1mM benzamidine HCl, 0.2mM DTT, 0.4mM EDTA and 60µg/mL PMSF.

**50 mg/mL Ampicillin Stock Solution.** A 50mg/mL solution of Ampicillin in water was prepared followed by filter sterilisation using a 0.2µm Acrodisc®. The solution was stored at -20°C as 1mL aliquots and used in a working concentration of 50µg/mL.

**Bacteriophage T4 Polynucleotide Kinase Buffer (10x).** 0.5M Tris.HCl (pH 7.6), 0.1M Magnesium chloride (MgCl<sub>2</sub>), 50mM DTT, 1mM spermidine HCl, and 1mM

EDTA (pH 8.0). The solution was filter sterilised using a 0.2µm Acrodisc© and stored at -20°C.

**Bradford Assay Reagent.** 100mg Coomassie Brilliant Blue G250 and 50mL ethanol were mixed thoroughly. 100mL 85% phosphoric acid was added with the resulting solution diluted to 1 litre with EM water. After thorough mixing the solution was filtered through Whatman Filter paper to remove any insoluble matter.

**Buffer A (10x Stock Solution).** 60.55g Tris base, 1.566g benzamidine HCl, 0.309g DTT and 2.922g EDTA were diluted to 1 litre with EM water and the pH corrected to 7.5 using concentrated HCl. 100mL of stock solution was diluted to 1 litre and 3mL 20mg/mL PMSF added to give a solution containing 50mM Tris HCl, 1mM benzamidine HCl, 0.2mM DTT, 1mM EDTA and 60µg/mL PMSF.

**Buffer HA (10x Stock Solution).** 21.396g dipotassium hydrogen orthophosphate trihydrate, 21.264g potassium dihydrogen orthophosphate, 1.566g benzamidine HCl and 0.309g DTT were diluted to 1 litre with EM water. 100mL of stock solution was diluted to 1 litre and 3mL 20mg/mL PMSF added to give a solution containing 25mM potassium phosphate at pH 6.5, 1mM benzamidine HCl, 0.2mM DTT and 60µg/mL PMSF.

**Buffer HA High Salt.** 38.512g dipotassium hydrogen orthophosphate trihydrate, 38.275g potassium dihydrogen orthophosphate, 0.157g benzamidine HCl and 0.031g DTT were diluted to 1 litre with EM water. This gave a solution containing 450mM potassium phosphate at pH 6.5, 1mM benzamidine HCl, 0.2mM DTT and 60µg/mL PMSF.

**Buffer P1 (Resuspension Buffer) for Qiagen-tip 20.** 6.055g Tris base, 3.722g EDTA was dissolved in 800mL EM water and the pH adjusted to pH 8.0 with HCl. The solution was sterilised by autoclaving at 15 psi for 20 minutes. When sufficiently cool, 10mL of sterile 10mg/mL RNase A was aseptically added to give a final concentration of 50mM Tris/HCl, 10mM EDTA and 100µg/mL RNase A and the solution stored at 4°C.

**Buffer P2 (Lysis Buffer) for Qiagen-tip 20.** 8.0g NaOH pellets were dissolved in 950mL EM water and 50mL 20% SDS solution added to give a final concentration of 0.2M NaOH and 1% SDS. The solution was sterilised by autoclaving at 15 psi for 20 minutes.

**Buffer P3 (Neutralisation Buffer) for Qiagen-tip 20.** 294.45g potassium acetate was dissolved in 500mL EM water and the pH adjusted to pH 5.5 with glacial acetic acid before increasing the volume to 1L to give a final concentration of 3M potassium acetate. The solution was sterilised by autoclaving at 15 psi for 20 minutes and stored at 4°C.

**Buffer QBT (Equilibration Buffer) for Qiagen-tip 20.** 43.83g sodium chloride and 10.46g MOPS (free acid) were dissolved in 800mL EM water. The pH was adjusted to pH 7.0 and 15mL Triton X-100 added and the volume increased to 850mL. The solution was sterilised by autoclaving at 15 psi for 20 minutes. When sufficiently cool, 150mL of absolute ethanol was added to give a final concentration of 0.75M NaCl, 50mM MOPS, 15% ethanol and 0.15% Triton X-100.

**Buffer QC (Wash Buffer) for Qiagen-tip 20.** 58.44g NaCl and 10.46g MOPS (free acid) were dissolved in 800mL and the pH adjusted to pH 7.0. The volume was increased to 850mL and the solution sterilised by autoclaving at 15 psi for 20 minutes. When sufficiently cool, 150mL of absolute ethanol was added to give a final concentration of 1M NaCl, 50mM MOPS and 15% ethanol.

**Buffer QF (Elution Buffer) for Qiagen-tip 20.** 73.05g NaCl and 6.055g Tris base were dissolved in 800mL and the pH adjusted to pH 8.5. The volume was increased to 850mL and the solution sterilised by autoclaving at 15 psi for 20 minutes. When sufficiently cool, 150mL of absolute ethanol was added to give a final concentration of 1.25M NaCl, 50mM Tris/HCl and 15% ethanol.

**Butanol-Saturated Water.** 200mL EM water and 50mL butanol were mixed together thoroughly and stored at room temperature.

**50mM Calcium Chloride Solution.** 0.147g calcium chloride ( $\text{CaCl}_2 \cdot 2\text{H}_2\text{O}$ ) was added to 20 mL EM water. The solution was filter sterilised using a 0.2 $\mu\text{m}$  Acrodisc<sup>®</sup> and stored at -20°C.

**Cell Lysis Solution for Promega Magic Minipreps<sup>™</sup>.** 0.2M sodium hydroxide (NaOH) with 1% SDS. The solution was sterilised by autoclaving at 15 psi for 20 minutes.

**Cell Resuspension Solution for Promega Magic Minipreps<sup>™</sup>.** 50mM Tris.HCl and 10mM EDTA with 100 $\mu\text{g}/\text{mL}$  RNase A. The solution was filter sterilised using a 0.2 $\mu\text{m}$  Acrodisc<sup>®</sup> and stored at -20°C.

**24:1 Chloroform:Iso-amyl Alcohol.** 4mL iso-amyl alcohol was added to 96mL chloroform and the solution mixed thoroughly before storing at room temperature.

**Column Wash Solution for Promega Magic Minipreps<sup>™</sup>.** 40mM Tris.HCl, pH 7.5, 10mM EDTA pH 7.5, 0.4M NaCl made up to 500mL with EM water. After sterilising by autoclaving at 15 psi for 20 minutes, 500mL absolute ethanol was added. This resulted in a solution containing 20mM Tris.HCl, pH 7.5, 5mM EDTA pH 7.5 and 0.2mM NaCl with 50% v/v absolute ethanol.

**Deuterated 0.1M Phosphate Buffer, pH 8 for Nmr Spectroscopy.** 0.269g anhydrous disodium hydrogen orthophosphate and 0.0144g anhydrous potassium dihydrogen orthophosphate was made up to 20mL with 99.96% deuterium oxide. The pH was monitored (the meter reading not being corrected for isotope effects on the glass electrode) and corrected to pH 8 with either deuterated hydrochloric acid or sodium hydroxide.

**3mM Dithionitrobenzoate (Ellman's Reagent).** 11.889mg DTNB was made up to 10mL with 0.1M phosphate buffer, pH8.

**DNA Molecular Weight Markers.** A solution of DNA molecular weight markers

was purchased from Sigma Chemical Co. consisting of DNA fragments from a *Hind* III restriction enzyme digest of lambda phage DNA. The DNA fragment sizes were 23.0, 9.4, 6.6, 4.4, 2.3, 2.2 and 0.6 kbp.

**DNA Stop Dye.** 100mM Tris HCl (pH 8.0), 1mM EDTA, 40% sucrose and 0.05% bromophenol blue.

**Destain Solution for Coomassie Blue Staining of SDS-PAGE gels.** 100mL glacial acetic acid and 400mL methanol made up to 1L with distilled water.

**Enzyme Assay Buffer.** 473.5mL of 0.2M disodium hydrogen orthophosphate, 26.5mL of 0.2M potassium dihydrogen orthophosphate, 0.157g benzamidine HCl, 14 $\mu$ L  $\beta$ -mercaptoethanol and 3mL of 20mg/mL PMSF solution were made up to 1L with EM water.

**10mM Ferrous Ammonium Sulphate (Ammonium Iron (II) Sulphate Hexahydrate).** 196.1mg of the solid is made up to 50mL with degassed EM water. Cover the container with foil as light sensitive. This solution has to be made up freshly each time it is used.

**FPLC Buffer (10x Stock Solution).** 24.22g Tris base, 1.566g benzamidine HCl, 0.309g DTT and 2.922g EDTA were diluted to 1 litre with EM water and the pH corrected to 7.5 using concentrated HCl. 100mL of stock solution was diluted to 1 litre and 3mL 20mg/mL PMSF added to give a solution containing 20mM Tris HCl, 1mM benzamidine HCl, 0.2mM DTT, 1mM EDTA and 60 $\mu$ g/mL PMSF.

**4M Guanidine Hydrochloride/400mM Acetic Acid Solution for the Peroxide Assay.** A 6M stock solution of guanidine hydrochloride was prepared by adding 11.464g to 20mL of degassed EM water. At the same time, a 2M stock solution of acetic acid is prepared by making up 5.724mL glacial acetic acid to 50mL total volume with degassed EM water. The final solution is prepared by combining 6.667mL of the 6M guanidine hydrochloride, 2mL a 2M acetic acid with 1.333mL degassed EM water.

This solution is stable over a number of weeks.

**6M Guanidine Hydrochloride in 0.1M Phosphate Buffer for DTNB Assay.**

11.464g guanidine hydrochloride was added to 0.1M phosphate buffer, pH 8 and made up to a final volume of 20mL.

**1mM Hydrogen Peroxide Standard Solution.** This solution was prepared freshly by serial dilution. Three 30mL containers were cooled on ice. To each of these 19mL degassed EM water was added. 1mL of the 8.1M stock solution hydrogen peroxide was added to one container and mixed by pipeting. 1mL of this solution was transferred to the next container and mixed before 1mL of the resulting solution was transferred to the final container. The final solution was 1mM and was stored on ice.

**0.2M  $\beta$ -D-isopropyl-thiogalactopyranoside (IPTG) Stock Solution.** 1g of IPTG was dissolved in 21mL of EM water, filter sterilised using a 0.2 $\mu$ m Acrodisc<sup>®</sup> and stored at -20°C.

**PAGE Protein Sample Loading Buffer.** 125mM Tris (pH 6.8), 4% SDS, 20% glycerol, 10%  $\beta$ -mercaptoethanol and 0.01% w/v bromophenol blue.

**Polyethylene Glycol/Sodium Chloride (PEG/NaCl) Solution.** 20% PEG 6000 with 2.5M NaCl in EM water. The solution was filter sterilised using a 0.2 $\mu$ m Acrodisc<sup>®</sup> and stored at -20°C.

**68:31:1 Phenol:Water:Chloroform PCR Sequencing Solution.** 31mL chloroform and 1mL EM water were added to 68mL redistilled phenol. The resulting solution was thoroughly mixed and stored at 4°C.

**Phenol:0.1M Tris.HCl (pH 8.0) Buffer.** 50mL 0.1M Tris HCl at pH 8.0 was added to 50mL redistilled phenol and mixed thoroughly. The solution was stored at 4°C.

**Potassium Acetate Solutions.** The appropriate quantity of potassium acetate (MW

98.14) for solutions of either 3M or 2.55M was weighed out and dissolved in 50mL EM water. The solution was adjusted to the appropriate pH with glacial acetic acid and the volume increased to 100mL with EM water, before being sterilised by autoclaving at 15 psi for 20 minutes.

**2.5M Potassium Thiocyanate.** 4.859g of potassium thiocyanate is added to 20mL degassed EM water.

**20mg/mL PMSF Solution.** 1g PMSF was added to 50mL iso-propanol, mixed thoroughly and stored at -20°C.

**Protein High Molecular Weight Markers for SDS-PAGE.** A mixture of protein high molecular weight markers was purchased from Sigma Chemical Co., containing proteins of 29000 (carbonic anhydrase), 45000 (egg albumin), 66000 (bovine albumin), 97400 (phosphorylase b), 116000 ( $\beta$ -galactosidase) and 205000 (myosin) Daltons in weight. For use on SDS-PAGE gels, the solution was reconstituted using 1.5mL of 62mM Tris buffer at pH 6.8 containing 10% glycerol, 2% SDS, 5%  $\beta$ -mercaptoethanol and 0.001% bromophenol blue and stored at -20°C. Immediately prior to electrophoresis, the solution was thawed and incubated at 100°C for 5 minute.

**Protogel™ Acrylamide/Bisacrylamide (37:5:1) Stock Solution.** An acrylamide/bisacrylamide stock solution was purchased from Flowgen Instruments Ltd. containing 30% (w/v) acrylamide and 0.8% (w/v) bisacrylamide and was of protein and sequencing grade.

**10mg/mL RNase A (DNase free) Solution.** RNase A type I-A from Sigma Chemical Co. was dissolved in EM water to a final concentration of 10mg/mL. The solution was heated to 100°C for 15 minutes to denature any DNase present and allowed to cool to room temperature. The solution was stored in 1mL aliquots at -20°C.

**SDS-PAGE Gels: 8% Separating Gel.** The 8% separating gel monomer solution was prepared by adding together 3.78mL EM water, 2mL 1.5M Tris HCl at pH 8.8, 80 $\mu$ l

10% SDS, 2.13mL 37.5:1 acrylamide/bis solution, 8 $\mu$ L TEMED and 40 $\mu$ L 10% ammonium persulphate. The gel solution was thoroughly mixed and 3 mL used for the lower gel. After pipetting, the gel solution was overlaid with butanol-saturated water to prevent gel dehydration.

**3% Stacking Gel.** The 3% stacking gel monomer solution was prepared by adding together 2.35mL EM water, 1mL 0.5M Tris HCl at pH 6.8, 40 $\mu$ L 10% SDS, 0.52mL 37.5:1 acrylamide/bis solution, 8 $\mu$ L TEMED and 20 $\mu$ L 10% ammonium persulphate. The gel solution was thoroughly mixed and sufficient solution used to fill between the glass plates, surrounding the positioned sample comb.

**SDS-PAGE Running Buffer (10x).** 30g Tris base, 144g glycine and 10g SDS were added to 1 litre EM water.

**3M Sodium Acetate Solution (pH 4.8).** 40.81g sodium acetate was added to 50mL EM water. The solution was adjusted to pH 4.8 with glacial acetic acid before increasing the volume to 100mL. The solution was sterilised by autoclaving at 15 psi for 20 minutes.

**Stain Solution for Coomassie Blue Staining of SDS-PAGE Gels.** 2.5g Brilliant Blue R, 100mL glacial acetic acid and 400mL methanol made up to 1L with distilled water.

**STE (Sodium chloride-Tris-EDTA) Buffer.** 5.844g sodium chloride, 1.211g Tris base and 372.2mg EDTA were dissolved in 800mL EM water. The pH was adjusted to pH 8.0 with HCl and the volume increased to 1L. The solution was sterilised by autoclaving at 15 psi for 20 minutes.

**TAE (Tris-acetate-EDTA) DNA Electrophoresis Buffer (50x).** 242g Tris base, 57.1mL glacial acetic acid and 100mL of 0.5M EDTA (pH 8.0) were diluted to 1L with EM water and stored at room temperature.

**TE (Tris-EDTA) Buffer.** A solution of 10mM Tris.HCl (pH 8.0) and 1mM EDTA was prepared from stock solutions and sterilised by autoclaving at 15 psi for 20 minutes.

**Transformation Buffer 1.** 12g rubidium chloride, 9.9g manganese chloride, 30mL of 1M potassium acetate at pH 7.5, 1.5g calcium chloride and 150g glycerol were made up to 1L with EM water, adjusted to pH 5.8 using 0.2M acetic acid and filter sterilised using a 0.2µm Acrodisc© and stored at 4°C.

**Transformation Buffer 2.** 20mL of 0.5M MOPS pH 6.8, 1.2g rubidium chloride, 11.0g calcium chloride and 150g glycerol were made up to 1L with EM water, adjusted to pH 6.8 using 5M NaOH and filter sterilised using a 0.2µm Acrodisc© and stored at 4°C.

**Tris Buffer Stock Solutions.** 1M Tris stock solutions, at pH 7.5 and 8.0, were produced by adding 60.55g Tris base (MW 121.1) to 400mL EM water, adjusting to the required pH with HCl and then adding sufficient EM water to a final volume of 500mL. All Tris solutions were sterilised by autoclaving at 15 psi for 20 minutes.

**TSS Solution for Competent Cell Formation.** Solid PEG (MW 3350-8000) was added to LB media to make a final concentration of 10% (w/v). An aliquot of 2M magnesium (either the chloride or sulphate salt) was added to achieve a final concentration of 20-50mM. The pH was adjusted to between 6.5-6.8. The solution was filter sterilised using a 0.2µm Acrodisc© and stored in 3.8mL aliquots at -20°C. Immediately prior to use 0.2mL DMSO is added to achieve a final concentration of 5%.

**2% 5-bromo-4-chloro-3-indolyl-β-galactopyranoside (X-Gal).** 20mg X-Gal was dissolved in 1mL dimethylformamide (DMF). The solution was covered with foil and stored at -20°C.

### ***A2 Growth Media***

**H Top Agar.** 2g bactotrytone , 1.6g NaCl and 1.6g agar were made to 200mL with EM water. The solution was sterilised by autoclaving at 15 psi for 20 minutes. After sterilising, the solution was stored at 50°C until required to ensure the agar stayed molten.

**LB Broth.** 10g bactotryptone, 5g yeast extract and 10g NaCl were made up to 1L with EM water, adjusted to pH 7.5 using either HCl or 5M NaOH as required and sterilised by autoclaving at 15 psi for 20 minutes.

**LB Agar.** 10g bactotryptone, 5g yeast extract and 10g NaCl were made up to 1L with EM water and adjusted to pH 7.5 using either HCl or 5M NaOH as required. 15g agar was added and the solution sterilised by autoclaving at 15 psi for 20 minutes. When the solution had cooled to below 50°C, plates were poured using sterile petri dishes. After setting, the plates were stored at 4°C.

**Minimal Media Broth (M9).** 6g Na<sub>2</sub>HPO<sub>4</sub>, 3g potassium dihydrogen orthophosphate (KH<sub>2</sub>PO<sub>4</sub>) 0.5g NaCl and 1g ammonium chloride (NH<sub>4</sub>Cl) were made to 1L with EM water and the pH adjusted to 7.4 before sterilising the solution by autoclaving at 15 psi for 20 minutes. When the solution had cooled the following sterile solutions were added aseptically in the specified volumes: 1M magnesium sulphate (MgSO<sub>4</sub>), 1mL; 1M Thiamine HCl, 1mL; 0.1M CaCl<sub>2</sub>·H<sub>2</sub>O, 1mL and 20% glucose, 10mL.

**Minimal Media Agar.** This was made in an identical manner to the minimal media broth except 15g agar was added to the solution containing Na<sub>2</sub>HPO<sub>4</sub>, KH<sub>2</sub>PO<sub>4</sub>, NaCl and NH<sub>4</sub>Cl. When the solution had cooled to below 50°C, the additional solutions were added and the plates were poured using sterile petri dishes. After setting, the plates were stored at 4°C.

**SOB Broth.** 20g bactotryptone, 5g yeast extract, 0.6g NaCl, 0.5g KCl were made up to 1L with EM water and sterilised by autoclaving at 15 psi for 20 minutes. Immediately prior to use 1mL of magnesium chloride (MgCl<sub>2</sub>) and 1mL of 1M magnesium sulphate (MgSO<sub>4</sub>) were added aseptically.

**Terrific Broth (TB).** This media consists of two solutions: solution I; 12g bactotryptone, 24g yeast extract, 4mL glycerol made up to 900mL with EM water and solution II; 12.54g dipotassium hydrogen orthophosphate (K<sub>2</sub>HPO<sub>4</sub>) and 2.31g potassium dihydrogen orthophosphate (KH<sub>2</sub>PO<sub>4</sub>) made up to 100mL with EM water.

Both solution were sterilised by autoclaving at 15 psi for 20 minutes. Immediately prior to use a solution II was added to solution I.

**TYP Broth.** 16g bactotryptone, 16g yeast extract, 5g NaCl and 2.5g of dipotassium hydrogen orthophosphate ( $K_2HPO_4$ ) were made up to 1L with EM water and sterilised by autoclaving at 15 psi for 20 minutes.

**2YT Broth.** 16g bactotryptone, 10g yeast extract and 5g NaCl were made up to 1L with EM water. The solution was sterilised by autoclaving at 15 psi for 20 minutes.

### ***A3 Spectrophotometric Conversions for DNA***

1  $A_{260nm}$  unit of double stranded DNA (ds DNA)= 50 $\mu$ g/mL.

1  $A_{260nm}$  unit of either single stranded DNA (ss DNA) or single stranded oligonucleotide = 33 $\mu$ g/mL.

To evaluate the purity of a sample of DNA, the absorbance at 260nm and 280nm was measured and the  $A_{260}/A_{280nm}$  ratio calculated. The ratio for a pure sample of ds DNA should be 1.8.

### ***A4 Calculation of the Melting Temperature of Oligonucleotides***

Oligonucleotide primers were designed such that the melting temperature was above 56°C, the annealing temperature used during the PCR method for preparation of single and double stranded DNA for automated sequencing. The melting temperature ( $T_m$ ) of the oligonucleotide was calculated using the following equation:

$$T_m = n (G/C) \times 4^\circ C + n (A/T) \times 2^\circ C \quad \text{Equation A1}$$

The  $T_m$  of a GC bp and a AT bp was taken to be 4°C and 2°C respectively.

## References

Adesnik, M. and Atchinson, M. (1986) "Genes for cytochrome P-450 and their regulation." Critical Reviews in Biochemistry **19** (3): 247-305.

Alterman, M. A., Chaurasia, C. S., Lu, P., Hardwick, J. P. and Hanzlik, R. P. (1995) "Fatty acid discrimination and  $\omega$ -hydroxylation by cytochrome P450 4A1 and a cytochrome P4504A1/NADPH-P450 reductase fusion protein." Archives of Biochemistry and Biophysics **320** (2): 289-296.

Amarneh, B., Corbin, C. J., Peterson, J. A., Simpson, E. R. and Graham-Lorence, S. (1993) "Functional domains of human aromatase cytochrome P450 characterized by linear alignment and site-directed mutagenesis." Molecular Endocrinology **7** (12): 1617-1624.

Atkins, W. M. and Sligar, S. G. (1987) "Metabolic switching in cytochrome P-450<sub>cam</sub>: Deuterium isotope effects on regiospecificity and the monooxygenase/oxidase ratio." Journal of the American Chemical Society **109** (12): 3754-3760.

Bambal, R. B. and Hanzlik, R. P. (1996) "Effects of steric bulk and conformational rigidity on fatty acid omega hydroxylation by a cytochrome P450 4A1 fusion protein." Archives of Biochemistry and Biophysics **334** (1): 59-66.

Barton, G. J. (1993) "ALSCRIPT a tool to format multiple sequence alignments." Protein Engineering **6** (1): 37-40.

Bernhardt, R. (1995) "Cytochrome P450: Structure, function, and generation of reactive oxygen species." Review of Physiological and Biochemical Pharmacology **127**: 137-221.

Björkhem, I. and Danielsson, H. (1970) " $\omega$ - and ( $\omega$ -1)-oxidation of fatty acids by rat liver microsomes." European Journal of Biochemistry **17** (3): 450-459.

Black, S. D. and Coon, M. J. (1987) "P-450 cytochromes: Structure and function." Advances in Enzymology **60**: 35-87.

Black, S. D., Linger, M. H., Freck, L. C., Kazemi, S. and Galbraith, J. A. (1994) "Affinity isolation and characterisation of cytochrome P450 102 (BM-3) from barbiturate-induced *Bacillus megaterium*." Archives of Biochemistry and Biophysics **310** (1): 126-133.

Boddupalli, S. S., Estabrook, R. W. and Peterson, J. A. (1990) "Fatty acid monooxygenation by cytochrome P-450<sub>BM-3</sub>." Journal of Biological Chemistry **265** (8): 4233-4239.

Boddupalli, S. S., Oster, T., Estabrook, R. W. and Peterson, J. A. (1992) "Reconstitution of the fatty acid hydroxylation function of cytochrome P450<sub>BM-3</sub> utilising its individual recombinant hemo- and flavoprotein domains." Journal of Biological Chemistry **267** (15): 10375-10380.

Bonfils, C., Balny, C. and Maurel, P. (1981) "Direct evidence for electron transfer from ferrous cytochrome *b*<sub>5</sub> to the oxyferrous intermediate of liver microsomal cytochrome P-450 LM<sub>2</sub>." Journal of Biological Chemistry **256** (18): 9457-9465.

Boucher, J.-I., Genet, A., Vadon, S., Delaforge, M., Henry, Y. and Mansuy, D. (1992) "Cytochrome P450 catalyses the oxidation of N $\omega$ -hydroxy-L-arginine by NADPH and O<sub>2</sub> to nitric oxide and citrulline." Biochemical and Biophysical Research Communications **187** (2): 880-886.

Bradford, M. M. (1976) "A rapid and sensitive method for the quantitation of microgram quantities of protein utilizing the principle of protein-dye binding." Analytical Biochemistry **72**: 248-254.

Bredt, D. S., Hwang, P. M., Glatt, C. E., Lowenstein, C., Reed, R. R. and Snyder, S. H. (1991) "Cloned and expressed nitric oxide synthase structurally resembles cytochrome P-450 reductase." Nature **351**: 714-718.

Brocklehurst, K. (1979) "Specific covalent modification of thiols: Applications in the study of enzymes and other biomolecules." The International Journal of Biochemistry **10**: 259-274.

CaJacob, C. A., Chan, W. K., Shephard, E. and Ortiz de Montellano, P. R. (1988) "The catalytic site of rat hepatic lauric acid  $\omega$ -hydroxylase." Journal of Biological Chemistry **263** (35): 18640-18649.

Capdevila, J. H., Wei, S. Z., Helvig, C., Falck, J. R., Belosludtsev, Y., Truan, G., Graham-Lorence, S. E. and Peterson, J. A. (1996) "The highly stereoselective oxidation of polyunsaturated fatty-acids by cytochrome P450<sub>BM-3</sub>." Journal of Biological Chemistry **271** (37): 22663-22671.

Chang, Y. and Loew, G. H. (1996) "Construction and evaluation of a three-dimensional structure of cytochrome P450choP enzyme (CYP105C1)." Protein Engineering **9** (9): 755-766.

Cheng, L., Qian, S. J., Rothschild, C., d'Avignon, A., Lefkowitz, J. B., Gordon, J. I. and Li, E. (1991) "Alteration of the binding specificity of cellular retinol-binding protein II by site-directed mutagenesis." Journal of Biological Chemistry **266** (36): 24404-24412.

Chung, C.T. and Miller, R.H. (1993) "Preparation and storage of competent *Escherichia coli* cells." Methods in Enzymology **218**: 621-627.

Cupp-Vickery, J. R. and Poulos, T. L. (1995) "Structure of cytochrome P450eryF involved in erythromycin biosynthesis." Nature Structural Biology **2** (2): 144-153.

Curnow, K. M., Mulatero, P., Emeric-Blanchouin, N., Aupetit-Faisant, A., Corvol, P. and Pascoe, L. (1997) "The amino acid substitutions Ser288Gly and Val320Ala convert the cortisol producing enzyme, CYP11B1, into an aldosterone producing enzyme." Nature Structural Biology **4** (1): 32-35.

Darwish, K., Li, H. and Poulos, T. L. (1991) "Engineering proteins, subcloning and hyperexpressing oxidoreductase genes." Protein Engineering **4** (6): 701-708.

Dawson, J. H. (1988) "Probing structure-function relations in heme-containing oxygenases and peroxidases." Science **240**: 433-439.

De Groot, M. J., Vermeulen, N. P. E., Kramer, J. D., van Acker, F. A. A. and Donné-Op den Kelder, G. M. (1996) "A three-dimensional protein model for human cytochrome P450 2D6 based on the crystal structures of P450 101, P450 102 and P450 108." Chemical Research in Toxicology **9** (7): 1079-1091.

Delphi (1993) Delphi user guide, Version 2.4. Biosym Technologies, San Diego, CA, USA.

De Voss, J. J. and Ortiz de Montellano, P. R. (1995) "Computer aided, structure-based prediction of substrates for cytochrome P450<sub>cam</sub>." Journal of the American Chemical Society **117** (14): 4185-4186.

Dhalla, A. M., Li, B., Alibhai, M. F., Yost, K. J., Hemmingsen, J. M., Atkins, W. M., Schineller, J. and Villafranca, J. J. (1994) "Regeneration of catalytic activity of glutamine synthetase mutants by chemical activation: Exploration of the role of arginines 339 and 359 in activity." Protein Science **3**: 476-481.

Dwek, R. A. (1973) Nuclear Magnetic Resonance (NMR) in Biochemistry. pp 11-142, Oxford University Press, London.

Ellin, Å., Orreius, S., Pilotti, Å. and Swahn, C.-G. (1973) "Cytochrome P-450<sub>K</sub> of rat kidney cortex microsomes: Further studies on its interaction with fatty acids." Archives of Biochemistry and Biophysics **158**: 597-604.

Ellman, G. L. (1959) "Tissue sulphhydryl groups." Archives of Biochemistry and Biophysics **82**: 70

English, N., Hughes, V. and Wolf, C. R. (1994) "Common pathways of cytochrome-P450 gene-induction by peroxisome proliferators and barbiturates in *Bacillus megaterium* ATCC14581." Journal of Biological Chemistry **269** (43): 26836-26841.

Estabrook, R. W., Cooper, D. Y. and Rosenthal, O. (1963) "The light reversible carbon monoxide inhibition of the steroid C21-hydroxylase system of the adrenal cortex." Biochemische Zeitschrift **338**: 741-755.

Falk, J.E. (1975) in Porphyrins and Metalloporphyrins (Smith, K.M. ed.) pp. 30-93, Elsevier, Amsterdam.

Fukuda, T., Imai, Y., Komori, M., Nakamura, M., Kusunose, E., Satouchi, K. and Kusunose, M. (1994) "Different mechanisms of regioselection of fatty acid hydroxylation by laurate ( $\omega$ -1)-hydroxylating P450s, P450 2C2 and P450 2E1." Journal of Biochemistry **115**: 338-344.

Fulco, A. J. (1991) "P450<sub>BM-3</sub> and other inducible bacterial P450 cytochromes: Biochemistry and Regulation." Annual Review of Pharmacology and Toxicology **31**: 177-203.

Garfinkel, D. (1957) "Isolation and properties of cytochrome *b*5 from pig liver." Archives of Biochemistry and Biophysics **71**: 111-120.

Gerber, N. C. and Sligar, S. C. (1994) "A role for asp-251 in cytochrome P-450cam oxygen activation." Journal of Biological Chemistry **269** (6): 4260-4266.

Gillette, J. R., Brodie, B. B. and La Du, B. N. (1957) "The oxidation of drugs by liver microsomes: On the role of TPNH and oxygen." Journal of Pharmacology and Experimental Therapeutics **119**: 532-540.

Gonzalez, F. J. (1990) "Molecular genetics of the P-450 superfamily." Pharmacology and Therapeutics **45**: 1-38.

Gonzalez, F. J. and Nebert, D. W. (1990) "Evolution of the P450 gene superfamily." Trends in Genetics **6** (6): 182-186.

- Gorsky, L. D., Koop, D. R. and Coon, M. J. (1984) "On the stoichiometry of the oxidase and monooxygenase reactions catalysed by liver microsomal cytochrome P-450." Journal of Biological Chemistry **259** (11): 6812-6817.
- Gotoh, O. (1992) "Substrate recognition sites in cytochrome P450 family 2 (CYP2) proteins inferred from comparative analyses of amino acid and coding nucleotide sequences." Journal of Biological Chemistry **267** (1): 83-90.
- Gotoh, O. and Fujii-Kuriyama, Y. (1989) Evolution, structure and gene regulation of cytochrome P-450. In Ruckpaul K. and Rein, H. (Eds) Frontiers in Biotransformation Volume No 1. pp. 195-243, Taylor and Francis, London.
- Graham-Lorence, S., Sanders, D. and Peterson, J. A. (1994) Mutants affecting substrate recognition and substrate binding in P450BM-P. In M. C. Lechner (Ed.), 8th International Conference on Cytochrome P450: Biochemistry, Biophysics and Molecular Biology, (pp. 471-473). Lisbon, Portugal: John Libby, Eurotext.
- Graham-Lorence, S., Amarneh, B., White, R. E., Peterson, J. A. and Simpson, E. R. (1995) "A three dimensional modes of aromatase cytochrome P450." Protein Science **4** (6): 1065-1080.
- Graham-Lorence, S. E. and Peterson, J. A. (1996a) "Structural alignments of P450s and extrapolations to the unknown." Methods in Enzymology **272**: 315-326.
- Graham-Lorence, S. and Peterson, J. A. (1996b) "P450's: Structural similarities and functional differences." FASEB Journal **10**: 206-214.
- Graham-Lorence, S., Truan, G., Peterson, J. A., Falck, J. R., Wei, S., Helvig, C. and Capdevila, J. H. (1997) "An active site substitution, F87V, converts cytochrome P450 BM-3 into a regio- and stereoselective (14S, 15R)-arachidonic acid epoxygenase." Journal of Biological Chemistry **272** (2): 1127-1135.
- Guengerich, F. P. (1991) "Reactions and significance of cytochrome P-450 enzymes." Journal of Biological Chemistry **266** (16): 10019-10022.
- Hahn, E. L. (1950) "Nuclear induction due to free larmor precession." Physics Review **25**: 297-298.
- Hanahan, D. (1985) In DNA cloning, D. M. Glover (Ed.), IRL Press, pp. 109-135.
- Hardwick, J. P., Song, B. J., Huberman, E. and Gonzalez, F. J. (1987) "Isolation, complementary DNA sequence, and regulation of rat hepatic lauric acid  $\omega$ -hydroxylase (cytochrome P-450<sub>LA $\omega$</sub> )." Journal of Biological Chemistry **262** (2): 801-810.

Harikrishna, J. A., Black, S. M., Szklarz, G. D. and Miller, W. L. (1993) "Construction and function of fusion enzymes of the human cytochrome P450<sub>sc</sub> system." DNA and Cell Biology **12** (5): 371-379.

Hasemann, C. A., Ravichandran, K. G., Peterson, J. A. and Deisenhofer, J. (1994) "Crystal structure and refinement of cytochrome P450<sub>terp</sub> at 2.3Å resolution." Journal of Molecular Biology **236**: 1169-1185.

Hasemann, C. A., Kurumbail, R. G., Boddupalli, S. S., Peterson, J. A. and Deisenhofer, J. (1995) "Structure and function of cytochromes P450: A comparative analysis of three crystal structures." Structure **3** (1): 41-62.

He, S., Modi, S., Bendall, D. S. and Gray, J. C. (1991) "The surface-exposed tyrosine residue Tyr83 of pea plastocyanin is involved in both binding and electron transfer reactions with cytochrome *f*." The EMBO Journal **10** (13): 4011-4016.

He, Y. Q., He, Y. A. and Halpert, J. R. (1995) "*Escherichia coli* expression of site-directed mutants of cytochrome P450 2B1 from six substrate recognition sites: Substrate specificity and inhibitor selectivity studies." Chemical Research in Toxicology **8** (4): 574-579.

Hildebrandt, A. G., Roots, I., Tjoe, M. and Heinmeyer, G. (1978) "Hydrogen peroxide in hepatic microsomes." Methods in Enzymology **52**: 342-350.

Hirasawa, M. and Knaff, D. B. (1993) "The role of lysine and arginine residues at the ferredoxin-binding site of spinach glutamate synthase." Biochimica et Biophysica Acta **1144** (1): 85-91.

Ho, P. P. and Fulco, A. J. (1976) "Involvement of a single hydroxylase species in the hydroxylation of palmitate at the ω-1, ω-2 and ω-3 positions by a preparation from *Bacillus megaterium*." Biochimica et Biophysica Acta **431**: 249-256.

Hrycay, E. G., Gustafsson, J., Ingelman-Sundberg, M. and Ernster, L. (1976) "The involvement of cytochrome P-450 in hepatic microsomal steroid hydroxylation reactions supported by sodium periodate, sodium chlorite, and organic hydroperoxides." European Journal of Biochemistry **61**: 43-52.

Imai, M., Shimada, H., Watanabe, Y., Matsushima-Hibiya, Y., Makino, R., Koga, H., Horiuchi, T. and Ishimura, Y. (1989) "Uncoupling of the cytochrome P-450cam monooxygenase reaction by a single mutation, threonine-252 to alanine or valine: A possible role of the hydroxy amino acid in oxygen activation." Proceedings of the National Academy of Sciences USA **86**: 7823-7827.

Jardetsky, O. and Roberts, G. C. K. (1981) NMR in Molecular Biology. Academic Press, New York.

Johnson, E. F. (1992) "Mapping determinants of the substrate selectivities of P450 enzymes by site-directed mutagenesis." Trends in Pharmacological Sciences **13**: 122-126.

Johnson, E. F., Kronbach, T. and Hsu, M. H. (1992) "Analysis of the catalytic specificity of cytochrome P450 enzymes through site-directed mutagenesis." FASEB Journal **6**: 700-705.

Kim, B. H. and Fulco, A. J. (1983) "Induction by barbiturates of a cytochrome P450-dependent fatty acid monooxygenase in *Bacillus megaterium*: Relationship between barbiturate structure and inducer activity." Biochemical and Biophysical Research Communications **116** (3): 843-850.

Kimata, Y., Shimida, H., Hirose, T. and Ishimura, Y. (1995) "Role of Thr-252 in cytochrome P450<sub>cam</sub>: A study with unnatural amino acid mutagenesis." Biochemical and Biophysical Research Communications **208** (1): 96-102.

Klingenberg, M. (1958) "Pigments of rat liver microsomes." Archives of Biochemistry and Biophysics **75**: 376-386.

Knowles, J. R. (1991) "Enzyme catalysis: Not different, just better." Nature **350**: 121-124.

Koga, H., Rauchfuss, B. and Gunsalus, I. C. (1985) "P450<sub>cam</sub> gene cloning and expression in *Pseudomonas putida* and *Escherichia coli*." Biochemical and Biophysical Research Communications **130** (1): 412-417.

Koymans, L., Vermeulen, N. P. E., van Acker, S. A. B. E., te Koppele, J., Heykants, J. J. P., Lavrijsen, K., Meuldermans, W. and Donne-Op den Kelder, G. M. (1992) "A predictive model for substrates of cytochrome P450-debrisoquine (2D6)." Chemical Research in Toxicology **5** (2): 211-219.

Kunkel, T. A. (1985) "Rapid and efficient site-specific mutagenesis without phenotypic selection." Proceedings of the National Academy of Sciences USA **82**: 488-492.

Lamas, S., Marsden, P. A., Li, G. K., Tempst, P. and Michel, T. (1992) "Endothelial nitric oxide synthase: Molecular cloning and characterisation of a distinct constitutive enzyme isoform." Proceedings of the National Academy of Sciences USA **89**: 6348-6352.

- Lewis, D. F. V. (1995) "Three-dimensional models of human and other mammalian microsomal P450s constructed from an alignment with P450102 (P450<sub>bm3</sub>)."  
Xenobiotica **25** (4): 333-366.
- Lewis, D. F. V. and Lake, B. G. (1995) "Molecular modelling of members of the P4502A subfamily: Applications to studies of enzyme specificity." Xenobiotica **25** (6): 585-598.
- Li, H., Darwish, K. and Poulos, T. L. (1991) "Characterisation of recombinant *Bacillus megaterium* cytochrome P-450<sub>BM-3</sub> and its two functional domains." Journal of Biological Chemistry **266** (18): 11909-11914.
- Li, H. and Poulos, T. L. (1995) "Modelling protein-substrate interactions in the heme domain of cytochrome P450<sub>BM-3</sub>." Acta Crystallographia Section D **51**: 21-32.
- Li, H., Narasimhulu, S., Havran, L. M., Winkler, J. D. and Poulos, T. L. (1995) "Crystal structure of cytochrome P450cam complexed with its catalytic product, 5-exo-hydroxycamphor." Journal of the American Chemical Society **117** (23): 6297-6299.
- Li, H. and Poulos, T. L. (1997) "The structure of the cytochrome P450BM-3 heme domain complexed with the fatty acid substrate, palmitoleic acid." Nature Structural Biology **4** (2): 140-146.
- Lindberg, R. L. P. and Negishi, M. (1989) "Alteration of mouse cytochrome P450<sub>coh</sub> substrate specificity by mutation of a single amino-acid residue." Nature **339**: 632-634.
- Loida, P. J. and Sligar, S. C. (1993) "Molecular recognition in cytochrome P-450: Mechanism for the control of uncoupling reactions." Biochemistry **32** (43): 11530-11538.
- Lu, A. Y. and Coon, M. J. (1968) "Role of hemoprotein P-450 in fatty acid  $\omega$ -hydroxylation in a soluble enzyme system from liver microsomes." Journal of Biological Chemistry **243** (6): 1331-1332.
- Lumper, L., Busch, F., Seherazade, D., Henning, J. and Lazar, T. (1980) "Studies on the cosubstrate site of protease solubilized NADPH-cytochrome P450 reductase." International Journal of Peptide and Protein Research **16**: 83-96.
- Martinis, S. A., Atkins, W. M., Stayton, P. S. and Sligar, S. G. (1989) "A conserved residue of cytochrome P-450 is involved in heme-oxygen stability and activation." Journal of the American Chemical Society **111**: 9252-9253.

Martinis, S. A., Ropp, J. A., Sligar, S. G. and Gunsalus, I. C. (1991) Molecular recognition by cytochrome P-450cam: Substrate specificity, catalysis and electron transfer. In K. Ruckpaul & H. Rein (Eds.), Microbial and Plant Cytochrome P-450 (pp. 54-86). Berlin: Taylor and Francis.

Matson, R. S., Hare, R. S. and Fulco, A. J. (1977) "Characterisation of a cytochrome P-450-dependent fatty acid  $\omega$ -2 hydroxylase from *Bacillus megaterium*." Biochimica et Biophysica Acta **487**: 487-494.

McKnight, J., Chessman, M. R., Thomson, A. J., Miles, J. S. and Munro, A. W. (1993) "Identification of charge-transfer transitions in the optical spectrum of low-spin ferric cytochrome P-450 *Bacillus megaterium*." European Journal of Biochemistry **213**: 683-687.

McMillan, K., Bredt, D. S., Hirsch, D. J., Snyder, S. H., Clark, J. E. and Masters, B. S. S. (1992) "Cloned, expressed rat cerebellar nitric oxide synthase contains stoichiometric amounts of heme which binds carbon monoxide." Proceedings of the National Academy of Science USA **89**: 11141-11145.

McMillan, K., Salerno, J. C. and Masters, B. S. S. (1996) "Nitric oxide synthases: Analogues to cytochrome P450 monooxygenases and characterization of recombinant rat neuronal nitric oxide synthase hemoprotein." Methods in Enzymology **268**: 460-472.

Means, G. E. and Feeney, R. E. (1971) Chemical modifications of proteins. San Francisco: Holden-Day, Inc.

Miles, J. S., Munro, A. W., Rosendowski, B. N., Smith, W. E., McKnight, J. and Thompson, A. J. (1992) "Domains of the catalytically self-sufficient cytochrome P-450 BM-3." Biochemistry Journal **288**: 503-509.

Miura, Y. and Fulco, A. J. (1974) " $\omega$ -2 Hydroxylation of fatty acids by a soluble system from *Bacillus megaterium*." Journal of Biological Chemistry **249** (6): 1880-1888.

Miura, Y. and Fulco, A. J. (1975) " $\omega$ -1,  $\omega$ -2 and  $\omega$ -3 hydroxylation of long-chain fatty acids, amides and alcohols by a soluble enzyme system from *Bacillus megaterium*." Biochimica et Biophysica Acta **388**: 305-317.

Modi, S., Behere, D. V. and Mitra, S. (1989) "Interaction of thiocyanate with horseradish peroxidase." Journal of Biological Chemistry **264** (33): 19677-19684.

Modi, S., Primrose, W. U., Lian, L.-Y. and Roberts, G. C. K. (1995a) "Effect of replacement of ferriprotoporphyrin IX in the haem domain of cytochrome P-450 BM-3 on substrate binding and catalytic activity." Biochemical Journal **310**: 939-943.

Modi, S., Primrose, W. U., Boyle, J. M. B., Gibson, C. F., Lian, L.-Y. and Roberts, G. C. K. (1995b) "NMR studies of substrate binding to cytochrome P<sub>450</sub><sup>BM3</sup>: Comparisons to cytochrome P 450<sub>cam</sub>." Biochemistry **34** (28): 8982-8988.

Modi, S., Paine, M. J., Sutcliffe, M. J., Lian, L.-Y., Primrose, W. U., Wolf, C. R. and Roberts, G. C. K. (1996a) "A model for human cytochrome P450 2D6 based on homology modeling and NMR studies of substrate binding." Biochemistry **35** (14): 4540-4550.

Modi, S., Sutcliffe, M. J., Primrose, W. U., Lian, L.-Y. and Roberts, G. C. K. (1996b) "The catalytic mechanism of cytochrome P450 BM3: Reduction leads to a 6Å movement of the bound substrate." Nature Structural Biology **3** (5): 414-417.

Mueller, E. J., Loida, P. J. and Sligar, S. G. (1995) Twenty five years of P450<sub>cam</sub> research: Mechanistic insights into oxygenase catalysis. In P. R. Ortiz de Montellano (Ed.), Cytochrome P450: Structure, Mechanism, and Biochemistry (Second Edition). pp. 83-124, New York: Plenum Press.

Munro, A. W., Lindsay, J. G., Coggins, J. R., Kelly, S. M. and Price, N. C. (1994) "Structural and enzymological analysis of the interaction of isolated domains of cytochrome P-450 BM3." FEBS Letters **343**: 70-74.

Murakami, H., Yabusaki, Y., Sakaki, T., Shibata, M. and Ohkawa, H. (1987) "A genetically engineered P450 monooxygenase: Construction of the functional fused enzyme between rat cytochrome P450c and NADPH-cytochrome P450 reductase." DNA **6** (3): 189-197.

Murataliev, M. B. and Feyereisen, R. (1996) "Functional interactions in cytochrome P450BM3. Fatty acid substrate binding alters electron-transfer properties of the flavoprotein domain." Biochemistry **35** (47): 15029-15037.

Nakayama, N., Takemae, A. and Shoun, H. (1996) "Cytochrome P450foxy, a catalytically self-sufficient fatty acid hydroxylase of the fungus *Fusarium oxysporum*." Journal of Biochemistry **119**: 435-440.

Narhi, L. O. and Fulco, A. J. (1982) "Phenobarbital induction of a soluble cytochrome P-450-dependant fatty acid monooxygenase in *Bacillus megaterium*." Journal of Biological Chemistry **257** (5): 2147-2150.

Narhi, L. O., Kim, B. H., Stevenson, P. M. and Fulco, A. J. (1983) "Partial characterisation of a barbiturate-induced cytochrome P-450-dependent fatty acid monooxygenase from *Bacillus megaterium*." Biochemical and Biophysical Research Communications **116** (3): 851-858.

Narhi, L. O. and Fulco, A. J. (1986) "Characterisation of a catalytically self-sufficient 119,000-Dalton cytochrome P-450 monooxygenase induced by barbiturates in *Bacillus megaterium*." Journal of Biological Chemistry **261** (16): 7160-7169.

Narhi, L. O. and Fulco, A. J. (1987) "Identification and characterisation of two functional domains in cytochrome P-450<sub>BM-3</sub>, a catalytically self-sufficient monooxygenase induced by barbiturates in *Bacillus megaterium*." Journal of Biological Chemistry **262** (14): 6683-6690.

Narhi, L. O., Wen, L.-P. and Fulco, A. J. (1988) "Characterisation of the protein expressed in *Escherichia coli* by a recombinant plasmid containing the *Bacillus megaterium* cytochrome P-450<sub>BM-3</sub> gene." Molecular and Cellular Biochemistry **79**: 63-71.

Nebert, D. W. and Gonzalez, F. J. (1987) "P450 genes: Structure, evolution and regulation." Annual Review of Biochemistry **56**: 945-993.

Nebert, D. W., Nelson, D. R. and Feyereisen, R. (1989) "Evolution of the cytochrome P450 genes." Xenobiotica **19** (10): 1149-1160.

Nebert, D. W., Nelson, D. R., Coon, M. J., Estabrook, R. W., Feyereisen, R., Fujii-Kuriyama, Y., Gonzalez, F. J., Guengerich, F. P., Gunsalus, I. C., Johnson, E. F., Loper, J. C., Sato, R., Waterman, M. R. and Waxman, D. J. (1991). "The P450 superfamily: Update on new sequences, gene mapping, and recommended nomenclature." DNA and Cell Biology **10** (1): 1-14.

Negishi, M., Uno, T., Darden, T. A., Sueyoshi, T. and Pedersen, L. G. (1996) "Structural flexibility and functional versatility of mammalian P450 enzymes." FASEB Journal **10**: 683-689.

Nelson, D. R. and Strobel, H. W. (1987) "Evolution of cytochrome P-450 proteins." Molecular Biology of Evolution **4** (6): 572-593.

Nelson, D. R., Kamataki, T., Waxman, D. J., Guengerich, F. P., Estabrook, R. W., Feyereisen, R., Gonzalez, F. J., Coon, M. J., Gunsalus, I. C., Gotoh, O., Okuda, K. and Nebert, D. W. (1993) "The P450 superfamily: Update on new sequences, gene mapping, accession numbers, early trivial names of enzymes and nomenclature." DNA and Cell Biology **12**(1): 1-51.

Nelson, D. R., Koymans, L., Kamataki, T., Stegeman, J. J., Feyereisen, R., Waxman, D. J., Waterman, M. R., Gotoh, O., Coon, M. J., Estabrook, R. W., Gunsalus, I. C. and Nebert, D. W. (1996) "P450 superfamily: Update on new sequences, gene mapping, accession numbers and nomenclature." Pharmacogenetics **6**: (1): 1-42.

Nicholls, A. and Honig, B. (1993) GRASP: Graphical representation and analysis of surface properties. Columbia University, New York, NY 10032, USA.

Oguri, K., Yamada, H and Yoshimura, H. (1994). "Regiochemistry of cytochrome P450 isoenzymes." Annual Review of Pharmacology and Toxicology **34**: 251-279.

Okita, R. T., Parkhill, L. K., Yasukochi, Y., Masters, B. S. S., Theoharides, A. D. and Kupfer, D. (1981) "The  $\omega$ - and ( $\omega$ -1)-hydroxylase activities of prostaglandin A<sub>1</sub> and E<sub>1</sub> and lauric acid by pig kidney microsomes and a purified kidney cytochrome P-450." Journal of Biological Chemistry **256** (12): 5961-5964.

Okita, R. T., Clark, J. E., Okita, J. R. and Masters, B. S. S. (1991) " $\omega$ - and ( $\omega$ -1)-hydroxylation of eicosanoids and fatty acids by high-performance liquid chromatography." Methods in Enzymology **206**: 432-441.

Oliver, C. F., Modi, S., Sutcliffe, M. J., Primrose, W. U., Lian, L.-Y. and Roberts, G. C. K. (1997a) "A single mutation in cytochrome P450 BM3 changes substrate orientation in a catalytic intermediate and the regioselectivity of hydroxylation." Biochemistry **36**: 1567-1572.

Oliver, C. F., Modi, S., Primrose, W. U., Lian, L.-Y. and Roberts, G. C. K. (1997b) "Engineering the substrate specificity of *Bacillus megaterium* cytochrome P-450 BM3: Hydroxylation of alkyl trimethylammonium compounds." Biochemical Journal **327**: 537-544.

Omura, T. and Sato, R. (1964) "The carbon monoxide-binding pigment of liver microsomes." Journal of Biological Chemistry **239** (7): 2370-2378.

Ortiz de Montellano, P. R., Chan, W. K., Tuck, S. F., Kaikaus, R. M., Bass, N. M. and Peterson, J. A. (1992) "Mechanism-based probes of the topology and function of fatty acid hydroxylases." FASEB Journal **6**: 695-699.

Ortiz de Montellano, P. R. (1995a) Oxygen activation and reactivity. In P. R. Ortiz de Montellano (Ed.), Cytochrome P450: Structure, Mechanism and Biochemistry (Second Edition). pp. 245-304, New York: Plenum Press.

Ortiz de Montellano, P. R. (1995b) "Arylhydrazines as probes of hemoprotein structure and function." Biochimie **77**: 581-593.

Oster, T., Boddupalli, S. S. and Peterson, J. A. (1991) "Expression, purification, and properties of the flavoprotein domain of cytochrome P-450<sub>BM-3</sub>." Journal of Biological Chemistry **266** (3): 22718-22725.

Paulsen, M. D. and Ornstein, R. L. (1995) "Dramatic differences in the motions of the mouth of open and closed cytochrome P450<sub>BM-3</sub> by molecular dynamics simulations." Proteins: Structure, Function and Dynamics **21**: 237-243.

Penman, B. W., Reece, J., Smith, T., Yang, C. S., Gelboin, H. V., Gonzalez, F. J. and Crespi, C. L. (1993) "Characterization of a human cell-line expressing high levels of cDNA-derived CYP2D6." Pharmacogenetics **3**: 28-39.

Peterson, J. A., White, R. E., Yasukochi, Y., Coomes, M. L., O'Keefe, D. H., Ebel, R. E., Masters, B. S. S., Ballou, D. P. and Coon, M. J. (1977) "Evidence that purified liver microsomal cytochrome P-450 is a one-electron acceptor." Journal of Biological Chemistry **252** (13): 4431-4434.

Peterson, J. A., Lorence, M. C. and Amarneh, B. (1990) "Putidaredoxin reductase and putidaredoxin." Journal of Biological Chemistry **265** (11): 6066-6073.

Peterson, J. A., Deisonhofer, J., Hasemann, C., Ravichandran, K. G., Boddupalli, S. S. and Graham-Lorence, S. (1994) Structure and function in P450's: are bacterial P450's good models for eukaryotic P450's. In M. C. Lechner (Ed.), 8th International Conference on Cytochrome P450: Biochemistry, Biophysics and Molecular Biology, (pp. 271-277). Lisbon, Portugal: John Libby, Eurotext.

Peterson, J. A. and Graham-Lorence, S. A. (1995) Bacterial P450s: Structural similarities and functional differences. In P. R. Ortiz de Montellano (Ed.), Cytochrome P450: Structure, Mechanism and Biochemistry (Second Edition). pp. 151-182, New York: Plenum Press.

Plapp, B. V. (1995) "Site-directed mutagenesis: A tool for studying enzyme catalysis." Methods in Enzymology **249**: 91-119.

Plummer, S. M., Hall, M. and Faux, S. (1995) "Oxidation and genotoxicity of fecapentaene-12 are potentiated by prostaglandin H synthase." Carcinogenesis **16** (5): 1023-1028.

Porter, T. D. and Kasper, C. B. (1986) "NADPH-cytochrome P-450 oxidoreductase: Flavin mononucleotide and flavin adenine dinucleotide domains evolved from different flavoproteins." Biochemistry **25** (7): 1682-1687.

Porter, T. D. (1991) "An unusual yet strongly conserved flavoprotein reductase in bacteria and mammals." Trends in Biological Sciences **16**: 154-158.

Porter, T. D. and Coon M. J. (1991) "Cytochrome P450." Journal of Biological Chemistry **266** (21): 13469-13472.

Poulos, T. L. (1996) "Ligands and electrons and haem proteins." Nature Structural Biology **3** (5): 401-403.

Poulos, T. L., Finzel, B. C., Gunsalus, I. C., Wagner, G. C. and Kraut, J. (1985) "The 2.6-Å crystal structure of *Pseudomonas putida* cytochrome P-450." Journal of Biological Chemistry **260** (30): 16122-16130.

Poulos, T. L., Finzel, B. C. and Howard, A. J. (1986) "Crystal structure of substrate-free *Pseudomonas putida* cytochrome P-450." Biochemistry **25** (18): 5314-5322.

Poulos, T. L. and Howard, A. J. (1987) "Crystal structures of metyrapone- and phenylimidazole-inhibited complexes of cytochrome P-450<sub>cam</sub>." Biochemistry **26** (25): 8165-8174.

Poulos, T. L., Finzel, B. C. and Howard, A. J. (1987) "High-resolution crystal structure of cytochrome P450<sub>cam</sub>." Journal of Molecular Biology **195**: 687-700.

Poulos, T. L. and Raag, R. (1992) "Cytochrome P450<sub>cam</sub>: Crystallography, oxygen activation, and electron transfer." FASEB Journal **6**: 674-679.

Raag, R., Swanson, B. A., Poulos, T. L. and Ortiz de Montellano, P. R. (1990) "Formation, crystal structure and rearrangement of a cytochrome P450<sub>cam</sub> iron-phenyl complex." Biochemistry **29** (35): 8119-8126.

Raag, R. and Poulos, T. L. (1991) "Crystal structures of cytochrome P-450<sub>CAM</sub> complexed with camphane, thiocamphor and adamantane: Factors controlling P-450 substrate hydroxylation." Biochemistry **30** (10): 2674-2684.

Raag, R., Martinis, S. A., Sligar, S. G. and Poulos, T. L. (1991) "Crystal structure of the cytochrome P-450<sub>CAM</sub> active site mutant Thr252Ala." Biochemistry **30** (48): 11420-11429.

Raag, R., Li, H., Jones, B. C. and Poulos, T. L. (1993) "Inhibitor-induced conformational change in cytochrome P-450<sub>CAM</sub>." Biochemistry **32** (17): 4571-4578.

Ramarao, M. and Kemper, B. (1995) "Substitution at residue 473 confers progesterone 21-hydroxylase activity to cytochrome P450 2C2." Molecular Pharmacology **48**: 417-424.

Ravichandran, K. G., Boddupalli, S. S., Hasemann, C. A., Peterson, J. A. and Deisenhofer, J. (1993) "Crystal structure of hemoprotein of P450<sub>BM-3</sub>, a prototype for microsomal P450's." Science **261**: 731-735.

Riordan, J. F., McElvany, K. D. and Borders Jr., C. L. (1977) "Arginyl residues: Anion recognition sites in enzymes." Science **195**: 884-885.

Ruettinger, R. T., Kim, B. H. and Fulco, A. J. (1984) "Acylureas: A new class of barbiturate-like bacterial cytochrome P-450 inducers." Biochemical and Biophysical Research Communications **801**: 372-380.

Ruettinger, R. T., Wen, L.-P. and Fulco, A. J. (1989) "Coding nucleotide 5' regulatory and deduced amino acid sequences of P-450<sub>BM3</sub>, a single peptide cytochrome P-450:NADPH-P-450 reductase from *Bacillus megaterium*." Journal of Biological Chemistry **264** (19): 10987-10995.

Sacchettini, J. C., Scapin, G., Gopaul, D. and Gordon, J. I. (1992) "Refinement of the structure of *Escherichia coli*-derived rat intestinal fatty acid binding protein with bound oleate to 1.75Å resolution." Journal of Biological Chemistry **267** (33): 23534-23545.

Salaün, J.-P., Weissbart, D., Durst, F., Pflieger, P. and Mioskowski, C. (1989) "Epoxidation of *cis* and *trans* D<sup>9</sup>-unsaturated lauric acids by a cytochrome P-450-dependant system from higher plant microsomes." FEBS Letters **246** (1,2): 120-126.

Sariaslani, F. S. (1991) "Microbial cytochromes P-450 and xenobiotic metabolism." Advances in Applied Microbiology **36**: 133-178.

Sass, M. and Ziessow, D. (1977) "Error analysis for optimized inversion recovery spin-lattice relaxation measurements." Journal of Magnetic Resonance **25**: 263-276.

Sawadago, M. and Van Dyke, M. W. (1991) "A rapid method for the purification of deprotected oligodeoxynucleotides." Nucleic Acids Research **19** (3): 674.

Schaefer, F. C. and Peters, G. A. (1961) "Base-catalysed reaction of nitriles with alcohols. A convenient route to imidates and amidine salts." Journal of Organic Chemistry **26**: 412-418.

Scheller, U., Zimmer, T., Kärigel, E. and Schunck, W. (1996) "Characterization of the n-alkane and fatty acid hydroxylating cytochrome P450 forms 52A3 and 52A4." Archives of Biochemistry and Biophysics **328** (2): 245-254.

Schindler, J. F. and Viola, R. E. (1996) "Conversion of cysteinyl residues to unnatural amino acid analogs. Examination in a model system." Journal of Protein Chemistry **15** (8): 737-742.

Sevrioukova, I., Truan, G. and Peterson, J. A. (1997) "Reconstitution of the fatty acid hydroxylase activity of cytochrome P450<sub>BM-3</sub> utilising its functional domains." Archives of Biochemistry and Biophysics **340** (2): 231-238.

Shaw, G. and Fulco, A. J. (1992) "Barbiturate-mediated regulation of expression of the cytochrome P450<sub>BM-3</sub> gene of *Bacillus megaterium* by Bm3R1 protein." Journal of Biological Chemistry **267** (8): 5515-5526.

Shaw, G. and Fulco, A. J. (1993) "Inhibition by barbiturates of the binding of Bm3R1 repressor to its operator site on the barbiturate-inducible cytochrome P450<sub>BM-3</sub> gene of *Bacillus megaterium*." Journal of Biological Chemistry **268** (4): 2997-3004.

Shaw, G., Sung, C. and Chiang, A. (1996) "Induction by long-chain fatty acids and sodium dodecyl sulfate of cytochrome P450<sub>BM-3</sub> in *Bacillus megaterium*." Current Microbiology **32**: 124-128.

Shimizu, T., Tateishi, T., Hatano, M. and Fujii-Kuriyama, Y. (1991) "Probing the role of lysines and arginines in the catalytic function of cytochrome P450<sub>d</sub> by site-directed mutagenesis." Journal of Biological Chemistry **266** (6): 3372-3375.

Shiota, N., Nagasawa, A., Sakaki, T., Yabusaki, Y. and Ohkawa, H. (1994) "Herbicide-resistant tobacco plants expressing the fused enzyme between rat cytochrome P4501A1 (CYP1A1) and yeast NADPH-cytochrome P450 oxidoreductase." Plant Physiology **106**: 17-23.

Shirane, N., Sui, Z., Peterson, J. A. and Ortiz de Montellano, P. (1993) "Cytochrome P450<sub>BM-3</sub> (CYP 102): Regiospecificity of oxidation of  $\omega$ -unsaturated fatty-acids and mechanism-based inactivation." Biochemistry **32**(49): 13732-13741.

Shoun, H., Sudo, Y. and Beppu, T. (1985) "Subterminal hydroxylation of fatty acids by a cytochrome P-450-dependant enzyme system from a fungus, *Fusarium oxysporum*." Journal of Biochemistry **97**: 755-763.

Sibbesen, O., De Voss, J. J. and Ortiz de Montellano, P. R. (1996) "Putidaredoxin reductase-putidaredoxin-cytochrome P450<sub>cam</sub> triple fusion protein." Journal of Biological Chemistry **271** (37): 22462-22469.

Sligar, S. G., Lipscomb, J. D., Debrunner, P. G. and Gunsalus, I. C. (1974) "Superoxide anion production by the autoxidation of cytochrome P450<sub>cam</sub>." Biochemical and Biophysical Research Communications **61** (1): 290-296.

Sligar, S. G. and Murray, R. I. (1986) Cytochrome P-450<sub>cam</sub> and other bacterial P-450 enzymes. In P. R. Ortiz de Montellano (Ed.), Cytochrome P450: Structure, Mechanism, and Biochemistry. Pp. 429-503, New York: Plenum Press.

Smith, H. B. and Hartman, F. C. (1988) "Restoration of activity to catalytically deficient mutants of ribulosebiphosphate carboxylase/oxygenase by aminoethylation." Journal of Biological Chemistry **263** (10): 4921-4925.

Solomon, I. and Bloembergen, N. (1956) "Nuclear magnetic interactions in the HF molecule." Journal of Chemical Physics **25** (1): 261-266.

Stuehr, D. J. and Ikeda-Saito, M. (1992) "Spectral characterisation of brain and macrophage nitricoxide synthases." Journal of Biological Chemistry **267** (29): 20547-20550.

Szklarz, G. D., He, Y. A. and Halpert, J. R. (1995) "Site-directed mutagenesis as a tool for molecular modeling of cytochrome P450 2B1." Biochemistry **34** (44): 14312-14322.

Tuck, S. F., Peterson, J. A. and Ortiz de Montellano, P. R. (1992) "Active site topologies of bacterial cytochromes P450101 (P450<sub>cam</sub>), P450108 (P450<sub>terp</sub>) and (P450<sub>BM-3</sub>)." Journal of Biological Chemistry **267** (8): 5614-5620.

Tuck, S. F., Graham-Lorence, S., Peterson, J. A. and Ortiz de Montellano, P. R. (1993) "Active sites of the cytochrome p450<sub>cam</sub> (CYP101) F87W and F87A mutants." Journal of Biological Chemistry **268** (1): 269-275.

Ungar, B. P., Gunsalus, I. C. and Sligar, S. G. (1986) "Nucleotide sequence of the *Psuedomonas putida* cytochrome P-450<sub>cam</sub> gene and its expression in *Escherichia coli*." Journal of Biological Chemistry **261** (3): 1158-1163.

University of Wisconsin (1991) GCG package. 7. 575 Science Drive, Madison, WI 53711.

Vermillion, J. L., Ballou, D. P., Massey, V. and Coon, M. J. (1981) "Separate roles for FMN and FAD in catalysis by liver microsomal NADPH-cytochrome P-450 reductase." Journal of Biological Chemistry **256** (1): 266-277.

Vieira, J. and Messing, J. (1987) "Production of single-stranded plasmid DNA." Methods in Enzymology **153**: 3-11.

- Von Wachenfeldt, C. and Johnson, E. F. (1995) Structure of eukaryotic cytochrome P450 enzymes. In P. R. Ortiz de Montellano (Ed.), *Cytochrome P450: Structure, Mechanism and Biochemistry* (Second Edition). pp. 183-224, New York: Plenum Press.
- Wait, R. (1993) Introduction to mass spectrometry. In C. Jones, B. Mulloy, & A. H. Thomas (Eds.), *Spectroscopic methods and analyses: NMR, mass spectroscopy, and metalloprotein techniques*. pp. 191-213, Totowa, NJ: Humana Press Inc.
- Wang, M., Roberts, D. L., Paschke, R., Shea, T. M., Masters, B. S. S. and Kim, J. P. (1997) "Three-dimensional structure of NADPH-cytochrome P450 reductase: Prototype for FMN- and FAD-containing enzymes." Proceedings of the National Academy of Sciences USA **94**: 8411-8416.
- Waterman, M. R. (1992) "Cytochrome P450: Cellular distribution and structural considerations." Current Biology **2**: 384-387.
- Wen, L.-P. and Fulco, A. J. (1987) "Cloning of the gene encoding a catalytically self-sufficient cytochrome P-450 fatty acid monooxygenase induced by barbiturates in *Bacillus megaterium* and its functional expression and regulation in heterologous (*Escherichia coli*) and homologous (*Bacillus megaterium*) hosts." Journal of Biological Chemistry **262** (14): 6676-6682.
- White, K. A. and Marletta, M. A. (1992) "Nitric oxide synthase is a Cytochrome P-450 type hemoprotein." Biochemistry **31** (9): 6627-6631.
- White, R. E. and Coon, M. J. (1980) "Oxygen activation by cytochrome P450." Annual Review of Biochemistry **49**: 315-356.
- Williams, D. H. and Fleming, I. (1995) Spectroscopic methods in organic chemistry. (Fifth Edition). London: McGraw-Hill Book Company.
- Wynn, R. and Richards, F. M. (1993) "Unnatural amino acid packing mutants of *Escherichia coli* thioredoxin produced by combined mutagenesis/chemical modification techniques." Protein Science **2**: 395-403.
- Xie, Q. W., Cho, H. J., Calaycay, J., Mumford, R. A., Swiderek, K. M., Lee, T. D., Ding, A., Troso, T. and Nathan, C. (1992) "Cloning and characterisation of inducible nitric oxide synthase from mouse macrophages." Science **256**: 225-228.
- Yabusaki, Y. (1995) "Artificial P450/reductase fusion enzymes: What can we learn from their structures?" Biochimie **77**: 594-603.

Yeom, H., Sligar, S. G., Li, H., Poulos, T. L. and Fulco, A. J. (1995) "The role of Thr268 in oxygen activation of cytochrome P450<sub>BM-3</sub>." Biochemistry **34** (45): 14733-14740.

Zvelebil, M. J. J. M., Wolf, C. R. and Sternberg, M. J. E. (1991) "A predicted three-dimensional structure of human cytochrome P450: Implications for substrate specificity." Protein Engineering **4** (3): 271-282.